Biophysical Chemistry of EcoKI in Physiological Solutions: Emulating the Cell Interior

Steven Alexander Keatch

Thesis presented for the degree of Doctor of Philosophy
School of Chemistry
University of Edinburgh
2005

Declaration

I declare that this thesis was composed by myself, and the research presented is my own except where otherwise stated.

To my family.

Acknowledgements

I would like to thank my supervisor David Dryden for his limitless advice and encouragement. He has been an inspirational mentor throughout this project. I would also like to thank T.J. Su and Mark Tock for their helpful discussions and guidance.

Thanks must go to my parents, who have been a constant source of encouragement and support without ever putting me under any pressure, and continually reminding me that there is no such thing as a bad result. Special thanks to my wife Natasha for supporting and looking after me throughout my PhD, and for always finding a bright side to anything that has gone wrong.

I would like to thank Professor John Ladbury for kindly supplying StpA protein, Dr Robert Henderson and Dr Torun Berge for their help with the AFM work, and Rick Higham for assistance with rheology measurements. I would also like to thank the MRC and EPSRC for funding this project. A final special mention must go to Chris, Stuart, Elaine, Kate and Dave for keeping me sane with lunchtime cheer.

Abstract

The genomic DNA of bacteria exists in a compact and organised conformation within the cell. This conformation is maintained by macromolecular crowding and binding of nucleoid-associated proteins, polyamines, and other non-specific DNA-binding ligands. Production of polyamines and nucleoid-associated proteins is tightly regulated and restructures the nucleoid under environmental conditions that induce DNA damage into an even more highly condensed conformation. These 'stressful' conditions can cause the specific methylation sequence of DNA to be lost, which leaves the DNA open to self-attack by restriction enzymes. One such enzyme is EcoKI, a type I restriction enzyme that protects the bacterial cell by destroying foreign invading DNA. Upon loss of specific methylation, EcoKI could potentially destroy the host DNA and kill the bacteria. This damaging restriction is alleviated due to partial proteolysis of EcoKI by ClpXP, although a reduced ability to destroy incoming foreign DNA is maintained. However, this method of alleviation does not exist for all type I enzymes, implying that additional restriction alleviation is required to protect bacteria. In this thesis, it has been found that the condensed structure of DNA produced by the polyamine spermidine and the nucleoid-associated protein StpA, as well as the non-specific DNA-binding of the ligand YOYO, dramatically inhibit EcoKI ATP hydrolysis and restriction activities. These results show that condensation may be a method used by bacteria to protect the nucleoid from self-attack by EcoKI under DNA-damaging conditions, and therefore forms a second mechanism of restriction alleviation. Such a condensed DNA structure may inhibit access of the enzyme to its binding site as well as inhibiting the physical ability to translocate DNA. This is in contrast to invading foreign 'naked' DNA in the cytoplasm, which adopts a more open conformation, and therefore forms an ideal substrate for EcoKI translocation and restriction.

Table of Contents

List of Figures

List of Tables

Abbreviations

A_x	absorbance at x nm
A	adenine or adenosine
ADP	adenosine diphosphate
AFM	atomic force microscopy
ATP	adenosine triphosphate
bp	base-pair(s)
BSA	bovine serum albumin
C	cytosine or cytidine; carboxyl
Da	Dalton
DEAE	diethylaminoethyl
DMSO	dimethyl sulfoxide
DNA	deoxyribonucleic acid
DNaseI	deoxyribonucleaseI
dNTP	deoxynucleoside triphosphate
DTT	dithiothreitol
EDTA	diaminoethanetetraacetic acid
EtBr	ethidium bromide
g	gram or relative centrifugal force
G	guanine or guanosine
H33258	Hoescht 33258 dye
hsd	host specificity for DNA
HsdM	modification subunit
HsdR	restriction subunit
HsdS	specificity subunit
k	rate constant; kilo (10^3)
kb	kilobase
K_d	dissociation constant
K_m	Michaelis constant
l	litre
LDH	lactate dehydrogenase
M	molar
mA	milli-ampere
min	minutes

N	amino
NAD(H)	nicotnamide adenine dinucleotide (hydride)
NMR	nuclear magnetic resonance
PAGE	polyacrylamide gel electrophoresis
PCR	polymerase chain reaction
PEG	polyethylene glycol
PEP	phosphoenol pyruvate
pH	$-\log_{10}[H^+]$
P_i	inorganic phosphate
PK	pyruvate kinase
RNA	ribonucleic acid
RNase	ribonuclease
R/M	restriction-modification
s	second
SAM	S-adenosyl methionine
SDS	sodium dodecyl sulphate
Sp	spermidine
StpA	suppressor of *td* mutant phenotype A
T	thymine or thymidine
TBE	Tris-borate-EDTA (buffer)
TE	Tris-EDTA
TEMED	N,N,N',N'-tetramethylethyledediamine
T_m	melting temperature; thermal denaturation
TRD	target recognition domain
Tris	2-amino-2(hydroxymethyl)-1,2,-propandiol
U	unit
UV	ultra violet
V	volts
V_{max}	maximum rate
w/v	weight per volume
YOYO-1	dimeric oxazole yellow dye
Δ	deletion
ε	extinction coefficient
°C	degrees Centigrade
λ	wavelength

Chapter 1:

Introduction

1.1. General overview and perspectives

The genomic DNA of bacteria exists in a compact and organised conformation within the cell. It maintains this conformation by binding of nucleoid-associated proteins, polyamines, other non-specific DNA-binding ligands and macromolecular crowding. The expression of such condensation inducing nucleoid-associated proteins and polyamines is tightly regulated and nucleoid structure can therefore alter during the cell cycle. Cells under environmental 'stress' have also been seen to restructure their nucleoid into a highly condensed structure. DNA within bacteriophage heads is even more highly organised by the presence of polyamines. Upon infection of the bacterial cell by such a bacteriophage, the injected DNA immediately comes under the forces of macromolecular crowding from the high concentrations of protein and RNA present in the cytoplasm, also inducing a more compact conformation. Eukaryotes also maintain their genomes in highly organised and condensed states by the binding of histones, which also have an important role in regulating gene expression. Such varying conformations of DNA have been shown to effect enzyme activity due to many factors including binding site accessibility and volume exclusion effects.

However, most researchers analysing protein-DNA interactions do not take account of this physiologically relevant situation, preferring instead to carry out their reactions in buffers containing only low concentrations of salt in which DNA conforms to a random coil. As this is not the conformation that it adopts within the cell, the resultant interactions with proteins may not be physiologically relevant, and interactions that do occur *in vivo* may be missed. The crowded environment of the bacterial cell is represented in figure 1.1A with the condensed structure of the nucleoid of a bacterium undergoing attack by bacteriophage shown in figure 1.1B.

EcoKI is a type I restriction enzyme that has a primary role in intercepting invading bacteriophage DNA and deactivating it before it has a chance to kill the host bacterial cell. In carrying out this task it undergoes non-specific binding, target site recognition, specific binding, DNA translocation, and DNA restriction. This multifunctional enzyme is therefore a good model enzyme to investigate how DNA structure affects these different protein-DNA processes.

A

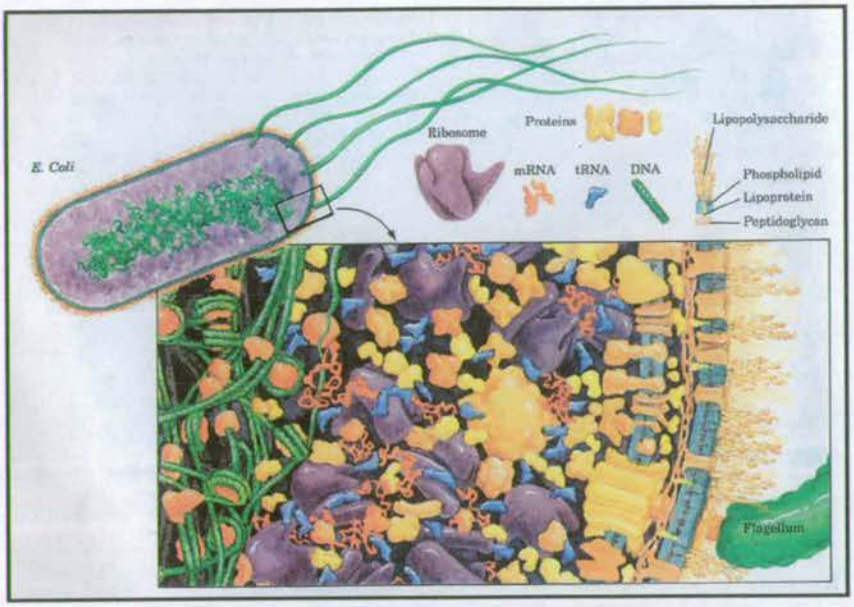

B

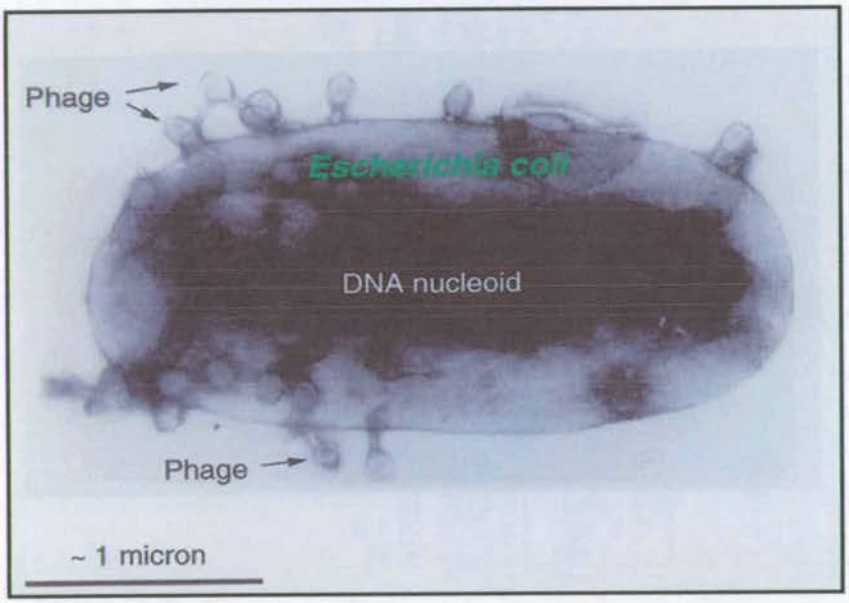

Figure 1.1. Intracellular crowding and bacteriophage attack of *E.coli*. Image A is a representation of the intracellular environment of an *E.coli* bacteria. The image shows how the DNA within the nucleoid is a compact conformation that occupies a small volume in the middle of the cell. The enlarged section from the box indicated shows the DNA bound to nucleoid-associated proteins, with the cytoplasm heavily crowded by macromolecules such as proteins and RNA. Image from Voet and Voet, 1995 (figure 1-13). Figure B shows an electron micrograph of *E.coli* under attack from bacteriophage. The bacteriophage bind to receptors on the cell membrane and inject their DNA into the crowded bacterial cytoplasm. The nucleoid can be seen as the dark region in the centre of the cell. Invading phage are indicated. Photograph by W.D. Donachie.

EcoKI also has the ability to distinguish the bacteria's genomic DNA from invading bacteriophage DNA due to its methylation state. Under situations of DNA damage when this methylation marker can be lost, EcoKI still manages to tell the two distinct targets apart. Although a protease has been found that partially degrades EcoKI when it is on the pathway to digest the bacterial genomic DNA, it is not present for all type I systems and does not prevent restriction of invading DNA. It has been proposed that the different conformations of the DNA in the nucleoid and the cytoplasm may allow distinction between these two types of DNA depending on their location in the cell.

It is therefore the aim of this thesis to investigate the different conformations of DNA formed by emulating the intracellular environment, and determine how these conformations affect EcoKI activities.

1.2. Restriction Endonucleases

1.2.1. Background

Restriction-modification systems were first found with the discovery that phages produced in one strain of a bacterial species would only rarely infect a different strain successfully, although readily infect the same strain. It was suggested from this that phages carried an imprint that identified their immediate origin and would require a new imprint in order to infect a different strain successfully *i.e.* to acquire a new host range (reviewed by Arber, 1965).

It was later shown that this host-controlled modification of the phage protected the DNA from an endonuclease, responsible for the restriction of successful propagation of the incoming phage genome. It was found that a specific sequence of DNA is recognised by a methyltransferase enzyme, which can modify the sequence by specific methylation (Smith *et al.*, 1972). The same sequence is recognised by the endonuclease, which proceeds to cleave the phage DNA in the absence of the specific modification. As the methyltransferase preferentially methylates the specific sequence in the bacterial DNA, foreign DNA entering the bacterial cell is recognised by the absence of specific methylation and is degraded by endonucleases, whilst the host DNA is

left unharmed (Murray, 2000; Dryden *et al.*, 2001)). There is only a low probability that an unmodified target sequence will escape attack by acquiring the correct modification. However, once acquired, this modification allows the phage to infect the new bacterial strain successfully.

As the host-controlled barrier to successful infection by phages was originally referred to as restriction, the relevant endonucleases have become known as restriction enzymes. Also, the methyltransferases are more commonly termed modification enzymes. Most restriction enzymes are accompanied by their cognate modification enzyme, with the two comprising a restriction-modification (R/M) system.

Classification of R/M systems is based upon their composition and cofactor requirements, the nature of their target sequence, and the position of the site of DNA cleavage with respect to the target sequence. Three different types of R/M systems have been characterised thus far and have been classified type I, II and III.

1.2.2. Type I restriction enzymes

1.2.2.1. Introduction

Type I R/M systems are hetero-oligomeric, multifunctional enzymes, capable of catalysing both restriction and modification. Methyltransferase activity requires S-adenosyl methionine (SAM) as the cofactor and methyl donor, whereas ATP, Mg^{2+}, and SAM are required for endonucleolytic activity (reviewed in Murray, 2000). Type I enzymes recognise specific asymmetric bipartite nucleotide sequences, comprising a 3-4bp specific sequence, separated by a nonspecific spacer of 6-8bp, before a 4-5bp specific sequence. For example, EcoKI recognises the sequence AACnnnnnnGTGC, where n can be any base (Kan *et al.*, 1979). All type I enzymes have been found to methylate adenine residues, one in each specific component of the target sequence, but on opposite strands. In the example for EcoKI above, the underlined A is a methylation site, whereas the underlined T represents the site of methylation for adenine on the complementary DNA strand. The methylation state of the target sequence determines whether the enzyme will act as an endonuclease or a methyltransferase. If the sequence is methylated, no activity takes place. If the sequence is hemimethylated, as in the case of newly replicated DNA,

the enzyme methylates the unmethylated strand (Vovis *et al.*, 1974). But if the sequence is unmethylated, the enzyme will pull the DNA towards itself from both directions whilst remaining bound to the target site (Bickle *et al.*, 1978; Davies *et al.*, 1999; Yuan *et al.*, 1980). Cleavage of the DNA then occurs when two translocating enzymes collide or translocation is generally impeded, which occurs at least 40bp (Dreier *et al.*, 1996), and typically several thousand base pairs from the target site (Studier and Bandyopadhyay, 1988). This general activity of type I R/M systems is summarised in figures 1.2 and 1.3.

Type I enzymes have been further characterised into four families; type IA, IB, IC and ID. Classification has been based upon genetic complementation, DNA hybridisation and antibody cross-reactivity (reviewed in Dryden *et al.*, 2001).

1.2.2.2. Subunit composition

Type I enzymes are made up from three subunits; HsdM (~50kDa), HsdS (50-60kDa) and HsdR (~140kDa) (reviewed in Dryden *et al.*, 2001; Bickle and Kruger, 1993). The acronym Hsd stands for "host specificity of DNA" due to the early nomenclature of R/M systems being referred to as host specificity systems. HsdS is the specificity subunit, and includes two target recognition domains (TRD), which confer target sequence specificity to both the restriction and modification activities of the complex. HsdM is the methylation subunit, and includes the binding site for SAM as well as the active site for methylation. HsdR is the restriction subunit and includes sequences essential for endonuclease activity, DNA translocation as well as the active site for ATP hydrolysis. A model of the domain structure of type I restriction enzymes is represented in figure 1.4.

It has been found that the stoichiometry of an active type I restriction enzyme is $R_2M_2S_1$ (Dryden *et al.*, 1997). However, the methyltransferase enzyme lacking endonuclease activity is also present *in vivo*, with a functional stoichiometry of M_2S_1 (Dryden *et al.*, 1993; Suri and Bickle, 1985; Taylor *et al.*, 1992).

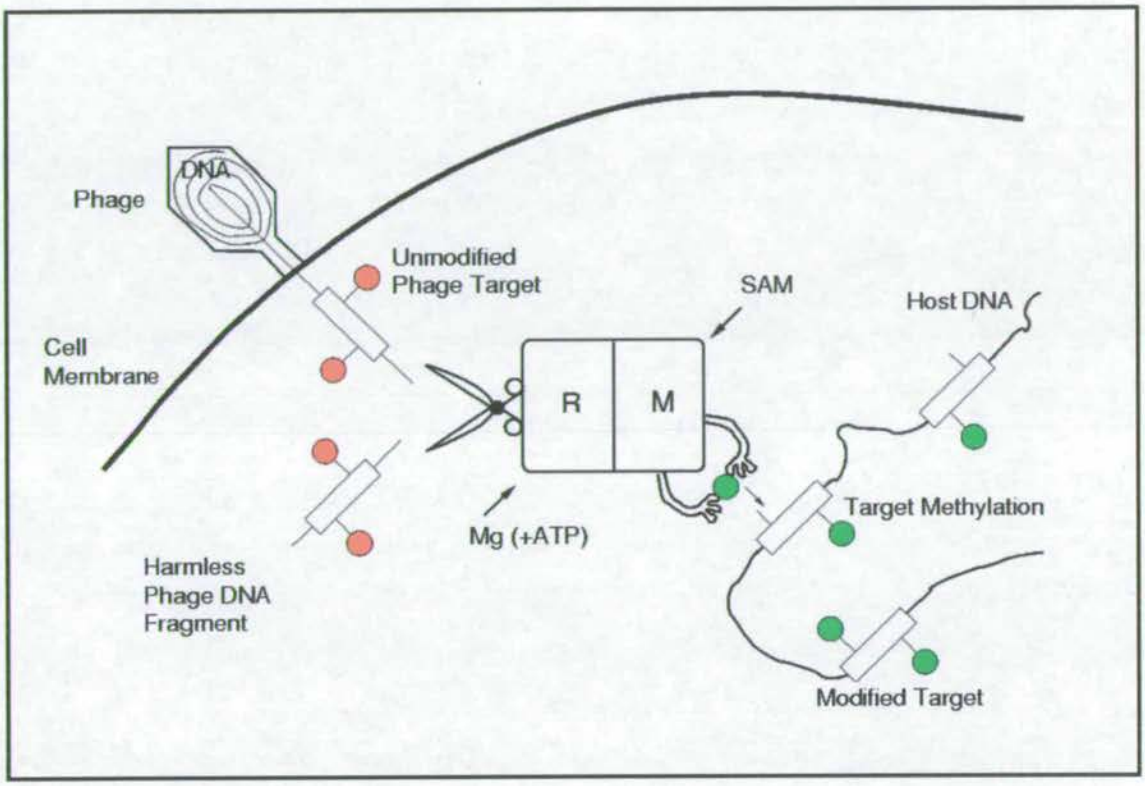

Figure 1.2. Type I restriction/modification systems. The type I restriction enzymes recognise the methylation state of their specific target sequence. When it comes across fully methylated DNA, it recognises this DNA as being part of the host bacterial genome and leaves it alone. If the DNA is hemimethylated, it is recognised as newly replicated bacterial host DNA, and the enzyme uses its methyltransferase activity to methylate the other strand. However, invading bacteriophage DNA lacks this specific methylation and is therefore recognised by the restriction enzyme as foreign. It uses its restriction activity to cut the invading DNA into harmless fragments. Image provided by David Dryden.

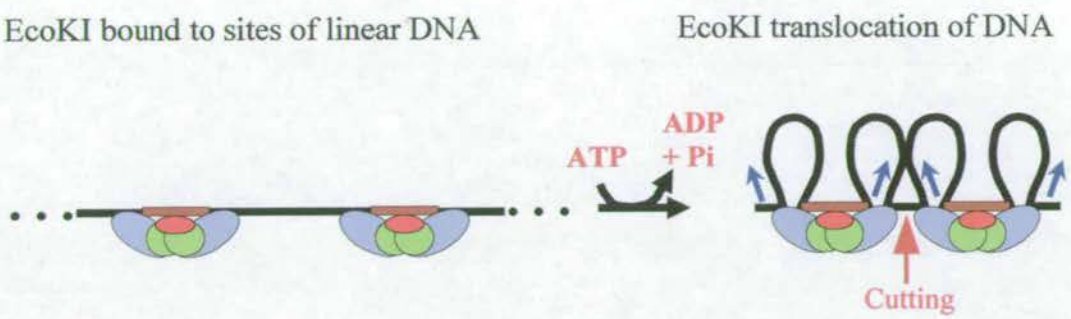

Figure 1.3. Cartoon of EcoKI restriction of DNA. EcoKI (composed of green, red and blue subunits) bind to specific sites on the DNA (red rectangles on black line). DNA is translocated using energy produced by the hydrolysis of ATP, whilst the EcoKI remain bound at the target site. Loops of translocated DNA are therefore formed. Eventually the two translocating EcoKI molecules bump into each other. If both enzymes started translocating at the same time and at a similar speed they should meet roughly half way between their target sites. When the two enzymes meet, this causes translocation to stall, triggering restriction, with each enzyme introducing a single-stranded nick, producing a double-stranded cut in the DNA. After restriction EcoKI remains bound to its target site and continues to hydrolyse ATP. Dimerisation of the two EcoKI molecules can also occur prior to translocation, but has not been shown for clarity.

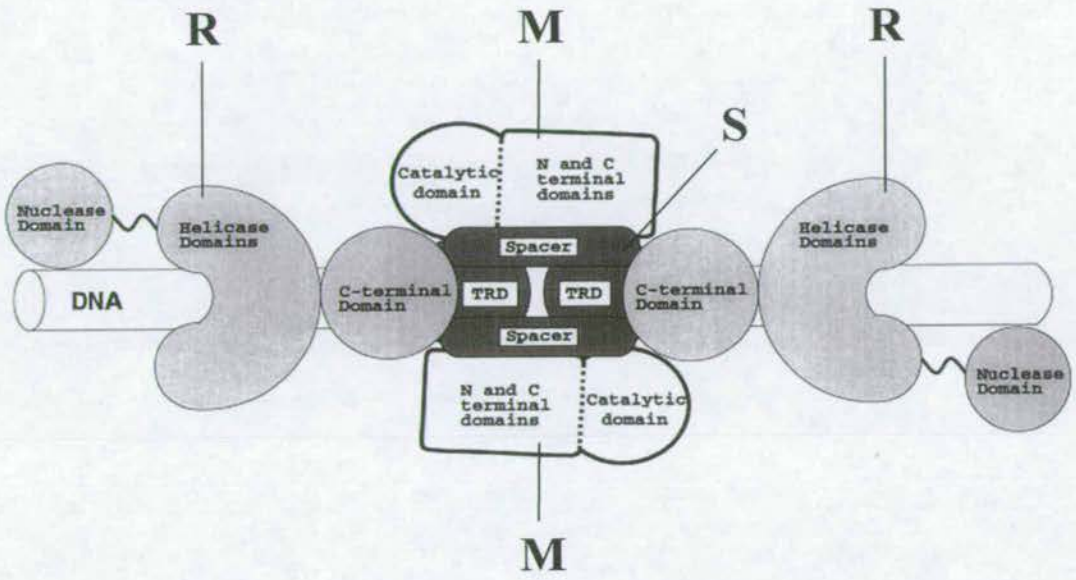

Figure 1.4. Model of the domain structure of a type I restriction enzyme. The S subunits (black) comprise two target recognition domains (TRDs) which recognise and bind to specific target sites on DNA (white cylinder). The TRDs are joined by two spacer regions. The M subunits (bold outline, white) are made up of a catalytic domain and N- and C-terminal domains. The N-terminal domain is involved in recognition and methylation, whereas the C-terminal domain is involved in the assembly of the S subunit. The R subunits (light grey) comprise an endonuclease domain, capable of single-stranded cleavage, domains 1A and 2A of the DNA helicases, and a C-terminal domain which is involved in association with the M and S subunits. Image adapted from Davies *et al.*, 1999.

1.2.2.3 DNA recognition and specificity

The N- and C-terminal TRDs of the HsdS subunit (each of 150-180 amino acids) recognise the 3′ and 5′ sections of the bipartite target sequence respectively (Fuller-Pace *et al.,* 1984; Gann *et al.,* 1987; O'Neill *et al.,* 1998). The amino acid sequences of the TRDs are poorly conserved between systems and do not contain any obvious DNA-binding motifs (Murray, 2000). However, secondary structure predictions have found that a common tertiary structure may be present in TRDs, similar to that found in the solved structure of the TRD of the type II methyltransferase HhaI (Sturrock and Dryden, 1997). This has led to the prediction of a DNA interaction region comprising a loop-β-strand-loop within the TRD that could make specific contacts with bases within the major groove (Chen *et al.,* 1995), and has been supported by random and site-directed mutagenesis experiments (O'Neill *et al.,* 1998).

1.2.2.4. Methylation

Type IA and IC families have a strong preference for methylating only hemimethylated target sites, and cleaving only unmethylated DNA (Dryden *et al.,* 1993; Janscak *et al.,* 1996; Suri and Bickle, 1985). However, it has been shown that EcoAI, a type IB representative, shows little or no preference for modifying hemimethylated DNA over unmethylated DNA (Suri and Bickle, 1985). EcoKI methyltransferase has a much greater binding affinity for its specific target sequence compared to nonspecific DNA. It was also shown that the methylation state of the target sequence had no effect on this binding affinity. This suggests that the preference for methylating hemimethylated over unmethylated DNA is due to recognition of the methylation state after binding has occurred (Kelleher *et al.,* 1991; Powell *et al.,* 1993, 1998a).

HsdM has been found to contain two conserved sequences; motif I and motif IV. Motif I is essential for binding the cofactor SAM, whereas motif IV is characteristic of other methyltransferases and is vital for catalysis. This has been shown by mutations in these motifs abolishing these respective activities (Willcock *et al.,* 1994).

The type I modification enzymes catalyse the transfer of the methyl group from SAM to the N-6 position of specific adenine residues in their respective target sequences. DNaseI and

exonuclease III footprinting experiments have shown that the M_2S_1 complexes of both EcoKI and EcoR124I cover 25-30bp of DNA (Mernagh and Kneale, 1996; Powell, 1993, 1998a). It has also been found that the partially assembled form (M_1S_1) protects the same length of DNA as the active form, indicating that both of the HsdM subunits must be positioned on either side of the HsdS subunit. Evidence that the HsdM subunits enwrap the DNA by a large-scale movement has been found by small angle X-ray scattering of EcoR124I methyltransferase (Taylor *et al.*, 1994). This would allow them to gain access to their methylation sites by the catalytic domain of HsdM moving into the minor groove (Dryden *et al.*, 1995). Methylation is then predicted to occur by a base-flipping mechanism whereby the target base is rotated 180° out of the DNA helix, into the catalytic site of the enzyme (Roberts and Cheng, 1998). In support of this, two sites that are associated with the adenine substrates for methylation have been located, that are hypersensitive to hydroxyl radical cleavage (Mernagh and Kneale, 1996). It is possible that SAM is responsible for determining the methylation state of the target sequence by blocking the positioning of a methylated base within the active site by steric hindrance, after the adenine residues become exposed (Burckhardt *et al.*, 1981; Powell *et al.*, 1995).

Although HsdS contains the determinants of specificity, it has been shown that these subunits are not soluble enough to form a stable complex with DNA in EcoKI or EcoR124I, and an HsdS fusion protein from EcoR124I is unable to bind to its target site efficiently (Powell *et al.*, 1998a and references therein). The type I enzyme HsdM subunits are therefore thought to be essential for DNA sequence recognition and binding even though they lack specificity determinants and can be exchanged between closely related R/M systems. This is supported by the finding that the presence of SAM increases the affinity of the methyltransferase for the specific DNA target site by 4-20 fold but has little affect on its affinity for nonspecific DNA (Powell *et al.*, 1998a).

1.2.2.5. DNA translocation and cleavage

Type I R/M systems cleave DNA at variable positions remote from their target sites (Horiuchi and Zinder, 1972). The cleavage sites are reached by translocating the DNA towards the enzyme simultaneously from both sides of the complex using energy from ATP hydrolysis (Studier and Bandyopadhyay, 1988). This results in the formation of twisted and untwisted loops emanating from the complex, which have been visualized by electron microscopy (Bickle *et al.*, 1987;

Endlich and Linn, 1985; Yuan *et al.*, 1980). Studier and Bandyopadhyay, (1988), have suggested a model for type I enzymes in which cleavage occurs when translocation of DNA from both sides of the enzyme causes two translocating complexes to meet. This model predicts that cleavage would occur roughly half way between adjacent recognition sites. In agreement with this, synchronised restriction reactions produced diffuse bands on gels, indicating the production of relatively discrete DNA fragments (Dryden *et al.*, 1997; Murray *et al.*, 1973; Studier and Bandyopadhyay, 1988). Also, according to this model, the trigger for cleavage is the hindrance of translocation, which agrees with the finding that cleavage occurs when two restriction enzymes from different families collide, and also when the enzyme encounters an unpassable Holliday junction (Janscak *et al.*, 1999). ATP hydrolysis continues after cleavage but the enzyme remains bound to the target site and therefore does not turn over in the restriction reaction (Suri and Bickle, 1985)).

EcoKI has been observed by atomic force microscopy during translocation and cleavage (Ellis *et al.*, 1999). It was seen that on DNA with two target sites, EcoKI dimerised prior to addition of ATP and translocation. This can still be accounted for by the Studier and Bandyopadhyay model, as the loop formed between R/M systems by dimerisation would reduce in size during translocation until it disappeared, at which time cleavage would take place between the two complexes due to translocation hindrance, analogous to a collision. However, as only one site is required for translocation (Garcia and Molineux, 1999; Janscak *et al.*, 2000), and translocation by individual EcoR124I enzymes has been studied by single molecule techniques (Seidel *et al.*, 2004), DNA-dependent dimerisation does not appear to be an absolute requirement for translocation. Dimerisation could enhance restriction by facilitating cooperation between two complexes, allowing the enzymes to remain stationary and translocate DNA only, without having to pull another R/M complex through a crowded solution of macromolecules.

The translocation activity of EcoKI has been studied by measuring the rate at which T7 phage DNA is pulled into an *E.coli* cell. In this study, the T7 phage has a single EcoKI target site at the end of its genome, first to enter its bacterial host, where EcoKI is the only method of translocation (Garcia and Molineux, 1999). It was found that the entire ~39kb genome could be translocated at a rate of 100-200bp/s. This is similar to the *in vitro* results that found the rate to be 200-400bp/s for EcoKI and EcoR124I (Studier and Bandyopadhyay, 1988; Firman and Szczelkun, 2000).

Single molecule imaging using magnetic tweezers has recently been used to study the translocation of the type I restriction enzyme, EcoR124I (Seidal *et al.*, 2004). In EcoR124I, the second R subunit is more weakly bound than the first. This allows the formation of an enzyme with either one or two motor subunits, although both subunits are required for cleavage. It was found that at zero force, EcoR124I with a single R subunit could translocate around 1300bp DNA at about 550bp/s. This is in agreement with the translocation rate measured by Firman and Szczelkun, (2000), of around 400bp/s at 20°C using a triplex displacement assay. When two R subunits were present, EcoR124I translocated over three times more DNA at about twice the translocation rate (Seidal *et al.*, 2004). The results indicate that the two motors work independently and without coordination. Further to this, switches in translocation direction were also seen for the single motor complex. This has been reconciled with the proposal that the R subunit can dissociate and reassociate at either R position, allowing either a continuation of translocation in the same direction, or a switch in direction. EcoR124I with a single R subunit has been also shown to generate positive supercoils ahead of the translocating complex. Furthermore, the fact that around 11bp were translocated per supercoil introduced, suggests that the R subunit follows the DNA helical pitch during translocation.

Work by Bianco (2004, personal communication) has revealed that EcoR124I ATP hydrolysis is dramatically reduced following cleavage of a supercoiled substrate. The cleavage event has also been shown to release the DNA ends. Furthermore, RecBCD was able to displace EcoR124I after restriction, in an active form that was able to cut other DNA molecules. In this way EcoR124I is able to turn over, and catalyze more than one reaction if assisted.

All type I enzyme HsdR subunits contain conserved motifs, characteristic of ATP-binding proteins. This is consistent with the requirement for ATP for restriction. There are also other conserved sequences that share homology with ATP-dependent helicases and putative helicases. These motifs are found in helicase superfamily 2 (SF2), and are referred to as DEAD-box motifs due to their amino acid sequence (Gorbalenya and Koonin, 1991). It was shown by mutagenesis studies that in EcoKI, each of its seven DEAD-box motifs was essential for restriction *in vivo* (Davies *et al.*, 1998). It has also been found that the DEAD-box motifs are organised within domain structures like those deduced for DNA helicases (Davies *et al.*, 1999). It is therefore possible that these conserved motifs are responsible for translocating the DNA by a mechanism

similar to helicases. In accordance with a role in coupling ATP hydrolysis to DNA translocation, amino acid substitutions within the DEAD-box motifs have been found to prevent ATP hydrolysis activity. These substitutions, however, do not affect the conformational changes that confer tight binding to the target sequences (Davies *et al.,* 1998). Although helicases also posses strand separating ability, type I restriction enzymes are thought to translocate double-stranded DNA without separating strands. This is due to the finding that when the DNA strands were cross-linked together at a low level by psoralen, enzyme translocation was not impeded (Reviewed in Singleton and Wigley, 2002).

HsdR also contains another conserved motif which has sequence homology with motifs associated with DNA nicking in both type II restriction enzymes (Pingoud and Jeltsch, 1997) and the RecBC family of nucleases. This sequence is referred to as motif X. Substitutions within this region did not affect either ATP hydrolysis or translocase activities of EcoAI (Janscak *et al.,* 1999) or EcoKI (Davies *et al.,* 1999), suggesting that this motif is in a different domain to that of the DEAD-box motifs. However, these substitutions did block the nicking and cutting activities of the enzymes, consistent with their proposed function in cleavage. This homology with type II enzymes implies that both systems (type I and II) may utilise a common mechanism for the hydrolysis of phosphodiester bonds.

If the enzyme follows the helical path of the DNA during translocation, as occurs with helicases, the three points of contact made by the enzyme (two HsdR and one HsdS) to the DNA would impart topological stress as translocation proceeds. DNA ahead of the translocating complex would become overwound and the DNA behind would become underwound (Davies *et al.,* 1999). As the build up topological stress does not prevent translocation, it was thought that this would need to be relieved by nicking. However, the nicking ability of motif X was shown not to affect translocation *in vivo* and *in vitro* and no other topoisomerase activity has so far been observed (Davies *et al.,* 1999; Janscak *et al.,* 1999).

Footprinting studies have found that the footprint of EcoKI restriction endonuclease, in the presence of SAM, shortens upon the addition of ATP to the same size as the methyltransferase, even though HsdR remains bound to the complex (Powell *et al.,* 1998b). It has been suggested that in the presence of cofactors, the tight binding of the target site is weakened in HsdR, allowing the conformational change required for translocation. The two HsdR subunits, situated

on either side of the methyltransferase would pull the DNA towards the complex from either side, generating DNA translocation in both directions (Powell *et al.*, 1998b).

1.2.2.6. Restriction alleviation

In every cell it is important to be able to distinguish between different DNA molecules, for example between replicated DNA versus non-replicated DNA or host DNA versus foreign DNA. In both of these situations the cell contrives to ensure that the DNA molecules are chemically different. In both eukaryotes and prokaryotes, DNA methylation, where cytosine is modified to C5-methyl-C or N4-methyl-C and adenine is modified to N6-methyl-A, is of particular importance for this chemical distinction. These different chemical modifications allow various enzyme systems to distinguish between the methylation states of the DNA and carry out appropriate reactions. However, there are situations in which chemically identical DNA molecules have to be differentiated by an enzyme. The normally impressive chemical ability of an enzyme to discriminate between different substrates is of no use in this situation, so how is this discrimination achieved?

Such a situation occurs in restriction alleviation (RA) in bacteria, where the DNA restriction/modification (R/M) system of the host bacterium is switched off or reduced in effectiveness for a period of time (Bertani and Weigle, 1953; Makovets *et al.*, 2004). This pause in restriction capability is of importance when a new R/M system is introduced into a naïve host to allow the establishment of modification upon the chromosome (O'Neill *et al.*, 1997). Following the acquisition of genes encoding EcoKI, there is a long lag period before *E.coli C* becomes restriction proficient (Prakash-Cheng and Ryu, 1993). This would allow the host DNA time to become modified by the methyltransferase and acquire protection from the action of the restriction-proficient enzyme. Although *hsdM* and *hsdS* (genes encoding HsdM and HsdS respectively) share the same promoter, and *hsdR* (gene encoding HsdR) has its own promoter, there has been no evidence found for transcriptional regulation of gene expression for type I enzymes (Murray, 2000), thereby implying there is no control over the production of either the methyltranferase or restriction enzyme. RA can also be induced by the loss of the modification function by mutation (Doronina and Murray, 2001; O'Neill *et al.*, 2001) and is of vital importance when cellular DNA is damaged, for example after exposure to UV light of nalidixic

acid. This is due to the fact that the repair machinery can leave the DNA unmethylated and therefore a potential target for restriction (Bertani and Weigle, 1953; Makovets *et al.*, 2004; Doronina and Murray, 2001). R/M systems usually methylate newly replicated, hemimethylated host DNA, which contains the methylated parental strand and the unmethylated daughter strand, and destroys unmethylated foreign DNA. In situations of incomplete modification of the host DNA, R/M systems can be lethal. It is known that type I R/M systems have RA control to prevent such lethality (O'Neill *et al.*, 1997) whilst type II R/M systems function as selfish genetic elements (Kobayashi, 2001) and kill their hosts.

RA raises two important questions about the nature of the DNA in the cell. Firstly, when the chromosomal DNA sequences recognised by the R/M system exist in a partly methylated state during DNA repair or a fully unmethylated state when a new R/M system is acquired by a naïve host, how does the host cell control the potentially lethal activity of the host type I R/M system on its chromosome (Makovets *et al.*, 2004)? Secondly, during RA a reduced level of restriction activity is still present and forms a barrier to phage infection (Bertani and Weigle, 1953) indicating that the unmodified target sequences on the phage DNA can be distinguished from the unmodified target sequences on the host DNA by the resident type I R/M system. How is this accomplished when both DNA molecules are chemically identical (Makovets *et al.*, 2004)?

The RA phenomenon appears to apply only to type I R/M systems that comprise both restriction endonuclease and modification methyltransferase activities within a single multifunctional enzyme complex (reviewed in Bourniquel and Bickle, 2002; Dryden *et al.*, 2002, Murray, 2000, 2002). These systems, despite their complexity, are very widespread in prokaryotes occurring in most sequenced bacteria (Roberts *et al.*, 2003).

There appear to be (at least) two forms of RA. For type IA and IB R/M systems, RA has been linked to a genotypic effect involving the products of the *clpXP* genes (O'Neill *et al.*, 1997; Makovets *et al.*, 1998). This will be referred to as *family-specific RA* that so far is known for only the type IA and IB families. ClpXP is a proteolytic enzyme complex and it has been shown to degrade the restriction subunits of the type I R/M enzyme but only if the R/M enzyme has commenced the complex restriction process (Doronina and Murray, 2001). It has been shown that it is the translocation process during restriction that signals the ClpXP protease to attack the type I R/M enzyme and degrade the restriction subunits. In this manner the potentially lethal

effects of the type I R/M enzyme on the chromosome are prevented at least for the IA and IB families. However, not all type I R/M systems are subject to RA via the clpXP protease but RA is still observed and no specific genotype has so far been associated with this second form of RA (Makovets *et al.*, 2004). This will be referred to as *general RA* and is proposed to apply to all type I R/M systems including those that also have family-specific RA (Keatch *et al.*, 2004, Appendix F). The two forms of RA, general and family-specific are effective in limiting damage to the host chromosome. The physical basis of general RA is unknown but Makovets *et al.*, (2004) suggested that it may be related to the difference between the higher order structure of the chromosomal DNA which is present in the nucleoid and foreign DNA which will adopt less compact conformation as it enters the cytoplasm of the cell. Thus the type I R/M enzyme will see two different DNA structures and it effectively exists in two different 'compartments' in the cell, either associated with the nucleoid where its main function is to maintain methylation or in the cytoplasm where its role is to intercept foreign unmethylated DNA. In relation to this, there is some evidence that the enzyme can associate with the inner membrane when in the cytoplasmic fraction (Doronina and Murray, 2001; Holubova *et al.*, 2004).

In the absence of cell stress, the bacterial nucleoid is always partially coated with a range of nucleoid-associated proteins (Azam and Ishihama, 1999) and their concentration varies depending on growth conditions (Azam *et al.*, 1999). Such an extensive array of non-sequence-specific ligands bound along the DNA is likely to hinder a translocating type I R/M enzyme. Although it has been demonstrated that a single repressor protein bound to DNA does not hinder translocation (Dreier *et al.*, 1996), it is noteworthy that in early experiments the presence of saturating concentrations of intercalating dye molecules did substantially hinder restriction (Burckhardt *et al.*, 1981; Dreier and Bickle, 1996) implying that a barrier of non-specifically bound ligands would be a problem for translocation by type I R/M enzymes. Whilst the nucleoid DNA is typically only partially compacted by bound protein thereby allowing DNA replication to proceed, under conditions of stress which induce RA, it has recently been observed that the nucleoid can slowly convert to a semicrystalline form and undergoes a well known process termed 'condensation' in which the DNA double strands become aligned with each other in compact arrays (Levin-Zaidman *et al.*, 2000; Frenkiel-Krispin *et al.*, 2004). This condensed DNA is not available for replication or transcription as these processes are shut down during conditions of DNA damage to allow time for DNA repair. Hence, it is therefore possible that the condensed nucleoid is generally resistant to restriction. It has been shown that a variety of simple

type II restriction enzymes are inhibited *in vitro* by DNA condensation (Oana *et al.*, 2002; Pingoud *et al.*, 1984; Kuosmanen and Poso, 1985) but for these enzymes there is no indication of any association with the RA phenomenon (Efimova *et al.*, 1988). Condensation is likely to be an even more acute problem for a type I R/M system dependent upon DNA translocation.

1.2.2.7. Bacteriophage Defences

There are many mechanisms by which phages and transmissible plasmids avoid restriction by R/M systems. These include a low frequency of target sequences, unusual modifications to the DNA, and the production of a protein that binds to and inactivates R/M systems (reviewed in Bickle and Kruger, 1993). When the genome of phage T3 or T7 is infecting an *E.coli* cell, the first gene is transcribed before the rest of the DNA has entered the cell. This gene produces a protein, called Ocr (for 'overcome classical restriction'), that protects the rest of the phage DNA from attack by type I enzymes. Ocr acts as a DNA mimic, which binds strongly to EcoKI, rendering it inactive (Walkinshaw *et al.*, 2002). The Ocr protein of T3, but not T7, also degrades SAM, the cofactor for type I restriction and methyl donor for modification (Studier and Movva, 1976; Kruger *et al.*, 1985).

1.2.2.8. Biological Relevance of Type I R/M Systems

Although there is much support for the effect of R/M systems on phages, there is no proof that bacteria maintain these systems to protect themselves against phage attack. It has been shown that bacteria sharing a habitat with phages acquire resistance from attack rapidly. In such a case, a specific R/M system is only likely to provide an advantage to bacteria colonizing a new habitat. This advantage may be sufficient to induce selection (Korona *et al.*, 1993; reviewed in Murray, 2000).

However, why have type I enzymes evolved to be so complicated? Type I restriction enzymes are more 'expensive' for a cell to maintain compared to type II enzymes, and use up a large quantity of ATP. Type II enzymes are also efficient at protecting cells from phage attack. Why, therefore has nature kept type I restriction enzymes?

Type I enzymes carry out both methylation and restriction using the same specificity domain. Therefore, any mutation in this domain that changes sequence specificity will affect specificity for both the methylation and restriction activities. This would not happen in type II systems as separate enzymes carry out these different functions. Therefore it is possible that type I restriction enzymes have evolved to provide the bacterial cell with a kind of adaptive immunity (Bickle and Kruger, 1993).

It has also been suggested that the fragments of DNA produced by restriction, could be used by the bacteria for recombination. A special sequence called χ has been shown to be important in DNA degradation and recombination (Dixon and Kowalczykowski, 1993)). As type I enzymes cut DNA at random positions, there is a greater chance that a fragment will contain χ (Endlich and Linn, 1985). Random fragments of the phage DNA could hereby become inserted into the host's genome, thereby increasing diversity (Milkman *et al.*, 1999). The finding that RecBCD can displace EcoR124I from its target site in an active form has lead to the proposal that these two enzymes could work together, by destroying incoming DNA and producing single-stranded DNA templates for recombination (Bianco, 2004, personal communication).

Type I restriction enzymes also exhibit the peculiar characteristic of continuing to hydrolyse ATP long after they have carried out their restriction reaction (Bourniquel and Bickle, 2002; Dreier and Bickle, 1996; Eskin and Linn, 1972). This has been suggested as a potential method of cell self-destruction, due to a massive ATP consumption. This would remove the infected cell from population, thereby further reducing the chance of phage propagation (Dreier and Bickle, 1996).

1.2.3. Type II Restriction Endonucleases

1.2.3.1. Introduction

Unlike type I enzymes, type II systems comprise two separate enzymes; a restriction endonuclease, which in general requires Mg^{2+}, but not ATP or SAM (although there are exceptions to this), and a monomeric methyltransferase, which only requires SAM as a cofactor.

Both components recognise the same specific DNA sequence, which in most cases, is palindromic and of 4, 6, or 8 consecutive base pairs in length (Gormley *et al.*, 2000). Modification takes place within the recognition sequence, and double-stranded cleavage occurs at a fixed site either within or in the immediate vicinity of the recognition sequence. Some type II enzymes have been found to possess unusual properties and have been classified into subgroups. Type IIe enzymes (such as EcoRII) require two recognition sites for DNA cleavage, where the endonuclease is allosterically activated by binding to the second effector target site. Another subgroup is type IIs (typified by FokI) where the DNA is cleaved at a defined distance outside the non-palindromic recognition sequence by the monomeric endonuclease (reviewed in Pingoud and Jeltsch, 1997).

As both the methyltransferase and endonuclease components of type II enzymes recognise the same target sequence, they are in direct competition with each other. However, to inactivate invading phage DNA, the restriction endonuclease only has to cut at a single site, whereas the methyltransferase has to methylate all sites to fully protect the DNA. The restriction endonuclease therefore binds quickly, and nonspecifically anywhere on the DNA. It then proceeds to scan the DNA for its recognition site by either three-dimensional steps or linear diffusion or a combination of both.

1.2.3.2. Target site location

Translocation through three-dimensional space comprises many dissociation and re-association steps. As the distances between different DNA molecules are much larger than those between different segments of an individual DNA chain, the re-association steps are more likely to occur on the same molecule of DNA (Stanford *et al.*, 2000). If the enzyme dissociates and re-associates before it diffuses a threshold distance away from its original site, it will rebind at or near the initial site in a process termed 'hopping'. However, if the enzyme diffuses beyond the threshold distance from the initial site but still re-associates with the same DNA molecule, the association may be with an uncorrelated site. This process is known as 'jumping'. The efficiency of transfer through three-dimensional space depends upon the straight-line distance between the sites. The mean distance between two sites n base pairs apart in a random coil is $n^{1/2}$ (reviewed in Halford, 2001). Target site location by one-dimensional linear diffusion, on the other hand, is

predicted to take place as a random 'walk', where the enzyme moves along the DNA covering one unit at a time with equal probabilities of forward or reverse motions. Therefore, the mean number of steps required to move from one position to another, n units away, is n^2 (Stanford *et al.*, 2000).

Experimental results by Stanford *et al.*, (2000), using EcoRV showed that the fraction of encounters that resulted in cleavage of two sites, relative to those where the enzyme failed to reach the second site (processivity factor) showed a close correlation to the three-dimensional $n^{1/2}$ dependence, rather than a dependence on n^2. This evidence supports target site location by hopping and jumping steps rather than linear diffusion. However, it was found that these results could be more accurately explained by three-dimension dissociation and re-association events, combined with scanning of the region ~25 base pairs either side of the 'landing site' by linear diffusion and/or hopping. A combination of these processes could therefore be used by the enzymes (Stanford *et al.*, 2000).

1.2.3.3. DNA binding and specificity

Nonspecific binding to DNA has been studied in EcoRV and it has been found that there are no direct contacts between the protein and DNA bases. The DNA and enzyme do not have complementary surfaces, and it was found that a layer of water molecules could separate the complexes. It is thought that the transition to specific binding leads to the highly cooperative restructuring of the protein-DNA interface, accompanied by release of solvent molecules and ions, but retention of some water molecules. This has had support from studies of BamHI and EcoRV where it was demonstrated that tightly bound water molecules had a vital role in recognition and formed hydrogen bonds at the protein-DNA interface that are involved in catalysis (reviewed in Pingoud and Jeltsch, 1997).

Restriction enzymes are highly accurate in recognizing their target sites. Sequences that differ from the specific recognition sequence of the enzyme by only one base pair are cleaved several orders of magnitude more slowly than the correct target site. Any cutting that does occur at methylated or non-target sites, has been shown to occur mainly as single-stranded nicks (Jen-Jacobson *et al.*, 1996) which could be repaired *in vivo* by DNA ligases.

1.2.3.4. Structural properties

There has been no evidence found of any common DNA-binding motifs in any type II enzymes studied so far. The solved co-crystal structures of EcoRI, BamHI, EcoRV and PvuII, have shown that each enzyme uses different structures to bind DNA. Although the catalytic centres of the four enzymes have been found to be similar, EcoRI and BamHI approach the DNA major groove whereas EcoRV and PvuII contact the DNA at the minor groove. This can be related to the position of the scissile phosphodiester bonds cleaved by the enzymes. EcoRI and BamHI create 5' overhangs that are most easily formed from the major groove, whereas the scissile bonds cleaved to form blunt ends by EcoRV and PvuII are more accessible from the minor groove (reviewed in Pingoud and Jeltsch, 1997, 2001).

EcoRV causes a 55° kink in the DNA upon specific binding. Many other type II enzymes cause more subtle distortions of the DNA but all serve to mould the DNA to the enzyme. Most enzymes make contacts with every base in their recognition sequence although there are exceptions, such as EcoRV. EcoRV doesn't contact the central two bases of its recognition sequence even though they are specifically required. It is thought that only these specific bases can conform to the structural alterations induced by the specific binding of EcoRV (reviewed in Halford, 2001).

1.2.3.5. Coupling of specific binding to catalysis

Mg^{2+} or Mn^{2+} ions are vitally required for a successful recognition process that leads to cleavage. As recognition is a cooperative process, metal ion binding may have a role to play in coupling specific binding to catalysis. Intersubunit communication is particularly important in this respect, as double-stranded cleavage of the phage DNA is required for destruction, due to the ability of DNA ligases to seal any single-stranded nicks. Double-stranded cleavage requires that the rate constants for phosphodiester hydrolysis are greater than the rate constant for enzyme dissociation from the DNA, allowing both strands of the DNA to be cut before the enzyme dissociates.

1.2.3.6. Cleavage

One of the few conserved sequences found in restriction enzymes, has been located in the active site of all type II enzymes where the structure has been solved (Pingoud and Jeltsch, 2001). The motif is $PDX_{10-20}(D/E)XK$ (Thielking *et al.*, 1991) where both acidic amino acids have been found to be vital for cleavage. However, this motif is not present in all type II restriction enzymes, and two copies are present in others, where one is not involved in catalysis. The presence of this motif is therefore not sufficient to define an active site.

The general model of phosphodiester bond hydrolysis, as occurs in restriction enzyme cleavage of DNA, requires the presence of three entities (Pingoud and Jeltsch, 1997): a general base that activates the attacking nucleophile, which could be fulfilled by the semi-conserved lysine residue in the active site motif; a Lewis acid that stabilises the negatively-charged transition complex that could be served by the two conserved acidic amino acids acting as ligands for Mg^{2+} that binds the phosphate group to be attacked and; an acid to protonate or stabilise the leaving group, which is thought to be a water molecule from the inner hydration sphere of Mg^{2+} (Pingoud and Jeltsch, 2001).

However, although attempts have been made to produce a general mechanism for all restriction enzymes (Pingoud and Jeltsch, 2001), the actual mechanisms appear to differ between enzymes. This is not completely unexpected, as the active site motif itself is not totally conserved between different enzymes.

1.2.3.7. Star activity

Star activity is the phenomenon of restriction enzymes acting less accurately, and cleaving sites that differ from their cognate site by one base pair. This occurs under certain buffer conditions where the osmotic pressure is increased or Mn^{2+} is used instead of Mg^{2+} or where the pH is alkaline. Under star conditions, the DNA is cleaved even though not all the specific contacts are formed. This implies that lower activation energy is required to trigger the catalytic activity of the enzyme (reviewed in Pingoud and Jeltsch, 1997). Due to the varied range of causes of star activity, it is unlikely that it can be explained by a single mechanism. However, these star

activity-inducing conditions could cause slight conformational changes in the DNA, with this slight deformation allowing the interaction between protein and DNA to be less exact (Pingoud *et al.*, 1984).

1.2.3.8. Methyltransferases

Type II methyltransferases transfer a methyl group from S-adenosyl-L-methionine (SAM) to a base on their specific DNA recognition sites in order to prevent restriction by their cognate restriction enzymes (Cheng and Roberts, 2001). The cytosine 5-methyltransferase HhaI is the most widely studied methyltransferase and serves as a structural paradigm for this group of enzymes (Cheng and Roberts, 2001; Daujotyte *et al.*, 2004; Huang *et al.*, 2003). HhaI methylates the inner cytosine (underlined) in the sequence G<u>C</u>GC, and gains access to this nucleotide as it is rotated out of the DNA helix and into the HhaI catalytic pocket (Klimasauskas *et al.*, 1994). This is commonly referred to as base flipping.

The mechanism of base flipping has been inferred from the various structures obtained with different substrates and cofactors. It is thought that the methyltransferase binds first to the DNA and then to SAM. Following successful methyl transfer, SAM dissociates from the enzyme, followed by methylated DNA (O'Gara *et al.*, 1999). However, it has been found that SAM can bind the methyltransferase in the absence of DNA, although DNA is thought to be required to orientate SAM correctly for methyl transfer (O'Gara *et al.*, 1999). There is also the question of whether base flipping occurs via a passive or active mechanism.

A passive mechanism could be involved due to base-pair breathing, where the bases flip out of the helical structure in the absence of methyltransferase with a reported half-life of 1-100ms (Moe and Russu, 1992). In such a scenario, the methyltransferase would bind its specific target site, and wait for the cytosine base to flip out of the helix unaided. The enzyme would then catch the flipped-out base and carry out the methylation reaction (O'Gara *et al.*, 1998).

Alternatively, an active mechanism could be accomplished if the base is 'pushed' out of the helix, and/or 'pulled' into the active site pocket by the methyltransferase. It has been suggested that Gln237 could dislodge the cytosine from the helix by either 'pushing' it out of the helix

(Daujotyte *et al.*, 2004) or by stacking along side it (Huang *et al.*, 2003). The latter mechanism would facilitate flipping by destabilisation of the helix. In both mechanisms, Gln237 binds and stabilises the resultant unpaired guanine. The finding that removal of the Gln237 side chain produces a stable non-flipped complex supports the involvement of this amino acid (Daujotyte *et al.*, 2004). It has also been found that mismatches at the target base increase the binding of the methyltransferase (Klimsauskas and Roberts, 1995). This can be explained by the fact that less energy is required to flip out mismatched bases, as they are inherently unstable, thereby forming a more stable flipped-out complex. It was also shown that although the methylation reaction is sensitive to the base at the target position, the flipping reaction is not (Klimsauskas and Roberts, 1995 and O'Gara *et al.*, 1998).

Such results have led to the proposal that methyltransferases may have evolved from DNA mismatch binding proteins (Klimsauskas and Roberts, 1995). In this way they may have flipped out mismatched bases, thereby targeting them for removal and subsequent replacement. In accordance with this, base flipping has since been found as a mechanism used by a variety of DNA repair enzymes in base excision and direct reversal repair mechanisms (see references in Cheng and Roberts, 2001).

1.2.4. Type III restriction enzymes

Type III R/M systems are complex proteins that possess both modification and restriction activities. They comprise two polypeptides termed Res (106kDa) and Mod (75kDa). The Mod subunit can act alone to function as a methyltransferase using SAM as a cofactor, but both subunits are required for restriction activity (Bickle and Kruger, 1993; Bourniquel and Bickle, 2002).

Type III systems recognise an asymmetrical recognition sequence, with only one methylation site. A successful restriction reaction requires two unmethylated target sequences in head to head orientation (Meisel *et al.*, 1992). The active endonuclease has been found to have a stoichiometry of Res_2Mod_2 that cleaves the DNA at a fixed position 25-27 base pairs downstream of one of the unmethylated target sites. The target site that is next to the cleavage position appears to be chosen at random. The restriction reaction requires ATP hydrolysis as

well as Mg^{2+} (Meisel *et al.*, 1995) and SAM (Bourniquel and Bickle, 2002). ATP is also used by type III systems for DNA recognition, DNA translocation, and DNA cleavage (Meisel *et al.*, 1995 and reviewed in Dryden *et al.*, 2001).

The methyltransferase only methylates a single DNA strand within the recognition sequence. This produces completely unmodified sequences upon replication and should therefore be a target for restriction. However, the requirement for type III enzymes to have their recognition sequences in head-to-head orientation prevents such restriction. This is due to the fact that replication of such hemimethylated DNA would always produce unmodified sites in head-to-tail orientation, and therefore not form a target for restriction (Bouriquel and Bickle, 2002).

Like type I enzymes, type III R/M systems remain bound to their target site as they translocate DNA past themselves. They have also been found to contain DEAD-box motifs present in helicase enzymes (Gorbalenya and Koonin, 1991), although no other evidence of helicase activity has been found. However, unlike type I R/M systems, type III enzymes dissociate from their recognition site after DNA cleavage, and can therefore turn over (reviewed in Dryden *et al.*, 2001).

1.3. Helicases

DNA helicases are ubiquitous motor proteins that use energy from ATP to translocate themselves along double-stranded DNA, separating it into single strands (Soultanas and Wigley, 2000)). This reaction is essential to many cellular processes involving DNA, including repair, replication and recombination (Soultanas *et al.*, 2000). Helicases contain 'helicase signature motifs' which appear to be vital for DNA translocation activity (Soultanas and Wigley, 2001). The motifs found in helicase superfamilies 1 and 2 are also found in the type I restriction enzymes, inferring that a similar mechanism of translocation may exist for these different types of enzymes (Soultanas and Wigley, 2001; Seidel *et al.*, 2004). However, a global mechanism of translocation has not been found for helicases, as different enzymes function as monomers, dimers, trimers and hexamers (Dillingham *et al.*, 2000).

PcrA is a superfamily 1 (SF1) monomeric helicase involved in DNA repair and rolling circle replication (Soultanas *et al.,* 1999). It has been proposed, based on crystallographic data, that PcrA actively destabilises the DNA duplex in front of the enzyme, which is coupled to translocation along the resultant single-stranded product (Soultanas *et al.,* 2000). This produces a measured translocation speed of around 50bp/s, using 1 ATP per bp (Dillingham *et al.,* 2000). Although this is a seemingly large amount of ATP to use for translocation, it is apparent that helicases are powerful enough to displace streptavidin from the end of biotinylated DNA (Morris and Raney, 1999). Therefore this excessive use of ATP may enable helicases to overcome DNA secondary structure and displace bound proteins (Soultanas and Wigley, 2001).

It has been previously suggested that strand separation by duplex destabilisation in the SF2 HCV helicase may occur via a passive mechanism (Porter *et al.,* 1998). In this model, thermal fraying of the duplex at the DNA-helicase junction produces single-stranded product that is trapped by the helicase. This mechanism would limit the translocation speed of the helicase to the rate of thermal fraying of the DNA duplex (Soultanas and Wigley, 2001).

RecBCD is a complex helicase and nuclease involved in DNA repair and homologous recombination in *E.coli* (Smith, 2001). It can unwind 30000 bp in a single binding event, at a speed of around 1kb/s (Roman *et al.,* 1992). RecB is closely related to PcrA and translocates along DNA in a 3'→5' direction. RecD is also a helicase, but translocates along DNA in a 5'→3' direction (Dillingham *et al.,* 2003; Taylor and Smith, 2003). In this way, RecBCD uses these two complementary helicases to translocate along DNA in the same direction, using their opposing polarities. It has also been found that RecD is a faster helicase than RecB. If RecD translocates faster than RecB, and the two helicases are joined together, this would produce an expanding loop of single-stranded DNA that has not yet been translocated by RecB. It would also form a long and short tail of single-stranded DNA produced by RecD and RecB respectively. This agrees with electron microscopy data that shows just such translocating intermediates (Taylor and Smith, 2003). The individual RecB and RecD helicases possess very low processivity on their own, each only being able to translocate around 50bp in a single binding event (Dillingham *et al.,* 2003). Therefore, although RecB does not appear to contribute to the high rate of unwinding by RecBCD, it increases the processivity, as it is unlikely that both motors will dissociate from the DNA at the same time. Indeed, it has been found that both helicases are required for full enzymatic activity (Taylor and Smith, 2003). This activity

involves recognition of the recombination hotspot χ, in order to stimulate homologous recombination downstream of this site (Stahl *et al.*, 1975). Upon reaching χ, situated on the 3'-terminated strand, it is proposed that the RecC subunit recognises this sequence and the leading RecD helicase stops and waits for the slower RecB to catch up. The RecB helicase continues its translocation past χ and the nuclease activity that was previously used to degrade the 3'-terminated strand is switched to degradation of the 5'-terminated strand. This leaves the strand containing χ free from degradation downstream of this sequence, to allow recombination. RecBCD is then also able to load RecA protein onto the DNA, to permit the next step in homologous recombination to occur. It is thought that the slower translocation by the RecB helicase after χ recognition may be required for proper association of the RecA protein (Spies *et al.*, 2003). This model explains the behaviour of RecBCD observed by Spies *et al.*, (2003) using single molecule imaging.

Further elucidation of the mechanism of RecBCD action has been inferred by the recently determined crystal structure of RecBCD bound to DNA (Singleton *et al.*, 2004). It has been found that RecC forms a 'pin', which splits the strands of the DNA duplex, directing each strand to a helicase subunit. The strands pass along tunnels to the RecB subunit nuclease domain where cutting probably occurs. On its way to the nuclease domain, the 3' strand passes over a region of RecC that has been proposed to recognise the χ sequence.

RecG is a SF2 helicase that separates DNA strands by translocation of double-stranded, rather than single-stranded DNA. Mahdi *et al* (2003), have found RecG to contain a highly conserved helical hairpin motif and associated loop that is involved in translocation. They proposed a mechanism where ATP hydrolysis disrupts the helical hairpin associations, leading to the loop adopting a swinging arm motion that drives translocation. The loop is thought to directly contact the DNA and translocate it via either a mechanical levering action or by a ratcheting mechanism. It has been suggested that this method of double-stranded DNA translocation could also be used by other SF2 helicase-like proteins such as the chromatin remodeling factors and type I restriction enzymes (Mahdi *et al.*, 2003).

It has recently been proposed that SF1 and SF2 enzymes translocate DNA by mechanistically distinct methods (Singleton and Wigley, 2002). This hypothesis uses the available helicase structural data to infer that while SF1 enzymes translocate DNA via contacts with the DNA

bases, SF2 enzymes contact the DNA phosphates for translocation. This has been taken further to predict that SF1 enzymes would translocate along single-stranded DNA whereas SF2 enzymes could translocate along single or double-stranded DNA. This prediction agrees with the experimental evidence (reviewed in Singleton and Wigley, 2002). These different mechanisms of translocation may reflect the enzyme functions: SF1 enzymes involved in DNA repair would be able to recognise base abnormalities or specific sequences; SF2 enzymes involved in replication would not need to read the bases, but should be fast and highly processive. Binding to DNA by phosphates would therefore allow the enzyme to bypass any DNA damage (Singleton and Wigley, 2002).

1.4. Chromatin remodelling enzymes

Each eukaryotic cell has to organise their 2m long genomes into structures 2-10μm in size. This compaction is partly achieved by the binding of histones to condense DNA into chromatin. 146bp of DNA is wrapped around each histone octamer in 1.75 turns to form a nucleosome particle. This binding deforms the DNA causing kinks and unstacking of base pairs. These nucleosomes are associated with a linker histone that can be organised into higher ordered structures, which are not only important in DNA condensation, but are vital in controlling gene expression (Wolffe, 1998). If a nucleosome is situated on a gene, expression of that gene cannot take place without restructuring of the DNA, and it therefore said to be silenced. Therefore, in order to control gene expression, the cell needs to be able to manipulate chromatin structure. One such method of control involves ATP-dependent chromatin-remodelling enzymes (Whitehouse *et al.*, 2003).

Two families of remodelling machines, SWI/SNF and ISWI, induce perturbation of nucleosomal structure and position. These are both ATP-dependent enzymes in the SF2 superfamily of helicase-like proteins. It has been shown that SWI/SNF is involved in restructuring of DNA in the nucleosome by generating superhelical torsion, allowing release of the DNA from the histone octamer (Havas *et al.*, 2000). ISWI, on the other hand, is involved in repositioning of nucleosomes. It has been proposed to function by preferentially binding to nucleosomes, and

translocating DNA over the nucleosomal surface (Whitehouse *et al.*, 2003). This would account for the previously reported ISWI-induced sliding of nucleosome position (Langst *et al.*, 1999).

1.5. Looping

1.5.1. Introduction

Communication between distant sites on DNA is required by many genetic processes such as DNA replication, recombination, repair, transcription as well as numerous restriction systems. A common method to achieve this long-range communication is looping. DNA looping is generated when a protein or complex of proteins bind to two different sites on the same DNA molecule simultaneously. This causes the intervening DNA, which can vary in length from tens to thousands of base pairs, to loop out.

1.5.2. Loop generation and conformation

Restriction enzymes use different approaches to forming loops. Type I and III enzymes generate loops by one-dimensional translocation, driven by the hydrolysis of ATP (Rao *et al.*, 2000). This linear translocation produces loops with very different properties to those produced by interaction in three-dimensional space (Milsom *et al.*, 2001). For example, they increase in size as translocation progresses (Firman and Szczelkun, 2000), and also undergo alterations in their topology in response to the change in twist induced by the translocation (Janscak and Bickle, 2000). Also, EcoKI bound at two sites on a single DNA molecule has been shown, by atomic force microscopy, to dimerise prior to translocation (Ellis *et al.*, 1999). This most probably leads to the formation of a loop through association in three-dimensional space, due to the flexibility of the intervening DNA allowing EcoKI bound to separate sites to come together. This constrained loop formed between the dimerised enzymes would also change conformation upon translocation, as seen by a reduction in size. Also, for type I enzymes, it has been shown that they may introduce positive supercoils if they follow the helical pitch of the DNA (Seidel *et al.*, 2004). This would create a positively supercoiled contracting loop between the enzymes, at the

same time as expanding negatively supercoiled loops of translocated DNA (Halford *et al.*, 2003). In agreement with this, a restriction-deficient EcoAI mutant protein was shown to separate circular DNA into positively and negatively supercoiled regions by translocation (Janscak and Bickle, 2000).

Certain type II enzymes also form loops that can be produced by several different mechanisms (Friedhoff *et al.*, 2001). For example, group IIf contains tetrameric enzymes that possess two DNA binding sites such as SfiI, Cfr10I and NgoMIV. SgrAI, on the other hand, is dimeric, with one enzyme binding to each target site, before dimerisation produces a loop. FokI is also a dimer, but after one enzyme has bound its target site, a second enzyme binds to the first forming a tetrameric complex on one site. This complex then binds the second recognition site to form a loop.

The reaction scheme of either one- or three-dimensional contact between sites for interactions involving SfiI has been resolved using catenanes (linked plasmid rings) with one target site in each plasmid (Adzuma and Mizuuchi, 1989). A one-dimensional tracking process would not enable a single SfiI enzyme to bind sites on both rings. The cleavage rates of this reaction led to the discovery that SfiI must interact with its two sites by DNA looping through three-dimensional space. All other loop-forming type II enzymes, studied using this technique, have also been shown to produce loops via three-dimensional interactions (Embleton *et al.*, 2001). However, these enzymes show a preference for binding two sites in *cis* rather than *trans*. This can be explained by the relative proximity in space of sites located on the same DNA molecule compared to different DNA molecules (Watson *et al.*, 2000).

The loops generated by three-dimensional contacts can also have different configurations. It has been found that SfiI looping produces two distinct species (Watson *et al.*, 2000) with different electrophoretic mobility. Footprinting has shown that both forms are active, with similar local structures close to their natural configurations. This is due to fact that the DNA can take two different paths, with different relative orientations of the two palindromic recognition sites i.e. the DNA can follow a right handed or left-handed curve in three-dimensional space. This produces loops with topology similar to negatively and positively supercoiled DNA respectively (Watson *et al.*, 2000). However, other enzymes require specific topology of their target sequences and therefore this phenomenon does not occur. For example, the type III restriction

enzymes require their recognition sequences to occur in head to head orientation for a successful reaction to take place (Meisel *et al.,* 1992, 1995).

1.5.3. Biological Relevance of Looping

When a protein is bound to one of two target sites, it is held in close proximity to the second site. This is because the furthest apart the protein and second site can be is equal to the length of DNA between the two sites. This positioning of the protein acts to increase the concentration of the protein at the second site and therefore generates cooperativity in the binding to the two sites *i.e.* when one site is bound, the other site also tends to be bound. This process allows the proteins to saturate their binding sites at very low concentrations, well below the dissociation constant of the protein from an individual site. Therefore, although the protein can dissociate from a single site, overall, it remains bound at the two sites involved. Thus, the cooperative binding of looping allows a relatively low concentration of protein to saturate the DNA binding sites, which do not require particularly high affinities for the proteins (Schleif, 1992).

These properties are of use in the cell as there are a very large number of proteins that must be present at the same time within the nucleoid. Therefore, the concentration of any one individual protein will be relatively low. Although this concentration of protein could saturate sites with a very high dissociation constant, it is predicted that such high affinity binding could interfere with other important DNA functions, such as replication. Looping solves this problem by cooperative binding. Thus, looping enables low concentrations of proteins to bind to the DNA not too strongly, and occupy almost all the binding sites simultaneously (Schleif, 1992).

1.5.4. Flexibility

Looping through three-dimensional space is dependent upon DNA flexibility and the distance between the specific sites. The looping behaviour of naked DNA is best modelled as a polymer, where the inherent stiffness is expressed as its persistence length (P). The probability that two sites will interact to form a loop is expressed as the local molar concentration of one site with

respect to the other (J_M). Ringrose *et al.*, (1999), have managed to derive a single equation that determines J_M for all lengths of DNA, based upon a persistence length of 50nm, as previously calculated for naked DNA (Hagerman, 1988). Over an increasing distance between sites, it is shown that looping is difficult over short distances of DNA, due to lateral stiffness. An optimum distance for looping is reached at about 500 base pairs, before looping becomes more difficult again, due to less frequent interactions between sites. DNA supercoiling would affect these predictions by bringing distant sites into close proximity, thereby increasing J_M (Schleif, 1992). However, when compared to *in vivo* results, it was found that inside the cell, DNA could be looped over much shorter distances than were possible *in vitro*. Also, the *in vivo* data would only fit the Ringrose equation when the persistence length was decreased from 50nm to 27nm. This is evidence that chromatin acts to increase DNA flexibility within the cell by approximately two-fold (Ringrose *et al.*, 1999).

As well as lateral stiffness, torsional stiffness effects DNA looping. If two sites are incorrectly orientated around the DNA helix, DNA twisting is required to orientate the sites appropriately for looping. However, if the sites are orientated correctly, torsional stiffness acts to hold the sites in their appropriate positions, increasing the ease of looping. The flexibility of the loop-forming proteins will also have an effect upon the ease of looping. If the proteins are highly flexible, then they could accommodate a variety of DNA conformations to form a loop. However, inflexible proteins would require the DNA to assume the exact configuration for a loop to occur (Schleif, 1992).

1.6. Cyclisation

1.6.1. Introduction

Cyclisation occurs by complementary ('sticky') ends of DNA binding together, with the nicks in the phosphate backbone structure sealed by DNA ligase with hydrolysis of ATP, to a covalently closed structure (Crothers *et al.*, 1992; Shore *et al.*, 1981). The process of cyclisation of linear DNA is closely related to that of looping through three-dimensional space. As with looping,

cyclisation is also affected by lateral and torsional stiffness of the DNA. This is due to the fact that cyclisation requires the DNA to be sufficiently flexible to allow the two ends to meet, and that the DNA ends are correctly orientated for a successful interaction. However, as no proteins are involved in the initial interaction between the two ends in cyclisation, protein flexibility cannot aid the alignment and therefore the orientations have to be precise.

The probability of ring closure (j factor) is closely related to J_M, as used in looping. The j factor is defined as the cyclisation constant divided by the bimolecular equilibrium constant for joining two molecules (Shore *et al.*, 1981). This can be simplified to the effective concentration of one end of the linear molecule in relation to the other end. Cyclisation, like looping, is favoured over interactions between separate molecules due to the close proximity of the ends of the same molecule compared to the relatively large distances between molecules. This can be seen experimentally when low DNA concentrations lead to increased cyclisation reactions, compared to bimolecular and trimolecular associations (Kaiser and Inman, 1965; Jary and Sikorav, 1999).

1.6.2. Effect of condensation on cyclisation

Within the cellular cytoplasm, long DNA molecules are in globular states that are much denser than the random coil state. Physically, DNA condensation can be induced by polyamines that produce net-attractive intramolecular associations between the segments of the molecule (Jary and Sikorav, 1999; Minsky, 2004; Ha and Liu, 2001). The attractive forces produced by such condensing agents also cause multimolecular aggregation of DNA molecules. As condensation refers to the production of a highly dense, DNA-rich state, it applies to both single molecule compaction and multimolecular aggregation (Post and Zimm, 1982).

In previous experiments, it was observed that the cyclisation rate of λ DNA was too slow *in vitro* to account for the speed of the reaction *in vivo* (Wang and Davidson, 1968). This finding can now be explained by the fact that the DNA was in a random coil conformation, not a condensed state as found *in vivo*. In this thesis is will be demonstrated that the conformation of DNA can have a significant effect on reaction rates involving protein-DNA interactions. In a recent study, λ DNA cyclisation has been shown to depend greatly upon its condensation state (Jary and Sikorav, 1999): With increasing concentrations of condensing agent spermidine, the cyclisation

rate of λ DNA varied over six orders of magnitude, with fastest cyclisation occuring in the fully condensed configuration. It was calculated that in this conformation, the j factor is 87000 fold greater, and the cyclisation rate 40000 fold faster, than in the random coil state. The condensed state is also shown to lower the activation energy for the cyclisation reaction. These cyclisation rates are rapid enough to account for the rates seen *in vivo*.

These findings have a direct impact upon looping, and can act as models to aid in the understanding of such processes. DNA conformation must therefore be taken into account to more fully understand biological processes involving intramolecular DNA-DNA interactions.

1.7. Bacteriophage packaging

T4 bacteriophage DNA has a worm like coil volume of $4x10^9nm^3$. However, when packaged into the phage head, the DNA is confined to space with an outer radius of only 50nm and a volume of $5x10^5nm^3$ (Bloomfield, 1996). This corresponds to a reduction in volume of around 8000 times, which is similar to the order of compaction of T7 DNA within the phage head and other bacteriophages (Gosule and Schellman, 1976). Figure 1.5 depicts the large amount of DNA that is condensed into such a small volume in bacteriophage DNA packaging. To obtain a similar order of DNA condensation by force alone would require a pressure of over 100atm (Ha and Liu, 2001).

Several models have been suggested to produce such a degree of compaction and organisation of DNA within the bacteriophage head. These include the concentric shell or toroidal winding model, the spiral fold model, and the liquid crystal model (reviewed in Black, 1989). These models are represented in figure 1.6A.

Experiments looking at encapsidated T7 DNA using cryo-electron microscopy have revealed some striking images of DNA organisation (Cerritelli *et al.*, 1997). These micrographs reveal concentric rings of DNA, separated by around 2.5nm (figure 1.6B). Views from various angles along with computer modelling, can all be accounted for by the concentric shell model. Although none of the other models fit in with the observations of T7 DNA organisation, it is possible that other bacteriophage may use these mechanisms to arrange their DNA.

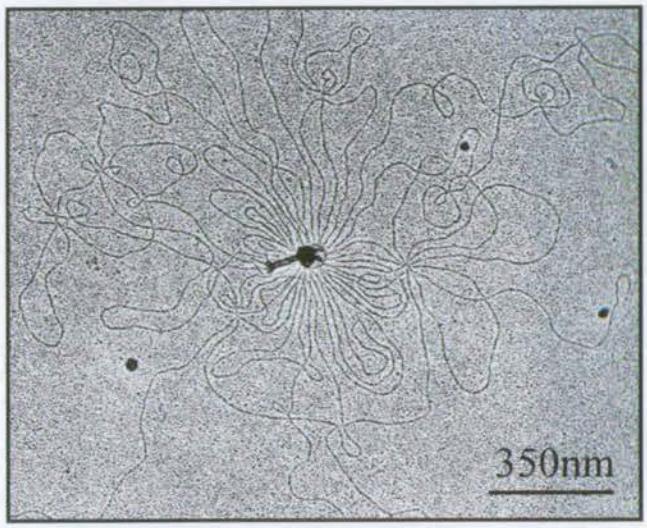

Figure 1.5. Bacteriophage DNA. Electron micrograph of T2 bacteriophage spilling its DNA from its broken capsid. The large amount of DNA that has to be organised within the small volume of the phage capsid is observed. Image from Kleinschmidt *et al.*, 1962.

A

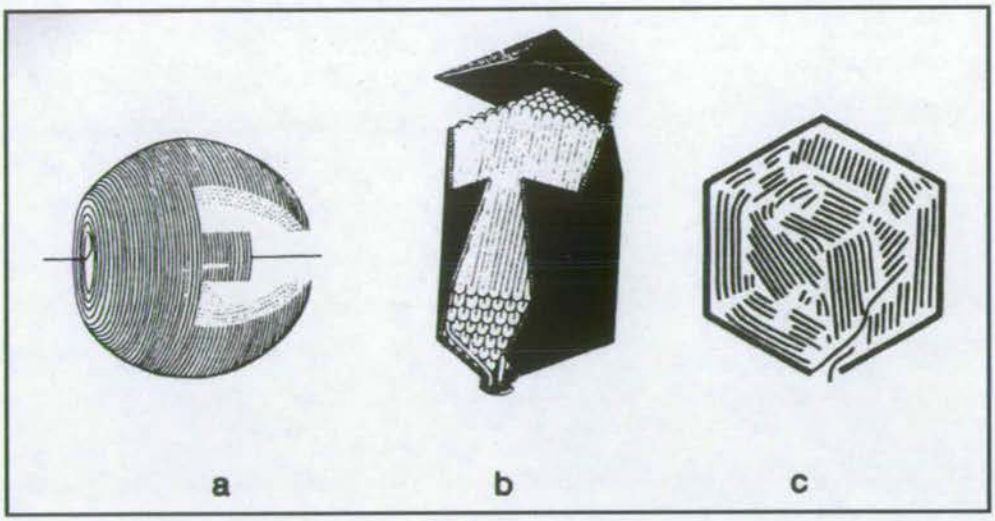

B

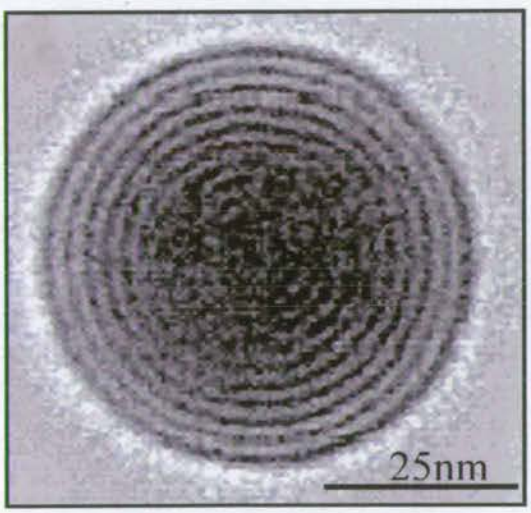

C

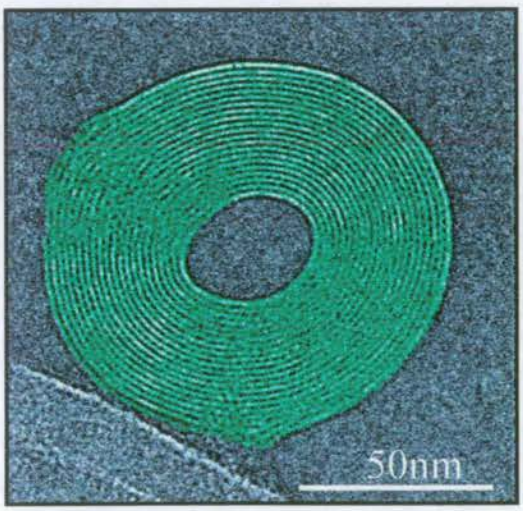

Figure 1.6. Polyamine condensed DNA *in vivo* and *in vitro*. Image A represents possible models of DNA packaging within the bacteriophage head: a) concentric shell or toroidal winding model; b) spiral fold model and; c) liquid crystal model with local parallel packaging. Images from Black, 1989. Electron micrograph B depicts the cross section through a bacteriophage T7 capsid. The image represent the average of 77 individual micrographs. Concentric rings of packaged DNA are clearly visible, revealing that this bacteriophage appears to use the concentric shell or toroidal winding model to package its DNA. Image from Cerritelli *et al.*, 1997. Electron micrograph C depicts bacteriophage λ DNA *in vitro*, condensed by hexammine cobalt (III). Concentric rings of DNA forming this toroid can also be seen. Image from Hud and Downing, 2001. The conformation of DNA formed *in vitro* by the addition of polyamines has striking similarities to the conformation DNA adopts within the head of bacteriophage.

1.8. Polyamine-induced DNA condensation

1.8.1. Physical aspects of condensation

1.8.1.1. Introduction

DNA is highly organised and compacted into the small volumes of cells and viruses. This condensation is achieved by different mechanisms and to different degrees of compaction. Viral genomes are condensed into the confined volume of the capsid by polyamines and internal viral proteins (Ames and Dubin, 1960; Laemmli, 1975) to a concentration of 800-1000mg/ml (Bohrmann *et al.*, 1993). Bacterial DNA is condensed by non-histone proteins, polyamines and crowding effects (Flink and Pettijhon,1975) to a concentration of 80-100mg/ml. Eukaryotic DNA is highly organised and compacted into chromatin by histones and non-histone proteins to a concentration during mitosis of 170-220mg/ml (Bohrmann *et al.*, 1993). However, polyamines are present and highly regulated in eukaryotic cells, and may have an as yet undiscovered role in the organisation of the higher-order structure of chromatin and therefore gene expression (Baeza *et al.*, 1987).

Polyamines are present in millimolar concentrations in bacteria, viruses, and actively proliferating animal cells (Ames and Dubin, 1960; Tabor and Tabor, 1976). Due to their positive charge they bind strongly to negatively charged DNA. When a sufficient polyamine concentration is added to DNA in a random coil conformation in dilute solution, the DNA condenses into toroidal conformations of a similar size and shape to the structures seen in bacteriophage heads *in vivo* (Ha and Liu, 2001). An example of this is shown in figure 1.6C. Other structures such as rods (Golan *et al.*, 1999) and flowers (Fang and Hoh, 1998) can also be formed depending on the preparation conditions.

1.8.1.2. Condensate morphology

Although the sizes of toroids produced by different preparations varies widely (Arscott *et al.*, 1990), the average toroid size is relatively unaffected by the length of DNA used (Bloomfield, 1991). Toroids have been modelled to have a hexagonal packing arrangement with a measured

interhelical separation of around 2.5nm (Schellman and Parthasarathy, 1984). pBR322 was condensed into toroids as well as large cylindrical aggregates by spermidine (Baeza *et al.,* 1987). These toroidal condensates were resistant to digestion to DNaseI, and became thicker and more defined, with a decreased diameter of hole with further increases in spermidine concentration.

Using DNA fragments of 258-4362bp with spermine, toroidal condensates were formed only by fragments of 738bp and larger (Marquet *et al.,* 1987). This can be explained as the calculated circumference of these toroids with a diameter of 70nm was around 680bp. Therefore, a DNA of at least this length would be required to form a nucleus for the growth of a toroid.

Varying morphologies of condensed DNA structures were observed by AFM, using a 6.8kb plasmid and a polylysine-asialoorosomucoid adduct (Golan *et al.,* 1999). These included thick flattened structures as well as rods and toroids. The volume of each condensate indicated that the majority were formed by the collapse of a single DNA molecule. However, a few condensates of each example appeared to be formed by the collapse of two or three plasmids combined. The similar volumes obtained for rods and toroids also indicates a similar degree of condensation of the structures, despite the differing morpholgies.

DNA that was condensed with spermidine and visualised by AFM (Lin *et al.,* 1998) produced mainly toroidal condensates, and some rod or U-shaped conformations. When the DNA concentration was increased, much larger toroidal and elliptical aggregates were seen. These structures appeared to be formed by the aggregation of individual toroidal condensates in a spiral arrangement.

1.8.1.3. Toroid Formation

DNA is condensed when 89-90% of its charge is neutralised (Wilson and Bloomfield, 1979). Experimentally, this requires polyvalent cations with a valency of three or greater. This was predicted by the widely accepted counterion condensation theory produced by Manning, (1978). It is thought that the simple reduction of repulsive forces between DNA phosphates is not sufficient to induce condensation, and that counterions therefore can also produce attractive forces between DNA segments (Marquet, 1991).

In an attempt to determine the mechanism of condensation by spermine, Porschke, (1984), found two separate processes. Firstly, an induction period was observed, followed by a fast reaction with a millisecond time range, which was assigned to single DNA molecules collapsing into a condensed state. Then a slower reaction on the 100s time scale occurred which was thought to represent the intermolecular association of condensed molecules. In order to account for the time scales observed, Monte Carlo simulations using a model of excluded site binding was used. This took into account that spermine molecules will bind at random to the DNA, and as they each cover four bases, they will leave smaller gaps that spermine cannot fit into. The rapid intramolecular condensation observed could be accounted for only if the spermine molecules were mobile along the DNA double helix with a rate constant of around $200s^{-1}$ for movement of spermine by one nucleotide. It is proposed that after initial random binding, the spermine molecules have to redistribute themselves by dissociation/reassociation steps and/or sliding, in order to pack along the DNA more efficiently. This allows the critical charge neutralisation threshold for condensation to be reached within the millisecond time scale seen. This fast mobility of spermine along the DNA was also seen by Marquet *et al.*, (1987). A two-step condensation process, in agreement with this, was also observed by Matulis *et al.*, (2000). They formed a similar model of polyamine binding and redistribution along the DNA to produce interstrand binding and condensation using spermidine and hexammine cobalt (III).

Spermidine is a trivalent polyamine essential to many if not all prokaryotes (Pingoud, 1985). The spermidine molecule is around 1.1-1.3nm long with the three basic groups orienting well with three adjacent phosphate groups of DNA when aligned (Liquori *et al.*, 1967). A representation of spermidine structure can be seen in figure 1.7A. Na^{+} and Mg^{2+} ions bind to the phosphate groups on DNA and can effectively compete with spermidine for DNA binding (Rubin, 1977). This implies that spermidine binds to DNA through association with the negative phosphate moeities.

A

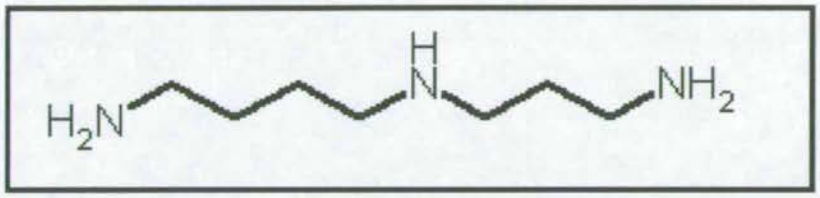

B

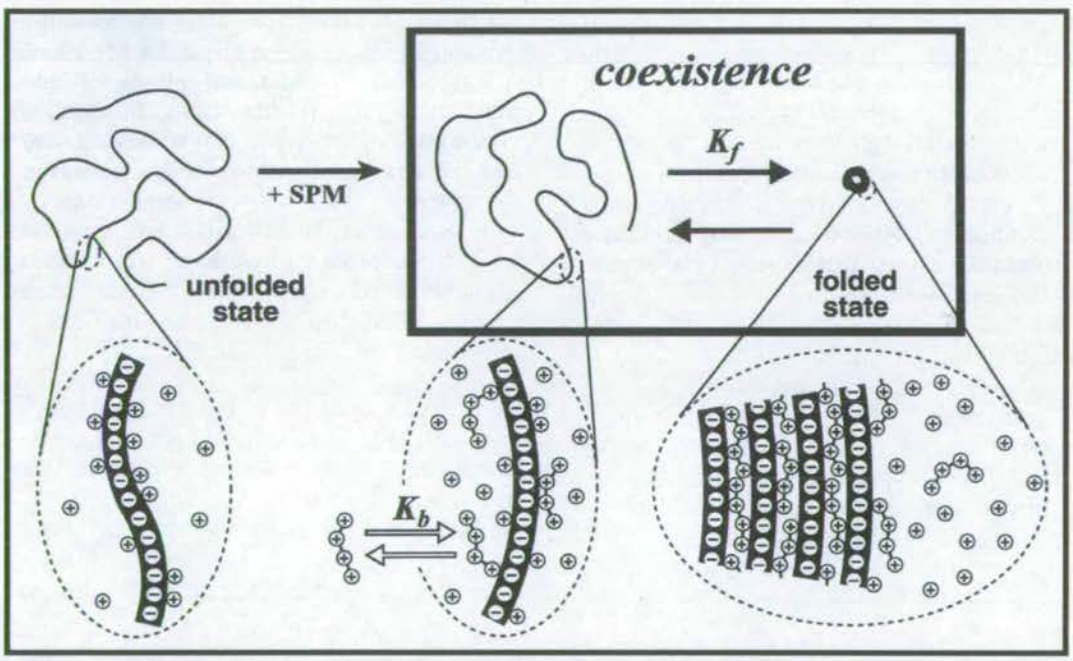

Figure 1.7. Polyamine structure and function. Image A shows the structure of the trivalent polyamine spermidine, with the three amine groups producing the positive charges required for DNA phosphate binding under appropriate buffer conditions. Image B is a schematic representation of the folding transition of DNA molecules with the addition of the tetravalent polyamine spermine. K_b is the binding constant of spermine to phosphate groups in an elongated DNA chain. K_f is the equilibrium constant between the elongated and compacted states of DNA, where the manner of binding of spermine changes dramatically. During condensation, spermine binding changes from a loose association with DNA to a tight binding situation also forming interstrand links. Image from Makita and Yoshikawa, 2002.

This suggestion is backed up by the findings by Srivenugopal *et al.*, (1987), and Schellman and Parthasarathy, (1984), that increasing the length of the methylene chain of spermidine, and thereby decreasing the alignment between the spermidine basic groups and DNA phosphate groups, decreased condensation. It was found that a higher concentration of spermidine analogue was required to condense DNA as the length of methylene bridge was increased. Moreover, the condensates produced were less tightly compacted than those condensed with spermidine. A representation of the different binding modes adopted by spermine to induce toroidal condensation in buffer containing monovalent cations is shown in figure 1.7B.

1.8.1.4. Charge correlation

Single molecule imaging of DNA extended by buffer flow was observed to be condensed from the free end of the DNA molecule after addition of protamine (Brewer *et al.*, 1999). Although this and theoretical predictions (Ostrovsky and Bar-Yarn, 1995) propose that nucleation of condensation occurs from one end of a DNA molecule, this cannot be a requisite for condensation as supercoiled DNA also forms toroids (for example, Baeza *et al.*, 1987). It has been predicted that a DNA molecule spontaneously forms a loop that is stabilised by the binding of molecules of condensing agent to the point of contact (Bloomfield, 1996). Further condensing agent binding to both looped and unlooped DNA continues toroid formation (Hud *et al.*, 1995). This model predicts formation of toroid sizes in good agreement with those observed experimentally.

It is thought that if two like-charged rods are parallel to each other, at close distances, their charges correlate and become attractive. Counterions bind inhomogeneously to the charged rod, producing positively charged and negatively charged regions. This can form electrostatic attractions if the charge patterns of two charged rods become complementarily adjusted to each other. Overlap of layers of counterions bound to the rods is also predicted to produce attractions between like-charge rods, due to the resultant increase in entropy (reviewed in Minsky, 2004). This counterion-induced attraction forms the basis of the charge correlation model of polyvalent-counterion-mediated condensation suggested by Ha and Liu, (2001). The like charges of two rods are repulsive at long distances, irrespective of the angle between them. This is because electrostatic repulsion is a long-range parameter. This repulsion also occurs at closer ranges if

the two rods are perpendicular or otherwise misaligned. However, if the two rods approach each other in a parallel or close to parallel orientation, the like charges will form attractions through charge correlation. In this way polyamines could reduce the repulsive charges between two DNA double helices enough to allow them to approach each other to a distance that would enable attraction to occur if the helices are orientated correctly.

This model also predicts a limit on the size of the condensate produced. This is due to the idea that as an individual charged rod approaches a bundle of already condensed rods, the rods in the facing bundle surface will repel it. The approaching rod has to be at an angle very close zero with respect to the bundle in order for the correlation to overcome the repulsion. As the bundle size increases so does the repulsion, and therefore an approaching rod is less likely to be able to join the bundle at a small enough angle for correlation attraction to overcome the general repulsion. This argument can be extended to the association of two bundles, and therefore limits on aggregate size are also predicted.

Studies using bacteriophage T5 have produced exceptionally large toroidal bundles of condensed DNA (Lambert *et al.*, 2000). However, in these experiments T5 DNA was injected from phage directly into liposomes in solution with polyvalent counterions. In this situation the DNA is inserted into the liposome base pair by base pair so that the orientation of the chain is already aligned with those already present in the growing bundle. This can explain the unusually large toroids produced, as the kinetic mechanism of bundle growth is very different from the usual *in vitro* toroid formation.

Although condensation of phage lambda DNA (48.5kb) forms single toroids, condensation of concatemers of 2-4 molecules forms multiple toroids (Brewer *et al.*, 1999). This implies that there may be a maximal length of DNA that can be condensed into a toroidal conformation, which would agree with the charge correlation model. As toroids of sperm DNA condensed by protamine have been shown to contain up to 60kb DNA (Hud *et al.*, 1993) it is clear that the maximal length of DNA that can condense into a single toroid is above this value.

Evidence against electrostatic attraction forces has been presented which showed interstrand spacing of hexagonally packed helices was independent of counterion valence, structure or concentration. Instead, it was proposed that hydration forces were the driving force of

condensation, where polyvalent ligands reconfigured the water molecules between DNA segments to create long-range attractions (Rau and Parsegian, 1992). This model has been interpreted to predict an orderly condensation process similar to a nucleation and growth process, enabling toroidal formation followed by aggregation (Lin *et al.,* 1998).

Both models agree that condensation is driven by attractive lateral interactions between adjacent helices, due to binding of a critical amount of multivalent cations.

1.8.1.5. Force considerations

Baumann *et al.,* (2000), have found that their results with DNA condensed with spermidine and hexammine cobalt (III) fit well to a model where the DNA persistence length decreases due to increased bending flexibility. As the DNA phosphate charges were neutralised, the DNA persistence length decreased. Under conditions of high concentrations of NaCl, DNA has a persistence length of around 50nm. However, with addition of hexammine cobalt (III) and spermidine the apparent persistence length decreased to 12-26nm and 25-38nm respectively.

A decreasing persistence length with increasing charge neutralisation was also seen by Marquet *et al.,* (1987). However, their electric dichroism experiments found that addition of spermine increased the stiffness of DNA, and introduced bending. They suggested that this induced bending was the cause of the decreased persistence length.

It has been found possible to decondense DNA mechanically by a force of less than 5pN (Baumann *et al.,* 2000). This value is less than the calculated stalling force of RNA polymerase (Yin *et al.,* 1995)). Seidel *et al.,* (2004), also found that type I restriction enzyme EcoR124I could still translocate when a force of 5pN was applied. Therefore it may be possible for such enzymes to generate enough mechanical force to unpackage such condensed DNA *in vivo*. However, the decondensation force is measured by pulling one end of condensed DNA, which would probably decondense via an unzipping mechanism. It may require more force to decondense DNA if this process occurs from the middle of the condensate, rather than from one end.

1.8.1.6. Valence

Makita and Yoshikawa, (2002), have found that the concentration of polyamines required to induce a condensed DNA conformation is reduced with increasing polyamine valency. Although it has been predicted that a valency of three is required for a counterion to induce DNA condensation, it has been found that Mn^{2+} can condense supercoiled, but not linear plasmid DNA, forming toroidal conformations (Ma and Bloomfield, 1994). Supercoiling and Mn^{2+} effects may combine to enhance lateral associations between DNA segments, and stabilise any helix distortions (Bloomfield, 1996). $MgCl_2$ and NaCl do not reverse the effect of Mn^{2+} and it is therefore thought that Mn^{2+}-induced condensation is not primarily dependent upon electrostatic interactions. It has been suggested that macromolecular crowding could affect condensation conditions to such an extent that DNA could be condensed *in vivo* by putrescine or Mg^{2+} (Murphy and Zimmerman, 1995).

1.8.1.7. DNA sequence and secondary structure

Specific DNA sequences are able to alter DNA secondary structure and therefore affect condensation. Long tracts of $(dC\text{-}dG)_n$ are converted into Z form by hexammine cobalt when inserted into pUC18 plasmids (Ma *et al.*, 1995). These insertions have been found to enhance condensation. Spermidine and spermine have also been shown to convert $(dA\text{-}dC)_n\text{-}(dG\text{-}dT)_n$ tracts into Z form when inserted into plasmids, at condensation-inducing concentrations (Thomas and Thomas, 1994). Long runs of adenines, which produce bent DNA, have been used to form unusually small toroids (Reich *et al.*, 1992).

1.8.1.8. Liquid crystal

DNA shorter than the length required to form one circle of a toroid is not capable of forming toroidal condensates (Bloomfield, 1991). However, at very high concentrations (around 200mg/ml) short mononucleosomal DNA can form a liquid crystalline arrangement (Rill, 1986). This liquid crystalline phase of short DNA has also been seen at low DNA concentrations in the

presence of spermidine (Sikorav *et al.*, 1994). This occurrence has been explained by the attractive forces present between parallel rods (Bloomfield, 1996). X-ray scattering has found that liquid crystalline domains are present in bacteria with high copy number plasmids (Reich *et al.*, 1994). This ordering may therefore be required for efficient packaging of high copy number plasmids *in vivo* (Bloomfield, 1996).

1.8.1.9. Conditions affecting condensation

At higher pHs, a greater proportion of spermine will be present in its trivalent form compared to a lower pH. Therefore polyamines, such as spermine, are more effective condensing agents at low pHs. Changes of intracellular pH *in vivo* could be used to control DNA conformation by the effects upon polyamine binding and DNA charge neutralisation. Such an increase in pH has been observed in *Physarum* during mitosis. Effects of pH within the physiological range on chromatin aggregation and stability have also led to suggestions that increasing pH could decondense chromatin and allow DNA synthesis to occur (Makita and Yoshikawa, 2002 and references therein).

An increase in temperature was seen to decondense spermidine-compacted DNA (Murayama and Yoshikawa, 1999). This temperature dependence was also observed by Matulis *et al.*, (2000), for hexammine cobalt (III) condensation of plasmid DNA. They also reported a strong dependence of spermidine- and hexammine cobalt (III)-induced condensation on ionic strength. As the ionic strength was increased by increasing the NaCl concentration, higher concentrations of polyamines were required to condense the DNA. This condensation dependence on ionic strength was also seen by Raspaud and de la Cruz, (1998), who found that the length of the DNA also affected its ability to condense and decondense. They observed that longer DNA molecules condensed at lower polyamine concentrations, and decondensed at higher polyamine concentrations than shorter DNA substrates.

The ionic strength dependence was predicted by Manning, (1978), and can be explained by direct competition for DNA binding between monovalent and divalent salt with the polyvalent condensing agents. These low valency salts will therefore inhibit the condensing agent from being able to neutralise the 89-90% of negative charge on the DNA required for collapse. In

order to reach this critical point, the polyvalent cation must bind to the DNA phosphate groups with all of its basic groups. Condensing agents will need to be present in higher concentration to out compete mono and divalent salt for phosphate binding to enable neutralisation of sufficient negative phosphate charge (Yoshikawa, 2001).

E.coli cells have been found to contain around 4.7μmoles/g wet weight cells spermidine (Tabor and Tabor, 1976). Using the estimated wet weight of a single bacterial cell as $9.5x10^{-13}$g (Moat and Foster, 1995) with a bacterial cell volume of 0.196μm^3 (Paul and Clark, 1996), this gives an overall spermidine concentration of around 23mM. Another estimate of spermidine concentration was measured as around 6.3mM (Tabor *et al.,* 1973) although the media the cells are grown on can affect these levels. Spermidine has been reported to be present in the cell with 90% bound to RNA, 5% bound to DNA and only 0.8% bound to membrane lipids (Ruiz-Herrera *et al.,* 1995). However, accurate measurement of cellular distribution is difficult, as spermidine will redistribute itself after cellular disruption and become associated with those species that bind it most strongly (Tabor and Tabor, 1976). It has been suggested that spermidine may actually be relatively free in the *E.coli* cell (Rubin, 1977). This can be explained if the ionic strength effects of monovalent and divalent ions are considered, as these would compete with spermidine for DNA binding. Concentrations of monovalent and divalent ions in non-metabolising *E.coli* have been estimated as around 0.24M and 0.043M respectively (Damadian, 1971), with total cation activity estimated as being between 0.17M and 0.24M in sodium ion equivalents (Kao-Huang *et al.*, 1977). The potassium ion and glutamate ion concentrations have also been measured by NMR, increasing from 0.23 molal to 0.93 molal potassium ions, and from 0.03 molal to 0.26 molal glutamate ions with increasing osmotic pressure (Richey *et al.*, 1987). As the association of polyamines to DNA is dependent on the monovalant and divalent ion concentrations, the condensed conformation of DNA produced by high concentrations of polyamines may not be maintained at this high ionic strength. DNA condensation by polyamines *in vitro* is an attractive model for DNA compaction in living cells, but is an oversimplification of the *in vivo* situation due to the high ionic strength found within this environment. However, the presence of DNA binding proteins, the compartmentalisation of polyamines as well as macromolecular crowding could all effect DNA condensation *in vivo* (Srivenugopal *et al.*, 1987).

1.8.2. Effect of condensation on enzyme activity

1.8.2.1. Introduction

The different DNA conformations produced by polyamine binding would be expected to affect enzyme-DNA interactions. It can be imagined that condensation could block access of enzymes to the DNA within the highly compact structure, and therefore be inhibitory to reactions. However, condensation would also bring sites that could otherwise be separated by several thousand base pairs into close proximity, thereby promoting reactions with enzymes that require simultaneous binding to these distant sites. The high concentration of DNA produced by condensation may produce a reduced search space for proteins to locate their binding sites more effectively. Also, the charge neutralisation effects of polyamines on DNA, or a possible polyamine-induced alteration of DNA secondary structure, could also affect the binding of proteins to their DNA binding sites. In fact, the effect of polyamines and DNA condensation appears to have multiple effects on enzyme activity.

1.8.2.2. Effect of polyamines on restriction enzymes

Although low concentrations of spermidine and spermine have been shown to increase restriction activity of EcoRI (Pingoud *et al.*, 1984), it has been shown that high concentrations of these polyamines inhibited the restriction activity of BamHI, EcoRI, HindIII, HpaI and PstI (Kuosmanen and Poso, 1985). ApaI restriction activity is also inhibited by high concentrations of spermine as found by Oana *et al.* (2002). In this study, a control was carried out using an 88bp oligomer, which was readily restricted by ApaI at high concentrations of spermine. As this 88-mer is too short to be condensed, this shows that it is the effect of spermine on the DNA structure that affects ApaI activity and not a direct effect of spermine on the enzyme. This also shows that ApaI can still bind its target site successfully in the presence of a high degree of bound spermine.

Polyamines can also increase the accuracy of restriction enzymes. At low concentrations of spermidine, which have been shown to enhance type II restriction enzyme activity, the non-specific 'star' activities of BamHI, BsuRI, EcoRI, EcoRV, HindIII, PstI and SalI were all

inhibited. This occurred regardless of the method used to induce star activity (*i.e.* high enzyme concentration, high pH, low ionic strength, organic solvents and Mn^{2+} ions) (Pingoud, 1985). It has been suggested that the spermidine may bind to and stabilise the DNA structure, which is optimal for accurate, efficient cleavage. It is therefore possible that the increased cutting at degenerate sites observed *in vitro*, is due to the lack of certain components present *in vivo*, which increase the accuracy of restriction (Pingoud, 1985).

1.8.2.3. Other effects of polyamines

It has been found that spermidine is of vital importance for certain cellular and bacteriophage functions. For example, bacterial cells are unable to grow without the presence of polyamines. Phage lambda are unable to grow on *E.coli* hosts lacking spermidine, which is also required for integration of lambda DNA *in vitro*, with spermidine also being required for packaging of lambda DNA into phage heads (reviewed in Tabor and Tabor, 1976; Pingoud, 1984). Polyamines have also been reported to speed up replication, transcription, and translation (Pingoud, 1984 and references therein), as well as stimulating the activity of DNA gyrase, and polymerase (Kuosmanen and Poso, 1985 and references therein).

1.8.2.4. Gene therapy

In gene therapy, an exogenous gene is transferred into cells where it can express its encoded protein. Such expression should compensate for the lack of naturally occurring protein in the cells (Mannisto *et al.*, 2002). Therefore, any disease caused by a genetic defect that produces insufficient or improper protein is a possible target for such an approach. Although this is relatively straightforward in theory, the practicalities of gene delivery have been more problematic. The majority of studies have used viruses as vectors to deliver the gene of choice to the target cells. However, although efficient at transferring foreign DNA into cells, viruses cause problems of immunogenicity, possible random genetic integration and difficulties of large-scale production (Mannisto *et al.*, 2002). In order to bypass these issues, non-viral gene delivery systems are receiving greater attention. These systems show significantly lower toxicity than viral vectors, although suffer from poor efficiency (Blagbrough *et al.*, 2003). Non-viral gene

delivery systems have been developed using polyamines and lipopolyamines, which condense the DNA by binding through their positive charges. These complexes are thought to bind to peptidoglycans on the cell surface and subsequently enter the cell by endocytosis (Blagbrough *et al.*, 2003). It has been proposed that the columnar hexagonal packing of DNA within polyamine-induced condensates can facilitate transport of DNA within cells (Liu *et al.*, 2001). However, nuclear localization is still inefficient in non-viral delivery systems (Blagbrough *et al.*, 2002). Polyamines and their derivatives therefore hold great potential in the development of gene therapy techniques and much research is being carried out to overcome the remaining barriers to produce optimal gene expression.

1.9. Protection of the bacterial genome *in vivo*

The genome of a bacterial cell suffers several thousand DNA lesions in every generation (Roca and Cox, 1997). These lesions can be single-stranded or double-stranded in nature, and therefore require different repair mechanisms. The cell can repair damage to only a single strand of DNA by either recognition of the damage by enzymes, or by the second, undamaged strand acting as a template for repair. However, repair of a double-stranded lesion is a more complicated process, as there is no undamaged template available at the repair site. Repair therefore requires the RecA-mediated repair pathway to use a different DNA molecule to obtain this information via homologous recombination (reviewed in Minsky, 2003).

This repair pathway has to overcome two major problems: 1) the location of the small target site by the repair machinery within the high concentration of non-target, but competitive DNA and; 2) the fact that the two ends of the damaged DNA that need to be joined and repaired may have diffused a great distance apart (Minsky, 2003).

It has been reported that upon exposure to treatments that induce double-stranded DNA breaks (UV-irradiation and nalidixic acid), the diffuse morphology of the *E.coli* genome is rearranged into a highly compacted and ordered conformation (Levin-Zaidman *et al.*, 2000). It appears that these stressed bacteria reorganise their nucleoid so that it occupies less than a fifth of the cytoplasmic volume, with DNA helices arranged in parallel orientation. Figure 1.8 shows this

organised structure of an *E.coli* nucleoid upon exposure to nalidixic acid. It was also shown that almost all the RecA molecules were sequestered to this region and that this morphology was lost after the removal of the DNA-damaging conditions. In this respect, it is interesting to note that the DNA-condensing polyamines spermine and spermidine have been found to induce the expression of *recA* in *E.coli* (Oh and Kim, 1999). A similar response to stress was seen by *Bacillus subtilis*, where DNA reconfiguration also occurred with co-localization of the repair machinery (Smith *et al.*, 2002).

It was therefore proposed that this condensation of bacterial DNA in response to DNA-damaging conditions would allow optimal DNA repair. It would allow the repair machinery to locate the double-stranded break rapidly due to the confinement of DNA, producing a smaller sampling volume. It would also potentially restrict the diffusion of the broken free ends of DNA, thereby effectively holding them together ready for repair (Minsky, 2003).

However, these DNA-damaging environments are often accompanied by nutrient depletion. DNA repair by homologous recombination is ATP dependent, and would be impaired under such conditions. Also, bacteria in stationary phase usually only contain one copy of their genome, thereby preventing repair by homologous recombination. This raises the question of how bacteria can protect and repair their genome without the use of ATP or a second DNA template (Frenkiel-Krispin *et al.*, 2001 and references therein)?

When *E.coli* cells are stressed by starvation, the nucleoid is seen to reorganise itself into toroidal condensates and forms co-crystals with the starvation-induced DNA-binding protein Dps (DNA-binding protein from starved cells) (Frenkiel-Krispin, 2004). The formation of the toroidal condensates is initiated at multiple sites within the nucleoid. It was proposed that these toroids acted as nucleation sites for the formation of the co-crystalline conformations. DNA condensation in these starved cells has been shown to be dependent upon the ionic conditions of the cell. It has also been found that starvation induced by a lack of phosphate increases the degradation of threonine and arginine to spermidine (Gerard *et al.*, 1999), which accelerates DNA collapse in starved cells in the absence of the nucleoid-associated protein Dps (Frenkiel-Krispin, 2004).

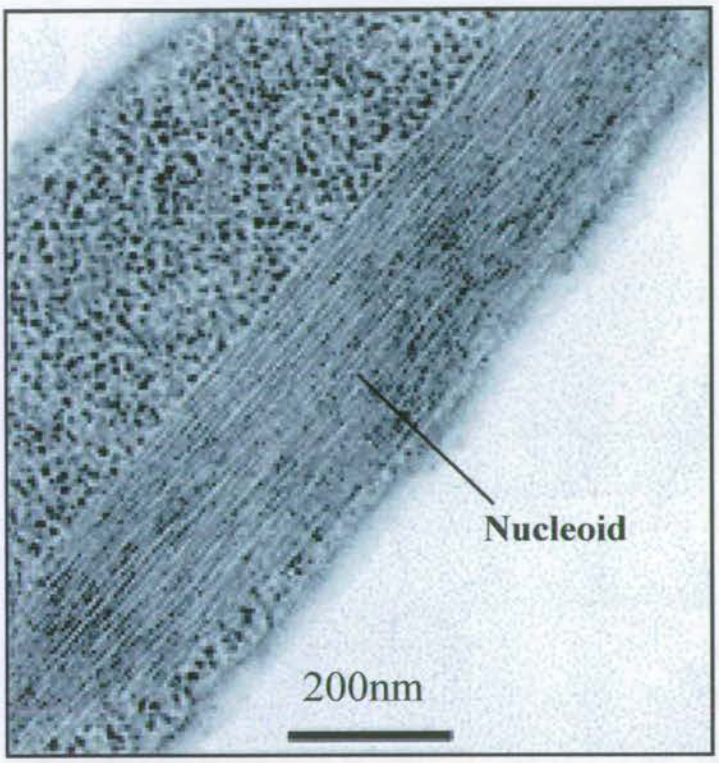

Figure 1.8. Nucleoid structure under 'stress'. Electron micrograph of *E.coli* bacteria after exposure to nalidixic acid, which induces double-stranded breaks into DNA. The bacterial nucleoid is seen to adopt a highly organised conformation, with the DNA helices arranged in parallel arrays. The dark spots present in the cytoplasm are thought to be ribosomes. Image adapted from Levin-Zaidman *et al.*, 2000.

Bacteria can survive in a number of environments that can induce double-stranded DNA lesions. For example, bacterial spores are resistant to a range of DNA damaging conditions, including desiccation, high temperature, UV and ionizing irradiation (Minsky, 2003). *Deinococcus radiodurans* can withstand DNA damaging radiation levels up to 15000 Gy, when less than 10 Gy are lethal to all other organisms (Daly and Minton, 1995; Battista, 1997). It is therefore of interest that the DNA of *Bacillus megaterium* spores as well as the genome of *D.radiodurans* adopt a toroidal conformation (Ragkousi *et al.*, 2000; Levin-Zaidman *et al.*, 2003). The formation of these laterally-ordered toroidal condensates as a protection mechanism against DNA damage agrees with the restriction diffusion model. Toroids have the DNA helices held together in lateral arrays (Hud and Downing, 2001), which would reduce diffusion of any damaged free ends. This would allow DNA repair through template-independent yet error free joining of free ends (Minsky, 2004). This is reinforced by the evidence that repair in *D.radiodurans* is promoted by factors which slow down molecular diffusion, such as freezing and desiccation. Also, repair in *D.radiodurans* is inhibited at high temperature, where diffusion is increased (reviewed in Minsky, 2003). As toroids have a reduced water content and have undergone a high degree of compaction, it is proposed that this will reduce the formation of reactive radicals and also restrict access of the free ends to potential degradation by nucleases (Minsky, 2003). In this way, DNA condensation in bacteria could produce energy independent protection for the genome, as well as providing an improved substrate for repair.

1.10. Nucleoid-associated proteins

The genome of *E.coli* comprises a single circular molecule of DNA, around 4.7 million bp in length (Azam and Ishihama, 1999). This large amount of DNA has to be organised into the small volume of the bacterial cell, represented in figure 1.9. The condensed state of the genome is, at least in part, due to its binding to several core nucleoid-associated proteins (Azam *et al.*, 1999, 2000; Lee *et al.*, 2003; Esposito *et al.*, 2002; Sonnenfield *et al.*, 2001). These nucleoid-associated proteins are thought to control the overall DNA conformation as well as gene regulation by different mechanisms, depending on the growth phase of the cell (Azam *et al.*, 1999).

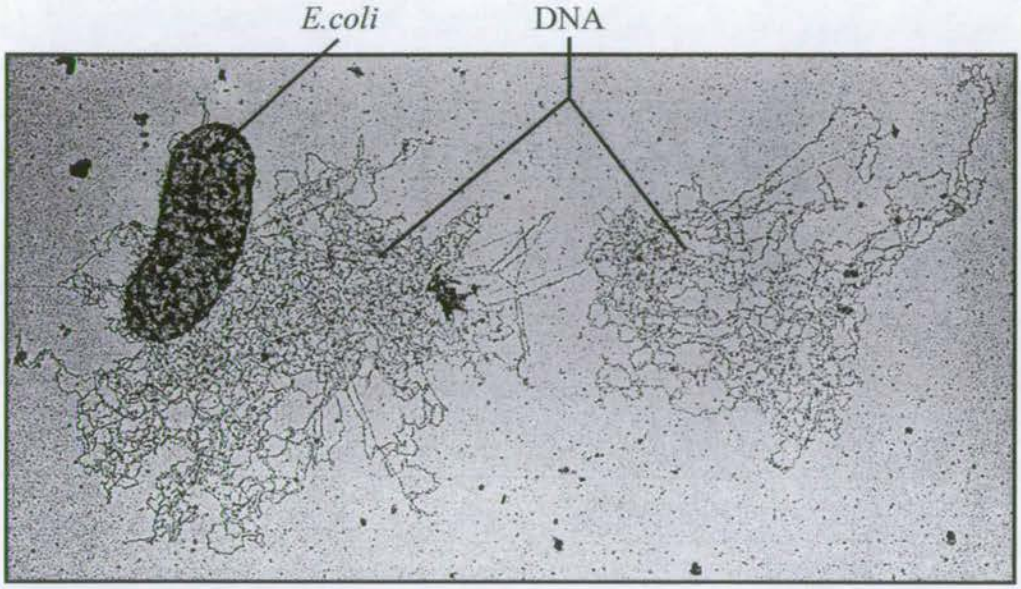

Figure 1.9. Lysed bacteria. Electron micrograph depicting a lysed *E.coli* cell spilling its genomic DNA. This shows the large amount of DNA that has to be organised within the small volume of the *E.coli* cell. Image adapted from Lewin, 2000, figure 18.5. Photograph by Jack Griffiths.

Nucleoid-associated proteins can be classified into two groups. The first group are uniformly distributed throughout the nucleoid, and thought to have a major role in DNA structuring (Azam *et al.*, 2000). These include H-NS (histone-like nucleoid structuring protein), HU (heat-unstable nucleoid protein), IHF (integration host factor), StpA (suppressor of *td* mutant phenotype A) and Dps (DNA-binding protein from starved cells). The second group bind at specific loci within the nucleoid and are therefore thought to be involved in gene regulation. They comprise CbpA (curved DNA-binding protein A), CbpB (curved DNA-binding protein B), Fis (factor for inversion stimulation), IciA (inhibitor of chromosome initiation A) and SeqA (sequestration A), and are all sequence specific DNA-binding proteins (Azam *et al.*, 2000).

In actively growing cells, the nucleoid is mainly associated with Fis, Hfq (host factor for phage Q_β), HU, StpA and H-NS. However, on entry into stationary phase, the nucleoid content of all these proteins is significantly reduced, with the starvation-induced nucleoid protein Dps becoming the most abundant. This change in nucleoid protein composition during stationary phase accompanies nucleoid condensation and gene silencing (Azam *et al.*, 1999).

H-NS is one of the most abundant bacterial nucleoid-associated proteins, and forms concentration-dependent, high-order, self-associated complexes (Esposito *et al.*, 2002). It has an important role in the packing of DNA within the nucleoid as well as regulation of many genes dispersed throughout the genome (Williams and Rimsky, 1997). Overproduction of H-NS has been seen to form highly condensed nucleoids, and is lethal to the cell (Spurio *et al.*, 1992). H-NS dimers are proposed to homo-oligomerise in a head to tail orientation, through their N-terminal domains. The C-terminal domains form the DNA binding regions, with each H-NS dimer therefore able to bind two separate DNA strands. In this way, H-NS oligomers can bind along the length of a DNA helix and form interstrand links with another DNA helix and therefore bind the DNA helices together in lateral arrays (Esposito, 2002).

This has been visualised by AFM *in vitro*, as high concentrations of H-NS were found to collapse plasmid DNA into varying conformations of condensates (Dame *et al.*, 2000). From the images obtained, a model of H-NS condensation was proposed where H-NS binds randomly to the open circle of DNA. When two points on the same DNA molecule come into close proximity, H-NS bound to one can also bind the second, thereby forming intramolecular bridges. The formation of the first bridge would make it easier for further bridging to occur, forming

many contacts, with intervening 'bubbles' of unbridged DNA. Further oligomerisation of H-NS would cause binding of these bubbles, completely linking the helices together, with a loop at either end. It is thought that the linked helices are possibly interwound to account for the observed loss in DNA length, and the fact that H-NS binding constrains DNA supercoiling. The DNA then undergoes a second order of condensation with increased concentrations of H-NS, where continued interactions between the bound H-NS molecules is thought to further collapse the bridged section of DNA (Dame *et al.*, 2000). This method of DNA bridging is similar to that of the eukaryotic linker histones H1 and H5, which also contain two DNA binding domains and form similar tracts of laterally condensed DNA (Clark and Thomas, 1988).

StpA shares 58% homology with H-NS, is of similar size and is present in bacterial cells at a similar concentration (Zhang and Belfort, 1992; Azam *et al.*, 1999). In fact, anti-StpA antibodies bind to both StpA and H-NS (Azam *et al.*, 1999). It is therefore thought that both proteins will have a similar function and mode of action (Azam *et al.*, 1999). In the absence of H-NS, over expression of StpA can suppress many of the effects of H-NS on gene expression. However, although there is an increase in the production of StpA in *hns* mutants, it is degraded by the Lon protease. This is due to the fact that in wild type cells, StpA and H-NS form heteromeric complexes which are resistant to Lon. StpA is therefore incapable of compensating for a loss of H-NS and *hns* mutant *E.coli* adopts a resultant pleiotropic phenotype. The heteromeric complexes formed by StpA and H-NS may possess novel properties, dependent upon the expression of both proteins (Sonnenfield *et al.*, 2001 and references therein).

StpA has been found to bind DNA with 4-6 times higher affinity than H-NS (Sonnenfield *et al.*, 2001). It has also been shown to interact with RNA, leading to the proposal that StpA may have a role in coupling DNA and RNA processes, such as the coordination of transcription and translation (Azam and Ishihama, 1999). H-NS and StpA have also been shown to have a preference for bent DNA (Sonnenfield *et al.*, 2001). However, Azam and Ishihama, (1999), used a shorter bent DNA substrate and found that only H-NS favoured bent DNA, with StpA binding with equal affinity to bent and straight substrates. This has been explained by the idea that StpA may recognise a longer curved segment of DNA than H-NS (Sonnenfield *et al.*, 2001).

1.11. Crowding

1.11.1. Introduction

Classically, measurements of biochemical rates, mechanisms and equilibria have been carried out under conditions selected to minimise the effects of nonspecific reactions that occur between reaction participants, and species that are not involved directly in the reaction. This typically involves using solutions containing low concentrations (<1mg/ml) of total protein and nucleic acid together with buffer salts, cofactors, and low molecular weight substrates. Information is then often extrapolated to the limit of infinite dilution to reflect the properties of individual reactants and products within an idealised bath of solvent (Minton, 2001; Zimmerman, 1993). However, the biological media of living systems is very different to this solvent bath. Such biological media typically contain 50-400mg/ml of macromolecules that can be predominantly composed of a single highly concentrated macromolecule (e.g. haemoglobin in red blood cells ~350mg/ml) (Zimmerman, 1993), or more commonly contain many different macromolecules in relatively low concentrations. In this case, although no single macromolecule is present in high concentration, altogether they take up a significant fraction of the total volume of the medium (e.g. ~340mg/ml total RNA + protein in *E. coli* cytoplasm) (Zimmerman and Trach, 1991). Such media are therefore termed crowded rather than concentrated. Also, especially in eukaryotic cells, the macromolecules may be present in large arrays, such as cytoskeletal fibres. These conditions are referred to as confining. These factors correspond macromolecules occupying between 5-40% of the total cellular volume (Ellis and Minton, 2003) leaving only a very small volume for reactions to take place.

1.11.2. Excluded volume theory

Independent of electrostatic and hydrophobic interactions, steric repulsion is always present between macromolecules in solutions of finite concentration. As two molecules cannot occupy the same position in space at the same time, other species are excluded from the volume taken up by any given protein molecule. Therefore, increasing the total protein concentration leaves less volume accessible to an individual molecule, as the exclusion volume increases. As an ideal

solution presents no hindrance to a test molecule moving at random anywhere within the solution, volume exclusion effects result in significant non-ideality of the environment encountered by the test molecule. Therefore, the packing of macromolecules at physiological concentrations leads to substantial non-ideality of biological media (Burg, 2000).

The size of the test molecule also affects the volume that it is excluded from. For example, a test molecule is not only excluded from the volume taken up by the background molecules; it is also excluded from the area surrounding them. This is as the centre of mass of the test molecule can only approach a background molecule to a distance equal to its own radius. Therefore, the excluded volume is much greater for a large test molecule than a small molecule. This can be more simply thought of as a small molecule being able to fit into the spaces between the background species, whereas the larger molecules cannot and are therefore excluded (Minton, 2001; Zimmerman, 1993). The volume exclusion principle is described further in figure 1.10.

1.11.3. Effect of crowding on reaction rates

In a biological medium, the local environment will have an affect upon the reactions taking place when the reactants come together, forming a precursor complex and then products, if each species interact unequally with the background species, or if the mobilities of the reaction participants are changed by the background species (Zimmerman, 1993). More specifically, when the rate of a reaction is limited by the rate of conversion of the precursor complex to the products, it is said to be precursor complex limited. However, when a reaction rate is limited by the rate of encounter of the reactants, it is said to be diffusion limited. As crowding is expected to enhance the relative abundance of the precursor complex and thus increase the forward reaction rate, crowding is predicted to increase the rate of precursor complex limited reactions. However, crowding retards diffusional motion, and will decrease the rate that reactants collide, thereby decreasing the rate of diffusion limited reactions (reviewed in Minton, 2001). It can therefore be seen that reactions tend to be precursor complex limited in the absence of large concentrations of background species, but become diffusion limited as the rate of encounter decreases as background species concentration increases (Minton, 1998). These reactions are represented in figure 1.11.

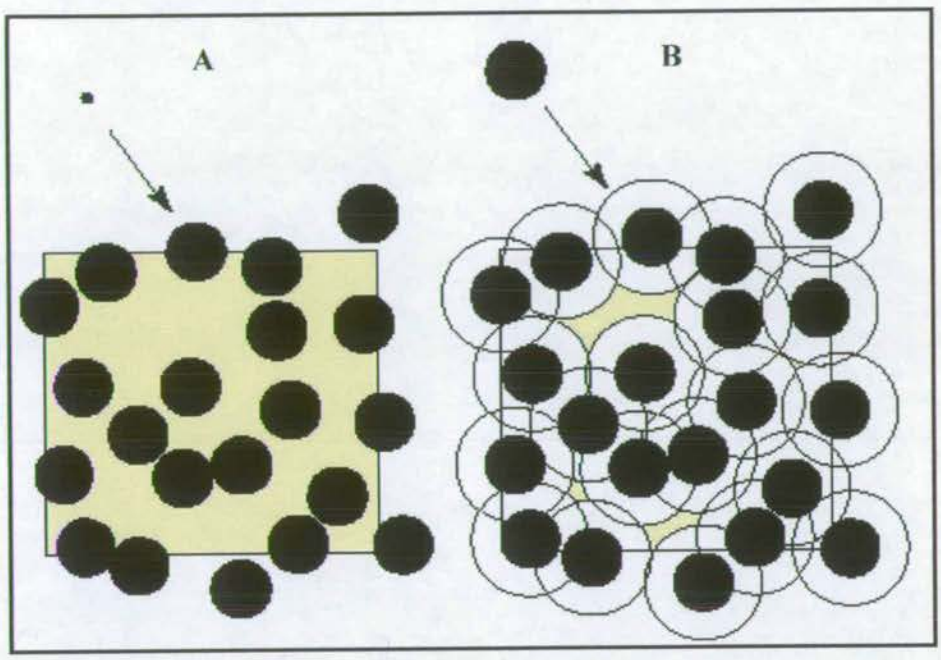

Figure 1.10. Effect of particle size on volume exclusion. In A the yellow box represents a specific volume. The large black spheres represent background molecules. The small black sphere is the test molecule. If the background molecules take up around 30% of the total volume, the small test molecule can only gain access to the remaining 70% of the available volume, as two molecules cannot occupy the same space at the same time. However, this principle is heavily dependent on the size of the test molecule. It is the centre of mass of the test molecule that represents the molecule's position. The centre of mass of a test molecule can only approach the background molecules to within a distance equal to its radius. At this point, the two molecules are touching and therefore cannot get any closer. Although this is insignificant for very small test molecules (as in A), when the test molecule is the same size as the background molecule (as in B), a specific volume around each background molecule is excluded from access by the centre of mass of the test molecule. This excluded shell (white sphere) is of the same radius as the sum of the background and test molecule radii. Therefore, in this case, the test molecule only has access to around 10% (remaining yellow regions) of the total volume, even though the background molecules only physically occupy around 30%. Therefore the bigger the test molecule, the greater the effects of volume exclusion. Image adapted from Minton, 2001.

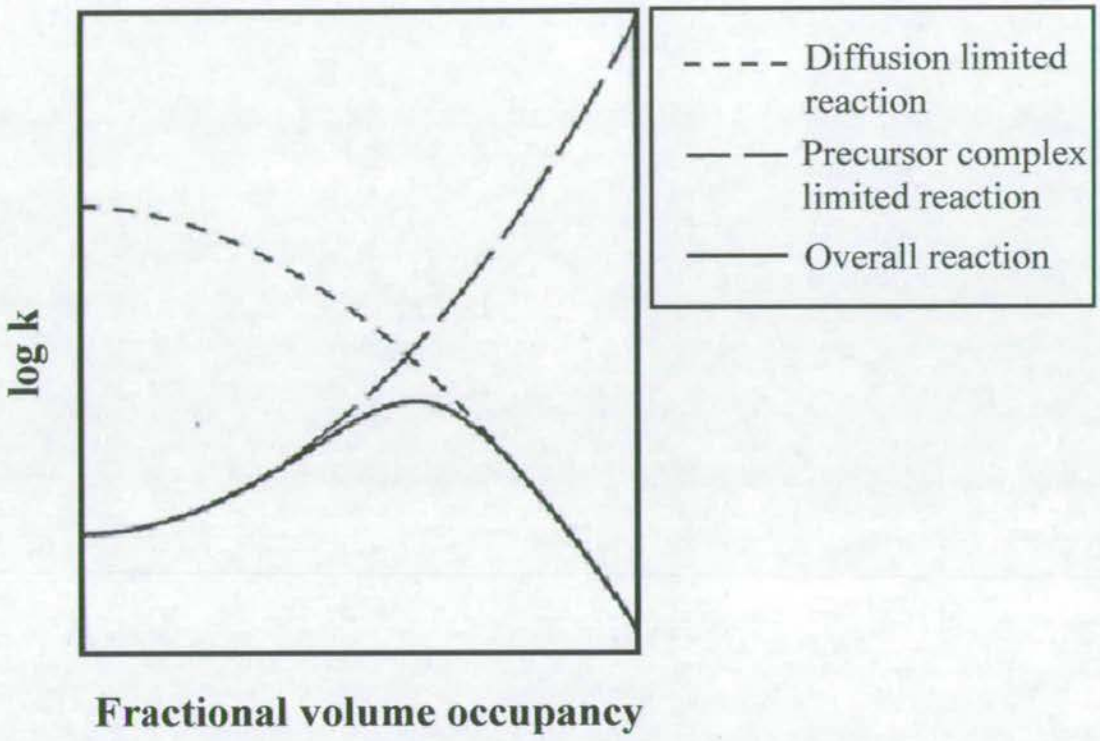

Figure 1.11. Effect of crowding on reaction rates. As the fractional volume occupancy (crowding) increases, the rate constant of reactions limited by the concentration of the precursor complex will increase as crowding increases the relative concentration of the reactants due to volume exclusion. However, the rate constant of reactions limited by the rate of encounter of reactants (diffusion-limited) will decrease due to decreasing diffusion. The overall reaction rate will therefore be precursor complex limited at low crowding levels, and diffusion-limited at higher levels of crowding. Image adapted from Zimmerman and Minton, 1993.

1.11.4. Nonspecific reactions

A nonspecific interaction is dependent upon the physical properties of interacting macromolecules, such as the polarity of surface residues, net charge, macromolecular shape, and dipole or multipole moment. Nonspecific interactions are substantially weaker than specific interactions, and can be attractive or repulsive in character. They are an unavoidable consequence of crowding and must be taken into account in order to gain greater understanding of the molecular processes taking place *in vivo* (Minton, 2001).

1.11.5. Crowding-induced condensation

DNA can become condensed due to the presence of crowding agents, such as polyethylene glycol (PEG). In this case, the repulsion between the DNA and the solvent is increased by PEG, thereby forcing the DNA segments to interact with each other, rather than with the solvent (Murphy and Zimmerman, 1995). This finding is reinforced as PEG-induced DNA collapse is enhanced by increasing monovalent salt concentration (Yoshikawa, 2001). This occurs as monovalent cations bind to the DNA phosphate groups, neutralising the negative charge. This reduces the repulsion between DNA segments, making it easier for the DNA to collapse into a condensed conformation (Yoshikawa, 2001). This crowding-induced DNA condensate would maintain its negative charge on its outer surface, with its interior neutralised.

1.11.6. Protein renaturation

In vivo, protein folding is promoted by chaperones that inhibit the aggregation of partially folded or incorrectly folded proteins. It is thought that in the absence of such processes, crowding would greatly increase the probability of partially and incorrectly folded protein aggregation, by excluded volume effects. These aggregates would therefore be lost from the pool of functional protein. In agreement with this, it was found that in the presence of a high concentration of background random coil polymers, the recoverable activity of most enzymes was markedly reduced. However, when high concentrations of a folded, stable protein were used as

background species, recoverable activity was increased. This can be explained as the probability of a random coil polymer forming an entangled complex with the unfolded protein is much greater than that for a native, stable protein (Minton, 2000b and references therein). It is also proposed that the native protein background species may stabilise the folded state of the test protein by preferentially destabilising the unfolded state (Minton, 2000a). Therefore, these studies suggest that different background species have varying effects on the behaviour of a given test protein.

1.11.7. Crowding as a cell volume sensor

Crowding has also been suggested as a mechanism by which the cell can monitor its volume (Burg, 2000). In eukaryotic cells it was found that a small loss of cell volume could invoke a disproportionately large increase in compensatory ion fluxes. It has been seen that in dog red cell ghosts containing protein mixtures, the activity of the swelling and shrinkage-activated membrane ion transporters correlated with total protein concentration rather than cell volume or concentration of any one particular constituent (Colclasure and Parker, 1991). Crowding as a cell volume sensor could act sensitively, as small changes in macromolecular crowding (which correlates with cell volume) would result in large changes in the thermodynamic activity of the macromolecular species. A drop in crowding would therefore indicate to the cell that its volume had decreased and could trigger appropriate compensatory mechanisms to restore the cell volume (Colclasure and Parker, 1991).

1.11.8. Crowding effects on enzymic activity

It has been found that crowding can greatly extend the range of conditions under which enzymes are active. For example, DNA ligases from T4 and *E.coli* have been shown to have their activity greatly stimulated by PEG in high salt concentrations that are otherwise inhibitory (Hayashi *et al.*, 1985). Crowding can also affect substrate specificity as blunt-end ligation that can be undetectable under normal assay conditions, can be strongly induced by crowding (Zimmerman and Pheiffer, 1983). It is thought that these effects are due to crowding inducing DNA

condensation, upon which, reaction rates are greatly dependent. For example, DNA condensation has been shown to increase the rates of DNA catenation (Krasnow and Cozzarelli, 1982), renaturation (Sikorav and Church, 1991), and sticky-end cohesion (Murphy and Zimmerman, 1995).

Crowding effects have been used to explain the tendency of phage lambda DNA to cyclise upon injection into the bacterial cytoplasm. It is proposed that DNA entering the cell will immediately succumb to the crowding effects of the cytoplasm, including restricted diffusion and condensation. As this conformation will hold the DNA ends in close proximity, the rate of cyclisation will be increased (Murphy and Zimmerman, 1995).

1.11.9. Direct and indirect effects of crowding on DNA

DNA is estimated to have a local concentration of up to 100mg/ml inside the bacterial nucleoid that is compacted into a small proportion of the total cell volume (Murphy and Zimmerman, 1994,1995). This condensed DNA state is thought to be promoted by supercoiling and macromolecular crowding as well as by the binding of polyamines and nucleoid-associated proteins (Zimmerman and Murphy, 1996). However, it is unknown to what extent each factor contributes to the condensation process *in vivo*. The excluded volume effects of macromolecular crowding favour compact molecular conformations and will therefore promote condensation (Lerman, 1971). It is thought that the concentrations of condensation-promoting DNA-binding proteins, found in the cell, are too low to account for DNA condensation on their own (Murphy and Zimmerman, 1994). But macromolecular crowding can also affect DNA condensation indirectly by increasing the binding of macromolecular ligands, such as nucleoid-associated proteins. This increases the effects of the condensation-promoting ligands so that the physiological concentrations of the major DNA-binding proteins are sufficient to condense the DNA of bacterial cells on their own. This effect was shown by Murphy and Zimmerman (1995), as lower concentrations of the nucleoid-associated protein HU were required to condense DNA when PEG was used to crowd the reaction. Such a mechanism will be of less importance in relation to increasing the binding of condensation-inducing polyamines due to their small size.

Much of the evidence gained so far on DNA condensation has come from experiments using isolated nucleoids. However, even in these purified preparations some degree of compaction has been lost, as they do not adopt such a condensed state as seen *in vivo* (Murphy and Zimmerman, 2000). Within *E.coli*, the DNA is localised to a compact and often dumbbell-shaped structure. Upon cell lysis, this structure decompacts to generally fill the residual cell boundaries. However, if polylysine is added immediately after lysis, the DNA remains in its highly compacted state (Murphy and Zimmerman, 2001). As lysis acts to lower the local concentration of macromolecules, and it was shown that the decompacted DNA state was not due to degradation, decompaction upon lysis is strong evidence for crowding effects upon DNA condensation.

Crowding is fundamentally different from the other condensing forces of enzymic supercoiling and DNA-binding proteins as these mechanisms depend upon binding interactions between the DNA and the respective proteins. This leaves them susceptible to changes in the local environment such as salt concentration and pH. Crowding, however, does not act through binding interactions and is therefore insensitive to environmental change (Zimmerman and Murphy, 1996). This has led to the proposal that the DNA adopts and maintains a condensed state that forms the active conformation of DNA (Sikorav and Church, 1991). This mandatory condensation would apply to all DNA within the cell; from the cell's own genome, to exogenous DNA introduced by viruses, transformation, conjugation or other means (Zimmerman and Murphy, 1996). The mandatory condensation of DNA introduced into the bacterial cytoplasm by a bacteriophage is shown in figure 1.12.

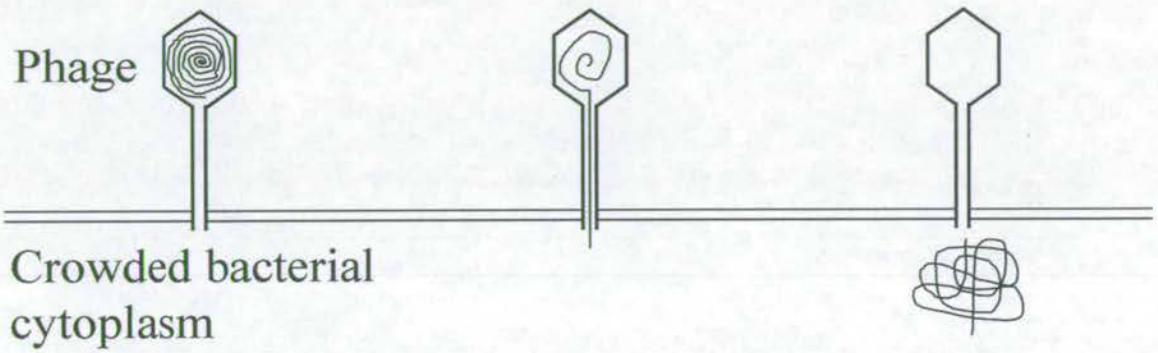

Figure 1.12. Mandatory condensation. Cartoon depicting DNA condensed within the phage head. Upon injection of DNA into bacterial cytoplasm, DNA is forced into a compact conformation due to macromolecular crowding.

1.11.10. Physiological consequences

It is becoming widely accepted that the physiological conditions of crowding have significant effects on the rate and equilibria of a wide range of reactions compared to those carried out in dilute solution. It is now appreciated that non-specific interactions, that experimenters have tried to eliminate in the past, make a significant contribution to the free energy balance of physiological systems and have to be accounted for. As reaction participants have evolved to function optimally under physiological conditions, reaction kinetics and equilibria depend sensitively upon available volume, which itself is dependent upon the total volume fraction of macromolecules. This therefore makes experimentation very difficult, as any small change in macromolecular concentration may have a substantial impact upon the equilibria and kinetics of intracellular reactions (reviewed in Minton, 2001).

1.12. DNA Fluorophores

1.12.1. Introduction

DNA-binding fluorophores can have a significant effect upon the structural conformation of DNA. Such effects include increased DNA persistence length and altered helical repeat, which occur due to intercalation of the fluorescent dye between bases or binding in the major or minor grooves (Meng *et al.,* 1996 and references therein). Examples of mono- and bis-intercalating dyes, and minor groove binding dyes are shown in figure 1.13. These structural alterations would be expected to affect many enzymatic activities, and in concordance with this, have been shown to inhibit several interactions between DNA and proteins involved in transcription, replication, repair and cleavage (Meng *et al.,* 1996; Parolin *et al.,* 1990).

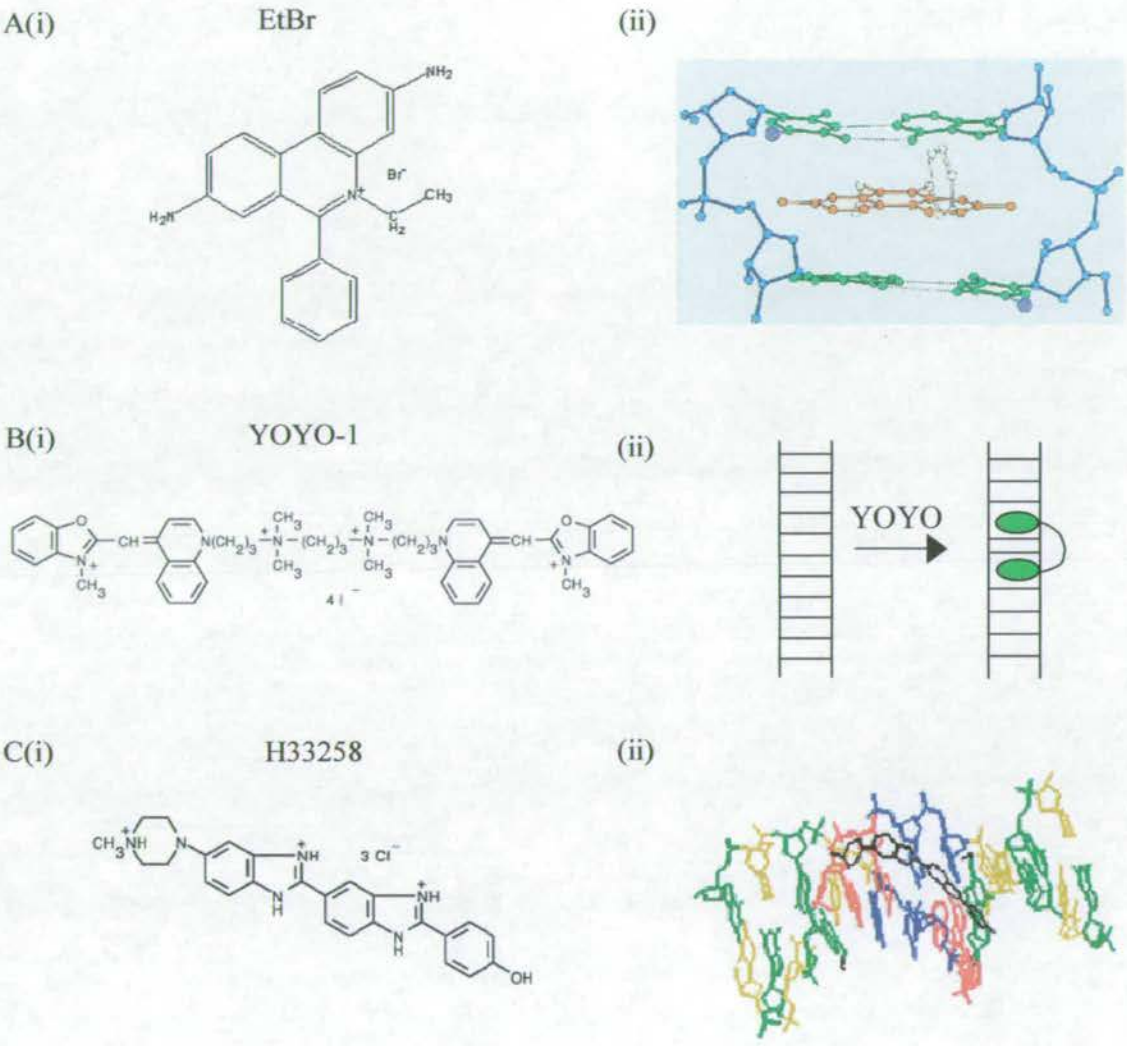

Figure 1.13. Dye structure and DNA-binding mechanism. Image A shows the structure of ethidium bromide (EtBr) (i), and the way in which it mono-intercalates in between two base pairs of DNA (ii), where EtBr is shown in orange, the bases in green and sugar-phosphate backbone in blue. Image B represents the structure of YOYO-1 (i), and the way it bis-intercalates between the base pairs of DNA (ii). In this image, the DNA is represented as a ladder, with the base pairings as the rungs. The green DNA-binding regions of YOYO intercalate between the base pairs causing an alteration of the DNA structure. Image C indicates the structure of Hoechst 33258 (H33258) (i), with it binding along the minor groove of DNA in (ii). The DNA double helix is shown with blue and red nucleotides representing T and A respectively, and green and yellow representing G and C respectively. H33258 is shown in black, bound in the minor groove.

To be an efficient fluorescent probe, the dye should be strongly fluorescent when bound to DNA, but non-fluorescent when free in solution. It should also possess a high DNA binding constant and a high molar absorptivity (Carlsson *et al.,* 1996). Six commonly used dyes that fulfil these criteria are; the thiozole orange monomer (TO) and dimer (TOTO), the oxazole yellow monomer (YO) and dimer (YOYO), and monomeric ethidium bromide (EtBr) along with ethidium dimer (EtD) (Rye *et al.,* 1992). These dyes have no specific base preferences and bind DNA by intercalation, with the dimeric compounds forming bis-intercalation interactions. Intercalating dyes stack in between base pairs and cause the DNA to unwind. They also alter phosphate bond length, thereby excluding the adjacent sites from binding other dye molecules. This forms the nearest neighbour exclusion principle (Soslau and Pirollo, 1983).

1.12.2. Agarose gel electrophoresis

Of these dyes, TO and YOYO show the greatest enhancement of fluorescence when bound to DNA. However, it is TOTO and YOYO that are the most sensitive, as they are able to detect as little as ~4pg DNA by agarose gel electrophoresis. This is ten-fold more sensitive than EtD and more than five hundred fold higher than that achieved using EtBr staining (Rye *et al.,* 1992). EtD, TOTO and YOYO produce a fluorescence intensity in agarose gels that is directly proportional to the DNA content (Rye *et al.,* 1992). This allows direct quantification of DNA content using these dyes in gels. Bis-intercalating dyes tend to form more stable complexes with DNA than mono-intercalating dyes (Carlsson *et al.,* 1995). This can be seen with TOTO and YOYO, which bind so tightly to DNA that they remain bound during electrophoresis, even when present only in the loaded sample. This allows the elimination of interfering background fluorescence that results from staining of the whole gel (Carlsson *et al.,* 1996; Rye *et al.,* 1992).

As dyes affect the charge, length and flexibility of DNA, this may cause the DNA bands in gels to change in width and position. In fact, bis-intercalating dyes have been shown to produce double bands where only one is expected. This can be due to a single molecule being mono-intercalated into two separate DNA molecules. However, YOYO caused this effect due to inhomogeneous distribution of the number of dye molecules per DNA molecule (Carlsson *et al.,* 1995).

Bis-intercalating dyes also seem to reduce the mobilities of DNA in electrophoresis much more than mono-intercalating dyes. Although YOYO decreases DNA mobility, and produces slower dynamics of orientation than pure DNA, it does not change the mode of migration of the DNA molecule through the gel. The mobility decrease is also the same for all DNA sizes investigated in this respect (2-164kb), and therefore the electrophoretic separation is not affected (Carlsson *et al.*, 1996). The main reason for the decrease in mobility is due to the alteration in charge that the dye places upon the DNA molecule. In fact, it has been seen that at ratios of dye:nucleotides greater than 1:1, the positively charged YOYO causes the DNA to migrate towards the negative electrode (Matsuura *et al.*, 2001).

As intercalating dyes cause DNA unwinding, the constrained structure of covalently closed supercoiled DNA will only be able to bind a certain amount of dye before topological stress prohibits further intercalation. Linear and nicked forms of DNA are unconstrained and therefore will bind saturating amounts of dye. This will affect the relative mobilities and band intensities of these species, as the supercoiled DNA will have less bound dye and therefore greater mobility but reduced fluorescence.

1.12.3. Effects of dyes upon enzyme activity

DAPI and H33258 are another set of fluorescent dyes that bind to the minor groove of the DNA double helix. These dyes prefer AT rich sequences and possess two binding modes: they have a high affinity binding mode that occurs at high DNA:dye ratio; and a low affinity binding mode at low DNA:dye ratio (Meng *et al.*, 1996). These dyes have been shown to have little effect upon the cleavage reactions of type II restriction enzymes, although at high concentrations, they both perturb DraI. This is as expected as the recognition sequence of this enzyme is composed entirely of A and T bases. Using the same method for the intercalating dyes EtBr, EtD, and TOTO, it was found that of the eleven type II enzymes studied, EtBr only perturbed NotI at saturating conditions. However, EtD completely inhibited SgrAI, SfiI, NotI and DraI, and perturbed CspI at high concentrations. TOTO also completely inhibited SfiI and NotI and perturbed CspI at high concentrations (Meng *et al.*, 1996). This appears to indicate that in general, intercalating dyes may have a greater effect upon type II restriction enzyme inhibition than groove-binding dyes, although these effects vary.

It has also been found that the minor groove binding dyes DAPI and H33258 have little effect on the helicase activity of RecBCD and UvrD (Eggleston *et al.*, 1996; George *et al.*, 1992). However, these dyes were found to inhibit superfamily 2 WRN and BLM helicases at high concentrations (Brosh *et al.*, 2000). In contrast to this, WRN and BLM helicases were found to be relatively insensitive to intercalating molecules with only slight inhibition caused by EtBr and the small anti-cancer and anti-multiple sclerosis intercalating drug mitoxantrone (Brosh *et al.*, 2000), whereas mitoxantrone was shown to exert a large inhibitory effect on the helicase activity of UvrD (George *et al.*, 1992). These widely different helicase sensitivities to similar DNA ligands have led to the proposal that these helicases may use different mechanisms to unwind double-stranded DNA (Brosh *et al.*, 2000).

It has been proposed that dye inhibition of type II restriction enzymes occurs through distortion of the recognition site, so as to become unrecognisable to the restriction enzyme (Goppelt *et al.*, 1981). Dye inhibition of helicases is proposed to be caused by the dye molecules forming a physical block to translocation along the DNA (George *et al.*, 1992). It is therefore interesting to note that the type I restriction enzyme EcoKI, a member of the helicase superfamily 2 which possesses both target site recognition and DNA translocation activity, has been found to have its methylation and restriction activity inhibited by EtBr (Burckhardt *et al.*, 1981). This reinforces the differences in effects that different dyes have upon different enzymes.

1.13. Summary of DNA functional control processes

DNA Manipulation Process	Functional Summary
Type I Restriction Enzymes	Cut DNA after ATP-driven DNA translocation stalls. DNA restriction and modification functions combined.
Type II Restriction Enzymes	Cut DNA at specific sites within or close to target site.
Type III Restriction Enzymes	Cut DNA after ATP-driven DNA translocation, beside one target site. DNA restriction and modification functions combined.
Helicases	Separate DNA into single strands using ATP hydrolysis.
Chromatin Remodelling Enzymes	Manipulate the position of nucleosomes or the wrapping of DNA around histones to aid DNA access by other proteins.
Looping	Brings regions of DNA separated by large distances into close proximity.
Cyclisation	Joining of free ends of linear DNA, forming circular molecule.
Condensation	Concentrated region of densely packed DNA of finite size.
Nucleoid-Associated Proteins	DNA-binding proteins which can cause DNA to adopt a condensed conformation and/or affect gene expression.
Crowding	Affect of background molecules on reactions through non-specific interactions
DNA Fluorophores	Small molecules that alter the structure of DNA and whose fluorescent signal is changed by DNA binding.

Table 1.1. Summary of DNA functional control processes.

1.14. Aims

It is the aim of this thesis to alter the environment and structure of DNA by addition of spermidine, StpA, dyes and polyethylene glycol 8000, and analyse how such changes affect the translocation and restriction activities of EcoKI. To more fully understand the processes involved in such affects on activity, some biochemical analysis of EcoKI activity under different conditions (such as pH) and with various DNA substrates is also required. In this way, the activity of EcoKI under more physiological conditions may be inferred, and the question of "how are unmodified sequences in the resident bacterial chromosome distinguished from those in DNA that has recently entered the bacterial cell?" (Makovets *et al.*, 2004; Murray, 2002) may be addressed.

These aims will be accomplished using DNA condensation assays, restriction assays and ATP hydrolysis assays involving agarose gel electrophoresis, SDS PAGE, AFM, PCR, spectrophotometry, DNA digestion by DNaseI, and restriction by EcoKI and type II restriction enzymes.

Chapter 2:

Materials and Methods

2.1. Reagents

AFM buffer: 2mM Tris-acetate, 2mM magnesium-acetate and 1.4mM 2-mercaptoethanol, pH7.9.

Alkaline solution: 0.2M NaOH; 1% SDS.

DNA loading buffer (10x): 20% Ficoll 400; 0.1M Na_2EDTA (pH 8.0); 1% SDS; 0.25% (w/v) bromophenol blue.

High salt EcoKI buffer: 33mM Tris-acetate; 10mM Mg-acetate; 66mM K-acetate; 0.5mM dithiothreitol; pH7.9.

LB (Luria-Bertani) agar: LB broth; 1.5g/l Difco agar, autoclaved.

LB broth: 10g/l NaCl; 10g/l Difco bacto-tryptone; 5g/l Difco yeast extract; pH adjusted to 7.2 with NaOH, autoclaved.

Low salt EcoKI buffer: 10mM Tris-acetate; 10mM Mg-acetate; 7mM 2-mercaptoethanol; pH7.9 (acetic acid).

Lysis buffer: 50mM glucose; 25mM Tris-HCl pH8.0; 50mM EDTA; 5mg/ml lysozyme (Sigma).

Mixed reagent: 5.72% (w/v) ammonium molybdate in 6M HCl; 2.32% (w/v) polyvinyl alcohol (ave. mol. wt. 30-70kD) (Sigma); 0.0812% (w/v) malachite green; distilled H_2O; all mixed respectively in a 1:1:2:2 ratio.

NEB buffer 4: 20mM Tris-acetate, 10mM Mg-acetate, 50mM K-acetate, 1mM dithiothreitol, pH7.9 (New England Biolabs).

SDS PAGE destaining solution: 7% acetic acid; 5% methanol; 88% H_20.

SDS PAGE staining solution: 1 part acetic acid; 3 parts isopropanol; 6 parts H_2O; 0.5% (w/v) Coomassie brilliant blue.

SDS sample buffer (2x): 1.51g Tris base; 0.1g SDS; made up to 25ml wth H_2O; pH adjusted to 6.8 with 1N HCl; filtered through 0.45-μm filter. Then added: 20ml glycerol; 4g SDS; 3.1g dithiothreitol; 1mg bromophenol blue; made up to 100ml with distilled H_2O and stored at -20°C.

TBE (10x): 0.89M Tris base; 0.89M boric acid; 20mM EDTA.

TE buffer: 10mM Tris-HCl pH8.0; 1mM EDTA.

2.2. Bacterial strains

***E.coli* ER2426**: *Hsd⁻*
Genotype: fhuA2 supE44 e14- rfbD1? relA1? endA1 spoT1? thi-1 Δ(mcrC-mrr)114::IS10 F' proA+B+ laqIq Δ(lacZ)M15 zzf::miniTn10 (KanR) (New England Biolabs, Beverley, Ma, USA)

***E.coli* NK301**: *Hsd⁺* (Makovets *et al.*, 1999).

***E.coli* NK311**: *Hsd⁻* (Makovets *et al.*, 1999).

2.3. Plasmids

pBR322 (Bolivar, 1977): 4361bp. Two EcoKI target sites (1664-1652, and 4024-4036, in tail-to-tail orientation at their closest separation) separated by 1976bp and 2359bp. One EcoRI target site (4359), one BamHI target site (375), one SalI target site (651), one BsgI target site (1650) and one PvuI target site (3733). Ampicillin resistant.

pBRsk1 (Davies, 2000): 4361bp, pBR322 T4033A, one EcoKI target site (1652-1664). One EcoRI target site (4359), one BamHI target site (375), one SalI target site (651), one BsgI target site (1650) and one PvuI target site (3733). Ampicillin resistant.

pBE 3 (O'Neil *et al.*, 1997): Contains genes *hsdR*, *hsdM* and *hsdS*. Ampicillin resistant.

2.4. Oligonucleotides

Primer3: 5'-CTGTCGTTGAGGACCCGGC-3', T_m = 63.1°C.

Primer4: 5'-CACGATACGGGTTACTGAT-3', T_m = 54.5°C.

PrimerA:

5'-CCAGCAGCATCCTGCGATGCAGATCCGGAACATAATGGTGC-3'

T_m = 76.4°C.

PrimerB:

5'-ACAACATGAATGGTCTTAACTTTCCGGTGCTCGTAAAGTCTGGAAAC-3'

T_m = 72.9°C.

PrimerC:

5'-ACTGCTGCTGCAAAACAACTGCGACGTGCGCAACAACATGAATGGT-3'

T_m = 76.4°C.

PrimerD:

5'-CCTTACTGGTTAGCAGAACGAATCAGTGCTACGCGAGCGAACGTGA-3'

T_m = 77.3°C.

PrimerG:

5'-TTCACCACTCCAAGAAAACGAGCCAGTGCATTCTTGCGGAGAACTG-3'

T_m = 75.5°C.

(All designed and made in this thesis)

2.5. Experimental Procedures

2.5.1. EcoKI purification

EcoKI was purified by a method based on that described briefly by Dryden *et al.*, 1997. All purification steps were carried out at 4°C unless otherwise stated. EcoKI was prepared from 8 litres NK311 cells (Makovets *et al.*, 1999) containing the plasmid pBE3 (O'Neill *et al.*, 1997) grown in LB broth containing 50μg/ml ampicillin (Beecham pharmaceuticals) for 18h at 37°C. Thirty six grams of cell paste was resuspended in 100ml of 20mM Tris-HCl, 10mM $MgCl_2$, 7mM β-mercaptoethanol, 10% glycerol, 10^{-5}M PMSF, and 10^{-5}M benzamidine, pH 7.5, buffer and sonicated on ice with intermittent cooling for 24min. The sonicated sample was diluted to 600ml with the same buffer and cell debris removed by centrifugation at 26000xg for 1h. The supernatant was then applied to a (17cm x 1.6cm diameter) DEAE-sepharose column with bound protein being eluted with a 500ml 0-0.5M NaCl gradient. Fractions were analysed by 10% SDS PAGE and those containing EcoKI were pooled and dialysed against buffer to remove NaCl before being applied to a (17cm x 1.6cm diameter) heparin-agarose column. A 500ml 0-1M NaCl gradient was used to elute bound protein. SDS PAGE was again used to locate the EcoKI containing fractions that were pooled and dialysed against buffer containing 0.2M NaCl. The dialysed sample was concentrated using 10kD cut off centrifugal concentrators (Vivascience) to a volume of 3ml. This was loaded onto a superdex 200 16/60 column and run in buffer containing 0.2M NaCl. The fractions containing EcoKI were again concentrated using the 10kD cut off centrifugal concentrators. Each 1ml of concentrated sample was diluted with 4ml buffer (0M NaCl) and run on a 1ml HPLC Resource Q column. Bound protein was eluted with an 11ml 0-0.5M NaCl gradient. SDS PAGE was used to identify the EcoKI containing fractions which were pooled before an equal volume of glycerol was added and stored at -20°C. Protein concentrations were measured by UV spectroscopy at 280nm, using the calculated extinction coefficient for EcoKI ($R_2M_2S_1$), 371606$M^{-1}cm^{-1}$ (Dryden *et al.*, 1997). The purification yielded about 20mg enzyme.

2.5.2. Competent cells

For all work with bacteria, sterile technique was used. The bacteria used to produce plasmid DNA were *E.coli* strain ER2426 as they are *Hsd*$^-$ and therefore any plasmids they produce

will be unmethylated at EcoKI target sites and therefore suitable for EcoKI restriction assays. For control experiments, plasmid DNA was made from bacterial strain NK301 (Makovets *et al.*, 1999), which is *Hsd*$^{+}$ and therefore produce plasmid DNA that is methylated at the EcoKI target sequence and therefore cannot be cut by EcoKI. Strain NK301 was treated in exactly the same way as ER2426 except that no kanamycin selection was used, as NK301 are not kanamycin resistant.

Cells were made competent for transformation by a method described by Ausubel *et al.*,1992. One bacterial colony was transferred from an LB agar plate to a 5ml LB broth overnight culture. This was incubated with shaking at 37°C for 16h. This was then diluted 1 in 50 in LB broth, and incubated for a further 2h at 37°C. Cells from 50ml culture were pelleted by centrifugation at 4500xg at 4°C for 10 min (Heraeus, biofuge stratos, with Heraeus swing-out rotor #3047 and Heraeus #8172 buckets). The supernatant was removed and the pellet was resuspended in 20ml ice-cold 100mM $MgCl_2$. This was centrifuged at 4500xg for a further10 min at 4°C. The supernatant was removed and the pellet resuspended in 10ml ice-cold 100mM $MgCl_2$. This was again centrifuged at 4500xg for 10min at 4°C. The supernatant was discarded and the pellet was resuspended in 2ml ice-cold 100mM $CaCl_2$. These competent cells were kept on ice and used for transformation within 24h.

2.5.3. Transformation

1µl plasmid DNA to be taken up by cells was added to 200µl competent cells. Cells were then left on ice for 30min. Cells were then heat-shocked by incubating them at 42°C for 90s. 1ml LB broth was added to the cells and they were incubated at 37°C for 1h. As all plasmids used were ampicillin resistant, and *E.coli* ER2426 is kanamycin resistant, 100µl cells were spread onto LB agar plates containing 50µg/ml ampicillin (and 30µg/ml kanamycin for *E.coli* ER2426). Colonies were grown by incubation of the plate at 37°C for 16h.

2.5.4. DNA plasmid preparation

Plasmid DNA was purified from *E.coli* strain ER2426 by a method based on that described by Baumann and Bloomfield, 1995. Cells transformed with the (ampicillin resistant) plasmid

of interest were grown in 500ml LB broth containing 50μg/ml ampicillin and shaken at 37°C for 16h. Cells were harvested by centrifugation at 4500xg at 4°C for 10min (Heraeus, biofuge stratos, with Heraeus swing-out rotor #3047 and Heraeus #8172 buckets). The supernatant was discarded and the pellet resuspended in 20ml lysis buffer. This was incubated for 10min at room temperature. Cells were lysed by the addition of 40ml freshly prepared alkaline solution and stored on ice for 10min. Cellular debris was precipitated by carefully adding 25ml saturated ammonium acetate. This was swirled rapidly to mix for 30s and then incubated on ice for 10min. The precipitate was pelleted by centrifuging at 10000xg for 10 min at 4°C (Heraeus, biofuge stratos, with Heraeus fixed angle rotor #3335). The supernatant was then passed through a single layer of autoclaved 'cheese cloth' which had been pre-washed with TE buffer. The crude plasmid DNA was precipitated by the addition of 60ml ice-cold isopropanol. This was mixed and incubated on ice for 20min. The precipitated DNA was pelleted by centrifugation at 10500xg for 15min at 4°C (Heraeus, biofuge stratos, with Heraeus fixed angle rotor #3335). The supernatant was discarded and the pellets allowed to drain. The pellet was resuspended in 2ml TE buffer and centrifuged at 22000xg for10min (Heraeus, biofuge stratos, with Heraeus fixed angle rotor #3332) to remove any undissolved material. 200units of (DNase-free) RNase (Sigma) was added to the supernatant, and incubated for 1h at 37°C. 2ml TE-saturated phenol was added to the digest and shaken for 30s. The sample was then centrifuged at 22000xg for 5 min at 4°C (Heraeus, biofuge stratos, with Heraeus fixed angle rotor #3332). The aqueous phase was removed and stored on ice. 2ml TE buffer were then added to the remaining lower phase containing 2ml TE-saturated phenol. This was mixed and re-centrifuged (22000xg, 5min, 4°C). The aqueous phase was removed and combined with the other previously removed aqueous phase in 10kD cut-off dialysis tubing (Sigma) in 1l TE buffer overnight at 4°C (or 2h at room temperature) with stirring. The sample was removed from the dialysis tubing and the plasmid DNA was precipitated by adding 0.1x volume of 5M NaCl and 2x volume of ice-cold ethanol. This was incubated at -20°C for 45min and the precipitate was pelleted by centrifugation at 12000xg for 30min at 4°C. The supernatant was removed and the pellet was washed twice with 70% ethanol before being allowed to air-dry. The pellet was then resuspended in 2ml sterile H_2O.

Once purified, plasmid DNA purity and concentration was measured by UV spectroscopy using an Hitachi U-2001 spectrophotometer. The absorbance was measured over a range of 220-340nm. The absorbance at 320nm was used as a baseline, and all other absorbances corrected for this accordingly. The ratio of absorbance at 260nm:270nm was always greater than 1.2 which indicates that the sample was free from phenol. The ratio of the absorbance at

260nm:280nm was approximately 2 which indicates that the sample was free from protein (Bauman and Bloomfield, 1995). The DNA concentration was calculated using the equation:

1 absorbance unit at 260nm = 50μg/ml double-stranded DNA.

An EcoRI restriction enzyme digest of a sample of purified plasmid DNA (pBR322 or pBRsk1) was carried out in order to confirm that the correct plasmid had been isolated. This was determined by agarose gel electrophoresis with ethidium bromide staining as described.

Unless otherwise stated, when linear DNA was required, plasmid DNA was cut with EcoRI in high salt EcoKI buffer as described.

2.5.5. Agarose gel electrophoresis

Separation of DNA fragments in different conformations from bacterial plasmids pBR322 and its derivative pBRskI was carried out by submerged horizontal electrophoresis in 0.8% agarose essentially as described by Ausubel *et al.*, (1992). 1xTBE buffer was used as both the gel and running buffer, supplemented with 0.5μg/ml ethidium bromide (EtBr). Electrophoresis was carried out at 8V/cm for 2h. Gels were then stained in 1xTBE buffer containing 0.5μg/ml EtBr for 45min in order to equalise the background fluorescence, before a 5min destain in distilled, deionised water to improve the ratio of band intensity to background fluorescence. DNA was visualized using a UV transilluminator (UVP, TFM-30) and images acquired using a CCD camera (initially Kodak DC3200 and later Fujifilm FinePix S602Zoom) with a 3mm thick, 570nm filter (Schott, Mainz, Germany) and Adobe Photoshop software. Densitometry was carried out on gel images using Scion Image software (Scion corporation).

In order to analyse the data thoroughly, a conversion factor was required to allow direct comparison between supercoiled DNA and the other forms of nicked and linear DNA. This is due to the fact that as EtBr causes DNA unwinding, the constrained structure of supercoiled DNA only allows it to bind a limited number of dye molecules. Nicked and linear DNA, however, are unconstrained and can bind more dye. Comparing the band intensities of identical quantities of linear and supercoiled DNA allowed the conversion factor (cf) to be calculated thus:

$$cf = \frac{\text{linear - nicked}}{\text{supercoiled}}$$

Nicked DNA needs to be accounted for, as a small fraction is always present in the supercoiled sample as a result of the purification procedure.

Agarose gels were also used for binding studies of EcoKI to DNA by mobility retardation. In these experiments, reactions were carried out with DNA in EcoKI high salt buffer, pH7.9, with 0.1mM SAM and 50µg/ml BSA. Varying concentrations of EcoKI were added, 5min prior to the addition of glycerol to a final concentration of 7% (instead of loading buffer). Samples were then loaded onto an appropriate agarose gel, which was run at $3Vcm^{-1}$, and the temperature of the running buffer maintained at 20°C. No dye was used in either the gel or the buffer during electrophoresis, with the gels being stained with EtBr after they were run, and then viewed as described.

2.5.6. SDS Polyacrylamide gel electrophoresis (PAGE)

One-dimensional gel electrophoresis under denaturing conditions was used to separate polypeptides based upon their molecular size. Mighty Small II (Hoefer Scientific instruments) vertical slab gel kits were used. 10-15% polyacrylamide gels were made as described by Ausubel *et al.*, 1992. Protein samples were prepared by addition of an equal volume of 2x sample buffer, prior to loading onto gel. Gels were run at 25-30mA per gel. Gels were removed from their casts and gently shaken in staining solution for about 2h, or until bands were clearly visible. Gels were then transferred to a destain solution and gently shaken for 3-16h. Gels were scanned and images optimised using Adobe Photoshop. Gels were also dried out overnight between stretched sheets of wet cellophane membrane, in order to retain gels.

2.5.7. Restriction enzyme digests

Type II restriction enzymes were purchased from Promega (Madison, WI, USA). Restriction digests using these enzymes were carried out according to the manufacturer's instructions, using approximately 1unit of enzyme per 2μg plasmid DNA with one target site, 50μg/ml bovine serum albumin (Promega) and 1x high salt EcoKI buffer. Heat-sensitive enzymes (such as EcoRI) were deactivated, when required, by incubation at 65°C for 30min. Samples were mixed with DNA loading buffer prior to loading onto agarose gel and run as described below.

Restriction assays with the type I restriction enzyme EcoKI, were typically carried out in low salt EcoKI buffer with the ionic strength adjusted with NaCl. Reactions were carried out with 50nM plasmid DNA; 0.1mM S-adenosyl methionine (SAM); 50μg/ml bovine serum albumin (BSA) and; 2mM ATP. 67nM EcoKI was used for digestion of DNA with one EcoKI target site and 134nM EcoKI for two-site DNA. Reactions were typically carried out in 180μl total volume, with 22μl being removed at specific time points and added to EDTA (77mM final concentration) in order to stop the reaction. EcoKI was denatured by heating the sample to 68°C for 30min. Loading buffer was then added to samples before being run on 0.8% agarose gels in 1x TBE buffer as described.

When restriction digests with EcoKI were carried out with spermidine or StpA, the DNA was incubated with the spermidine or StpA and buffer for 30min at room temperature prior to the addition of SAM, BSA and EcoKI. The reactions were started with ATP, 5min after the addition of EcoKI.

Restriction digests were also carried out in ATP regenerating buffer. These experiments used 50nM linear pBR322, 134nM EcoKI in low salt EcoKI buffer, pH 7.9, with 0.1mM SAM, 50μg/ml BSA, 10mM phosphoenol pyruvate, 2.5mM NADH, 13μg/ml pyruvate kinase/lactate dehydogenase mix, and 2mM ATP. The ionic strength was made up to 100mM with NaCl. Reactions were stopped by addition of 77mM EDTA and heating to 68°C for 30min.

2.5.8. Dynafit Modelling

Restriction assay timecourse data was analysed using Dynafit to fit curves to the data and calculate rate constants (Kuzmic, 1996). Scripts were written to provide several possible reaction mechanisms, with the most appropriate mechanism chosen by the program due to factors including the ability of the curves produced to of fit the data (least-squares fit), and the number of variables used. Initial estimates of the rate constants were provided and allowed to vary in order to determine which values optimally fitted the data. The mean values of several experiments were used to provide the data points as no function was available to produce explicit error bars in a program of this type. An example of the initial data and task file used to fit curves to the timecourse for EcoKI restriction of supercoiled pBR322 in the presence of 4mM spermidine at 100mM ionic strength as well as the output data produced can be seen in Appendix E.

2.5.9. DNaseI digestion of DNA

Assays were carried out in low salt EcoKI buffer with 1mM $CaCl_2$ and the ionic strength adjusted using NaCl. 50nM plasmid pBRsk1 DNA was incubated with a 0.1μg/ml DNaseI (final concentration) at 37°C. The reaction was stopped by the addition of EDTA (final concentration 77mM). Samples were then run on 0.8% agarose gels, in 1x TBE with EtBr staining.

2.5.10. Coupled ATP hydrolysis assay

EcoKI translocation was measured by a coupled enzyme ATP hydrolysis assay (Pullman *et al.*, 1960; Harris, 1987) based on the following reaction:

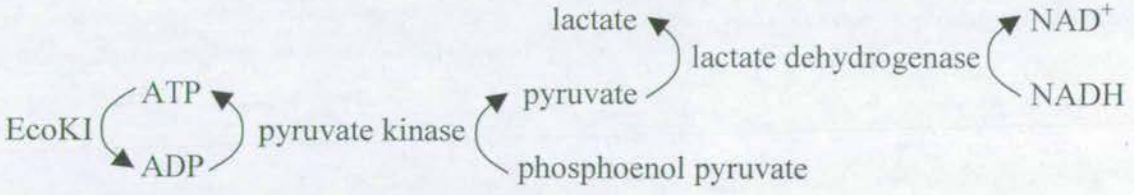

In this reaction, the rate of decrease in NADH is proportional to the rate of ATP hydrolysis by EcoKI. This decrease of NADH is measured spectrophotometrically at an absorbance of 340nm. For this assay, 5nM DNA with one EcoKI target site or 2.5nM DNA with two EcoKI target sites was incubated with 10nM EcoKI, 50µg/ml BSA, 0.1mM SAM, 1mM phosphoenol pyruvate, 250µM NADH, in low salt EcoKI buffer, pH 7.9, with a final reaction volume of 300µl. Pyruvate kinase/lactate dehydrogenase was dialysed against low salt EcoKI buffer and used fresh on the day of experiment at a concentration of 13µg/ml. A baseline was recorded at A_{340nm} on a time scan, before the reaction was started with the addition of 2mM ATP. After 30s, the rate of decrease of NADH was thereafter recorded and the corresponding rate of ATP hydrolysis calculated using the following extinction coefficient for NADH:

$$A_{340\,nm}^{1mM} = 6.22$$

2.5.11. P_i assay of ATPase activity

In this assay, the P_i that is produced from the hydrolysis of ATP by EcoKI is complexed and measured in a single step following the addition of mixed reagent, using a modification of the protocol described by Chan *et al.*, (1986), and Janscak *et al.*, (1996). The assay works on the principle that EcoKI hydrolyses ATP into ADP and P_i. ATP hydrolysis can therefore be assayed by measuring the amount of P_i produced. This can be carried out by a colorimetric assay as the liberated P_i forms a coloured complex with molybdate/malachite green that has a measurable absorbance at 630nm. The mixed reagent was made on the day of the experiment and allowed to stand at room temperature for at least 30 min, when it turned a golden brown colour.

EcoKI reactions were carried out as in the endonuclease assay. However, after the reaction had been stopped at each specific time point by the addition of EDTA, 7µl of sample was added to 243µl mixed reagent in a 1cm path length quartz cuvette. The absorbance at 630nm was then recorded in the UV spectrophotometer (Hitachi U-2001) after 100s. This absorbance was then converted into P_i concentration by use of a calibration graph that had been made by the measurement of known concentrations of KH_2PO_4. It should be noted that

in the endonuclease assay, the 0min time point contained no ATP and therefore would not be a valid blank for the P_i concentration of the other time points. The appropriate amount of ATP was therefore added to the 0min time point after the addition of EDTA. Also, it was seen that relationship between A_{630nm} and P_i concentration was only linear up to around an A_{630nm} of 1.2. Therefore any samples with an A_{630nm} of >1 were diluted and the P_i concentration adjusted accordingly.

2.5.12. Rheology

Rheology experiments were carried out to determine the viscosity of glycerol and polyethylene glycol (PEG) solutions. A CSL^2 Rheometer (TA) was used with a 4cm, 2° cone (700 µl volume) for highly viscous solutions, and with a 6cm, 0.31° cone (565µl volume) for more dilute solutions. Viscosity was measured at 25°C, by varying the shear strain. The rheometer calibration was checked on the day of each experiment using glycerol at 37°C.

2.5.13. Polymerase chain reaction (PCR)

PCR consists of a three-step cycle repeated many times. The three steps in a cycle are denaturation, annealing and extension. All three steps are temperature dependent and therefore the reaction can be pushed through each step in turn by changing the temperature.

Firstly a high temperature (typically 95°C) is used to denature double-stranded DNA into two single strands. Secondly, the temperature is reduced to allow the primers to anneal to their binding site. A primer is allowed to bind at each end of the DNA sequence that is to be amplified, with one primer being complementary to each strand. Thirdly, the temperature is raised to around 72°C to allow the enzyme Taq polymerase to replicate the DNA strands optimally. Taq polymerase extends the DNA sequence starting at each primer in a 5' to 3' direction. Therefore, the primers must be orientated so that they are extended over the region of DNA to be amplified. This extension occurs as the polymerase facilitates the binding and joining of nucleotides that are complementary to the original denatured single-stranded DNA.

This first PCR cycle produces two new DNA strands identical to the original target. In further cycles, newly synthesised DNA will also become a target for replication. Replication of this newly synthesised target will have a precisely defined length that is limited at either end by the 5' end of the two primers. This will produce double-stranded DNA consisting of the primers and the intervening DNA. As cycling continues, the amount of DNA producing full length original target will be overtaken by the amplification of the shorter DNA sequence from primer to primer.

A DNA thermal cycler (Perkin Elmer) and puRe Taq ready-to-go PCR beads (Amersham Biosciences) were used to conduct PCR experiments. PCRs were typically carried out in a total volume of 25µl containing 0.5µM of each primer, 2.5nM template DNA, 200µM each dNTP, 10mM Tris-HCl (pH 9.0), 50mM KCl and 1.5mM $MgCl_2$, for 30 cycles. The samples were covered with a thin layer of mineral oil to prevent evaporation.

2.5.14. Atomic Force Microscopy (AFM)

In modern AFM, a manufactured tip, attached to a cantilever, is dragged across a surface of interest, whilst a laser beam is deflected from the back of the cantilever and onto a position-sensitive detector. This laser beam deflection allows a picture of the surface to be built up. This technique, used with a tip in tapping mode (were the tip only contacts the surface intermittently), allows the study of fragile samples such as DNA.

AFM imaging was performed with a multimode atomic force microscope (Digital Instruments, Santa Barbara, CA). Samples were imaged in air, using tapping mode with a root mean square amplitude of 0.7V (9nm) and a drive frequency of 300kHz. Silicon cantilevers with a specified spring constant of 42N/m were used (NCH Pointprobes; Nanosensors, Wetzlar-Blankenfeld, Germany).

Samples were 20µl in volume and contained 0.2nM plasmid DNA pBR322 in AFM buffer. The spermidine concentration was varied from 0 to 7.3mM. Samples containing 0 to 0.1mM spermidine were adsorbed to mica coated with poly-L-lysine. Above 0.1mM spermidine, no poly-L-lysine was required for DNA attachment and so bare mica was used. The 20µl sample was applied to the slide, and left at room temperature for 10 min. Excess liquid was

gently blotted off before the samples were dried with a constant flow of nitrogen for a further 10 min. The samples were then viewed by AFM.

2.5.15. Ionic strength calculation

When required, the ionic strength of solutions was calculated using the following equation:

$$I = \frac{1}{2} (m_+ z_+^2 + m_- z_-^2)$$

(Atkins, 1978) where I is the ionic strength (M), and m and z are the molarity and charge respectively of cations (+) and anions (-). Ionic strength is an important parameter that corrects the concentration for differences in ion valences. The total ionic strength of a solution is calculated by summing the ionic strengths of each individual component electrolyte.

2.5.16. Ligation

Ligation experiments were carried out with 60nM pBR322, linearised with EcoRI to produce cohesive ends with a four base overhang. EcoRI was heat denatured before ligation experiments were conducted in low salt EcoKI buffer with 50μg/ml BSA, 4units ligase and 1mM ATP. Reactions contained varying concentrations of spermidine and were stopped by addition of 73mM EDTA and heating at 65°C for 10min. Samples were run on agarose gels with EtBr staining after addition of DNA loading buffer. The fractions of DNA present in each band were calculated by densitometry using Scion Image software.

2.5.17. Statistics

When three or more repeats of an experiment were carried out, the mean was taken, with errors calculated as the standard deviation. When an experiment was carried out twice, the mean was taken, with the error calculated as the standard error. The standard error was used for these experiments as the maximum and minimum limits of the error bars represent the values of the separate data points of each of the two individual experiments.

Chapter 3:

General EcoKI Biochemistry

3.1. Introduction

It is thought that the main purpose of EcoKI is to protect the bacterial cell from attack by invading bacteriophage DNA. EcoKI recognises a specific target sequence on the DNA and can determine by its methylation state whether or not the DNA is foreign. If it is found to be unmethylated and therefore foreign DNA, EcoKI translocates the DNA by pulling it towards itself from both directions, whilst remaining bound to its target site. This translocation requires ATP and continues until it is stalled by some impediment, such as another translocating EcoKI enzyme. Once translocation has stalled, the enzyme cuts the DNA in a process involving two single-stranded nicking events (Studier and Bandyopadhyay, 1988). This process is summarised in figure 1.2 and leaves the invading DNA harmless to the cell. As the cutting event occurs where the EcoKI meets the impediment to translocation, the cutting site varies in position. Once EcoKI has carried out these processes, it remains bound to its target site and therefore can only carry out one reaction. It also carries on hydrolysing ATP once the target DNA has been restricted (reviewed in Bickle and Kruger 1993; Bickle, 1993).

However, there is little known about the mechanism of translocation and the nature of the cutting sites. There has also been little research into the buffer conditions in which EcoKI carries out restriction. It is the aim of this chapter to investigate these matters.

3.2. EcoKI purification

Figure 3.1 shows EcoKI isolated and purified from *E.coli* NK311 cells. Around 20mg of enzyme was purified in 4 separate fractions. All fractions contained a small amount of contaminating protein. However, no contaminant had any effect on EcoKI specific activity, as all cofactors (SAM, Mg^{2+} and ATP) were required for restriction of unmethylated DNA (data not shown). Fraction 2 contained the least amount of contaminant and was therefore chosen for use in experiments described in this thesis.

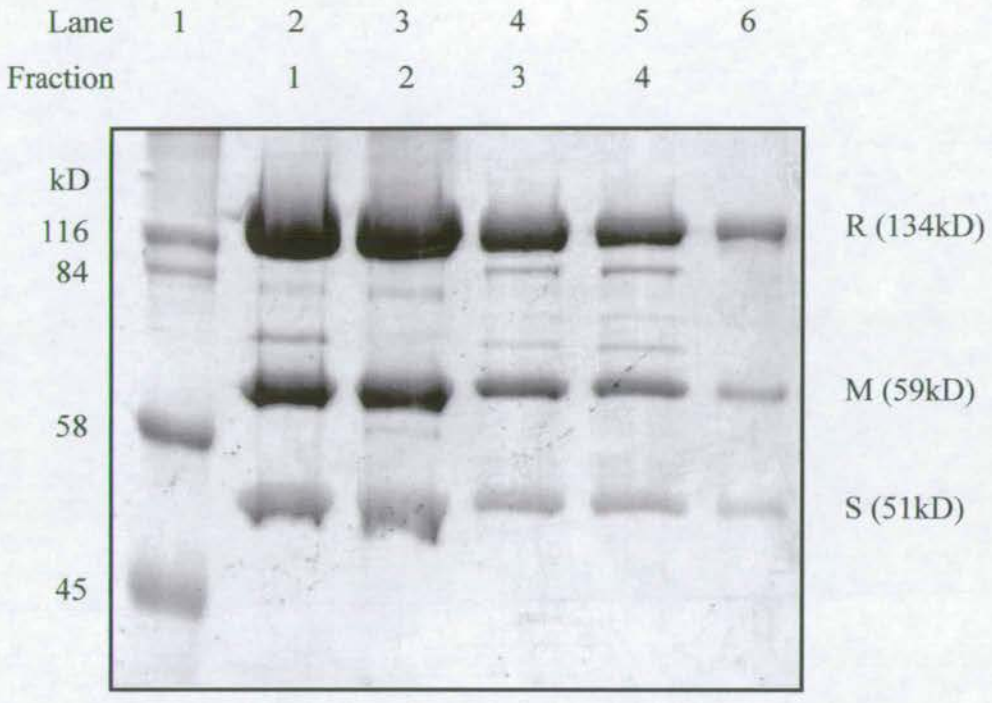

Figure 3.1. EcoKI purification. EcoKI was isolated as described in materials and methods. Fractions 1-4 were collected from the final column and run on a 10% polyacrylamide gel with coomassie blue staining. All fractions were overloaded in order to observe any contaminants. Fraction 2 was used for experiments in this thesis. Lane 1 contains a high molecular weight marker of sizes indicated. Lane 6 contains an EcoKI marker, containing R, M and S subunits of sizes indicated.

3.3. Mechanism of EcoKI restriction of different DNA substrates

EcoKI restricts DNA with varying numbers of target sites and varying conformations. Upon restriction of a DNA substrate with two EcoKI target sites, EcoKI was seen to dimerise prior to addition of ATP (Berge *et al.*, 2000). Although this is not an absolute requirement for restriction, it is thought to represent a change in EcoKI conformation upon specific binding to its target site. EcoKI has been shown to be able to restrict circular plasmid DNA with only one target site (Dreier *et al.*, 1996). It has been suggested that in this case, the trigger for restriction is stalling caused by the ever decreasing length of DNA between the R subunits, which becomes so small that at some point it cannot be translocated any further. Restriction of linear DNA with one target site has also been reported (Murray *et al.*, 1973; Szczelkun *et al.*, 1997; Janscak *et al.*, 1996), in the presence of excess enzyme over long time periods. However, the mechanism for this process is unknown, it is possibly due to EcoKI molecules being bound non-specifically to the DNA, and creating a block to the translocating, specifically bound EcoKI, thereby inducing restriction. The mechanism of EcoKI restriction of DNA is discussed further in chapter 1.

3.3.1. Expected products of restriction

Figure 3.2 represents the mechanism of restriction of supercoiled one-site pBRsk1. The diagram shows how a supercoiled plasmid is converted into a nicked intermediate, and then linear product. The situation in which EcoKI digests linear pBRsk1 is represented by figure 3.2C. Figure 3.3 represents the mechanism of restriction of supercoiled two-site pBR322. The diagram shows how supercoiled plasmid is converted into nicked and then linear intermediates, before conversion into linear fragment products. The situation where EcoKI restricts linear pBR322 is represented in figure 3.3C-E.

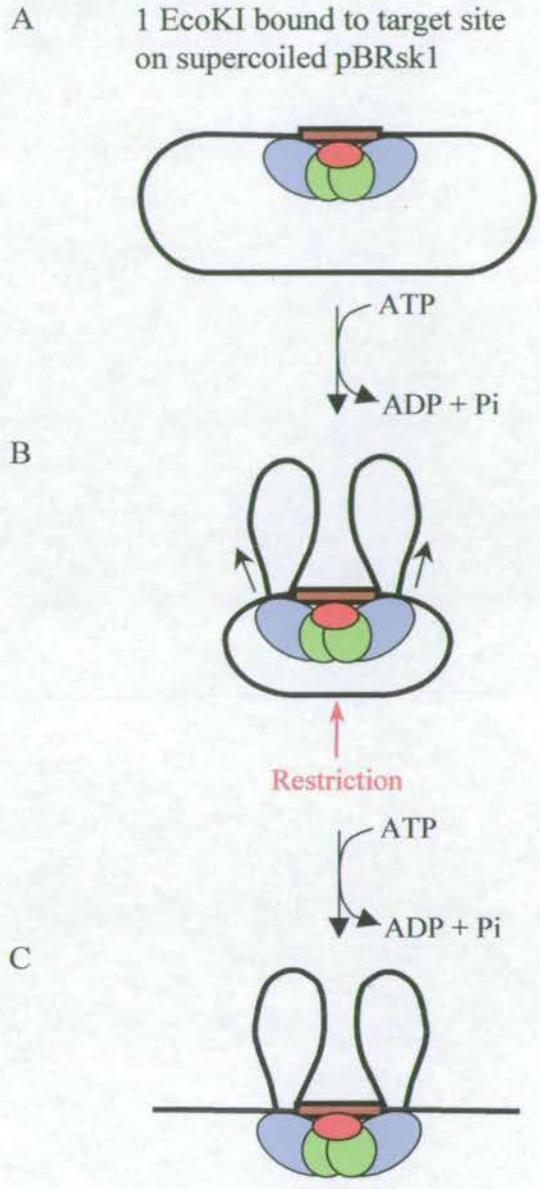

Figure 3.2. Diagram of EcoKI restriction of supercoiled pBRsk1. In this diagram, DNA is represented by a thick black line, EcoKI target sites are dark red rectangles, and EcoKI is made up of its subunits S (red oval), M (green ovals) and R (purple ovals). Although the DNA substrate is supercoiled, it is represented here as a relaxed open circle for clarity. A) EcoKI specifically binds to its target site. B) In the presence of ATP, EcoKI translocates the DNA towards itself from both directions whilst remaining bound to its target site, forming translocated loops of DNA. The loops produced are supercoiled but represented in relaxed conformation for clarity. When no more of the circular plasmid can be translocated, restriction is triggered. C) The cutting event is made up of 2 single-stranded nicking events. As the 2 nicks occur one after the other, this produces a relaxed nicked intermediate (not shown). The second nicking event produces linear DNA, where EcoKI remains bound to its target site. ATP hydrolysis continues after restriction.

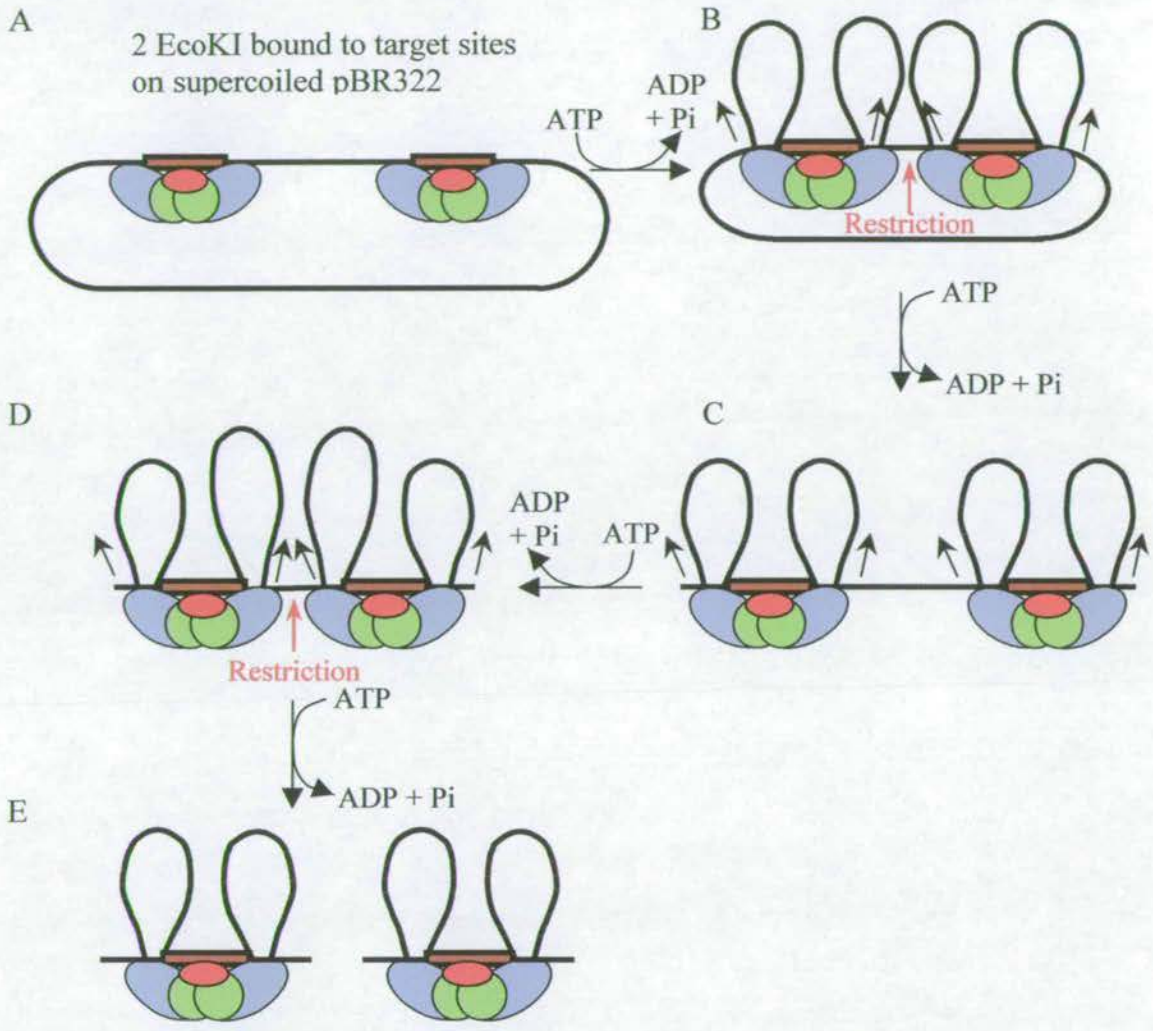

Figure 3.3. Diagram of EcoKI restriction of supercoiled pBR322. In this diagram, DNA is represented by a thick black line, EcoKI target sites are dark red rectangles, and EcoKI is made up of its subunits S (red oval), M (green ovals) and R (purple ovals). Although the DNA substrate is supercoiled, it is represented here as a relaxed open circle for clarity. A) Two EcoKI specifically bind to their target sites. Although dimerisation of the 2 bound EcoKI has been observed, this is not shown here for clarity. B) Upon addition of ATP, EcoKI translocates the DNA towards itself from both directions whilst remaining bound to its target site, forming translocated loops of DNA. The loops produced are supercoiled but represented in relaxed conformation for clarity. When the 2 EcoKI bump into each other, translocation is stalled, and restriction occurs. C) The cutting event is made up of 2 single-stranded nicking events. As the 2 nicks occur one after the other, this produces a relaxed nicked intermediate (not shown). The second nicking event produces linear DNA. D) The EcoKI molecules continue to translocate DNA, and bump into each again, on their other sides. This stalls translocation again and restriction occurs where they meet. This again occurs from 2 single-stranded nicking events. E) This produces 2 linear fragments of DNA, each with an EcoKI bound to its target site. EcoKI continues to hydrolyse ATP after restriction.

3.3.2. Observed products and time course of restriction

3.3.2.1. EcoKI restriction of supercoiled one-site pBRsk1

Figure 3.4 shows restriction of supercoiled pBRsk1 by EcoKI. The rapid conversion from supercoiled into nicked and then linear DNA can be seen in figure 3.4A and the accompanying densitometry of figure 3.4B. This data can be more clearly represented graphically as shown by figure 3.4C, where all supercoiled DNA can be seen to be digested after 450s. There is an initial increase in the fraction of nicked DNA after 60s, followed by a decrease as it is rapidly converted into linear DNA. The fraction of linear DNA increases after an initial lag, and levels off after around 600s, when the DNA has almost all been cut. The small lag between the loss of supercoiled DNA and the formation of linear DNA due to the presence of the nicked intermediate. This is due to the two separate single-stranded nicking events that EcoKI uses to linearise the DNA. Figure 3.4A also shows the linear product to be further digested after prolonged incubation. This is a commonly seen property of type I restriction enzymes when they are left for long periods with an excess of enzyme as discussed later.

3.3.2.2. EcoKI restriction of supercoiled two-site pBR322

Figure 3.5 shows restriction of supercoiled pBR322 by EcoKI. The rapid conversion from supercoiled (CCC) into nicked (OC) and linear (L) and then into linear fragments of DNA, which can be seen as a smear running down from the linear band, can be seen in figure3.5A and the accompanying densitometry of figure 3.5B. This data can be more clearly represented graphically as shown by figure 3.5C, where all supercoiled DNA can be seen to be digested after around 600s. There is an initial increase in the fraction of nicked DNA after 60s, followed by a decrease as it is rapidily converted into linear DNA. The fraction of linear DNA increases after an initial lag, before reaching a peak after around 150s and then decreasing and levelling off at a fraction of around 0.15 after 1800s, due to its conversion into linear fragments. The fraction of linear fragments increases rapidly after an initial lag of around 60s. After this, the fraction of linear fragments produced levels off at around 0.86 after 1800s. The reaction does not go to completion within the timeframe studied, as not all the linear DNA is restricted into linear fragments.

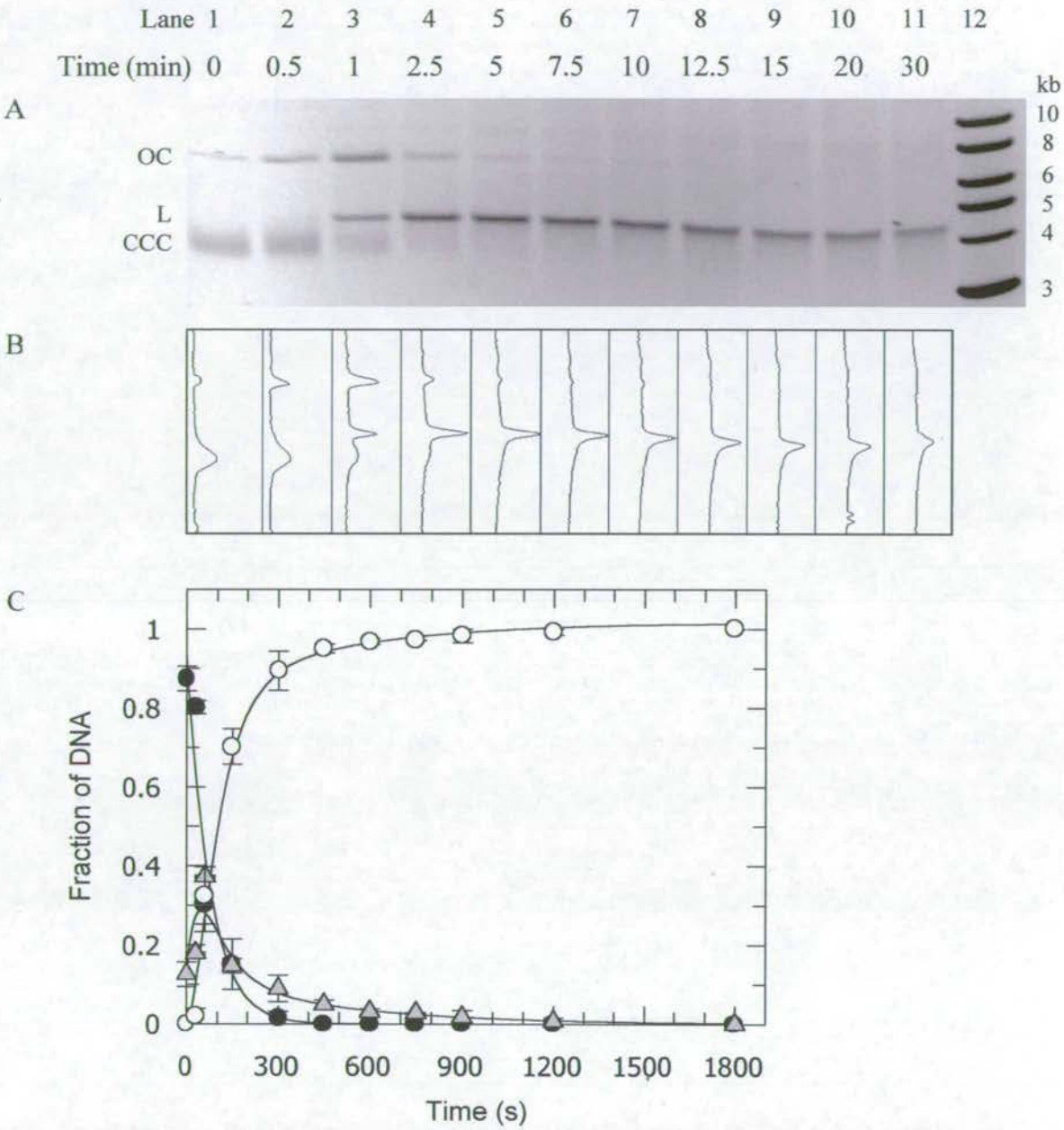

Figure 3.4. Restriction of supercoiled pBRsk1 by EcoKI. Degradation of 50nM supercoiled pBRsk1 by 67nM EcoKI in low salt EcoKI buffer, pH 7.9, with the ionic strength made up to 100mM with NaCl. A) Timecourse of EcoKI digestion of DNA with supercoiled (CCC) pBRsk1 being converted to nicked (OC) then to linear (L) DNA. Lane 1 contains a DNA 1kb ladder of sizes indicated. B) Densitometry of gel A as aligned, obtained using Scion Image software. C) Graph of conversion of CCC into OC and L over time. Curves were fitted to data using Dynafit software and a kinetic model described in the text. Points indicate the mean of 2 separate experiments.

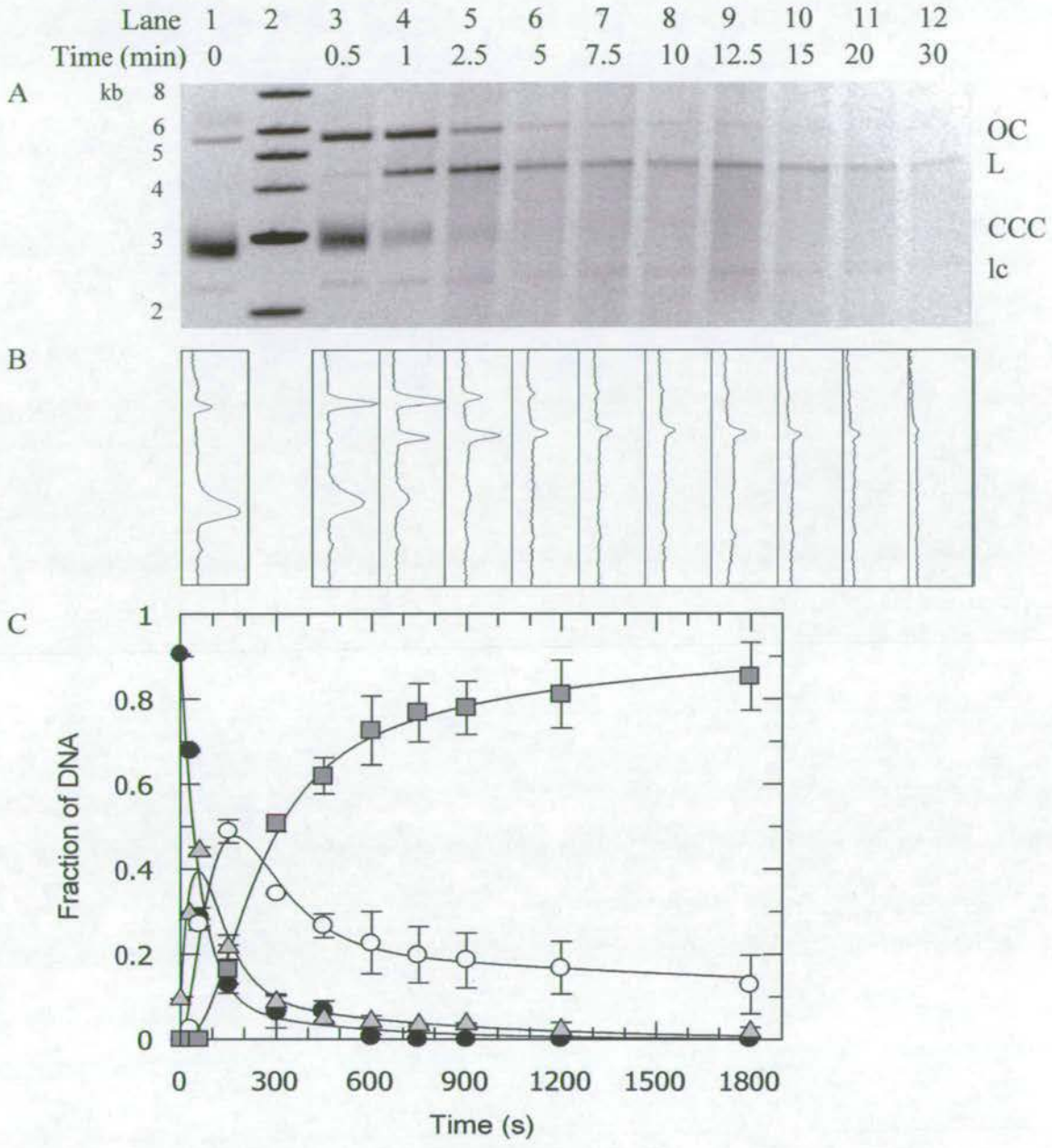

Figure 3.5. Restriction of supercoiled pBR322 by EcoKI. Degradation of 50nM supercoiled pBRsk1 by 134nM EcoKI in low salt EcoKI buffer, pH 7.9, with the ionic strength made up to 100mM with NaCl. A) Timecourse of EcoKI digestion of DNA with supercoiled (CCC) pBR322 being converted to nicked (OC) then linear (L), then to linear DNA fragments. Linear fragments of DNA can be seen as a smear running down from the linear band. Lane 2 contains a DNA 1kb ladder of sizes indicated. B) Densitometry of gel A as aligned, obtained using Scion Image software. C) Graph of conversion of supercoiled (black circles) into nicked (light grey triangles), linear (white circles) and linear fragments (dark grey squares) of DNA over time. Curves were fitted to data using Dynafit software and a kinetic model described in the text. Points indicate the mean of 2 separate experiments. A loading control can also be seen (lc) to indicate equal loading.

3.3.2.3. EcoKI restriction of linear two-site pBR322

Restriction of linear pBR322 by EcoKI is shown in figure 3.6. EcoRI-linearised pBR322 produces a specific banding pattern when cut with EcoKI. This produces a diffuse band at around 3.9kb, with a smear running from this. There is an absence of DNA seen between the linear pBR322 at 4.4kb and the restricted band at around 3.9kb. It can be seen under the reaction conditions used that not all linear pBR322 is cut by EcoKI after 20min. This can be seen more clearly in figure 3.6C, which shows an initial rapid cutting of DNA, which slows and levels off to a fraction of around 0.3 left uncut after 15min.

The fact that not all of the DNA is restricted is not due to a lack of enzyme as there is a sufficient amount to restrict all supercoiled pBRsk1 used at the same ratio of EcoKI:target sites. If one R subunit were inactive or dissociated, this would be observed as the production of a large amount of nicked DNA by supercoiled pBRsk1, which was not seen. However, although there is sufficient EcoKI to saturate the sites, it is possible that due to its binding equilibrium, EcoKI may be dissociating and re-associating with its target site prior to the onset of translocation. It is therefore possible that one EcoKI enzyme translocates past the other site when the second enzyme is not bound, leaving the translocating enzyme with no trigger for restriction.

3.3.2.4. EcoKI restriction of linear one-site pBRsk1

Restriction of linear one-site pBRsk1 by EcoKI is shown in figure 3.7. According to the model of restriction by Studier and Bandyopadhay (1988), linear DNA with only one target site should not be cut by EcoKI. However, this activity is seen during prolonged incubation with an excess of enzyme, as discussed previously. Figure 3.7A shows how the linear band of pBRsk1 is slowly digested into a smear of lower molecular weight. This slow digestion can be seen more clearly in figure 3.7C which shows that a fraction of around 0.2 of the DNA is digested after 30min.

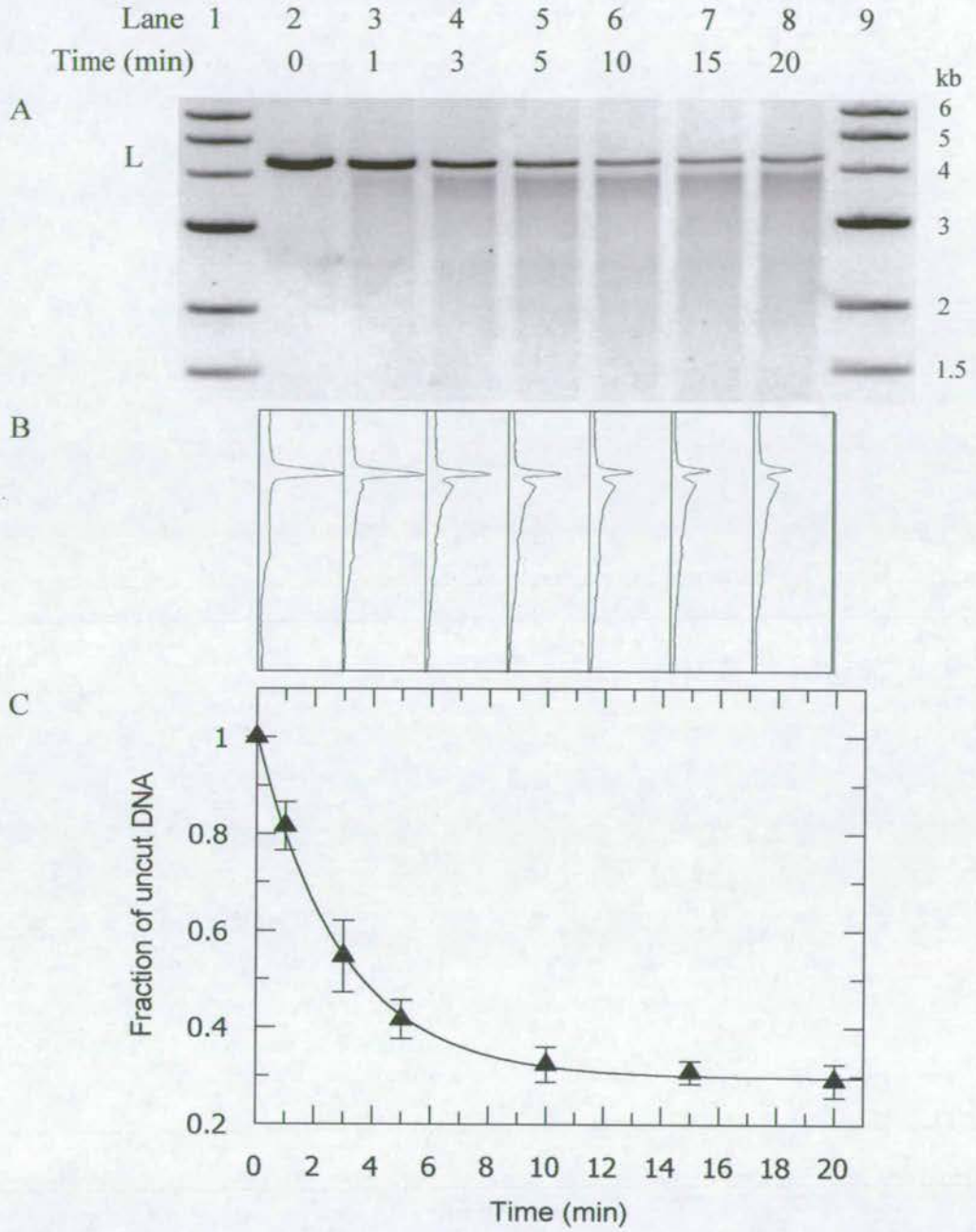

Figure 3.6. Restriction of linear pBR322 by EcoKI. Reactions were carried out in low salt EcoKI buffer, pH7.9, with the ionic strength made up to 100mM with NaCl. Concentrations of 50nM linear pBR322 and 134nM EcoKI were used. A) Agarose gel of linear pBR322 (L) being cut by EcoKI at specific time points. Linear pBR322 (L) is seen to be digested by EcoKI into a diffuse band at around 3.9kb with a smear from this, of lower molecular weight. Lanes 1 and 9 contain 1kb linear DNA marker of sizes indicated. B) Densitometry of aligned gel using Scion Image software. C) Graph showing the fraction of linear pBR322 cut with time. Points represent the mean of 4 separate experiments.

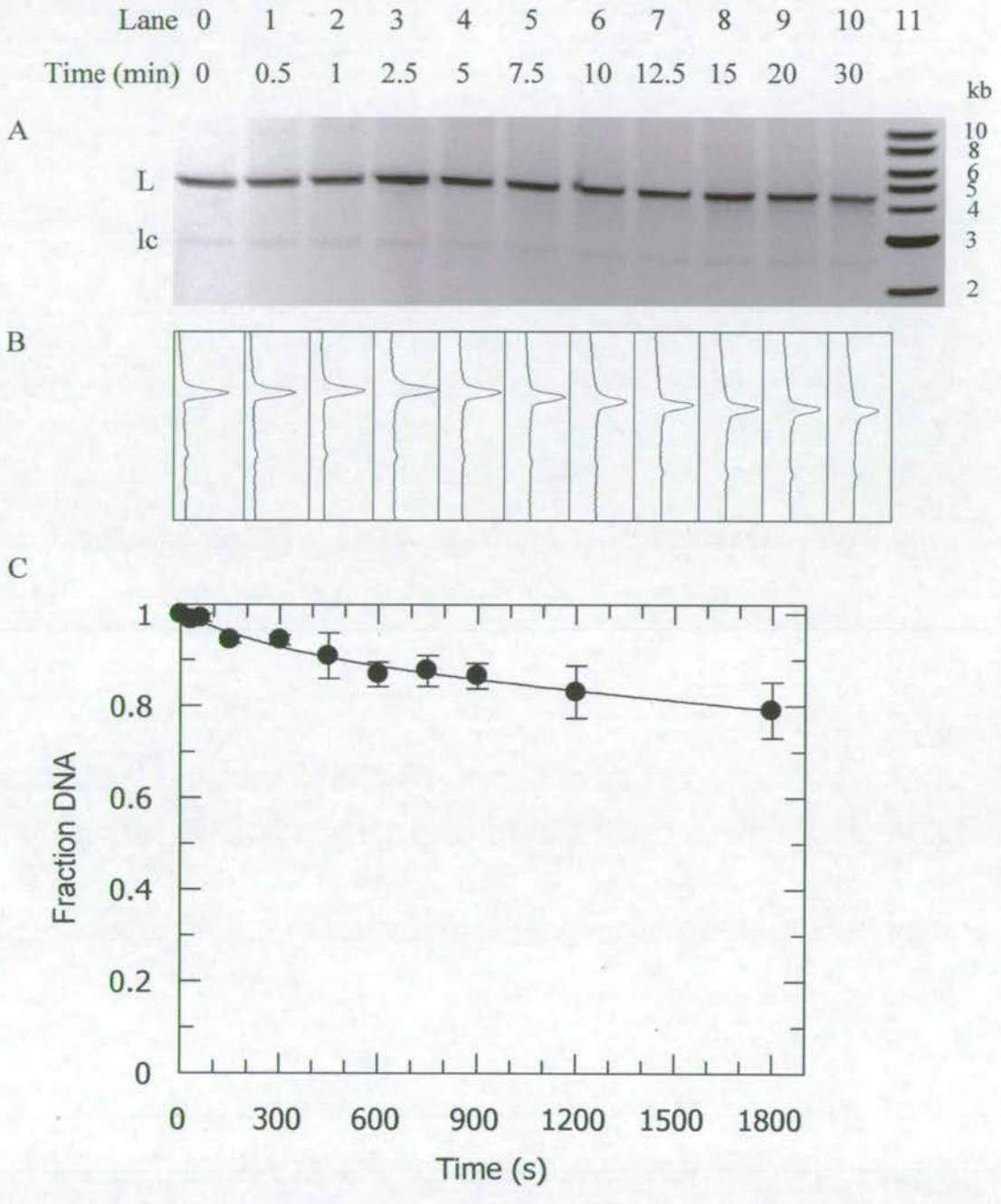

Figure 3.7. Restriction of linear pBRsk1 by EcoKI. Reactions were carried out in low salt EcoKI buffer, pH7.9, with 50nM linear pBRsk1 and 67nM EcoKI. A) Agarose gel of linear pBRsk1 (L) being cut by EcoKI at specific time points. EcoKI digests linear pBRsk1 into a diffuse smear of lower molecular weight. Lane 11 contains a 1kb linear DNA marker of sizes indicated. A loading control can also be seen (lc) to indicate equal loading. B) Densitometry of aligned gel using Scion Image software. C) Graph showing the fraction of linear pBRsk1 cut with time. Points represent the mean of 2 separate experiments.

3.4. Dynafit data fitting

All the densitometry data was fitted to the curves shown using the program Dynafit. Fitting of the data for the EcoKI restriction of all the various DNA substrates used the models shown above table 3.1. Fitting of the data for EcoKI restriction of one-site supercoiled pBRsk1 used a simple model where supercoiled plasmid was converted to nicked intermediate and linear product. However, EcoKI restriction of the other DNA substrates required more complicated models, where reversible steps are required to fit the data accurately. For example, the conversion of two-site linear pBR322 into linear fragments requires reversible steps to account for the fact that not all of the DNA is restricted. The DNA may therefore spend some time as an uncuttable intermediate (L*), which can become cleavable again by returning to the main pathway. The reasons for this complicated mechanism may be explained by the low concentration of EcoKI used, potentially allowing the possibility that both cutting sites may not be EcoKI-bound at the same time. This is analysed further in the discussion (Page 205). Similar mechanisms are required to describe the EcoKI restriction reactions of supercoiled two-site pBR322 and linear one-site pBRsk1 and can be accounted for by the same explanation as restriction of these substrates is also thought to require interaction of two EcoKI. These 'extra' reversible steps are also used to accurately describe the restriction of supercoiled one-site pBRsk1 when restriction is inhibited to such an extent that not all DNA is restricted (see later).

Table 3.1 indicates the rate constants calculated by Dynafit for the fitting of restriction data to these reaction mechanisms. It can be seen that in the restriction of supercoiled pBRsk1, the rate constant for the conversion of supercoiled to nicked DNA ($k1 = 0.01266 \pm 0.001 s^{-1}$), is lower than the rate constant for the conversion of nicked to linear DNA ($k2 = 0.0228 \pm 0.0059 s^{-1}$). This trend is also seen for the first two steps of restriction of supercoiled pBR322 ($k1 = 0.0162 \pm 0.006 s^{-1}$ and $k2 = 0.0185 \pm 0.0034 s^{-1}$), which are of similar magnitude to those of supercoiled pBRsk1. The rate constant for the restriction of linear pBR322 into linear fragments (from initial supercoiled pBR322 substrate) is much lower ($k3 = 0.0066 \pm 0.0013 s^{-1}$), although comparable to the rate constant for conversion of linear pBR322 to linear fragments (from initial linear pBR322 substrate) ($k1 = 0.0079 \pm 0.0007 s^{-1}$). The rate constant for the restriction of linear pBRsk1 is even lower ($k1 = 0.0004 \pm 2 \times 10^{-5} s^{-1}$), indicating the slow rate at which this reaction proceeds. Except for this reaction, the reversible steps are all of low magnitude with large associated errors compared to the rate constants of the main reaction pathway, thus indicating that the main reaction pathway is the favoured route for procession of these reactions.

Supercoiled pBRsk1 (CCC)

$$CCC \xrightarrow{k1} OC \xrightarrow{k2} L$$

Supercoiled pBR322 (CCC)

$$\begin{array}{ccccccc} CCC & \xrightarrow{k1} & OC & \xrightarrow{k2} & L & \xrightarrow{k3} & LF \\ k4 \updownarrow k7 & & k5 \updownarrow k8 & & k6 \updownarrow k9 & & \\ CCC^* & & OC^* & & L^* & & \end{array}$$

Linear pBR322 (L)

$$\begin{array}{ccc} L & \xrightarrow{k1} & LF \\ k2 \updownarrow k3 & & \\ L^* & & \end{array}$$

Linear pBRsk1 (L)

$$\begin{array}{ccc} L & \xrightarrow{k1} & Smear \\ k2 \updownarrow k3 & & \\ L^* & & \end{array}$$

	Rate constant (s^{-1})								
Substrate	k1	k2	k3	k4	k5	k6	k7	k8	k9
pBRsk1 CCC	**0.01266** ± 0.0010	**0.0228** ± 0.0059	-	-	-	-	-	-	-
pBR322 CCC	**0.0162** ± 0.006	**0.0185** ± 0.0034	**0.0066** ± 0.0013	**0.0010** ± 0.0016	**$2x10^{-14}$** ± 0.0005	**0.0013** ± 0.0002	**0.0025** ± 0.0020	**0.0015** ± 0.0009	**0.0002** ± 0.0004
pBR322 L	**0.0079** ± 0.0007	**0.0012** ± 0.0003	**$5.1x10^{-5}$** ± 0.0002	-	-	-	-	-	-
pBRsk1 L	**0.0004** ± $2x10^{-5}$	**0.00210** ± 0.0001	**0.00064** ± $9.6x10^{-5}$	-	-	-	-	-	-

Table 3.1. EcoKI rate constants and mechanisms of restriction of various DNA substrates using Dynafit. The rate constants of EcoKI restriction of supercoiled (CCC) and linear (L) DNA substrates containing one (pBRsk1) and two (pBR322) EcoKI target sites are shown in the table. The mechanisms of restriction used to produce these rate constants are shown above. These mechanisms were used to fit the data shown in figures 3.4C, 3.5C, 3.6C, and 3.7C.

3.5. EcoKI ATP hydrolysis activity

EcoKI translocates DNA with the concomitant hydrolysis of ATP. Two assays were used to analyse EcoKI translocation based on this property. The ATP coupled assay, indirectly measuring the rate of ATP decrease, and the P_i ATP hydrolysis assay, which measures the rate of production of P_i.

3.5.1. ATP coupled assay

The ATP coupled assay was used to look at ATP hydrolysis of EcoKI translocating supercoiled pBRsk1. Figure 3.8A shows an initial drop in absorbance at 340nm with addition of ATP. This is due to the addition of ADP within the ATP sample. This is quickly converted by the coupled enzymes into a decrease in NADH, as visualised by the decrease in absorbance at 340nm. The decrease in absorbance then levels off as all ADP has been converted. This levelling off time represents the lag time of the experiment, as no meaningful data can be derived from reactions until all contaminating ADP has been used up. After the initial decrease in absorbance, there is no ATP hydrolysis activity in the absence of EcoKI. Upon addition of EcoKI, the absorbance increases slightly, before quickly reaching a linear rate of decrease after around 30s after addition of EcoKI. This linear absorbance decrease is due to EcoKI ATP hydrolysis activity. The fact that the linear rate is not achieved immediately is thought to represent the binding of EcoKI to its target site. Figure 3.8B shows a higher initial absorbance in the presence of EcoKI, with the same initial rapid drop following addition of ATP. This is followed immediately by a slower linear rate of decrease in absorbance. This linear decrease is due to EcoKI ATP hydrolysis activity. The linear rate of absorbance decrease due to EcoKI is the same irrespective of whether EcoKI is added before or after ATP.

The ATP assays were therefore started by the addition of ATP, and the rate of ATP hydrolysis was measured after around 30s, after the initial drop in absorbance and once the rate had become linear. This method was used to look at the rates of ATP hydrolysis of EcoKI translocating different DNA substrates.

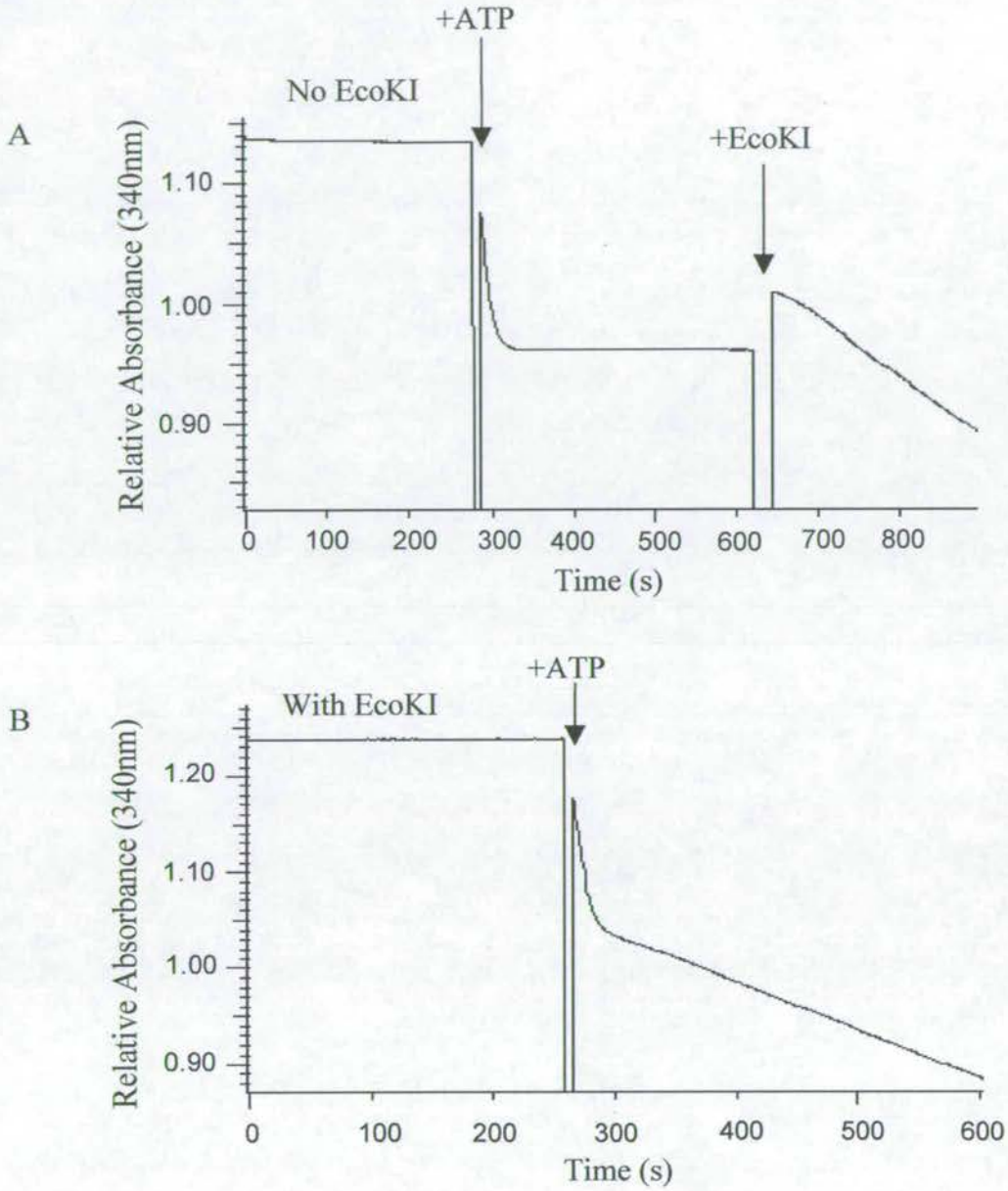

Figure 3.8. ATP hydrolysis coupled assay. Reactions were carried out in high salt EcoKI buffer, pH 7.9, with ATP regeneration system. 6nM supercoiled pBRsk1was used with 12nM EcoKI and 2mM ATP added as described. A) Graph showing reaction absorbance at 340nm over time with addition of ATP then EcoKI. B) Graph showing reaction absorbance at 340nm over time with EcoKI present from the start of the reaction, and addition of ATP.

3.5.1.1. EcoKI ATP hydrolysis activity with different DNA substrates

Figure 3.9 shows the effect of DNA substrate on ATP hydrolysis activity of EcoKI. ATP hydrolysis rates of 55±4nM/s, 88±4nM/s, 72±5nM/s and 74±4nM/s are achieved by 10nM EcoKI with substrates of 5nM supercoiled pBRsk1, 5nM linear pBRsk1, 2.5nM supercoiled pBR322 and 2.5nM linear pBR322 respectively. These correspond to ATP hydrolysis rates of around 11, 18, 15 and 15 ATP hydrolysed/EcoKI/s respectively.

The ATP hydrolysis rates measured here can be compared with those obtained using the same assay as described by Davies, (2000). In this work EcoKI hydrolysed ATP at a rate of around 105nM/s, 88nM/s and 70nM/s when incubated with 5nM supercoiled pBR322 and 5nM supercoiled and linear pBRsk1 respectively. Although the rates of hydrolysis are of similar magnitude, this shows that EcoKI hydrolyses ATP faster using supercoiled pBRsk1 than when linear pBRsk1 is the substrate. This is contrary to the results described in this thesis. These small irregularities in ATP hydrolysis rate could possibly be assigned to an inaccurate calculation of DNA concentration, or the different ionic composition of the DNA samples. The linearised DNA will also contain varying concentrations of denatured EcoRI, which may alter reaction rates, possibly due to the accompanying different concentrations of glycerol from the EcoRI stock.

3.5.1.2. Effect of EcoKI concentration on ATP hydrolysis rate

Figure 3.10 shows that increasing the EcoKI concentration from an EcoKI:target site ratio of 2 to 12 increases the ATP hydrolysis activity of EcoKI, with all substrates studied. As EcoKI can only hydrolyse ATP when bound specifically to its target site (Davies, 2000) all sites should be saturated at a concentration of 2 EcoKI per site.

This can be explained if increasing the EcoKI concentration increases the binding of EcoKI to its target site. As binding and release of EcoKI to its target will be in equilibrium, increasing the EcoKI concentration will favour binding. More EcoKI would be specifically bound to the DNA and therefore more EcoKI would be capable of hydrolysing ATP. This agrees with the finding that lower 'saturating' levels of EcoKI do not fully restrict DNA with two target sites (for examples see figures 3.5 and 3.6).

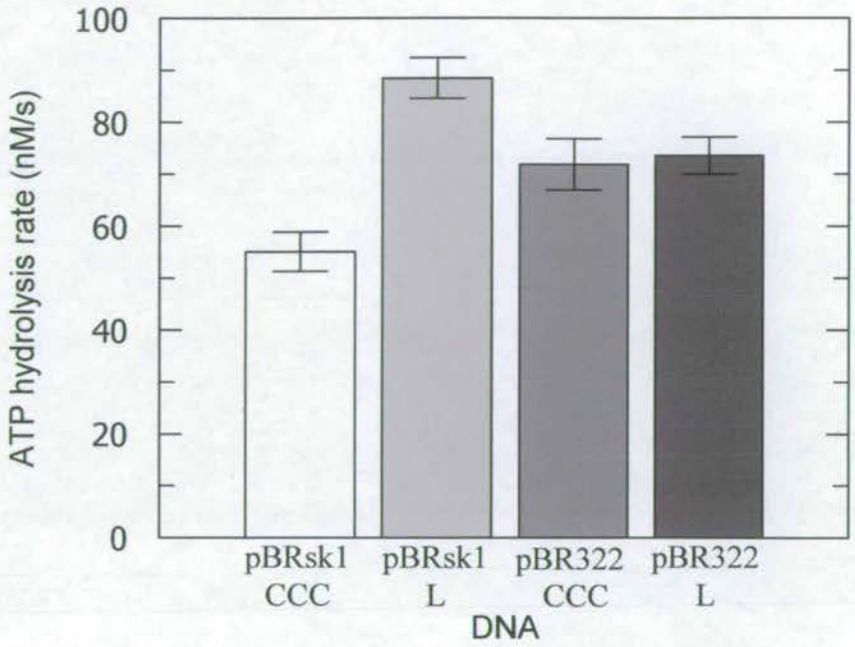

Figure 3.9. ATP hydrolysis rate of EcoKI with different DNA substrates. The reactions were carried out in high salt EcoKI buffer, pH 7.9, with 5nM EcoKI target sites in DNA (5nM pBRsk1, 2.5nM pBR322), 10nM EcoKI and 2mM ATP. The rate of ATP hydrolysis is shown when EcoKI is bound to supercoiled pBRsk1 (white), linear pBRsk1 (light grey), supercoiled pBR322 (dark grey) and, linear pBR322 (black). The results represent the mean of 3 separate experiments.

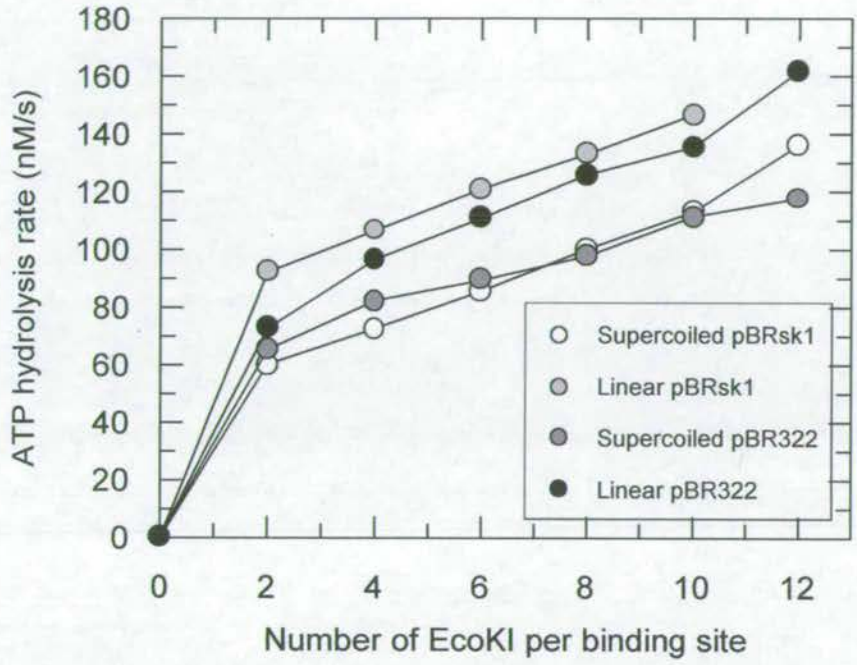

Figure 3.10. Effect of EcoKI concentration on rate of ATP hydrolysis. The reactions were carried out in high salt EcoKI buffer, pH 7.9, with 5nM EcoKI target sites of DNA (5nM pBRsk1, 2.5nM pBR322) and 2mM ATP. The graph shows the effect of increasing the EcoKI concentration on the rate of EcoKI ATP hydrolysis with supercoiled pBRsk1 (white circles), linear pBRsk1 (light grey circles), supercoiled pBR322 (dark grey circles) and, linear pBR322 (black circles).

It is also possible that a fraction of the enzyme is inactive, whereby increasing the EcoKI concentration would allow the specific binding and ATP hydrolysis activity of active species. However, as all supercoiled pBRsk1 is restricted by only a small excess of EcoKI (a ratio of EcoKI:DNA sites of 1.34:1) (see figure 3.4), the finding that an excess of up to 10 EcoKI per DNA site increases ATP hydrolysis activity is unlikely to be fully accounted for by inactive enzyme.

3.5.1.3. EcoKI restriction activity in ATP coupled assay buffer

Figure 3.11 shows restriction of linearised pBR322 by EcoKI in the same ATP regenerating buffer as used for the ATP hydrolysis coupled assay. When compared to figure 3.6 of restriction of linear pBR322 by EcoKI in low salt EcoKI buffer, the same banding patterns can be seen. Restriction occurs at a faster rate in the ATP regenerating buffer compared to low salt EcoKI buffer. More of the linear DNA is restricted after 20min, although the reaction still does not go to completion. These differences can be explained if the either the decrease in ATP, or increase in ADP and P_i, as ATP is hydrolysed by EcoKI, limit the rate of EcoKI translocation. This indicates that the reactions taking place in the ATP hydrolysis coupled assay is comparable to the situation observed in the restriction assays.

However, another ATP hydrolysis assay was developed in order to look at EcoKI ATP hydrolysis activity under identical conditions to the restriction assays.

3.5.2. P_i ATP hydrolysis assay

The results in figure 3.12 show how the amount of P_i produced by EcoKI varies with time. It can be seen that an initial rapid production of P_i is followed by a reduction and levelling off of the amount of P_i produced. This reduction in rate is possibly due to the use ATP, which will become limiting as it runs out, and/or due to the production of ADP and P_i, which may inhibit reactions. In order to eliminate these factors, the initial rate of reaction was measured.

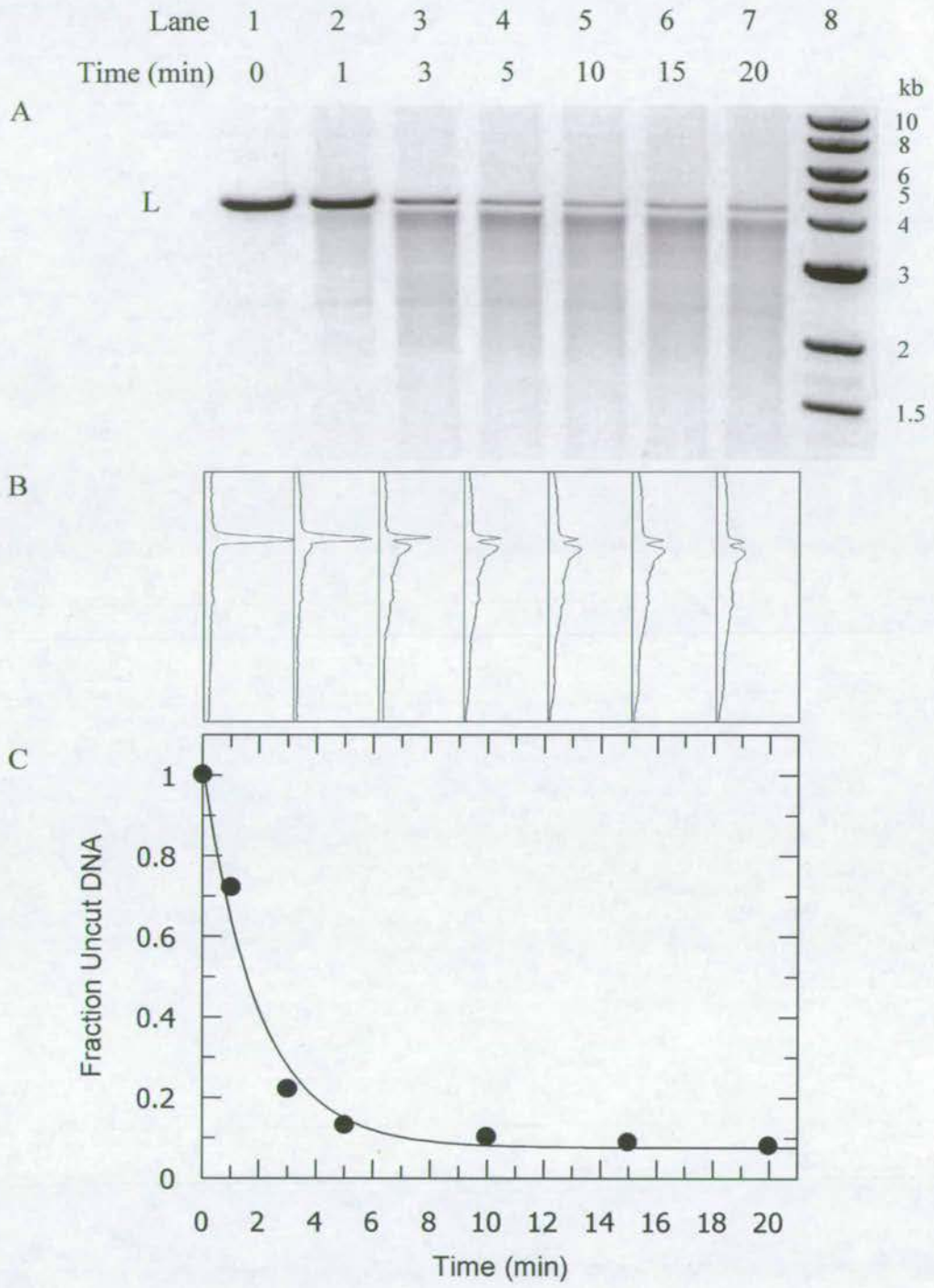

Figure 3.11. Effect of ATP regeneration buffer on EcoKI restriction of linear pBR322. Reaction was carried out using the same buffer as for ATP hydrolysis coupled assay, with 2.5mM NADH (instead of 250μM), pH 7.9, with 50nM DNA, and 134nM EcoKI. A) Linear pBR322 (L) can be seen to be restricted into lower molecular weights fragments with time. Lane 8 contains a linear 1kb DNA marker of sizes indicated. B) Densitometry of gel A, as aligned, using Scion Image software. C) Decrease in fraction of linear pBR322 with time, shown graphically.

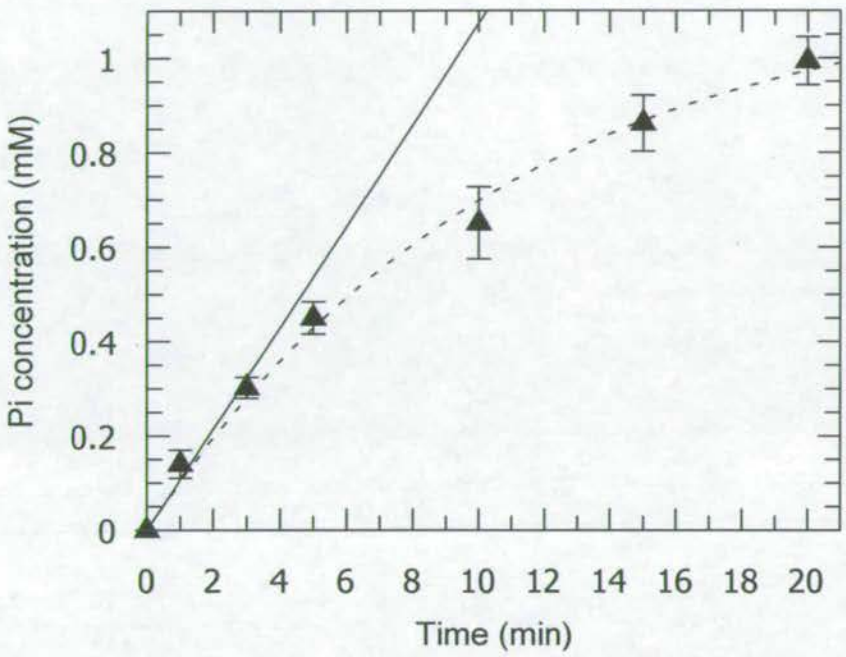

Figure 3.12. The production of P_i by EcoKI. Reactions were carried out with 50nM linear pBR322, 134nM EcoKI and 2mM ATP in low salt EcoKI buffer, pH 7.9, with the total ionic strength made up to 100mM with NaCl. Reactions were stopped with EDTA and absorbances measured at 630nm after 100s incubation with mixed reagent. The absorbances at 630nm were converted into P_i concentrations by using known concentrations of KH_2PO_4 to produce a calibration graph (as shown in figure 7.2). The graph shows the amount of P_i produced by EcoKI over time. The complete line represents the initial rate of reactions. All points represent the mean of 4 separate experiments.

The initial rate of production of P_i by 134nM EcoKI with 50nM linearised pBR322 is 1.8μM/s, which corresponds to a rate of around 21 ATP hydrolysed/EcoKI/s. This value is close to that obtained for EcoKI ATP hydrolysis of linearised pBR322 using the ATP hydrolysis coupled assay (15 ATP hydrolysed/EcoKI/s), as described in section 3.5.1.1.

This assay has also been carried out using EcoR124I by Janscak *et al.*, (1996). In these experiments, 10nM enzyme was used with an excess of DNA, with 10mM ATP. Their results showed an initial rapid linear increase in the P_i concentration to around 0.22mM after 2min. The rate of increase thereafter begins to level off, with around 0.7mM P_i produced after 15min. The shape of the curve produced is the same as that obtained for EcoKI in figure 3.12. The initial rate of P_i produced by EcoR124I (~1.9μM/s) is similar to that produced by EcoKI (1.8μM/s). However, 10 times less EcoR124I is used to produce these results than is used for EcoKI.

The fact that the production of P_i by EcoR124I levels off at around 0.7mM after 15min suggests that the decrease in ATP concentration is not the limiting factor for this reaction, as 10mM ATP was used. However, the production of ADP or P_i could still have an inhibitory affect on the ATP hydrolysis activity, causing the P_i production to level off.

Figure 3.13 shows the increase in P_i production by EcoKI over time with short initial time points. These shorter time points show that the initial rate of the reaction is linear. There is no initial lag seen under these experimental conditions.

The initial rate was calculated for the first 51s of the reaction alone, as well as for the full 20min reaction with and without the first 51s set of time-points. Each set of data points produced the same initial rate of ATP hydrolysis (data not shown). It is therefore reasonable to use the initial rate of a 20min reaction, without the need for very short time points over the first 51s, to accurately calculate the initial reaction rate for P_i ATP hydrolysis experiments.

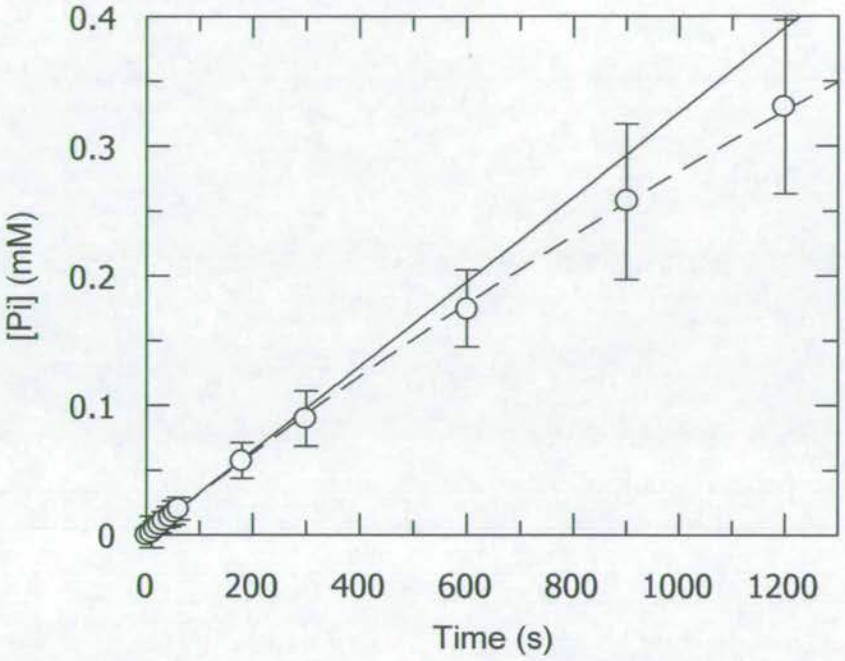

Figure 3.13. Production of P_i by EcoKI over short time points. Reactions were carried out with 50nM supercoiled pBRsk1 and 67nM EcoKI in NEB buffer 4, with 4mM ATP and 0.2mM SAM. The graph shows the amount of P_i produced by EcoKI over time. The complete line represents the initial rate of reactions. All points represent the mean of 6 separate experiments.

3.6. EcoKI cutting site location

The model of Studier and Bandyopadhyay, (1988), predicts that type I restriction enzymes cut the DNA when their translocation is stalled. Therefore a single EcoKI on a one-site supercoiled plasmid should cut the DNA about half way around the plasmid from its target site, if both R subunits are translocating DNA at the same rate. However, random cutting has been reported for this situation with EcoR124I (Szczelkun *et al.*, 1997) and EcoAI (Janscak *et al.*, 1999). The model also predicts that type I restriction of a two-site linear DNA substrate should occur about half way between target sites. This has been well reported in the literature (for examples see, Dryden *et al.*, 1997; Studier and Bandyopadhyay, 1988) but cutting around the target site has also been seen (Szczelkun *et al.*, 1997; and reviewed in Szczelkun 2002). It is the aim of this section to identify the cutting sites of EcoKI using single site supercoiled plasmids (pBRsk1) and two-site linearised DNA (pBR322) under the same conditions as the restriction assays.

3.6.1. Location of cutting site on supercoiled pBRsk1

Firstly, supercoiled pBRsk1 was cut with EcoKI and then restricted by either EcoRI or BsgI in order to locate the cutting site. Figure 3.14A shows that supercoiled pBRsk1 was only partially restricted with EcoKI as to not allow time for the EcoKI to digest the linear DNA produced into a smear. The EcoKI restriction products can be seen as linear, nicked and supercoiled DNA. After inactivation of EcoKI, these species were further restricted by EcoRI. This produced a linear band from restriction of the nicked and supercoiled substrates. A smear was also produced by restriction of the linear substrates. The same method was used to digest EcoKI-restricted pBRsk1 with BsgI. This also produced full length linear DNA from the partially restricted nicked and supercoiled species, and a smear from the linear products.

The fact that a smear is produced from both EcoRI and BsgI, with their respective cutting sites separated by around 1.64kb, shows that EcoKI cuts supercoiled pBRsk1 at random sites throughout the plasmid.

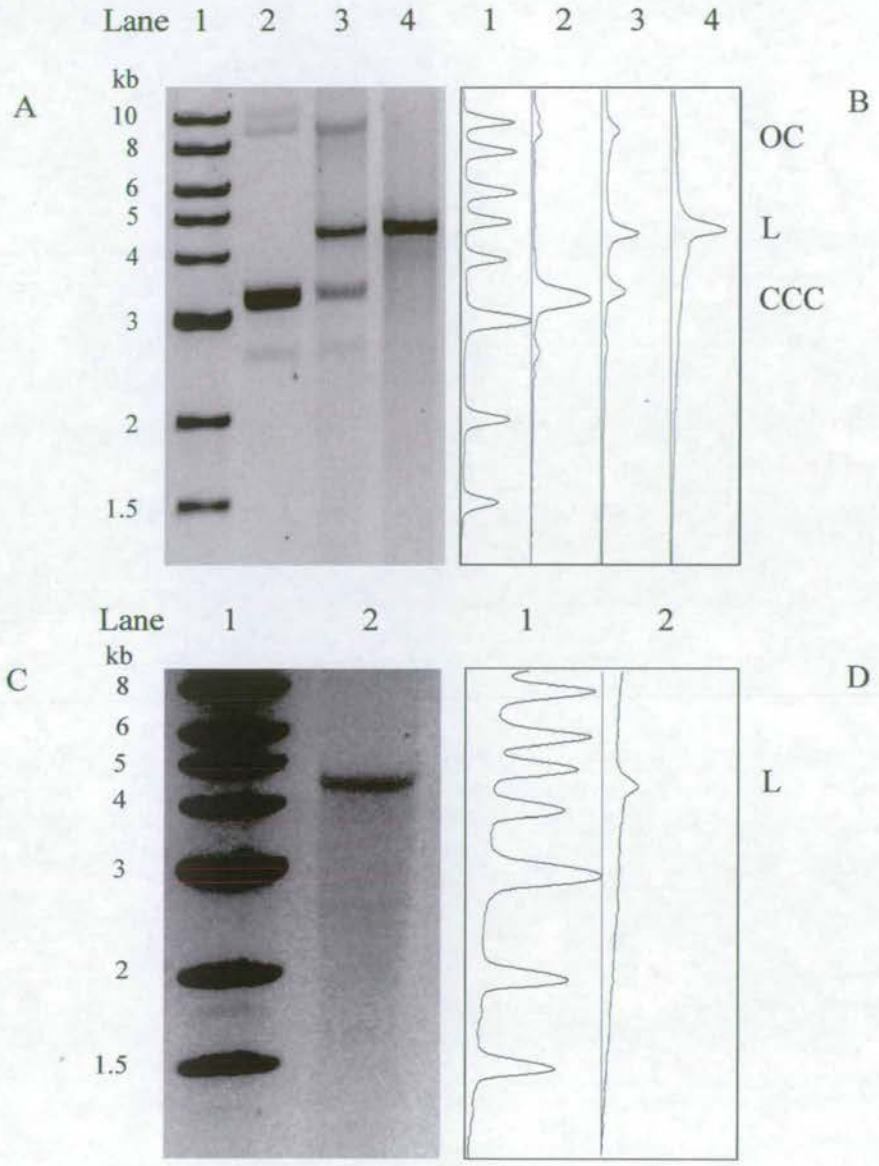

Figure 3.14. Double digestions of supercoiled pBRsk1. A) Gel showing supercoiled pBRsk1 (lane 2). This was restricted by EcoKI in low salt EcoKI buffer, pH 7.9 (lane 3). This partial restriction produced linear, nicked and supercoiled bands. Lane 4 shows the result of further digestion with EcoRI, producing a linear band and a smear of lower molecular weight species running down from this. Lane 1 contains a linear 1kb DNA marker of sizes indicated. B) Densitometry of gel A as aligned, using Scion Image software. C) Gel showing digestion of EcoKI-restricted pBRsk1 with BsgI (lane 2). Restriction with BsgI produces linear DNA (L) as well as a smear of lower molecular weight running down from this. Lane 1 contains a linear 1kb DNA marker of sizes indicated. D) Densitometry of gel C, as aligned, using Scion Image software.

3.6.2. Location of EcoKI cutting sites on linear pBR322

The position of EcoKI target sites and selected type II restriction enzyme cutting sites are shown in figure 3.15A. Restriction of pBR322 by these type II enzymes produces linear DNA with various distances between free ends and target sites. Further restriction of these linear substrates by EcoKI allow the identification of cutting sites of EcoKI. pBR322 that has been linearised by EcoRI, BamHI, SalI and BsgI will contain EcoKI target sites in head-to-head orientation. pBR322 linearised by PvuI will have its EcoKI target sites in tail-to-tail orientation.

Figure 3.16A shows that supercoiled pBR322 was successfully linearised by the different type II restriction enzymes. All reactions went to completion except for SalI, which left a small amount of unrestricted supercoiled plasmid. These linear species of pBR322 were then cut by EcoKI, in high salt EcoKI buffer, revealing different banding patterns shown in figure 3.16B. However, it should be noted that although these bands are prominent, much of the DNA is smeared, indicating that cutting occurs at various positions. By comparison of the sizes of fragments produced from the different linear species used, it is possible to locate the cutting sites of EcoKI on pBR322 that are responsible for the banding patterns observed.

This experiment was repeated in low salt EcoKI buffer, with the same banding patterns produced (data not shown). The following band sizes were produced when pBR322 was cut by EcoKI after being cut by a specific type II restriction enzyme: EcoRI produced a band of 3.9kb; BamHI produced a band of 3.4kb; SalI produced a band of 3.2kb; BsgI produced bands of 4.1kb and 2.3kb and; PvuI produced bands of 3.9kb and 2.3kb.

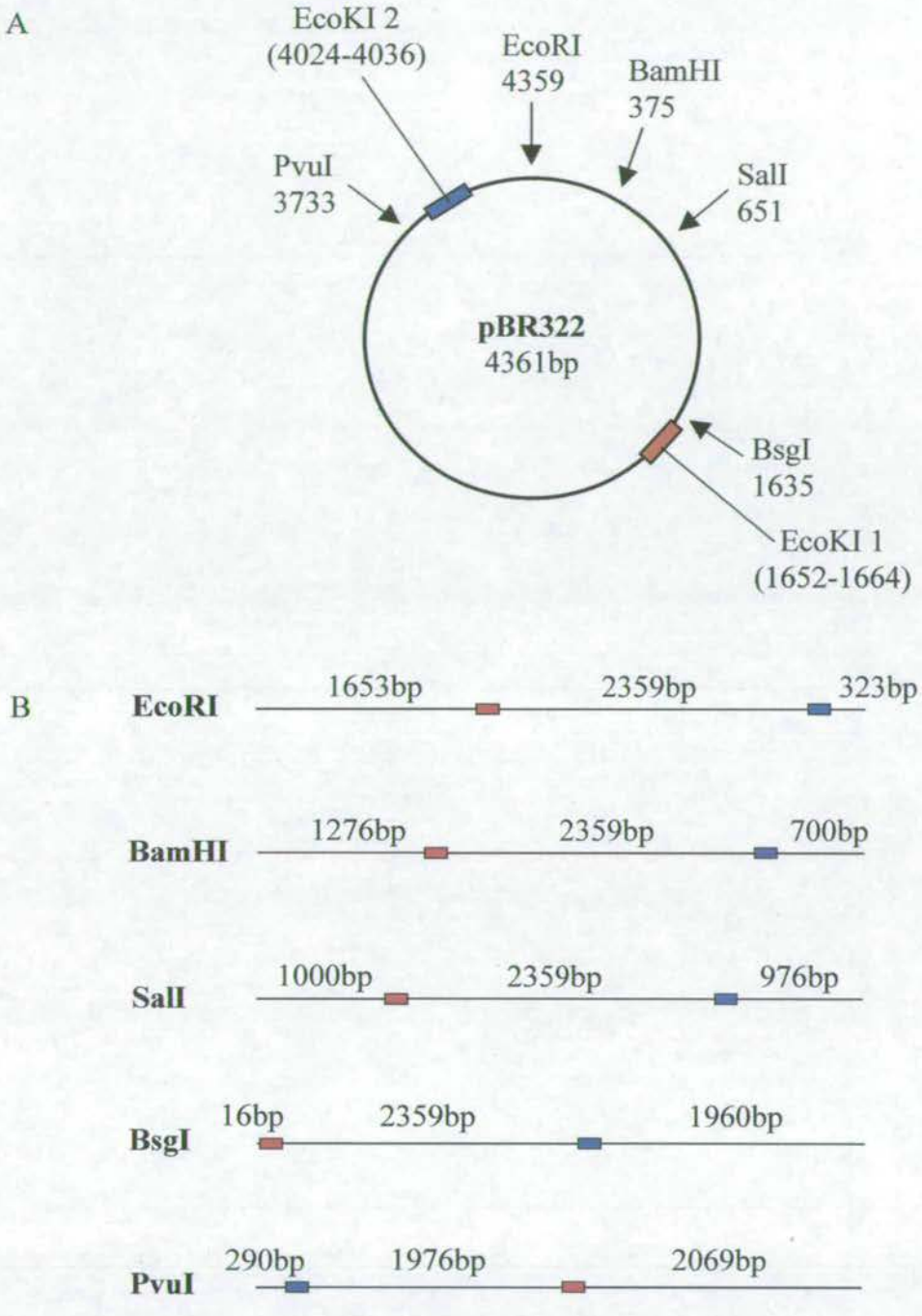

Figure 3.15. Restriction sites of different type II enzymes on pBR322, in relation to EcoKI target sites. A) Representation of plasmid pBR322 (black circle) with selected type II restriction cutting sites (arrows) and EcoKI target sites (dark red and blue rectangles). B) Representation of pBR322 after linearisation with selected type II restriction enzymes. Distances given indicate number of base pairs between the 2 EcoKI target sites(dark red and blue rectangles), and between EcoKI target sites and a free end. Cutting sites were obtained from NEB cutter (http://tools.neb.com/NEBcutter2/index.php).

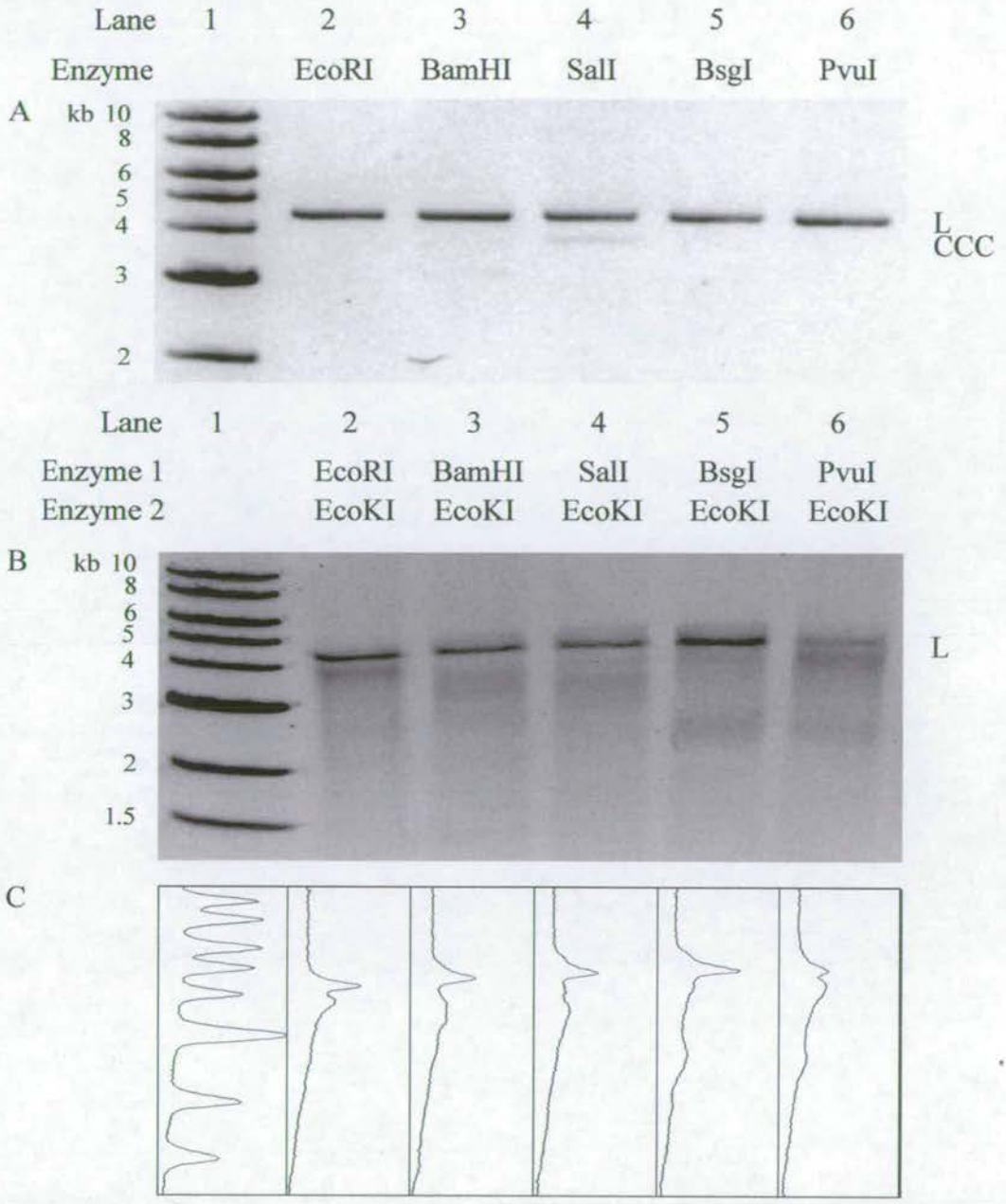

Figure 3.16. Location of EcoKI cutting site on pBR322. Reactions were carried out in high salt EcoKI buffer, pH 7.9. A) Gel showing restriction of pBR322 by different type II restriction enzymes. Each enzyme has only 1 cutting site on pBR322 and so produces full length linear DNA (L). A small amount of uncut supercoiled plasmid (CCC) can be seen to be left in lane 4 after incomplete digestion by SalI. Lane 1 contains a linear 1kb marker of sizes indicated. B) Gel showing Type II-linearised DNA after further digestion by EcoKI. Lane 1 contains a linear 1kb DNA marker of sizes indicated. C) Densitometry of Gel B, as aligned, using Scion Image software.

These sizes of bands can be explained by EcoKI restriction at positions shown in figure 3.17. If EcoKI cut pBR322 at the positions shown by the arrows, linear fragments of the sizes seen on the gel in figure 3.16B would be observed. These results clearly show that the bands are produced by cutting in close proximity to the EcoKI target sites. The mean distance of restriction from the target sites is 189±73bp. However, the measurement of the sizes of bands produced is made by comparison to a 1kb linear DNA marker. The actual size of the band produced is therefore an approximation to within 100bp. Also, the bands produced are broad, and the middle of the band is therefore used to indicate its mean size. It is possible that cutting at sites other than those indicated would also produce bands of the sizes observed. However, the majority of cutting at these sites would not occur between the two EcoKI sites, and therefore could not be explained by the model produced by Studier and Bandyopadhyay, (1988).

The banding patterns produced under the experimental conditions described may be different under different conditions. However, the same banding patterns were observed with high and low salt EcoKI buffer. EcoKI cutting at around its target site therefore represents the enzyme's behaviour under the same conditions as for the restriction and ATP hydrolysis assays. It should also be noted that the restriction reaction with EcoKI did not go to completion, as most DNA was left uncut. The smearing observed in figure 3.16B also indicates that not all the cutting occurs around the target sites, but also takes place at other locations on pBR322.

The Studier and Bandyopadhyay model indicates that two translocating type I enzymes should meet each other about half way between their target sites if they are translocating DNA at the same rate. However, the results described where cutting occurs beside one of the target sites could be explained by the possibility that EcoKI translocates all the intervening DNA between two target sites before bumping into the other EcoKI which has not begun translocating. This would cause restriction at the target site of the non-translocating enzyme.

The fact that cutting at around the target site was not observed for single-site supercoiled pBRsk1 agrees with this idea, as the two translocating R subunits of the same enzyme are less likely to be out of sync with each other than different R subunits from two separate enzymes. However, they also cannot be translocating at exactly the same time as this would have produced a band from restriction of the plasmid at about half way around the plasmid. The fact that Szczelkun *et al.*, (1997) observed cutting at around the target sites for EcoR124I may reflect the ability of this enzyme to completely dissociate from one of its R subunits (Seidel *et al.*, 2004).

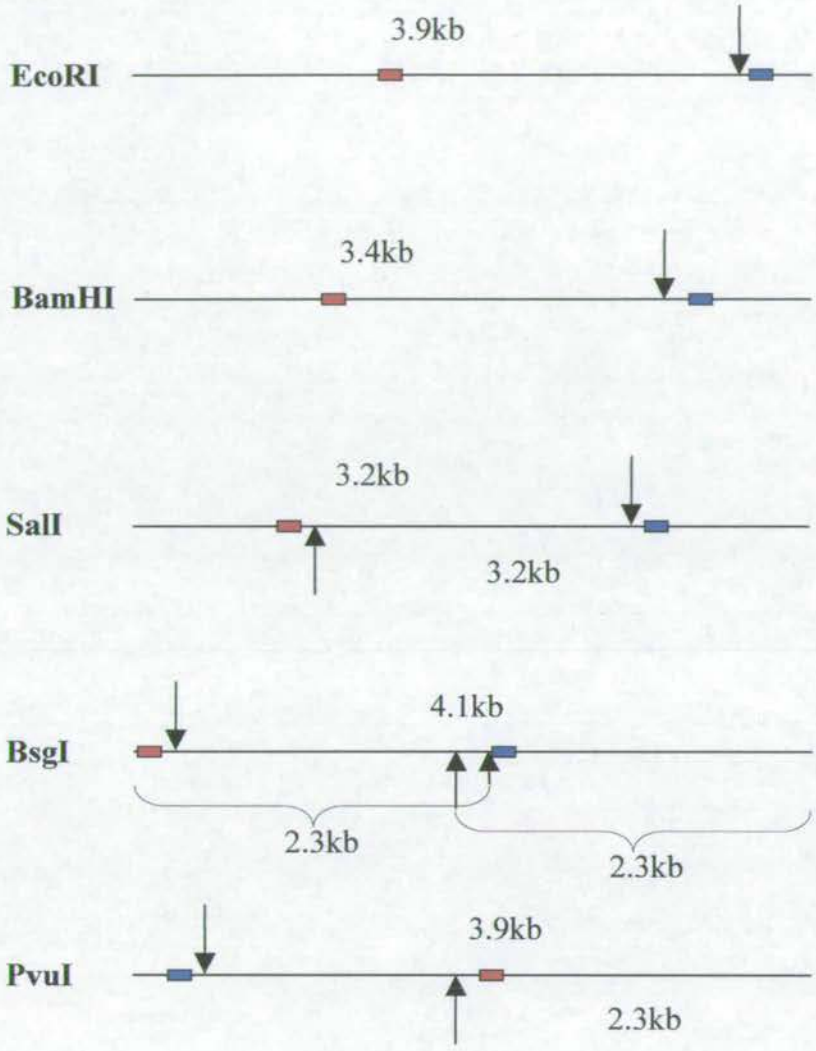

Figure 3.17. Possible cutting sites for EcoKI on linear pBR322. pBR322 DNA that have been linearised by the type II restriction enzymes indicated are represented by black lines. EcoKI target sites are represented by dark red and blue rectangles. The distances between target sites and free ends are the same as shown in figure 3.15. The sizes of fragments produced by restriction by EcoKI, as seen in figure 3.16, are estimated from comparison with 1kb linear DNA size marker, and can be accounted for by cutting at the positions shown, represented by arrows. The sizes of fragments produced by cutting at these sites are indicated.

It is possible that as this restriction appears to take place around 189±73bp from the target site, that EcoKI may have a larger footprint than expected. This is because restriction should occur where the two R subunits meet, thereby implying that the non-translocating R subunit introduces its cut 189±73bp from its target site without moving. However, the accuracy of these measurements is limited, as discussed earlier (section 3.6.2).

3.6.3. EcoKI binding and restriction of small two-site linear fragments

3.6.3.1. Formation and restriction of two-site fragments

As EcoKI has to translocate its DNA substrate large distances in order to restrict pBR322, primers were designed to produce small linear fragments of DNA, with varying distances between two EcoKI target sites. It was thought that restriction of these smaller substrates might further elucidate the cutting position of EcoKI.

Figure 3.18 shows that DNA products of expected sizes were produced by PCR and contain two EcoKI target sites. PCR product AB is 105bp, with 34bp between target sites. AC is 138bp with 67bp between target sites. AD is 188bp with 117bp between target sites. AG is 388bp with 317bp between target sites. All these substrates will contain EcoKI target sites in tail-to-tail orientation.

Figure 3.19 reveals ATP hydrolysis activity of EcoKI with each of the two-site fragments, indicating that EcoKI is able to bind to at least one of the specific target sites present on each substrate and hydrolyse ATP.

Restriction of these short substrates with EcoKI are shown in figure 3.20. Only substrate AG appears to be restricted by EcoKI. Upon incubation with EcoKI, AG is restricted and forms a smear of between 100-200bp, as well as a less intense smear at around 250bp. Although all samples incubated with EcoKI, appear to produce slightly less intense bands than without EcoKI, no other bands or smears are visible. Therefore AB, AC and AD do not appear to be restricted, with the reduction in intensity possibly due to a fraction of the DNA-bound EcoKI sticking to the reaction tube. It is possible that fragments AB, AC and AD can only bind a single EcoKI, thereby preventing restriction.

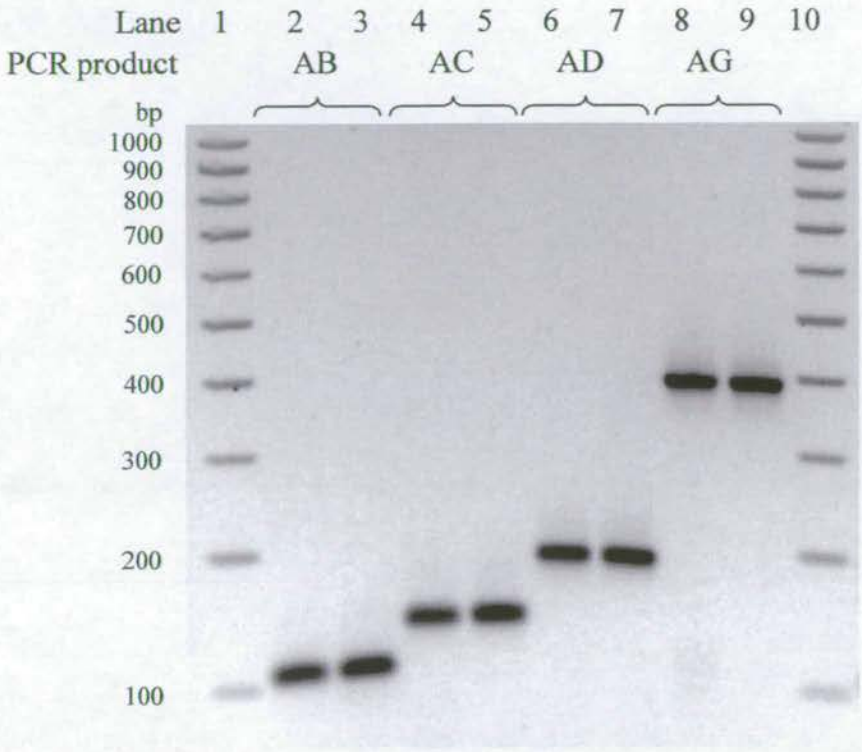

Figure 3.18. PCR products of various sizes, containing 2 EcoKI target sites. PCR reactions were carried out, using 33 cycles of 95°C 1min, 54°C 1min, 72°C 1min, with 2μM each primer and supercoiled pBRsk1 template. PCR products AB, AC, AD, and AG were formed using primers A + B, A + C, A + D, and A + G respectively. PCR products were run on a 2.5% agarose gel, with EtBr staining. Lanes 1 and 10 contain linear 100bp DNA markers of sizes indicated.

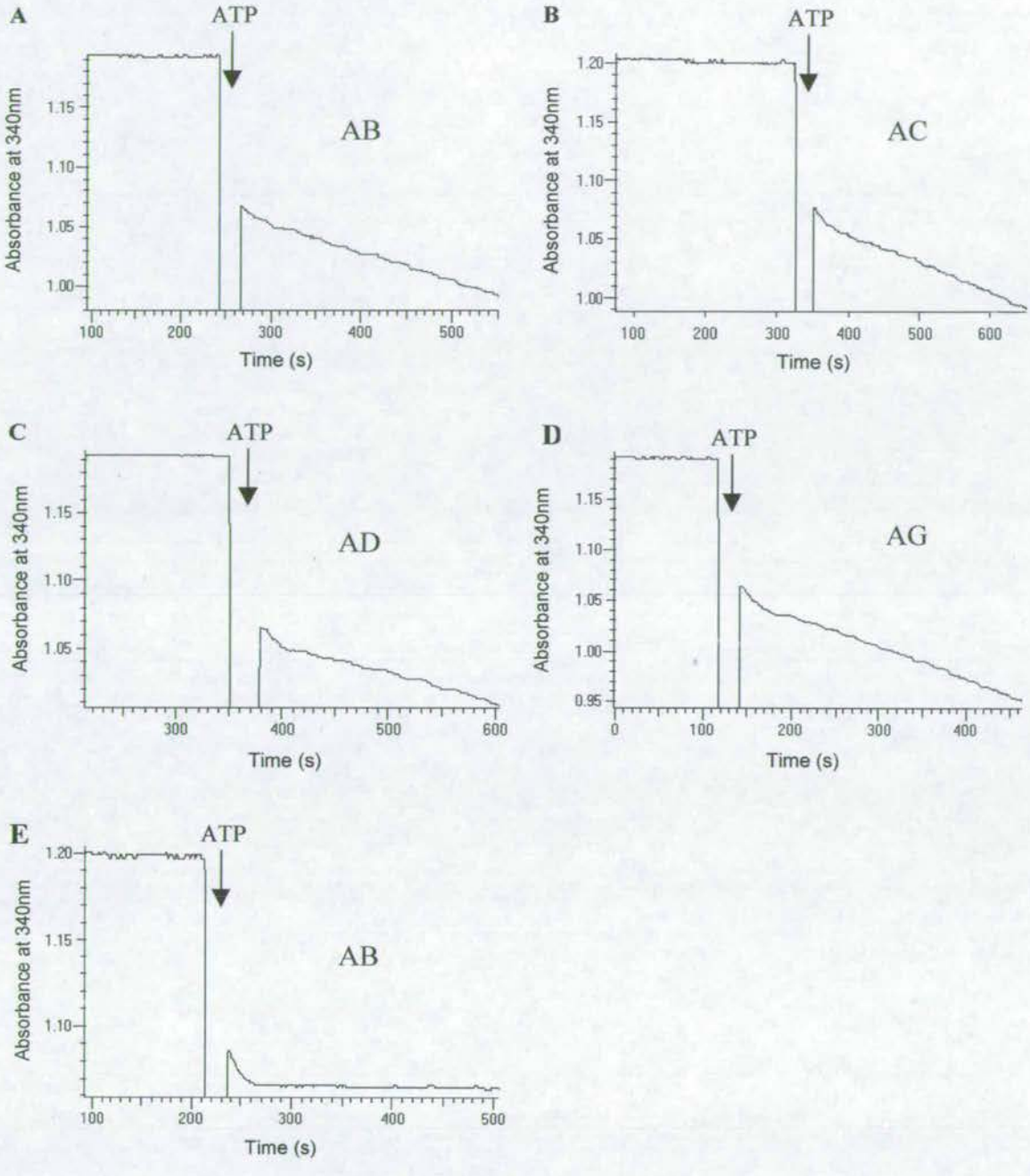

Figure 3.19. ATP hydrolysis coupled assay of short DNA fragments with two EcoKI sites. Reactions were carried out in high salt EcoKI buffer, pH 7.9, with ATP regeneration system. 5nM AB (A), AC (B), AD (C), AG (D) was used with 10nM EcoKI and 2mM ATP added as described. 2mM ATP was also added to 5nM AB in the absence of EcoKI (E) as a control. The decrease in absorbance at 340nm with time indicates hydrolysis of ATP.

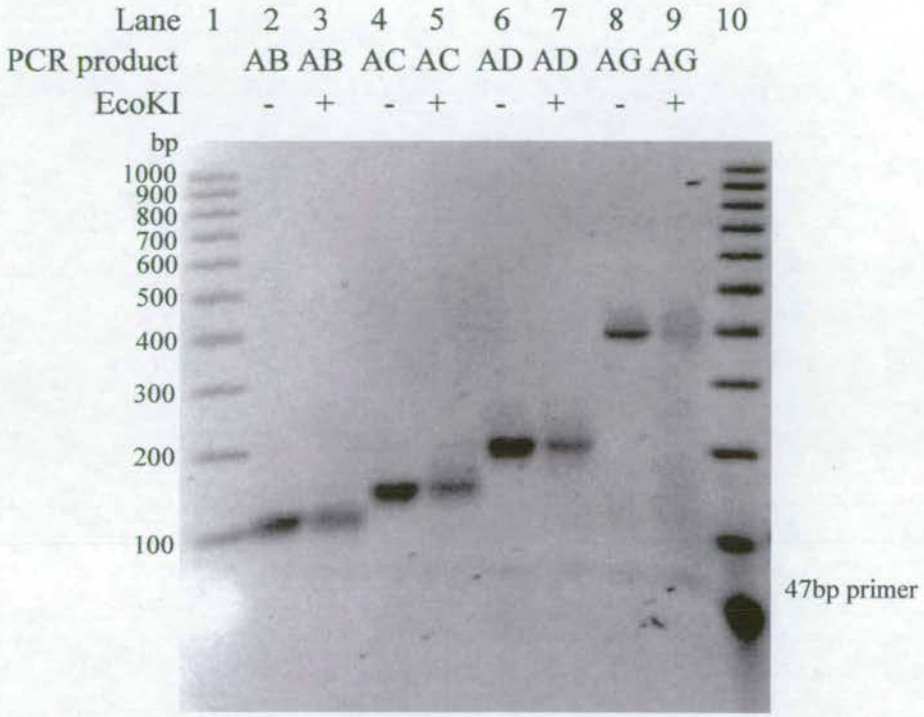

Figure 3.20. Restriction of small 2-site linear PCR products with EcoKI. Reactions were carried out in high salt EcoKI buffer, pH 7.9, with a ratio of EcoKI per target site of 1.33:1 for 45min at 25°C. DNA samples are run in tandem, with and without the addition of EcoKI. Lanes 1 and 10 contain linear 100bp DNA markers of sizes indicated. Lane 10 also contains 47bp primer B as shown. Samples are run on a 2.5% agarose gel with EtBr staining.

It therefore appears that EcoKI cannot restrict a fragment which has only has 117bp or less between its target sites. Fragment AG has 317bp between its target sites and is successfully restricted. If this is the case, and two EcoKI molecules cannot bind to two target sites separated by 117bp, then this indicates a large footprint of EcoKI. Dreier *et al.*, (1996), have previously found that EcoR124II requires at least 40bp between its target site for restriction to occur, and that cutting appears to increase as this distance is lengthened. They concluded that inability of the enzyme to cut DNA with a shorter distance between the target sites was due to steric hindrance only allowing binding of a single EcoR124II enzyme.

However, the footprint of EcoKI was found to be 45bp prior to addition of ATP and only around 30bp after addition by Powell *et al.*, (1998)b, when specifically bound to its target site. The method of analysis used was exonuclease III digestion. The results shown here can be explained if the R subunits are positioned, as suggested (Davies *et al.*, 1999; Powell *et al.*, 1998b), on each end of the molecule, arranged parallel to the DNA. These R subunits would therefore require a certain length of free DNA to allow the whole EcoKI molecule to bind successfully, but would not necessarily protect the underlying DNA from exonuclease digestion. It is also possible that EcoKI is able to bind to a smaller region of DNA successfully, but is required to translocate DNA a certain distance before a stall in translocation can trigger restriction.

3.6.3.2. Binding of EcoKI to one- and two-site fragments

In order to measure the number of EcoKI molecules that substrate AB and AG could bind, a gel retardation assay was carried out as shown in figure 3.21. In figure 3.21B, the band at 388bp represents DNA fragment AG alone with no EcoKI bound. The higher molecular weight bands running to positions equivalent to around 700bp and 1000bp are proposed to represent AG bound to one and two EcoKI respectively. At high EcoKI concentrations (375nM and 500nM) a faint band can also be seen at a position equivalent to 1300bp. This band may represent some form of multimolecular aggregate, possibly due to the ability of EcoKI to dimerise.

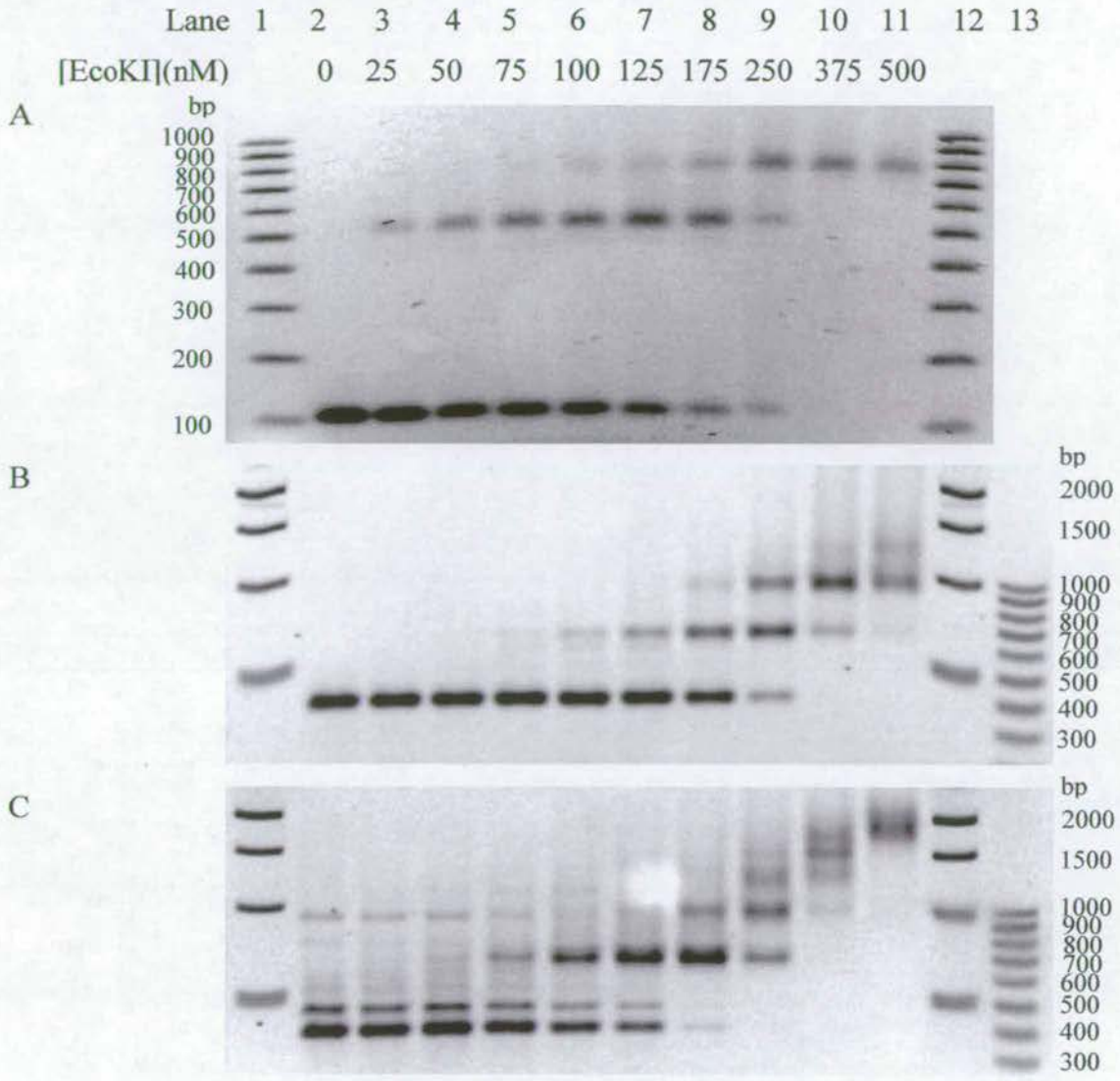

Figure 3.21. Gel retardation of DNA bound to EcoKI. Reactions were carried out in high salt EcoKI buffer, pH7.9, with a concentration of 0.1mM SAM, 50µg/ml BSA, 250nM DNA and varying concentrations of EcoKI as indicated. A) Gel retardation of AB containing 2 EcoKI sites separated by 34bp. The gel shows bands at 105bp, indicating fragment AB with no EcoKI attached. Bands at higher positions represent AB fragments with a number of EcoKI molecules bound to them, thereby inhibiting their mobility through the gel. B) Gel retardation of AG containing 2 EcoKI sites separated by 317bp. The gel shows bands at 388bp, indicating fragment AG with no EcoKI attached. Bands at higher positions represent AG fragments with a number of EcoKI molecules bound to them. C) Gel retardation of fragment 34 containing 1 EcoKI site. The gel shows bands at 400bp, indicating fragment 34 with no EcoKI attached. The presence of other bands in the absence of EcoKI at 450 and 900bp are due to mispriming during the production of the DNA fragment during PCR. Other bands that run to positions of higher molecular weight than 400bp in the presence of EcoKI represent fragment 34 with a number of EcoKI molecules bound to them. Lanes 1, 12 and 13 contain linear DNA markers of sizes indicated. Agarose content of gels A, B and C are 2.5%, 1.1% and 1.1% respectively.

Figure 3.21C indicates the mobility shift of a DNA fragment with one EcoKI target site made by PCR using primer3 and primer4, forming fragment 34, of 400bp. In lane 2, where no EcoKI is present, fragment 34 can be seen at 400bp. However, other bands are also present at positions of around 450bp and 950bp. These bands have been produced by mispriming during the PCR reaction. As the EcoKI concentration is increased a band is seen at a position equivalent to around 700bp, which is proposed to represent fragment 34 with one EcoKI bound. However, with further addition of EcoKI, bands appear at increasing molecular weight, equivalent to around 1000bp, 1300bp, 1500bp and 1800bp. At the highest concentration of EcoKI used (500nM), where there are two EcoKI for every target site, only the band equivalent to 1800bp is present. These high molecular weight bands (appearing above 700bp) are thought to represent multimolecular aggregates, with all forms of DNA (fragment 34 and misprimed products) included.

In figure 3.21A, bands of 105bp represent AB alone, with no EcoKI bound. Bands that run to a position equivalent to that of around 550bp represent fragment AB with one EcoKI bound. The higher bands, running to a position equivalent to around 800bp, are proposed to represent two EcoKI molecules bound to each AB fragment.

It is possible that the higher molecular weight bands present for fragments AG and AB represent DNA binding to different forms of the EcoKI, such as $R_2M_2S_1$, M_2S_1 or M_1S_1. Also, as EcoKI is known to dimerise, the single highest molecular weight bands for these DNA fragments could represent two DNA fragments, each bound to a single EcoKI, dimerised together. However, as AG can be successfully restricted by EcoKI (see figure 3.20), this fragment of DNA must be able to bind two EcoKI molecules simultaneously. Therefore the assignment of the three bands produced in figure 3.21B as AG alone, AG bound to one EcoKI and AG bound to two EcoKI is necessary to fulfil this requirement. Also, as the banding pattern of AB is very similar to that of AG, it may be inferred that the three bands produced in figure 3.21A also represent AB alone, AB bound to one EcoKI and AB bound to two EcoKI. The slight differences in banding pattern between AB and AG can be explained by the presence of contaminating primers remaining from the PCR reactions from which AB and AG were formed, leading to slight variations in the calculated DNA concentrations. As the banding pattern for AB is very different from that seen with fragment 34, it is unlikely that AB can only bind a single EcoKI molecule. However, this comparison is complicated by the presence of misprimed products of unknown sequence present in the fragment 34 reactions.

As there are only 34bp between EcoKI target sites, the intervening DNA is too rigid to allow dimerisation of two EcoKI molecules on the same AB substrate. Therefore, if each AB could bind two EcoKI, dimerisation may be expected between EcoKI molecules bound to a separate AB substrate. This would produce extra bands of higher molecular weight. No such bands were seen.

3.7. Effect of pH on EcoKI restriction activity

Little research has been done to find the optimal conditions for EcoKI activity. Therefore, EcoKI restriction activity was measured with varying pH, in order to discover the optimal conditions for cutting by EcoKI. Linear and supercoiled pBRsk1 were restricted by EcoKI in bis-tris propane buffer, over a pH range of 6.3-10.

Figure 3.22A shows the rapid conversion of supercoiled pBRsk1 into nicked and then linear DNA at pH 9.5. After an initial increase in intensity, the linear band can be seen to decrease. This could be due to EcoKI-bound DNA becoming stuck to the reaction tube, and/or also due to the previously described activity of EcoKI to slowly degrade one-site linear DNA in an excess of enzyme.

A graphical representaion of the results can be seen in figure 3.22C. Although the graph shows an increase in linear DNA throughout, the gel and densitometry clearly show an increase and decrease. This decrease, due to an unknown mechanism of EcoKI activity, is not analysed here where the fraction of linear DNA and accompanying degraded linear DNA are grouped todether for analysis. Analysis of restriction of linear one-site DNA is described and analysed in figure 3.23. Figure 3.23A shows the conversion of linear pBRsk1 into smeared DNA at pH 9.5. This digestion of one-site linear DNA has been previously described in the presence of excess type I enzymes (Janscak *et al.*, 1996). A graphical representaion of the results can be seen in figure 3.23C. The graph shows a decrease in linear DNA with an accompanying increase in smeared DNA. Curves were fitted to the data using models as described previously (section 3.4).

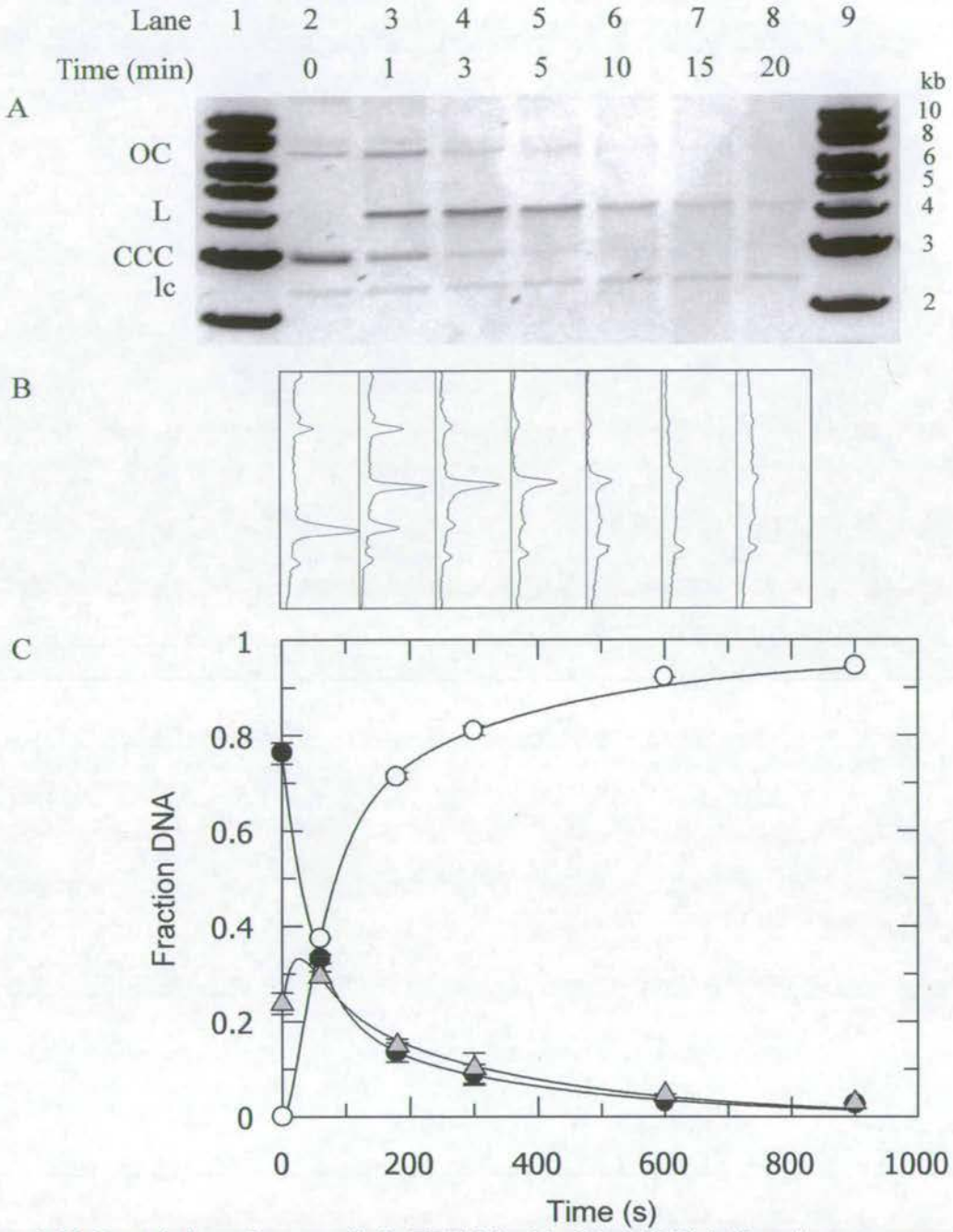

Figure 3.22. Restriction of supercoiled pBRsk1 by EcoKI at pH 9.5. Reactions were carried out in bis-tris propane buffer, pH 9.5, with 50nM supercoiled pBRsk1 and 67nM EcoKI. A) Agarose gel showing restriction of supercoiled pBRsk1 (CCC) into nicked (OC) and then linear (L) DNA. A loading control (lc) is also present which takes no part in the reaction. Lanes 1 and 9 contain linear 1kb DNA markers of sizes indicated. B) Densitometry of gel A, as aligned, using Scion Image software. C) Graph of fraction of DNA against time. This shows the conversion of the fraction of supercoiled pBRsk1 (shaded circles) into nicked (grey triangles) and linear DNA (open circles) with time. Each point is the mean of 2 separate experiments.

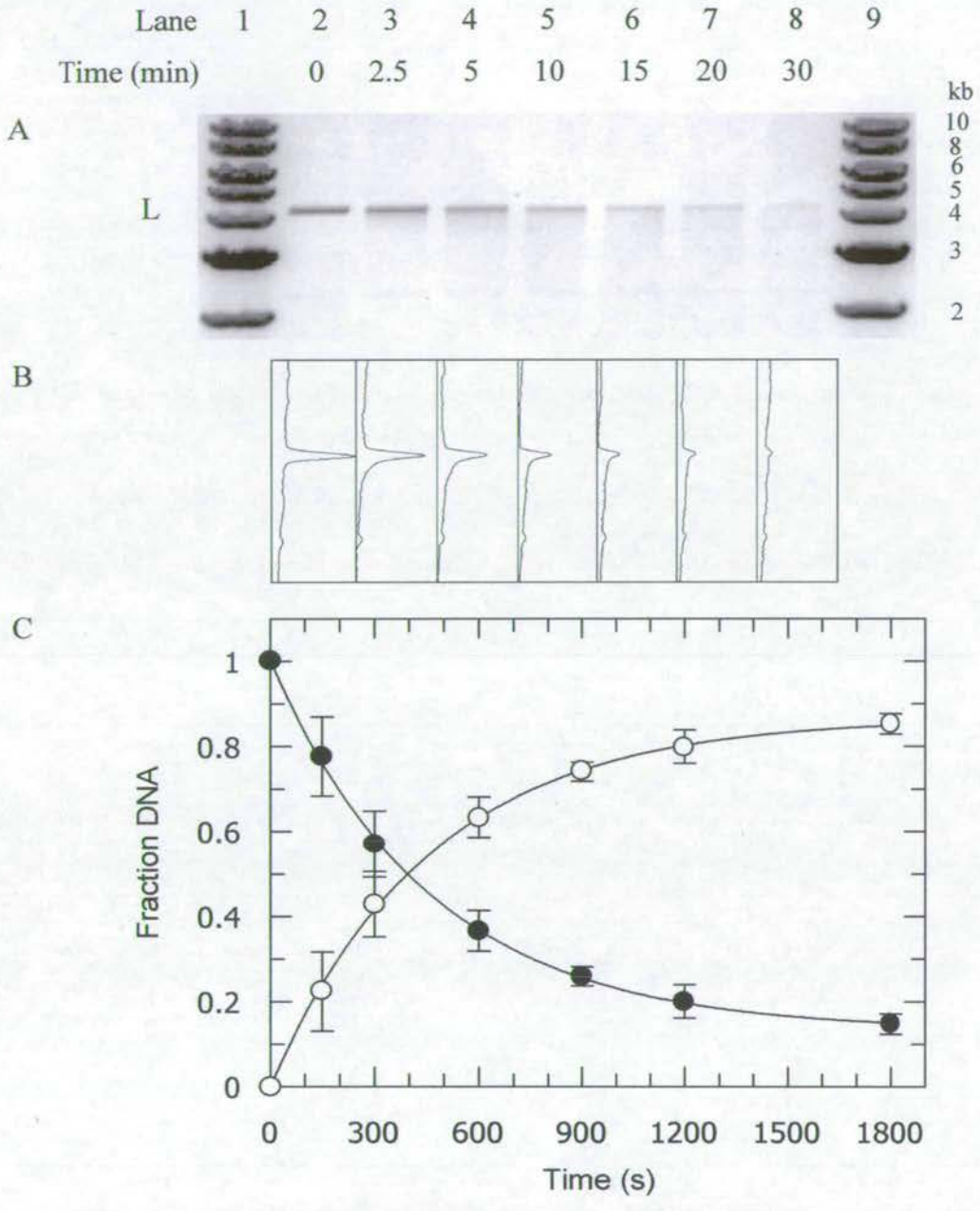

Figure 3.23. Restriction of linear pBRsk1 by EcoKI at pH 9.5. Reactions were carried out in bis-tris propane buffer, pH 9.5, with 50nM linear pBRsk1 and 67nM EcoKI. A) Agarose gel showing restriction of linear pBRsk1 (L) into a smear. Lanes 1 and 9 contain linear 1kb DNA markers of sizes indicated. B) Densitometry of gel A, as aligned, using Scion Image software. C) Graph of fraction of DNA against time. This shows the conversion of the fraction of linear pBRsk1 (shaded circles) into digested DNA (open circles) with time. Each point is the mean of 2 separate experiments.

Figures 3.24, 3.25 and 3.26 show how pH effects the EcoKI restriction activity of supercoiled and linear pBRsk1. The restriction activity of nicking supercoiled DNA, linearisation of the nicked DNA and digestion of the linear DNA have all been measured. In each case the rate constant of restriction is very low at a pH of 6.3. The rate constant increases with increasing pH until it peaks at pH 9.5. After this, the rate constant of restriction decreases again up to a pH of 10. This pH dependent activity of EcoKI was also seen with glycine and tris buffers (data not shown), indicating that this may be a general dependence of EcoKI and not a buffer specific property.

Figure 3.27A shows that all EcoKI cofactors are required for restriction of linear pBRsk1 at pH 8.9. This indicates that no contaminant in the sample is responsible for this increased restriction, unless its activity specifically requires all these cofactors also. Figure 3.27B shows that no restriction of methylated linear pBRsk1 occurs at pH 7.9 or 8.9, revealing that the restriction of this DNA at these pHs is due to EcoKI recognition of its specific target site and not due to star activity.

Therefore the dependence of EcoKI on pH reflects the situation in which EcoKI binds specifically to its target site and restricts DNA. From these results, it can be seen that under the assay conditions used, EcoKI restriction activity is highest at pH 9.5. This is significantly higher than the pH of most commercially available restriction buffers, which are usually around pH 7.9. This may reflect the optimal conditions for specific restriction by the more commonly used type II restriction enzymes. Unfortunately, it was not possible to measure the ATP hydrolysis rate at these varying pHs due to the pH dependence of the assays used.

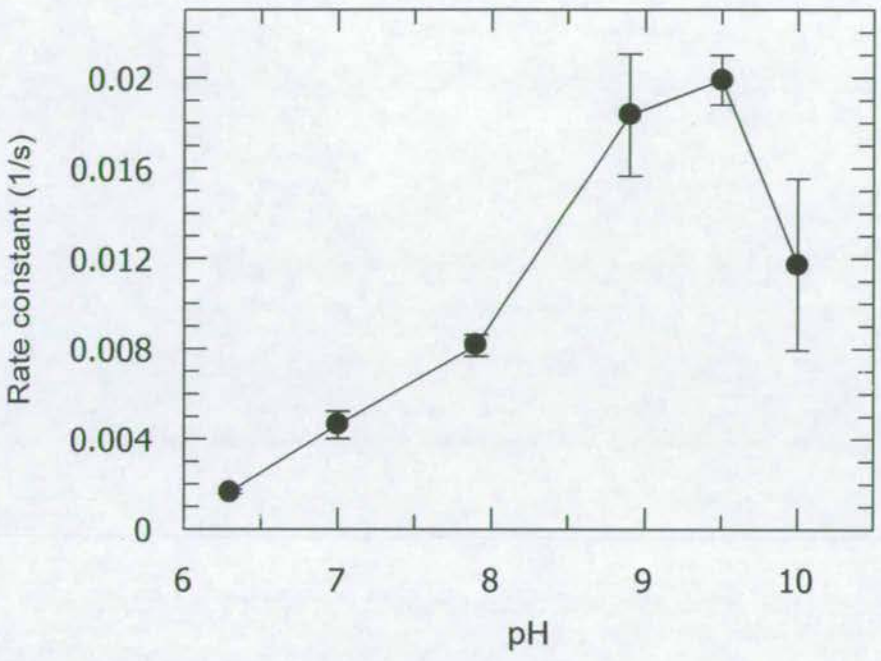

Figure 3.24. Effect of pH on EcoKI nicking of supercoiled pBRsk1. This graph shows the effect of pH on the rate constant of EcoKI nicking under the conditions described for figure 3.22. A peak in EcoKI rate constant of nicking of supercoiled pBRsk1 can be seen at pH 9.5. Each point represents the mean of 2 separate experiments. (see Appendix A).

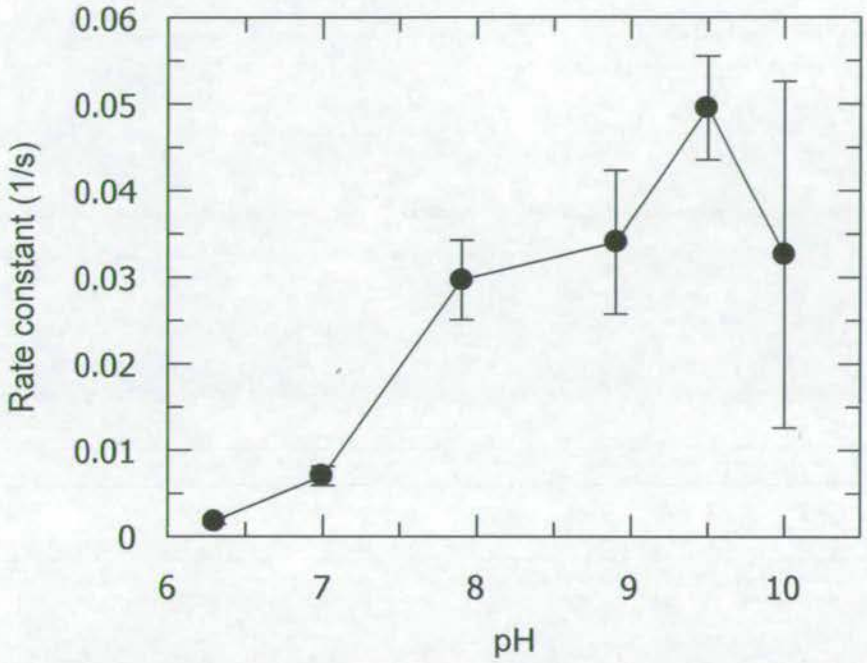

Figure 3.25. Effect of pH on EcoKI restriction of nicked pBRsk1. This graph shows the effect of pH on the rate constant of the second single-stranded nicking event by EcoKI under the conditions described for figure 3.22. A peak in EcoKI rate constant of restriction of nicked pBRsk1 can be seen at pH 9.5. Each point represents the mean of 2 separate experiments. (see Appendix A).

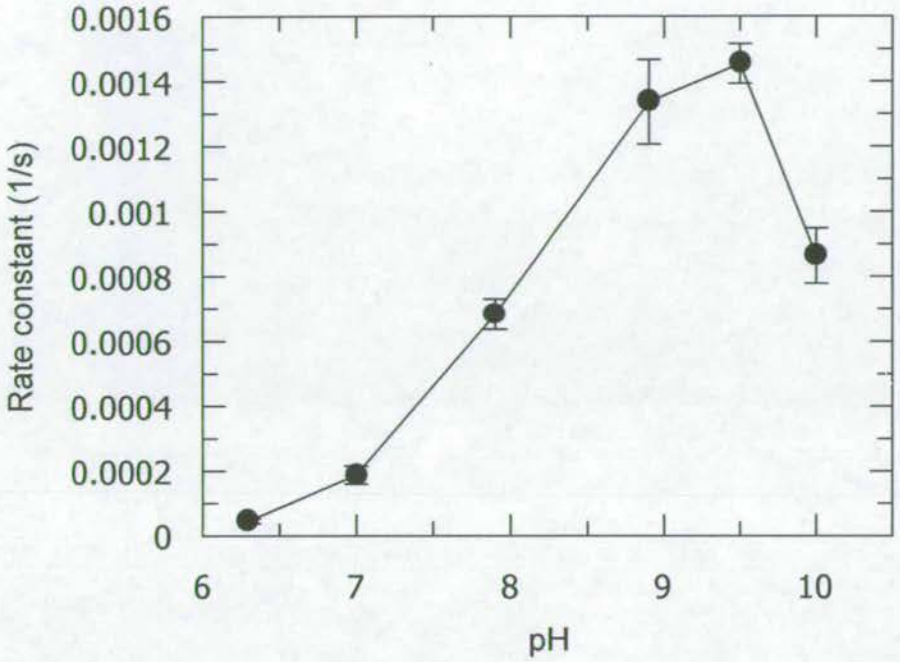

Figure 3.26. Effect of pH on EcoKI digestion of linear pBRsk1. This graph shows the effect of pH on the rate constant of EcoKI digestion of 1-site linear DNA under the conditions described for figure 3.23. A peak in EcoKI rate constant of digestion of linear pBRsk1 can be seen at pH 9.5. Each point represents the mean of 2 separate experiments. (see Appendix A).

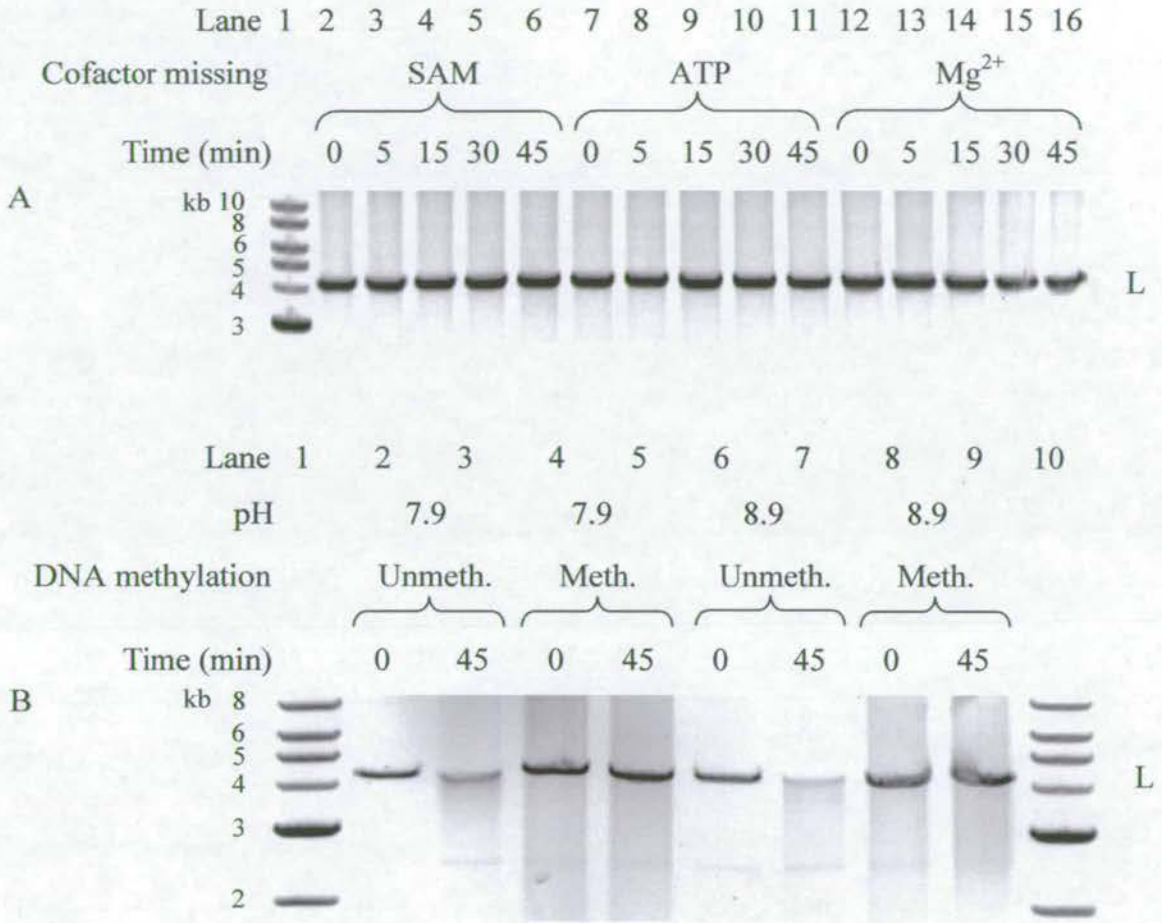

Figure 3.27. Specificity of EcoKI restriction at high pH. A) Gel A shows incubation of 67nM EcoKI with 50nM linear pBRsk1 (L) at pH 8.9. A time course up to 45min is followed, where a vital cofactor is missing. Lane 1 contains linear 1kb DNA markers of sizes indicated. B) Gel B shows the effect of using linear pBRsk1 that is either unmethylated (Unmeth) or methylated (Meth) at the EcoKI target site, at a concentration of 50nM, with a concentration of 67nM EcoKI at pH 8.9 with all cofactors present. Unmethylated DNA is the usual substrate for EcoKI, whereas methylated DNA should be left uncut by EcoKI. Digested unmethylated linear pBRsk1 can be seen as a smear. Lanes 1 and 10 contain linear 1kb DNA markers of sizes indicated.

3.8. Summary

This chapter has shown that EcoKI digests one- and two-site linear and supercoiled plasmids as expected from the literature. ATP hydrolysis activity of EcoKI can be measured by the ATP hydrolysis coupled assay as well as the P_i ATPase assay. Increasing the EcoKI concentration increases the ATP hydrolysis rate even above saturating concentrations. EcoKI restricts a one-site supercoiled plasmid at random positions all over the plasmid. EcoKI appears to cut a two-site linear plasmid at random positions between the target sites, but also in close proximity to one of the target sites. It also appears that EcoKI cannot restrict a linear two-site DNA fragment with 117bp or less between the target sites, even though both sites may be simultaneously bound by EcoKI. However, EcoKI can restrict a two-site linear DNA fragment with 317bp between the target sites. EcoKI shows optimal specific restriction activity at pH 9.5 for both linearised and supercoiled one-site plasmids.

Chapter 4:

Dyes

4.1. Introduction

Dyes are commonly used to stain DNA to aid in their direct visualisation. Recently they have been much used with single molecule imaging, as a method to measure protein-DNA interactions. However, dyes can affect DNA conformation by their binding. Intercalating dyes (such as YOYO and EtBr) bind in between DNA base pairs and alter the DNA helical twist. Minor groove binding dyes (such as H33258) alter the conformation of the DNA by closing the minor groove around them. These effects on DNA conformation as well as the presence of dye molecules bound to the DNA could in turn affect the protein-DNA interactions being observed. It is therefore important to fully understand the effect of the dyes being used on the specific protein being studied.

Most dye molecules bind DNA non-specifically, although some have a preference for A and T bases (H33258). They also bind as individual molecules and do not undergo co-operative binding. In fact, intercalated dyes actually prevent other dye molecules binding between the base pair next to them as described by the nearest neighbour exclusion principle (Wilson, 1990). In this way, dyes could be used to represent the many non-specifically bound small molecules and proteins that are present on bacterial DNA *in vivo*.

In this study, the effect of the bis-intercalating dye YOYO on EcoKI restriction and ATP hydrolysis activity has been analysed. The effects of the mono-intercalator EtBr and the minor groove binder H33258 upon EcoKI restriction activity have also been analysed. From these effects it may be possible to infer details of the EcoKI mechanism of binding, translocation and restriction.

4.2. Dye inhibition of EcoKI restriction

4.2.1. Analysis method of the effect of dyes on EcoKI restriction activity

EcoKI restriction data was analysed as shown in figure 4.1. Figure 4.1A shows an agarose gel of the restriction of supercoiled pBRsk1 with 32bp per intercalated YOYO by EcoKI. The slow conversion of supercoiled to nicked and linear DNA can be followed on the accompanying densitometry (figure 4.1B) and is represented graphically in figure 4.1C. This shows that an initial rapid decrease is followed by a levelling off of the fraction of

supercoiled DNA, with around 22% left uncut after 3600s. An initial rapid increase in nicked DNA is followed by a slower decrease as it is converted in to linear form, until it reaches a level of around 29% nicked after 3600s. After an initial lag, the fraction of linear DNA produced increases rapidly before this rate increases more slowly until 3600s, where around 49% DNA is linearised.

When compared to figure 3.4, where no YOYO is present, it can be clearly seen that YOYO inhibits EcoKI restriction of supercoiled pBRsk1. It is also shown that not all the DNA that is nicked is further digested into linear DNA. This can be explained if YOYO molecules are blocking translocation and causing EcoKI to stall. This may induce EcoKI to nick the DNA with each R subunit where it stalls. If these two nicks are beyond a certain critical distance apart, the DNA, although nicked on both strands, will remain as an intact loop, held together by a sufficient number of complementary base pairings. This species would therefore appear nicked on an agarose gel.

In order to address this, the samples were heated to 100°C for 30min in order to allow the strands to separate, and linearisation to occur if two nicks were present on separate strands. However, there was no change in the proportions of nicked or linear DNA (data not shown). This does not rule out the possibility that two nicks are made too far apart to linearise the DNA as the complementary bases, although separated by heating, could re-anneal as the temperature is lowered for electrophoresis, and still appear as nicked form in an agarose gel.

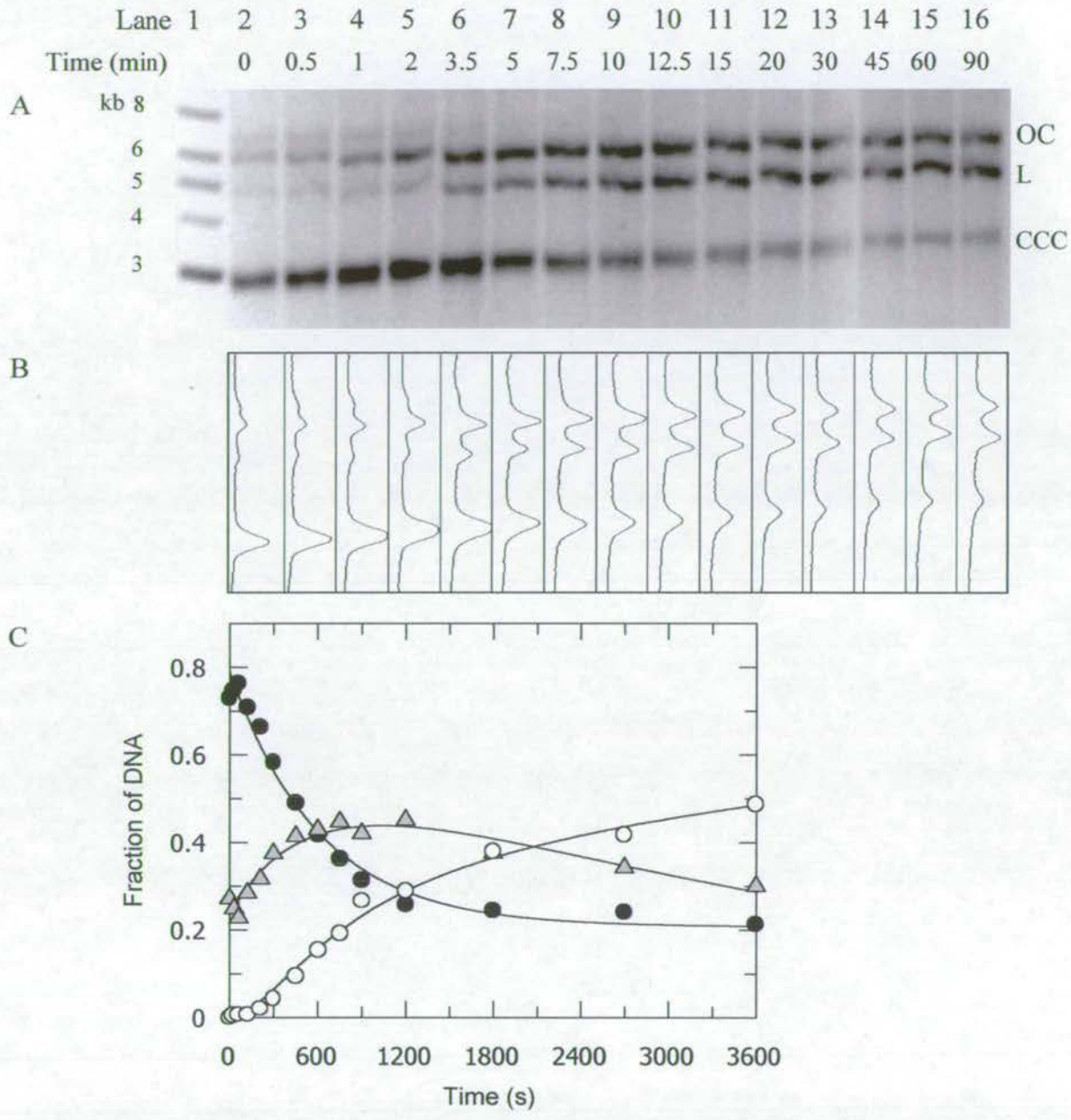

Figure 4.1. Restriction of pBRsk1 by EcoKI in the presence of 1 molecule of YOYO per 32bp DNA. Reactions were carried out using 50nM supercoiled pBRsk1 and 67nM EcoKI in high salt EcoKI buffer, pH 7.9. A) Agarose gel showing conversion of supercoiled pBRsk1 (CCC) into nicked (OC) and linear (L) forms over time. Lane 1 contains a 1kb linear DNA marker of sizes indicated. B) Densitometry of gel A as aligned, using Scion Image software. C) Graph of fraction of DNA converted from supercoiled to nicked to linear DNA by EcoKI in the presence of 1 YOYO per 32 bp DNA. Fitted lines are derived from the kinetic model described in the text. Points represent the mean of at least 3 separate experiments.

In order to fit this data to produce the graph shown in figure 4.1C, Dynafit modelling was used. However, although in the absence of dye a simple model could account for the restriction of supercoiled pBRsk1 (see section 3.4), addition of even a small amount of dye caused incomplete digestion of the DNA. The slow progression through the reaction pathway and the persistence of large amounts of uncleaved or nicked DNA suggests that dyes can sequester the DNA in uncleavable forms. In this case CCC* and OC* are the uncleavable forms of supercoiled and nicked DNA respectively. This therefore required a more complicated model of restriction as previously described for the digestion of two-site linear pBR322 (see section 3.4). In this case the model used was:

$$\begin{array}{ccccc} & & k1 & & k2 \\ CCC & & \rightarrow & OC & \rightarrow & L \\ k4 \updownarrow k6 & & & k3 \updownarrow k5 & & \\ CCC^* & & & OC^* & & \end{array}$$

It is of interest that these reversible steps are not required in the absence of dye, but become more important in the reaction mechanism as the dye concentration increases. This can be seen from table 4.1, which shows the rate constants for restriction of supercoiled pBRsk1 by EcoKI with varying concentrations of YOYO, using the model indicated above. EtBr and H33258 caused a similar inhibition of EcoKI restriction activity, and the same data-fitting model was used for their analysis (data not shown).

4.2.2. Effect of YOYO concentration on EcoKI restriction

Table 4.1 shows how the concentration of YOYO affects the rate constants of restriction of pBRsk1 by EcoKI. It also reveals how the reversible steps of the reaction mechanism become important when YOYO is present. This can be seen by the large equilibrium constants produced in the presence of YOYO. The rate constants for the main reaction pathway (k1 and k2) decrease with increasing YOYO concentration, and are shown graphically in figure 4.2.

[YOYO] (no. of DNA bp per YOYO)	Rate constants (s^{-1})						Equilibrium constants	
	k_1	k_2	k_3	k_4	k_5	k_6	k_3/k_5	k_4/k_6
∞ (No Dye)	**0.0218** ±0.0024	**0.0266** ±0.0042	**0.000212** ±0.00150	**1.12×10^{-9}** ±0.00064	**0.00378** ±0.0013	**0.005255** ±0.0022	**0.056**	**2.13×10^{-7}**
512	**0.0058** ±0.0006	**0.0145** ±0.0047	**7.82×10^{-5}** ±0.00031	**0.001449** ±0.00016	**1.87×10^{-5}** ±5.8×10^{-5}	**0.000149** ±6.4×10^{-5}	**4.189**	**9.71**
256	**0.0048** ±0.0005	**0.0085** ±0.0020	**0.000683** ±0.00018	**0.000829** ±0.00011	**4.70×10^{-5}** ±4.1×10^{-5}	**8.78×10^{-5}** ±6.2×10^{-5}	**14.53**	**9.44**
128	**0.0037** ±0.0002	**0.0046** ±0.0005	**0.001887** ±0.00019	**0.00117** ±0.00014	**2.93×10^{-5}** ±3.1×10^{-5}	**3.84×10^{-5}** ±4.3×10^{-5}	**64.38**	**30.5**
64	**0.0030** ±0.0005	**0.0027** ±0.0006	**0.000135** ±9.9×10^{-5}	**0.000413** ±6×10^{-5}	**2.75×10^{-5}** ±1.9×10^{-5}	**0.000113** ±6.2×10^{-5}	**4.891**	**3.65**
32	**0.0015** ±0.0001	**0.0026** ±0.0002	**0.001876** ±0.00014	**0.000126** ±2.5×10^{-5}	**0.000381** ±4.8×10^{-5}	**3.8×10^{-10}** ±4.6×10^{-5}	**4.919**	**3.32×10^{5}**
16	**0.0008** ±0.0001	**0.0014** ±0.0005	**0.000894** ±0.00021	**0.000447** ±9×10^{-5}	**2.71×10^{-5}** ±4.2×10^{-5}	**3.74×10^{-5}** ±9×10^{-5}	**33.00**	**11.9**

Table 4.1. Effect of YOYO concentration on EcoKI rate constants. Rate constants for the restriction of supercoiled pBRsk1 by EcoKI with varying concentrations of YOYO were calculated by Dynafit using the mechanism described in the text. The equilibrium constants for the reversible reaction steps are also shown. A graphical representation of rate constants k1 and k2 are shown in figure 4.2.

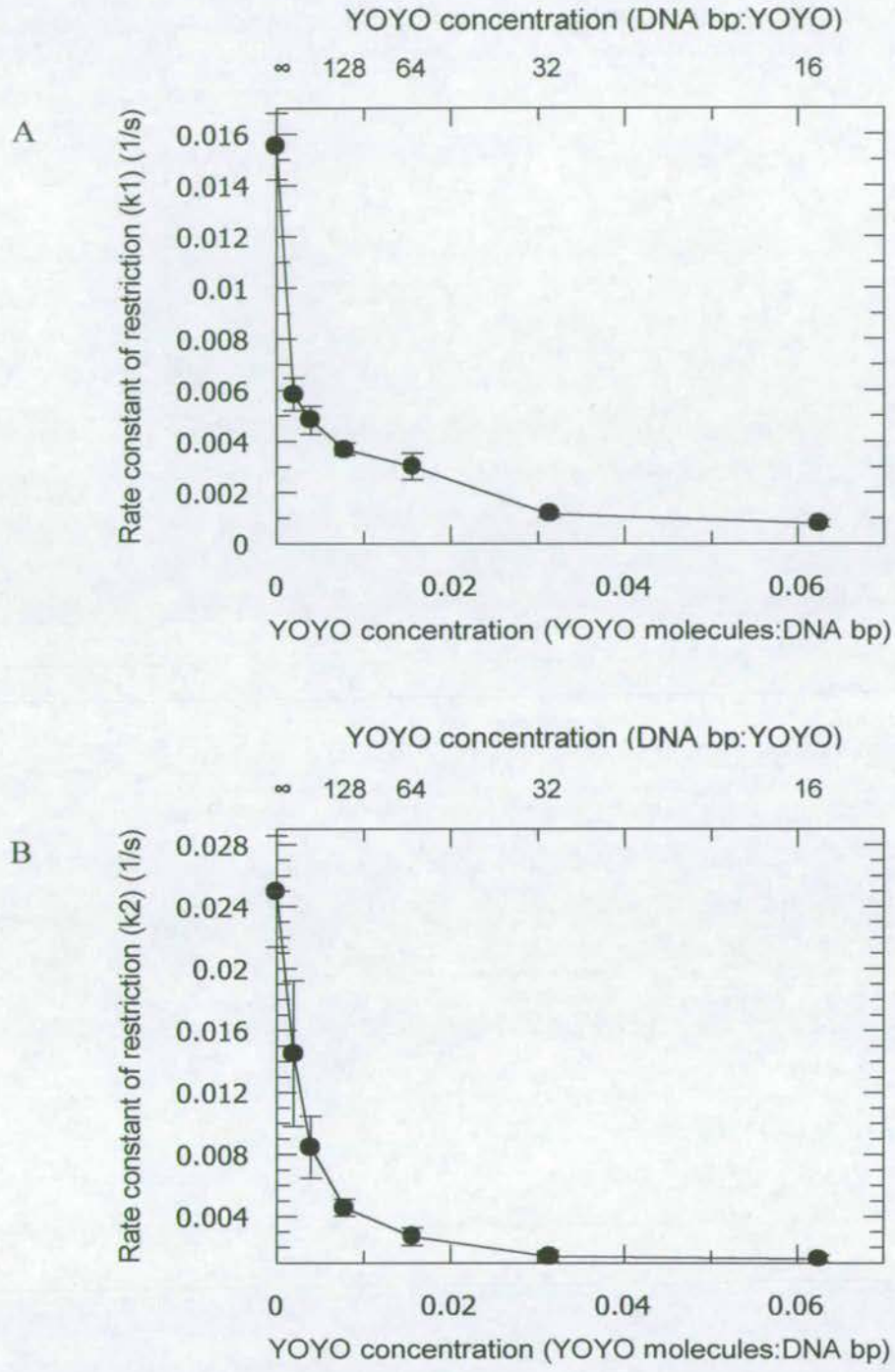

Figure 4.2. Effect of YOYO concentration on restriction of supercoiled pBRsk1 by EcoKI. Reactions were carried out with 50nM pBRsk1 and 67nM EcoKI in high salt EcoKI buffer, pH 7.9. Graphs show the rate constant of restriction of EcoKI nicking (k1) of supercoiled pBRsk1 (A), and then cutting this nicked intermediate (k2) into linear DNA (B), with varying concentrations of YOYO. In both graphs, the YOYO concentration is given as number of YOYO molecules per DNA bp by the bottom axis, and number of DNA bp per YOYO by the top axis. (See Appendix B).

Figure 4.2 reveals that even very small additions of YOYO severely inhibit EcoKI nicking of supercoiled pBRsk1 (k1) as well as the further restriction of this intermediate into linear DNA (k2). This can be seen by the fact that the restriction activity for k1 and k2 drops to around a third of its uninhibited level with the addition of only one YOYO per 256bp DNA (0.004YOYO:bp). After this very steep decrease, the EcoKI restriction activity levels off at a rate constant of around $0.001s^{-1}$ for k1 and k2 at 32bp per YOYO.

4.2.3. Effect of H33258 concentration on EcoKI restriction

Figure 4.3 shows how the concentration of H33258 affects the rate constants of restriction of pBRsk1 by EcoKI. EcoKI nicking of supercoiled DNA (k1), as well as further restriction into linear DNA (k2) is dramatically inhibited by very small additions of H33258. The k1 value can be seen to drop to around a fifth of its uninhibited level, and k2 to around an eighth of its uninhibited level with the addition of only one H33258 per 128bp DNA. After this very steep decrease, the EcoKI restriction activity levels off at a rate constant of around $0.002s^{-1}$ for k1 and k2 at concentrations obove 128bp per H33258.

4.2.4. Effect of EtBr concentration on EcoKI restriction

Figure 4.4 shows how the concentration of EtBr affects the rate constants of restriction of pBRsk1 by EcoKI. It can be seen that even very small additions of EtBr severely inhibit EcoKI nicking of supercoiled pBRsk1 (k1) as well as the further restriction of this intermediate into linear DNA (k2). The k1 value drops to around a half of its uninhibited level, and k2 to around a third of its uninhibited level with the addition of one EtBr per 128bp DNA. After this steep decrease, the EcoKI restriction activity levels off at a rate constant of around $0.001s^{-1}$ for k1 and k2 at 64bp per EtBr.

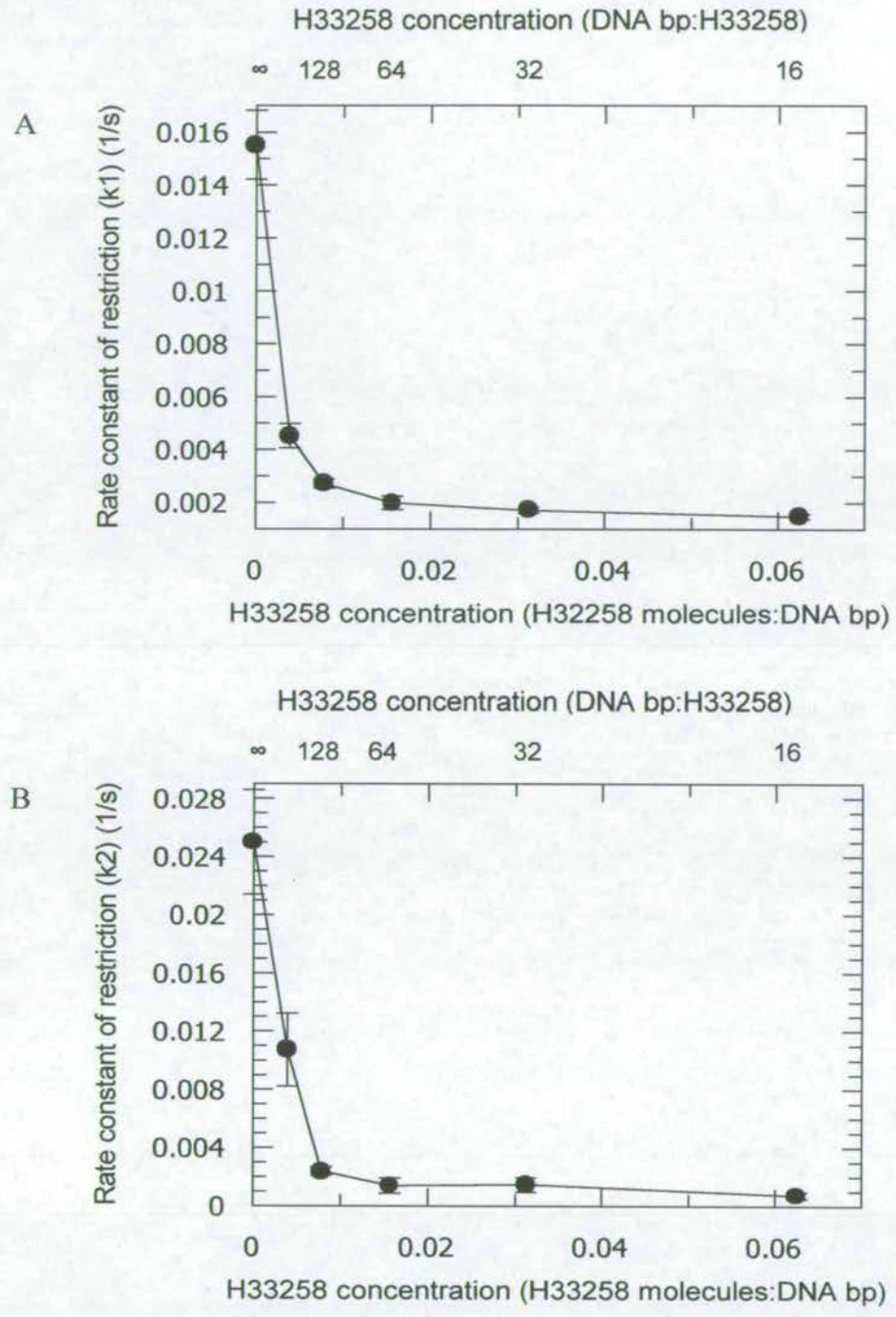

Figure 4.3. Effect of H33258 concentration on restriction of supercoiled pBRsk1 by EcoKI. Reactions were carried out with 50nM pBRsk1 and 67nM EcoKI in high salt EcoKI buffer, pH 7.9. Graphs show the rate constant of restriction of EcoKI nicking (k1) of supercoiled pBRsk1 (A), and then cutting this nicked intermediate (k2) into linear DNA (B), with varying concentrations of H33258. In both graphs, the H33258 concentration is given as number of H33258 molecules per DNA bp by the bottom axis, and number of DNA bp per H33258 by the top axis. (See Appendix B).

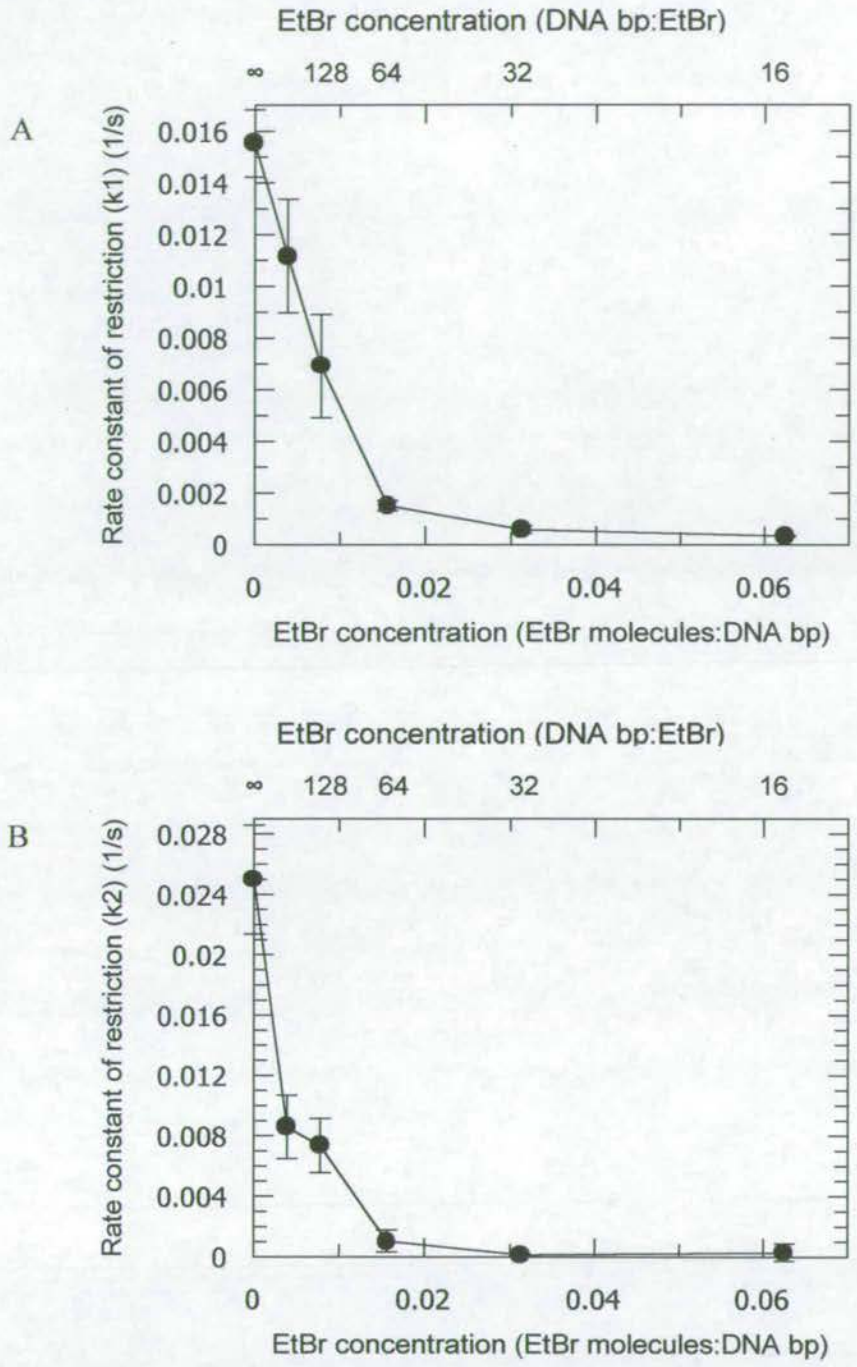

Figure 4.4. Effect of EtBr concentration on restriction of supercoiled pBRsk1 by EcoKI. Reactions were carried out with 50nM pBRsk1 and 67nM EcoKI in high salt EcoKI buffer, pH 7.9. Graphs show the rate constant of restriction of EcoKI nicking (k1) of supercoiled pBRsk1 (A), and then cutting this nicked intermediate (k2) into linear DNA (B), with varying concentrations of EtBr. In both graphs, the EtBr concentration is given as number of EtBr molecules per DNA bp by the bottom axis, and number of DNA bp per EtBr by the top axis. (See Appendix B).

4.3. Effect of YOYO concentration on EcoKI ATP hydrolysis

The effect of YOYO concentration on the ATP hydrolysis rate of EcoKI is shown in figure 4.5. The rate of ATP hydrolysis is greatly inhibited by only a small addition of YOYO. This can be seen as ATP hydrolysis activity drops to around a half of its uninhibited level with the addition of one YOYO per 128bp, and to around a third after the addition of one YOYO per 64bp. EcoKI ATP hydrolysis activity continues to decrease with further increase in YOYO concentration until almost no activity is seen with one YOYO per 8bp.

As YOYO stock is supplied in DMSO, the effect of DMSO on EcoKI activity was studied to ensure that the inhibition observed was not due to the effect of DMSO. A DMSO concentration equivalent to that which would be present when one YOYO per 8bp was used, produced no inhibition of restriction or ATP hydrolysis. This is shown in figure 4.6, where reactions containing a YOYO concentration of 1 YOYO per 8bp of DNA exhibit no ATP hydrolysis activity, whereas reactions without DMSO or YOYO, and with DMSO at an equivalent concentration to that present in YOYO when used at 1 YOYO per 8bp DNA show a much higher and equal ATP hydrolysis rate (within experimental error). Therefore the inhibition of EcoKI activity seen with the addition of YOYO is due to the presence of YOYO and not DMSO.

YOYO inhibition of EcoKI may at least partially be due to the binding of YOYO in the EcoKI target site and therefore inhibiting EcoKI binding. This was studied by binding EcoKI to its target site before the addition of YOYO. The ATP hydrolysis rates measured showed no difference to the rates observed with addition of YOYO before EcoKI. This may indicate that binding of YOYO to EcoKI target site does not inhibit EcoKI binding, but could also reflect YOYO competing off EcoKI from its target site due to its very tight binding of DNA. Dreier and Bickle, (1996), found that EcoR124II ATP hydrolysis activity was also inhibited by an intercalating dye (EtBr) when it was added either before or after the addition of EcoR124II. However, they found that the level of inhibition was greater when the dye was added prior to the addition of EcoR124II. They suggested that the different mechanisms of target site exclusion, and inhibited translocation of dye-bound DNA were responsible for the reduced ATP hydrolysis rates when EtBr was added before and after EcoR124II respectively.

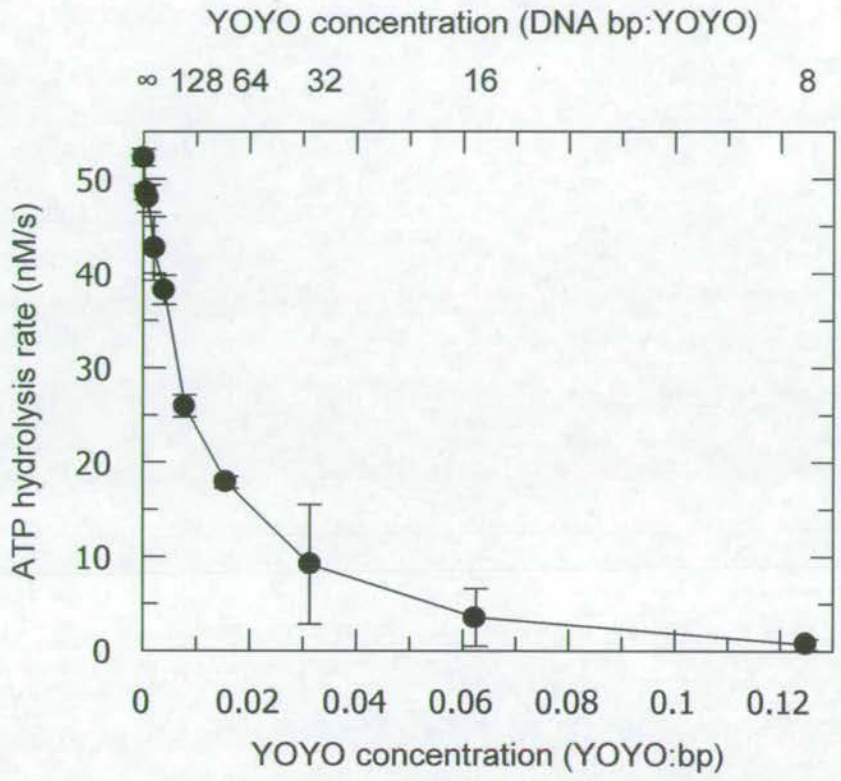

Figure 4.5. Effect of YOYO concentration on EcoKI ATP hydrolysis activity. Reactions were carried out with 5nM supercoiled pBRsk1 with 10nM EcoKI in high salt EcoKI buffer, pH 7.9. The ATP hydrolysis rate of EcoKI was measured by the ATP hydrolysis coupled assay with varying concentrations of YOYO bound to the DNA substrate. The YOYO concentration is given as number of YOYO molecules per DNA bp by the bottom axis, and number of DNA bp per YOYO by the top axis. The points represent the mean of 4 separate experiments.

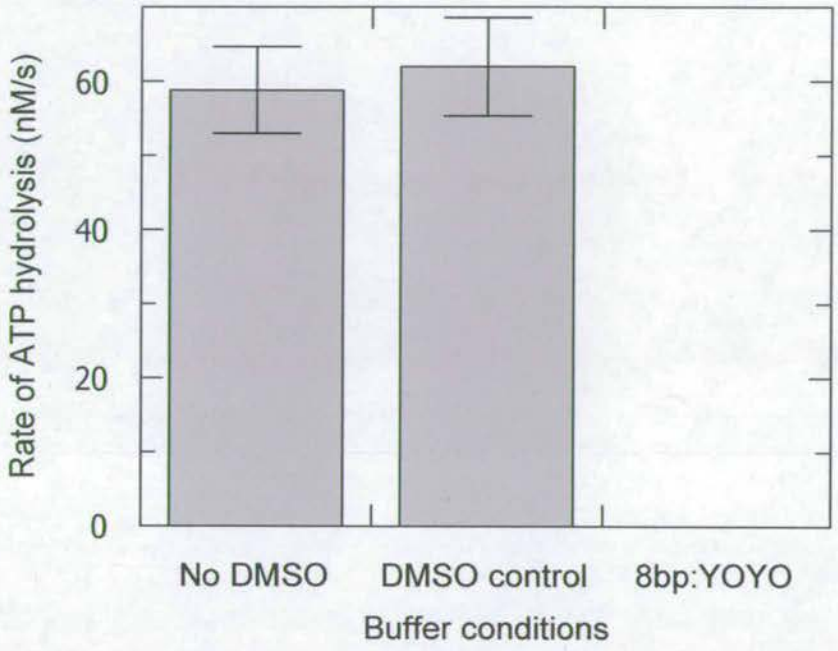

Figure 4.6. ATP hydrolysis coupled assay control. EcoKI ATP hydrolysis rate was measured using the ATP hydrolysis coupled assay in EcoKI high salt buffer, pH 7.9, with a concentration of 5nM supercoiled pBRsk1, 10nM EcoKI, 0.1mM SAM, 50µg/ml BSA and 2mM ATP. In the DMSO control (middle column), a concentration of DMSO was added that was equivalent to that present when a concentration of 1 YOYO molecule per 8bp DNA was used. In the far right column, the ATP hydrolysis rate is shown when YOYO is added at a concentration of 1 YOYO per 8bp DNA. The points represent the mean of three separate experiments with no DMSO, and the mean of 2 separate experiments in the DMSO control and with 8bp:YOYO.

4.4. Car parking model

YOYO inhibition of EcoKI translocation and restriction is proposed to be at least partly due to reduced binding of EcoKI to its specific binding site due to site blockage by YOYO molecules. YOYO binds DNA non-specifically and will therefore bind at random, throughout the DNA molecule. Therefore the level of inhibition achieved can be correlated to the spacing of YOYO molecules and the potential binding footprint of EcoKI translocation and restriction activity calculated. In this way, binding of EcoKI to DNA in the presence of YOYO is like trying to park a lorry (EcoKI) at the side of the road (DNA) in a specific space (target site), where cars may already be randomly parked (YOYO). This can be carried out using an equation formulated by McGhee and von Hippel, (1974). This has been adapted to allow the probability of there being a gap of sufficient size to allow EcoKI to bind and therefore carry out a reaction. In this equation,

$$Pg = \frac{(1-n\upsilon)^{g}}{(1-(n-1)\,\upsilon)^{g-1}}$$

Pg is the probability of the presence of a sufficient gap, n is the size of the space occupied by a dye molecule, υ is the dye concentration and g is the size of the gap. As YOYO excludes other dye molecules from binding around it due to alterations in the DNA structure, YOYO occupies around 4bp of DNA. This makes n = 4, although the equation is not very sensitive to this constant, as n values of 1-8 have little effect on the results. The results in figure 4.7 show the effect of YOYO concentration on ATP hydrolysis rate as described by figure 4.5 on a linear scale. The curve fitted with the equation described predicts a gap of 69±6bp required between YOYO molecules to allow EcoKI to hydrolyse ATP. Figure 4.7 also shows data for the initial rate of EcoKI restriction of supercoiled pBRsk1, which was also fitted to this equation and predicted an even larger footprint of 290±49bp. However, this data did not appear to fit the data well, particularly at high concentrations of YOYO. This EcoKI activity at high YOYO concentrations that was not fitted by the model may be due to EcoKI being able to compete off YOYO molecules to enable binding and therefore restriction at these concentrations.

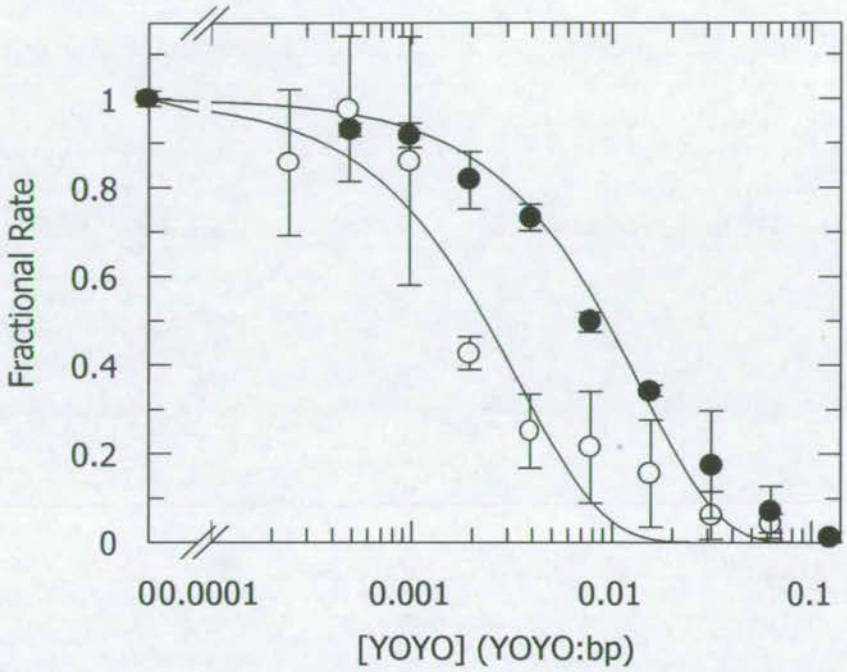

Figure 4.7. Car parking model. EcoKI initial restriction rates (open circles) and ATP hydrolysis rates (closed circles) with varying concentrations of YOYO. Reactions were carried out in EcoKI high salt buffer, pH 7.9, with 0.1mM SAM, 50μg/ml BSA and 2mM ATP. Curves have been fitted using the equation described in the text, in order to determine the probability of a gap occurring between dye molecules of a specific size to allow DNA binding of EcoKI. In this fitting, ATP hydrolysis or DNA restriction represent bound, active EcoKI enzymes, and the number of bound EcoKI inferred. The number of YOYO-1 molecules bound to the DNA are varied and so the probability of a specific gap is calculated over the concentration range (where nυ is the fraction of base pairs that are dye-bound) and compared to the EcoKI activity. From this, the gap required for successful EcoKI binding and activity is calculated.

The proposed footprint of EcoKI of around 290±49bp required for restriction would mean that EcoKI should not be able to restrict DNA with less than around 277bp between the target sites. This agrees with the large footprint prediction from the finding that EcoKI will not restrict DNA when there is 117bp or less between the target sites, but can restrict DNA with 317bp between target sites (see figure 3.20).

The fact that the model predicts that a larger footprint is required for restriction than for ATP hydrolysis activity implies that EcoKI would have to translocate the DNA a specific critical distance before a successful restriction reaction could be triggered.

4.5. Effect of YOYO on location of EcoKI restriction sites

4.5.1. Theory

The presence of pBRsk1 which is nicked but not linearised by EcoKI in the presence of YOYO has been visualised by agarose gel electrophoresis (see figure 4.1). This observation has led to the hypothesis that EcoKI translocation is stalled by intercalated YOYO molecules, which induces nicking at this site by one of the EcoKI R subunits. If both R subunits are induced to nick at a critical distance apart, although the nicks are on separate strands, the DNA will be held together by the large number of complementary base pairs. This species would therefore appear as nicked plasmid on agarose gels. This implies that DNA-bound YOYO molecules could prevent EcoKI translocation of DNA and trigger restriction activity.

4.5.2. Varying DNA substrates produced by type II restriction enzymes

In order to investigate the location of the EcoKI restriction sites when YOYO is present more precisely, pBR322 was linearised with different specific type II restriction enzymes, as shown before (figures 3.15 and 3.16). YOYO was then bound to these linear fragments at a concentration of 256bp per YOYO, before restriction with EcoKI. The banding pattern produced by this restriction can be seen in figure 4.8.

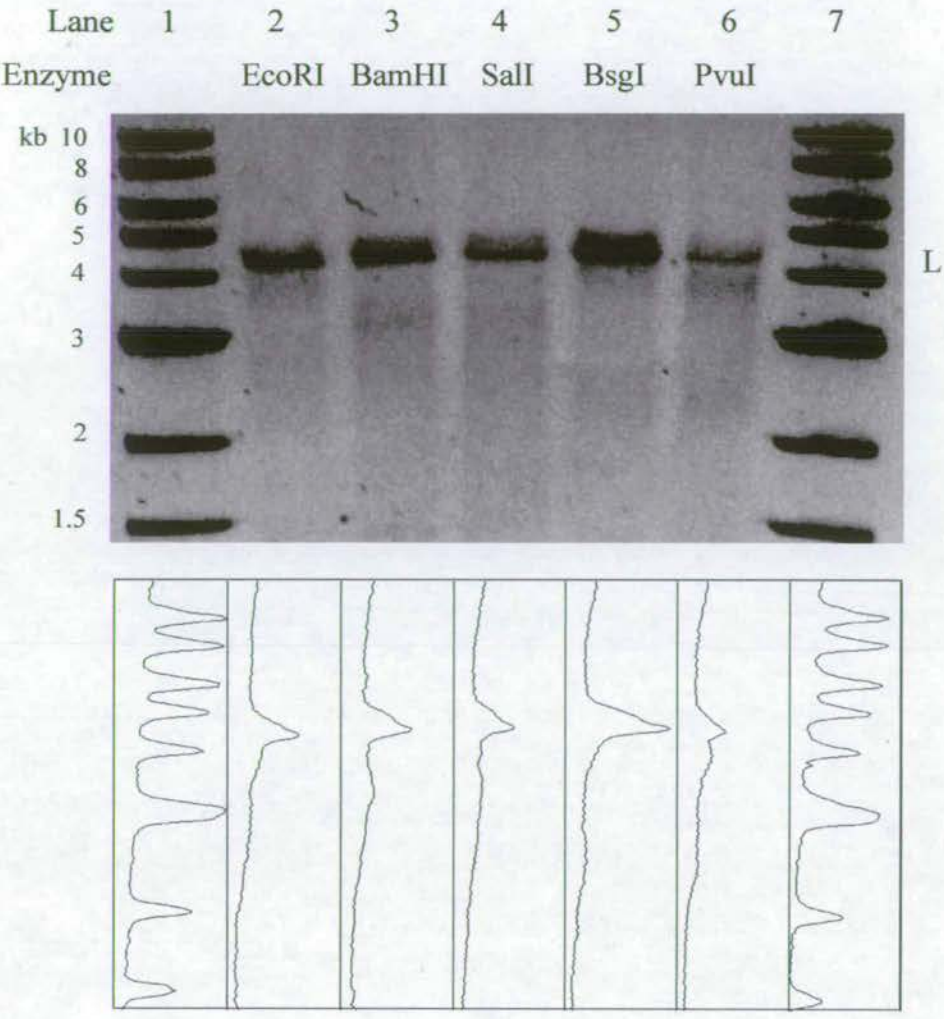

Figure 4.8. Location of EcoKI cutting site on pBR322 with 256bp per YOYO. Reactions were carried out in high salt EcoKI buffer, pH 7.9. pBR322 was linearised by a specific type II enzyme, as indicated, before addition of YOYO and restriction by EcoKI. A) Gel showing Type II-linearised DNA after further digestion by EcoKI. Lanes 1 and 7 contain a linear 1kb DNA marker of sizes indicated. B) Densitometry of Gel A, as aligned, using Scion Image software.

The banding pattern produced in the presence of 1 YOYO per 256bp DNA is the same as that achieved in the absence of YOYO (figure 3.16), implying that the position of the cutting site is not affected by YOYO intercalation at this low concentration. The DNA is cut into a smear representing random cutting between the target sites as well as into discrete bands produced by restriction within close proximity to the EcoKI target sites as described (see figure 3.17). However, this experiment was carried out at a low concentration of YOYO (1 YOYO per 256bp DNA), as not enough DNA was able to be restricted at higher concentrations of YOYO to produce visible bands on an agarose gel. Therefore, at higher YOYO concentrations, the EcoKI cutting site may be altered by YOYO. The mechanism of restriction occurring within close proximity to the target site is also unknown and may occur with limited DNA translocation.

4.6. Summary

YOYO, H33258 and EtBr all inhibit EcoKI restriction of one-site supercoiled plasmid DNA. All three dyes also appear allow EcoKI to nick some of the DNA without being able to restrict it further into linear form. YOYO has also been shown to inhibit EcoKI ATP hydrolysis activity. Using the car parking model, these experiments reveal that EcoKI has a footprint of ~69bp for ATP hydrolysis activity and ~290bp for restriction activity. EcoKI restriction of two-site linearised plasmids shows no difference in cutting site in the absence or presence of YOYO at low YOYO concentration (256bp:YOYO).

Chapter 5:

Spermidine

5.1. Introduction

Inside the head of bacteriophage, DNA adopts a highly ordered and condensed state due to the presence of polyamines (Cerritelli, 1997). This environment can be mimicked *in vitro* by the addition of spermidine, which condenses the DNA into toroidal structures which resemble the conformation of DNA within bacteriophage heads. Spermidine is a trivalent cation which binds to DNA, and acts to neutralise the charges of the highly negative DNA phosphate backbone. This results in a decrease of repulsive forces and decreases the persistence length of the DNA. When 89-90% of the charge is neutralised by spermidine, the DNA spontaneously adopts a condensed conformation (Manning, 1978).

This method has been used to great effect in gene therapy. This is due to the fact that when using non-viral DNA transfer techniques, transfer of DNA containing the gene of interest is greatly enhanced by the use of polyamines (Mannisto *et al.*, 2002; Blagbrough *et al.*, 2003; Liu *et al.*, 2001).

This condensed conformation is also relevant to the situation found in bacteria. Although the nucleoid of healthy growing cells is compacted into a small volume in the centre of the bacterial cell, under conditions of cell stress (such as exposure to UV light and nalidixic acid, which cause double-stranded breaks in the DNA) it has been seen that the nucleoid undergoes a further ordering process in which the bacterial nucleoid is arranged to align the DNA helices in parallel arrays. Under these conditions the nucleoid can also adopt a toroidal conformation. This finding has been explained by the 'restricted diffusion model' where it has been proposed as a method to allow easy repair of damaged DNA, by holding the broken ends close to each other in an ordered structure (reviewed in Minsky, 2004). Condensation is discussed in greater detail in chapter 1.

It is therefore of interest to see how enzymes such as EcoKI are affected by the spermidine-induced condensed conformation of DNA and how this is related to the situation found *in vivo*. In order to evaluate this effect of condensed DNA on EcoKI activity, an assay is first required to determine under what conditions DNA is condensed by spermidine.

5.2. Determination of DNA condensation state

5.2.1. Ligation

When linear DNA is in a condensed conformation, the free ends should be closer to each other in 3-D space than when DNA is in a random coil conformation. As the distance between the ends decreases, the enzyme DNA ligase is able to ligate the free ends together more readily. Ligase is an enzyme that fills in nicks in double-stranded DNA. Therefore, when two cohesive ends bind to each other by complementary base pairing, ligase is able to seal the ends together by forming covalent bonds to produce completely covalently bonded double-stranded DNA. It has been shown that condensation brings free ends into close proximity and can thereby increase the rate of cyclisation (Jary and Sikorav, 1999). Therefore, it was proposed that ligation could form the basis of an assay to determine the condensation state of linear DNA.

Figure 5.1A shows a typical gel from a ligation assay where linear DNA, produced by restriction with EcoRI, is converted into other forms due to ligation of its cohesive ends. Linear pBR322 is ligated into supercoiled monomers, nicked monomers, linear dimers and other multimeric forms over time. These products visualised on gels can be further analysed by densitometry (figure 5.1B) where the area under the peaks, produced by bands in the gels, can be calculated and used to form a graph. This is represented in figure 5.1C, which shows the decrease in linear monomeric pBR322 as it is ligated into these other products. There is an initial rapid decrease in monomeric linear DNA as the ends are ligated. This is followed by a slowing of ligation and levelling off after 135min, after which time around 90% monomeric linear DNA has been ligated. From this graph, it is possible to calculate the rate constant of ligation. This procedure was followed with increasing concentrations of spermidine, and the rate constants of ligation at each concentration are shown in figure 5.2.

Condensation is usually used to describe a concentrated region of densely packed DNA of finite size, and can comprise many or just a single DNA molecule. Therefore, the ligation of linear monomers into all other structures (monomeric and multimeric forms) was used to analyse the condensation state of DNA. This is due to the fact that this analysis describes the distance between free ends of the same molecule and other molecules.

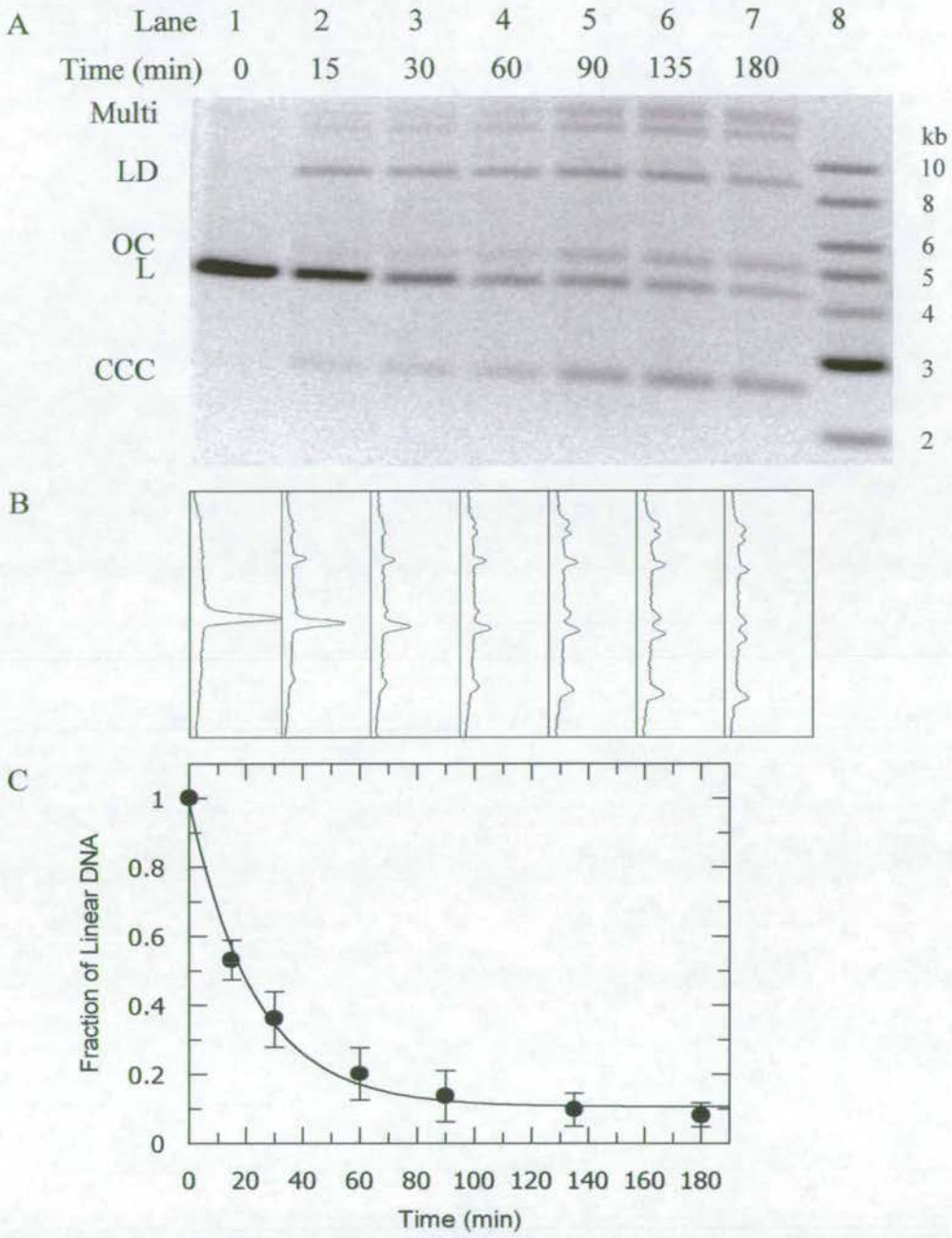

Figure 5.1. Ligation of linearised pBR322. A) Agarose gel showing timecourse of ligation of pBR322 that has been linearised with EcoRI (EcoRI was heat-inactivated prior to ligation reactions). Reaction contained 60nM DNA, 0.4units ligase, 50µg/ml BSA, 1mM ATP and low salt EcoKI buffer, pH7.9. Linear DNA (L) is converted into linear dimers (LD) as well as open circular (OC) and supercoiled (CCC) forms. Slow migrating DNA consisting of circularised dimers and higher multimeric species are also indicated (Multi). Lane 8 contains 1kb linear DNA marker of sizes indicated. B) Densitometry of gel A, as aligned, using Scion Image software. C) Graph of decrease of linear DNA against time. Graph represents the mean of 3 separate experiments.

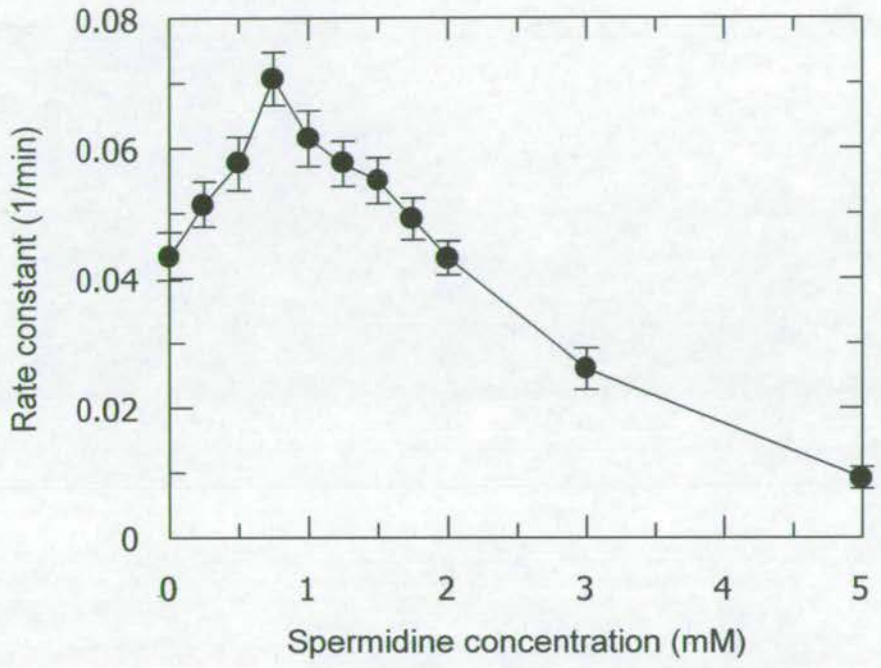

Figure 5.2. Effect of spermidine concentration on the ligation of linear pBR322. Reactions were carried out and analysed as seen in figure 5.1. The graph shows how the rate at which linearised pBR322 is ligated into circularised and multimeric species is effected by spermidine concentration. It should be noted that ionic strength was not kept constant in these experiments, and therefore increased with increasing spermidine concentration. (See Appendix C).

In order to look at monomeric DNA condensation, the data was also analysed as the production of nicked and supercoiled monomeric ligated products. This formed a graph essentially identical to that shown in figure 5.2 (data not shown).

The rate constant of ligation of linear pBR322 increases with an addition of spermidine from 0-0.75mM. Addition of spermidine to 2mM decreases the rate constant of restriction to a similar level to that obtained in the absence of spermidine. The rate constant of ligation continues to decrease with a further increase in spermidine concentration up to 5mM. These results agree with experiments carried out by Raae *et al.,* (1975), which showed a similar correlation between ligase activity and spermidine concentration.

As additions of spermidine decrease the persistence length of DNA, it may be expected that this would increase the ligation rate, as the ends are able to meet more readily. However, when the DNA is condensed, the ends may be held apart in the ordered condensed structure and therefore unable to bind. It is also possible that at high spermidine concentrations, DNA aggregates are formed thereby preventing access of the ligase to the free ends. It should also be noted that in these experiments, the ionic strength increased with increasing spermidine concentration. Therefore the results may reflect the effect of ionic strength on ligase activity. This dependence of ligase on ionic strength has been observed by increasing the monovalent salts concentration (Raae *et al.*, 1975). In these experiments, a concentration of around 70mM inhibited ligase activity, with a concentration of around 200mM almost completely preventing the occurrence of any ligase reactions.

In order to determine which of these situations was occurring in the reactions, an experiment was carried out where 116mM NaCl was added to a reaction with 3mM spermidine. It had been shown that this salt concentration could decondense DNA under conditions similar to these (Baeza *et al.*, 1987). Therefore, if the ends were being held rigidly apart by the condensed structure of DNA, or DNA aggregation was inhibiting access of the ligase to the DNA, decondensation with NaCl would increase the ligation rate, compared to a control reaction without NaCl, but with 3mM spermidine, and another without spermidine but with 116mM NaCl. The ligation rate of the reaction containing both 3mM spermidine and 116mM NaCl was the slowest, thereby suggesting that the effects observed may be mainly due to the increasing ionic strength of the reactions with increasing spermidine concentration (data not shown).

It would therefore be of interest to repeat these experiments, with the ionic strength maintained at a constant level throughout all additions of spermidine. However, as the ligation of linear pBR322 produces such a wide range of products, and the condensation of DNA may have both stimulatory and inhibitory effects on ligation of cohesive free ends, it was decided to look for a more straightforward method of determining the condensation state of DNA.

5.2.2. Atomic Force Microscopy

The AFM images (figure 5.3) show plasmid DNA in an uncondensed conformation in the absence of spermidine. However, with the addition a very small amount of spermidine (0.09mM) the DNA can be seen to partially condense into more compact forms. With the addition of a large concentration of spermidine (7.3mM) the DNA can be seen to form toroidal condensates of around 50-100nm in diameter. Although the background is full of other structures, these are also present in the control containing 7.3mM spermidine without DNA, which shows no toroidal structures.

However, image quality decreased as spermidine concentration increased, possibly due to the formation of salt crystals. It was only possible to obtain images in buffers of very low ionic strength and therefore conditions in which EcoKI is active were unobtainable. AFM sample preparation also produces the potential problems of inhomogeneous spermidine and other salt concentrations as the sample is dried to the mica. Therefore, the structures seen are representative of structures that may be obtained in solution-based reactions, but cannot describe the conditions of spermidine or other salt concentration required for DNA condensation to occur.

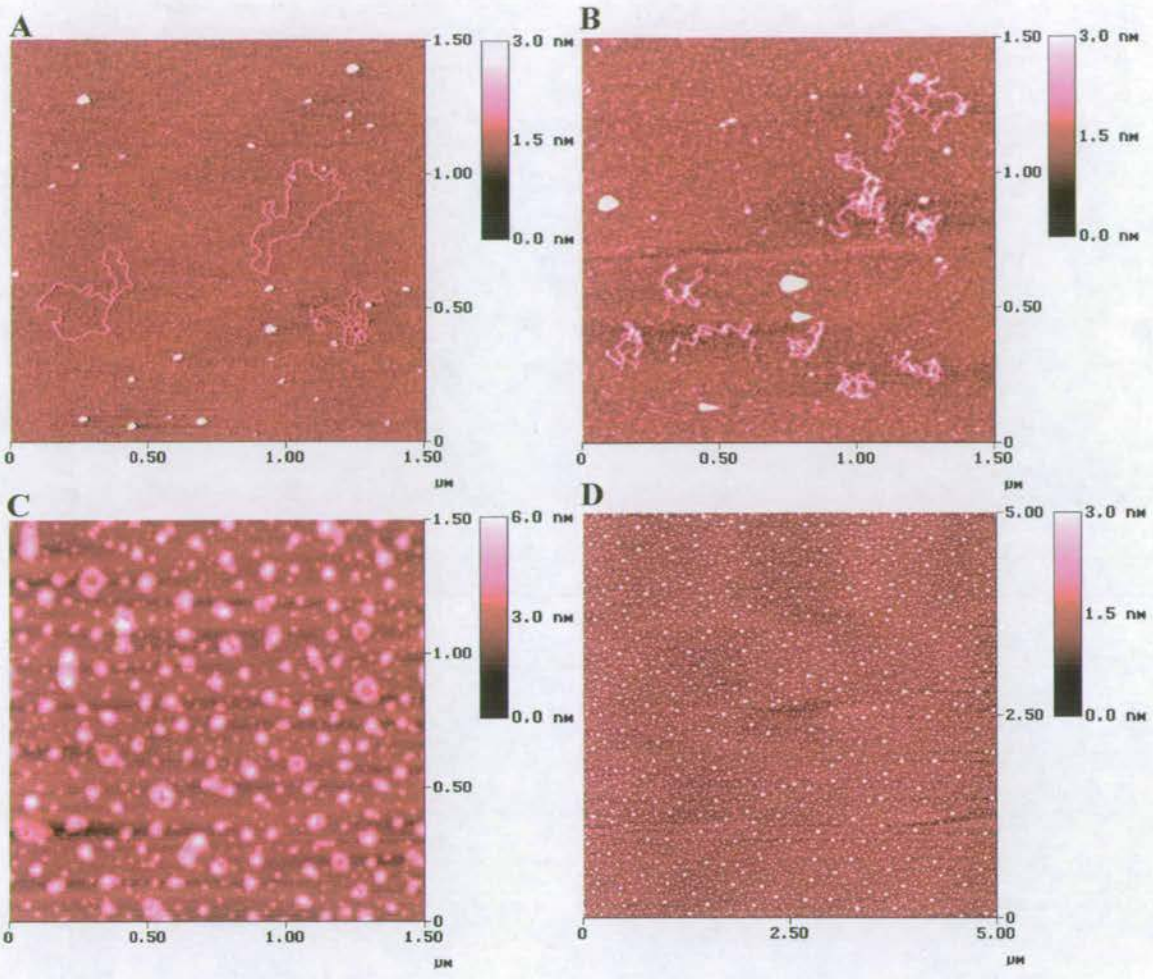

Figure 5.3. AFM images of spermidine-condensed DNA. AFM was used to image pBR322 in buffer containing 2mM Tris-acetate, 2mM Mg-acetate, 1.4mM 2-mercaptoethanol, pH 7.9 with (A) 0mM spermidine, (B) 0.09mM spermidine and, (C) 7.3mM spermidine. Image D shows 7.3mM spermidine without DNA.

5.2.3. DNaseI assay

5.2.3.1. Effect of spermidine on DNaseI digestion of DNA

DNaseI has been shown to be able to digest uncondensed DNA, but unable to digest DNA in a condensed conformation (Baeza *et al.*, 1987). This should therefore give a clear indication of the condensation state of the DNA with varying concentrations of spermidine. DNaseI is also active under EcoKI reaction conditions and therefore the same conditions can be used for the DNaseI assay as for EcoKI assays to follow.

At a total ionic strength of 100mM, both supercoiled and linear pBRsk1 were condensed by 6mM spermidine, as seen by their protection from digestion by DNaseI (figure 5.4). Some condensation can also be seen to occur with 5mM spermidine by the presence of faint bands. It can be seen that although the linear DNA appears completely condensed at 6mM spermidine, the supercoiled DNA is mainly in an open circular conformation with some linear, and virtually no supercoiled DNA. More of the supercoiled DNA is completely protected from DNaseI digestion at 10mM spermidine, shown by the large increase in the supercoiled band. At this concentration less DNA is linearised, as seen by the reduction in the linear band intensity. Condensed DNA still accessible to DNaseI for nicking activity as the open circular form is still produced (figure 5.4A). However, this nicking could also be taking place in the linear DNA (figure 5.4B) but is indistinguishable from fully intact linear DNA by agarose gel electrophoresis. Therefore supercoiled DNA shows structural changes that cannot be seen with linear DNA upon DNaseI digestion, due to its different structural conformations. It shows that the condensed structure becomes more condensed (and more resistant to DNaseI) with further additions of spermidine.

This experiment was also carried out at 75mM ionic strength. This showed the same trends in the protection of linear and supercoiled pBRsk1 as for the experiment carried out at 100mM ionic strength. However, at this lower ionic strength, linear and supercoiled DNA were condensed by only 4mM spermidine (data not shown). This dependence of polyamine-induced condensation upon ionic strength has also been demonstrated by Raspaud *et al.*, (1998), and agrees with the counterion condensation theory (Manning, 1978). The affects of altering other conditions upon spermidine-induced DNA condensation were investigated further.

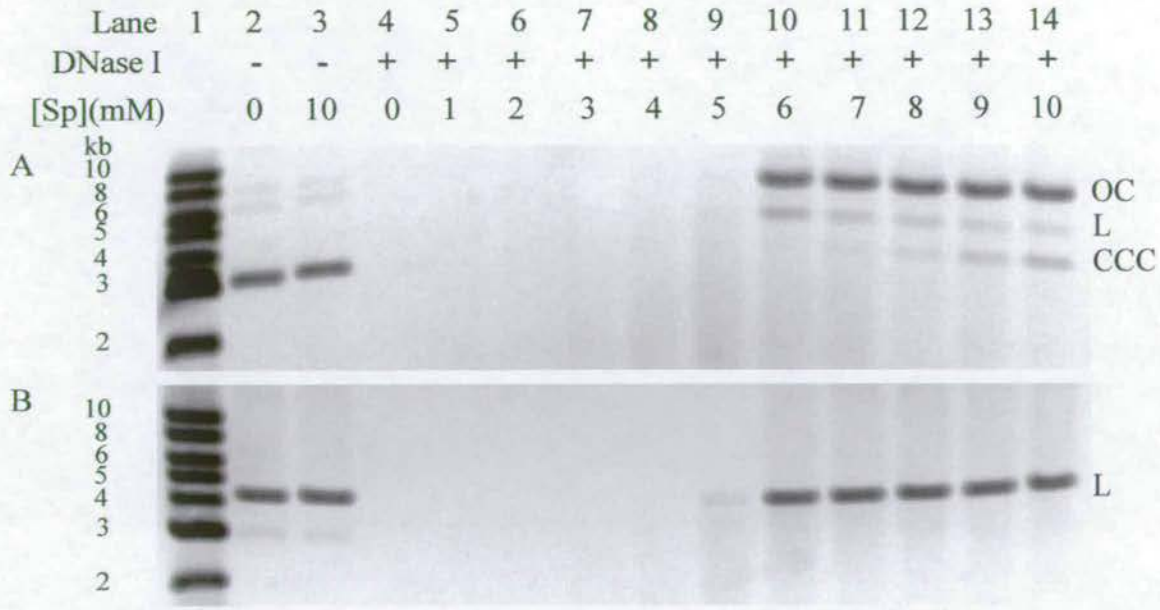

Figure 5.4. Effect of spermidine-induced condensation on digestion of linear and supercoiled DNA by DNase I. DNase I (0.1μg/ml) was used to digest supercoiled (A) and linear (B) pBRsk1 in low salt EcoKI buffer with the ionic strength made up to 100mM with NaCl. The concentration of spermidine (Sp) was varied from 0-10mM. The different conformations of DNA produced are indicated as supercoiled (CCC), nicked (OC), and linear (L). Lanes 2 and 3 of both gels contain pBRsk1 without DNase I but with 0 and 10mM spermidine respectively as controls. Lane 1 in both gels contains a DNA 1kb ladder of sizes indicated.

5.2.3.2. Effect of YOYO on DNA condensation

Figure 5.5 shows the effects of YOYO on spermidine-induced condensation of supercoiled and linear pBRsk1. A YOYO concentration of 50bp DNA per YOYO was used with varying concentrations of spermidine. The reaction conditions were the same as for figure 5.4 where pBRsk1, in the absence of YOYO, was condensed at 6mM spermidine. However, in the presence of YOYO, both supercoiled and linear pBRsk1 are condensed at a higher concentration of 10mM spermidine. A slight degree of protection from DNaseI digestion is also provided to the DNA by 8mM spermidine, as shown by the presence of faint bands. At this concentration, a smear running from the linear bands can also be seen indicating incomplete digestion of DNA. In figure 5.5A, at 10mM spermidine, supercoiled pBRsk1 can be seen to be digested by DNaseI into mainly nicked form with some linear and supercoiled also present. This indicates that even at this high spermidine concentration, pBRsk1 is not completely protected from the nicking activity of DNaseI. This is not seen with linear pBRsk1 (figure 5.5B), although as previously mentioned, this may be due to the fact that nicked and intact linear DNA cannot be separated by agarose gel electrophoresis.

These results show that at the concentration used, YOYO inhibits condensation of pBRsk1 by spermidine. This is shown by the higher concentration of spermidine (10mM) required to condense pBRsk1 with 50bp per YOYO, compared to the lower concentration (6mM spermidine) required for condensation in the absence of YOYO under the same ionic conditions. Both supercoiled and linear pBRsk1 are condensed at the same spermidine concentrations in the presence or absence of YOYO. These results agree with experiments carried out by Murayama and Sano, (2004), which also showed that YOYO inhibited DNA condensation by spermidine.

It is possible that further protection of pBRsk1 from DNaseI would take place at higher spermidine concentrations. However, this was not possible in these experiments due to the ionic strength constraints.

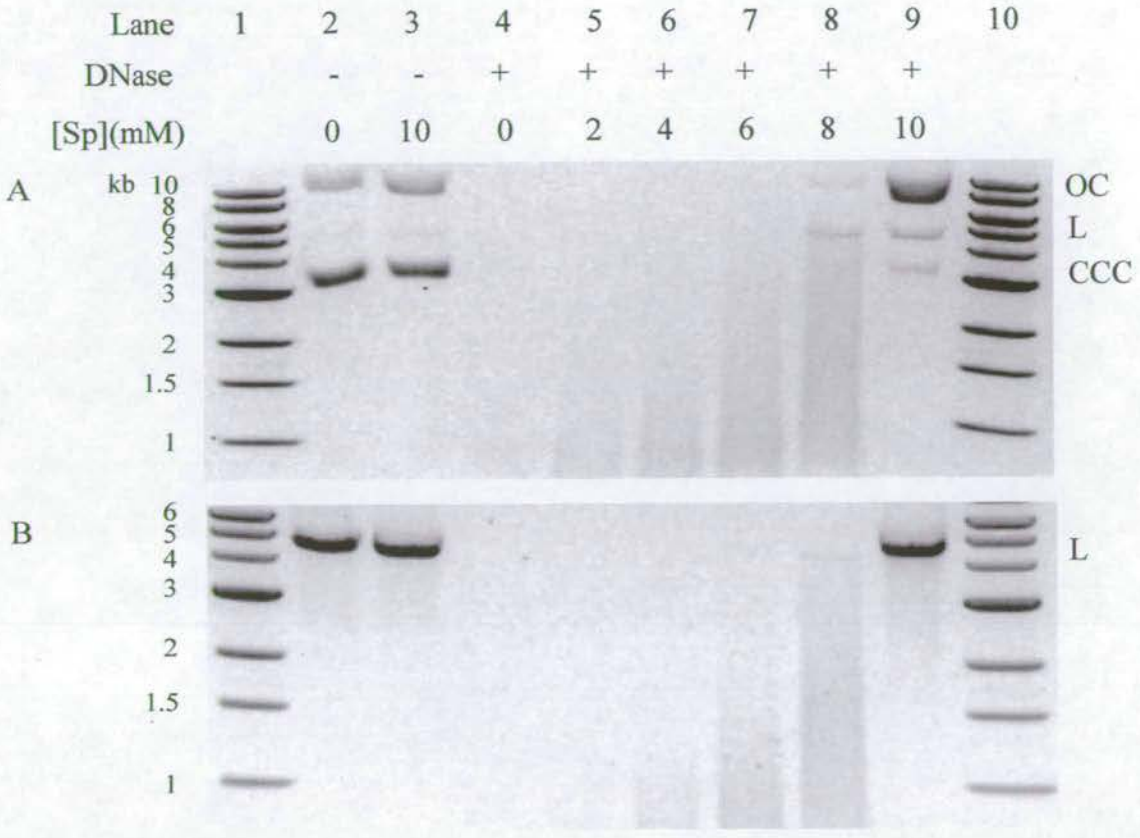

Figure 5.5. Effect of YOYO on spermidine-induced condensation of linear and supercoiled DNA, using DNase I digestion assay. DNase (0.1μg/ml) was used to digest supercoiled (A) and linear (B) pBRsk1 with a bp to dye ratio of 50 DNA bp per YOYO molecule. Reactions were carried out in low salt EcoKI buffer with the ionic strength made up to 100mM with NaCl. The concentration of spermidine (Sp) was varied from 0-10mM. The different conformations of DNA produced are indicated as supercoiled (CCC), nicked (OC) and linear (L). Lanes 2 and 3 of both gels contain pBRsk1 without DNase I but with 0 and 10mM spermidine respectively as controls. Lanes 1 and 10 of both gels contain a linear DNA 1kb ladder of sizes indicated.

5.2.3.3. Effect of ionic strength on DNA condensation

Figure 5.6 shows the effect of ionic strength on DNA condensation. When the ionic strength is kept constant at 681mM (figure 5.6A), it can be seen that even concentrations of spermidine up to 140mM are not capable of condensing DNA, as seen by the absence of a DNA band on the gel. However, when the ionic strength varies with the addition of spermidine, the DNA becomes condensed by 40mM spermidine, and decondenses at 100mM spermidine. Although the DNA is expected to be condensed at lower concentrations of spermidine, the long incubation times used in order to visualise DNaseI digestion of DNA at high ionic strengths limit the sensitivity of the assay to these condensates formed at lower ionic strengths. This condensation and decondensation behaviour has been seen in other studies where the ionic strength has varied (Jary and Sikorav, 1999; Murayama *et al.*, 2003). In its condensed form, the DNA seems to be nicked by DNaseI, due to its position on the gel, and therefore not completely protected from the action of DNaseI. It should be noted that binding of spermidine to DNA alters its mobility through an agarose gel due to its charge neutralisation affects. Although the two gels show different forms of DNA (linear and supercoiled), there is no difference in the condensation point of the two forms as shown previously (see figure 5.4). Also, the control in figure 5.6A, lane 14 shows that at lower ionic strength, 60mM spermidine is capable of condensing linear DNA, under the same conditions as in figure 5.6B, lane 7.

These results show how spermidine-induced condensation is affected by ionic strength, stressing how important it is to keep the ionic strength constant in such condensation studies.

5.3. Effects of DNA condensation on EcoKI activity

5.3.1. ATP hydrolysis coupled assay

As conditions were found that condense DNA, EcoKI assays could be carried out to determine the effect of the spermidine-induced condensed conformation of DNA on the ATP hydrolysis activity of EcoKI.

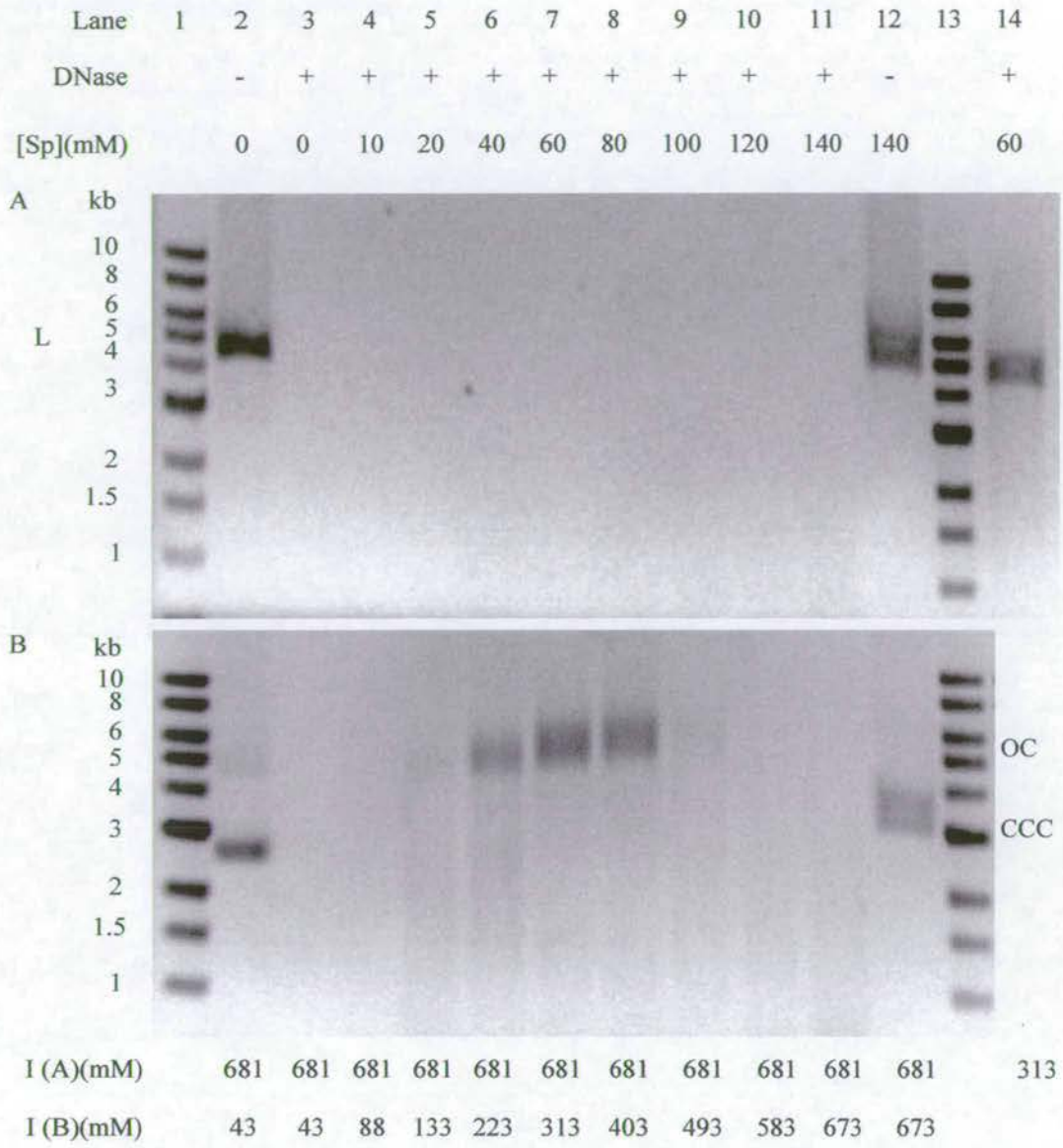

Figure 5.6. Effect of varying ionic strength (I) on DNA condensation, as seen by DNase I digestion. DNA was incubated with varying concentrations of spermidine and digested with 1μg/ml DNase I. Gel A shows digestion of linear pBRsk1 at a constant ionic strength of 681mM, except lane 14 which has an ionic strength of 313mM. Gel B shows the effect of varying the ionic strength, as indicated, on digestion of supercoiled pBRsk1. Lanes 1 and 13 contain 1kb linear DNA ladders of sizes indicated.

EcoKI ATP hydrolysis activity was studied using linear and supercoiled pBR322 and pBRsk1 (figure 5.7). It can be seen that the rate of ATP hydrolysis by EcoKI follows the same trend with varying concentrations of spermidine with each type of DNA substrate studied. With all substrates, ATP hydrolysis is slightly reduced by the addition of spermidine up to 4mM. The addition of spermidine up to 6mM causes a dramatic reduction in ATP hydrolysis activity of EcoKI. This is followed by a slower continued decrease in ATP hydrolysis activity with further increases in spermidine concentration, up to 10mM.

These experiments were carried out under the same conditions as the DNaseI experiments shown in figure 5.4, at 100mM ionic strength. Under these conditions, linear and supercoiled DNA was condensed by 6mM spermidine. Therefore EcoKI ATP hydrolysis activity is inhibited by the condensed conformation of DNA. This could be due to several possibilities: EcoKI may be

a) unable to bind to its target site due to inaccessibility of the condensed DNA structure;
b) unable to bind to its target site due to spermidine binding to EcoKI;
c) unable to bind to its target site due to competition of DNA binding from spermidine or;
d) able to bind its target site but unable to translocate DNA due to its condensed structure.
e) unable to locate its recognition site due to the reduced target for initial binding presented by condensed DNA

In order to determine if EcoKI can bind to its target site on condensed DNA, the ATP hydrolysis assay was repeated with supercoiled pBRsk1, where EcoKI was bound to its target site before the addition of spermidine. There was no change in the result from that obtained for the ATP hydrolysis rate of supercoiled pBRsk1 from figure 5.7, where spermidine was added before EcoKI (data not shown). This implies that EcoKI is able to bind to condensed DNA. However, this result can also be explained as EcoKI may be knocked off the DNA during the condensation process. Also, EcoKI could be competed off the DNA by spermidine. This second explanation is unlikely as spermidine has little effect on EcoKI ATP hydrolysis activity from 0-4mM. It is only when condensation-inducing concentrations of spermidine are reached that ATP hydrolysis activity is severely inhibited.

It should be noted that even when DNA is condensed, although ATP hydrolysis activity of EcoKI is inhibited, some ATP is still hydrolysed. Therefore some EcoKI, at least can bind the condensed DNA. If EcoKI can bind to condensed DNA but cannot translocate it, could this condensed, non-translocatable DNA potentially trigger restriction of the DNA?

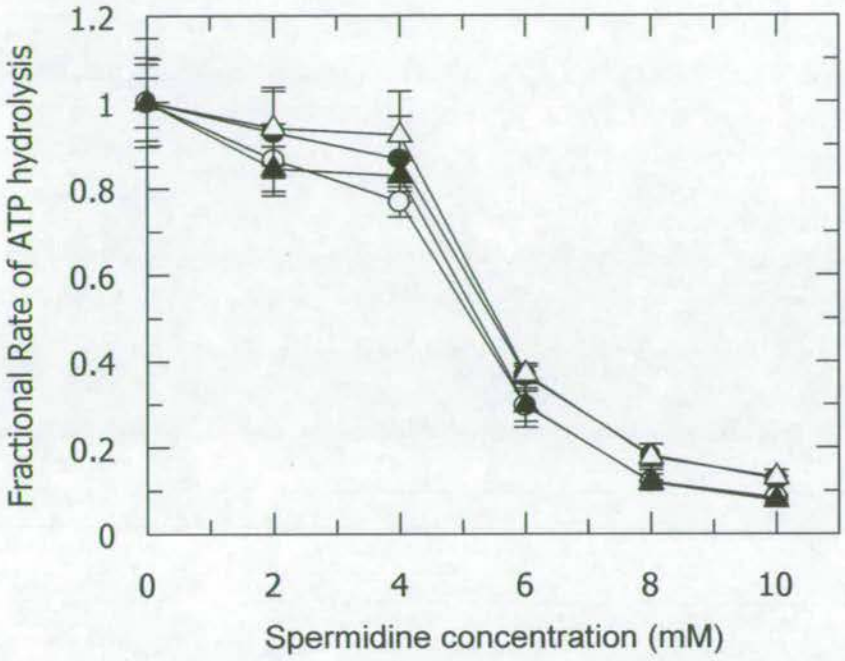

Figure 5.7. Effect of spermidine concentration on the rate of ATP hydrolysis of DNA by EcoKI. This graph represents the rate at which EcoKI hydrolyses ATP during translocation of supercoiled pBRsk1 (filled circles), linear pBRsk1 (open circles), supercoiled pBR322 (filled triangles) and linear pBR322 (open triangles). The concentration of EcoKI target sites on DNA was 5nM in all experiments. The reactions were carried out at an ionic strength of 100mM. Each point is the mean of 3 separate experiments.

5.3.2. EcoKI restriction assay

Figure 5.8 shows the effects of 6mM spermidine on the restriction of supercoiled pBRsk1 by EcoKI. This can be compared to a typical reaction carried out under the same conditions but in the absence of spermidine, in figure 3.4. When pBRsk1 has been condensed by 6mM spermidine, restriction by EcoKI does occur, but at a slower rate with less DNA being cut than in the absence of spermidine. This is shown in figure 5.8A, where the conversion of supercoiled pBRsk1 into nicked and linear DNA in the presence of 6mM spermidine can be seen. The total amount of DNA present in each well appears to decrease with time. This is possibly due to DNA bound EcoKI sticking to the reaction microcentrifuge tubes. As this would affect all conformations of DNA equally, the amount of each form of DNA in each lane was taken as a fraction of the total DNA present in each lane (figure 5.8B), thus overcoming this potential analytical problem. This can be seen in figure 5.8C, where the conversion of supercoiled to nicked to linear pBRsk1 can be followed. There is an initial rapid loss of supercoiled DNA as it is nicked. The supercoiled fraction then begins to level off after around 300s, and continues to decrease slowly until 1800s, where around 42% pBRsk1 remains as uncut, supercoiled DNA. The fraction of nicked DNA initially increases before levelling off after 150s at around 22% nicked DNA, at which level it remains until 1800s. There is a 30s lag before a rapid increase in linear DNA, up to around 300s. After this time there is a slow increase in linear DNA produced, where around 36% DNA is linearised after 1800s.

In order to fit this data to produce the graph shown in figure 5.8C, Dynafit modelling was used. For the restriction of one-site supercoiled pBRsk1, a simple model could account for the reaction mechanism in the absence of spermidine (see section 3.4). However, the addition of spermidine caused incomplete digestion of the DNA with a slow progression through the reaction pathway and the persistence of large amounts of uncleaved or nicked DNA. This suggests that spermidine can sequester the DNA in uncleavable forms which can be accounted for by their representation in the mechanism, where CCC* and OC* are the uncleavable forms of supercoiled and nicked DNA respectively. This therefore produces a more complicated model of restriction as previously described for the digestion of two-site linear pBR322 (section 3.4) and supercoiled pBRsk1 in the presence of dyes (section 4.2.1).

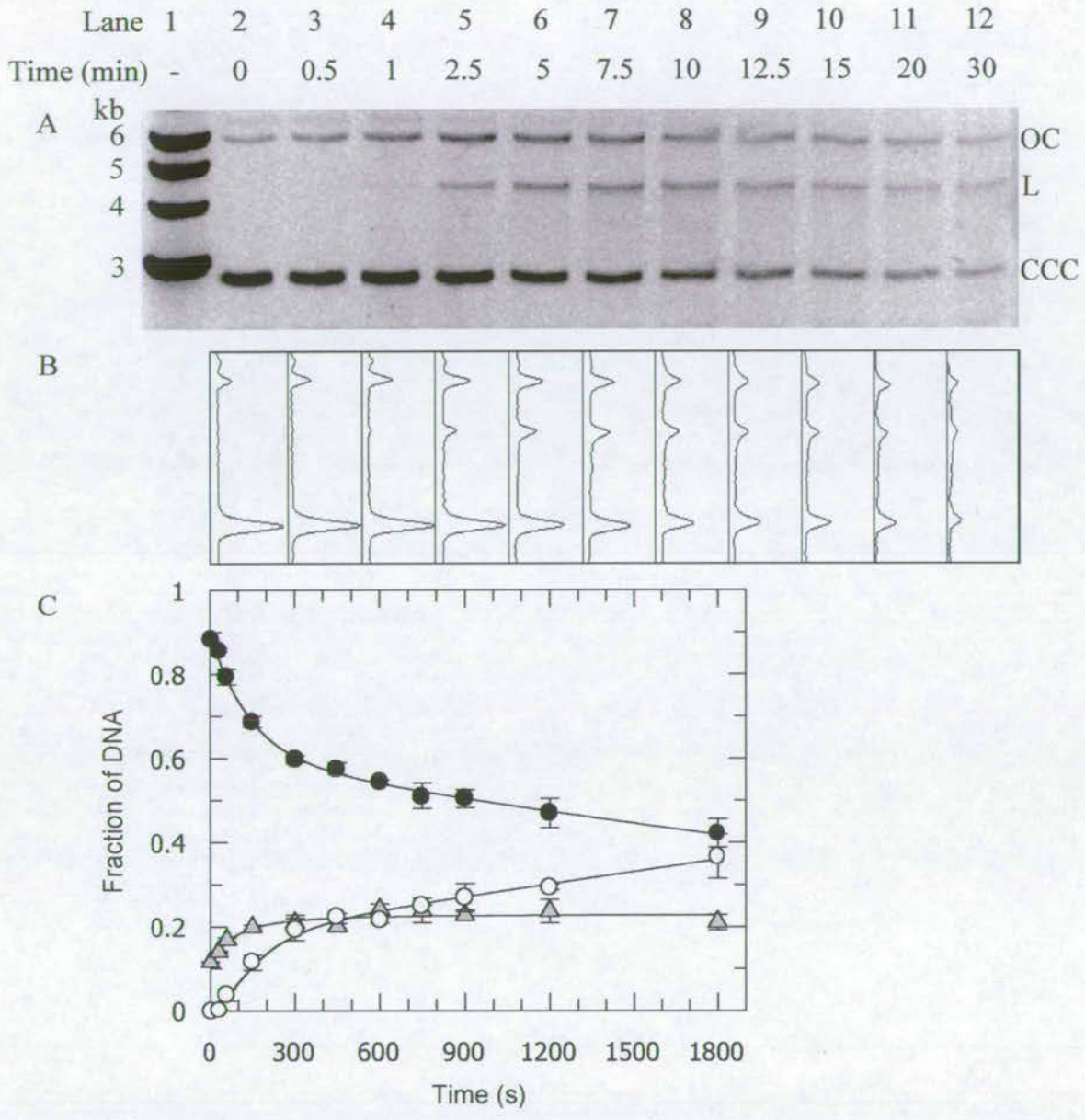

Figure 5.8. Restriction of condensed supercoiled pBRsk1 by EcoKI. Degradation of 50nM supercoiled pBRsk1 by 67nM EcoKI in low salt EcoKI buffer with 6mM spermidine and the ionic strength made up to 100mM with NaCl. A) Timecourse of EcoKI digestion of DNA with supercoiled (CCC) pBRsk1 being converted to nicked (OC) then to linear (L) DNA. Lane 1 contains a 1kb DNA ladder of sizes indicated. B) Densitometry of gel A obtained using Scion Image software. C) Graph of conversion of CCC (black circles) into OC (grey triangles) and L (white circles) over time. Curves were fitted to data using Dynafit software and a kinetic model described in the text. Points indicate the mean of 2 separate experiments.

The model used to fit the data for EcoKI restriction of supercoiled pBRsk1 was:

$$\begin{array}{ccccc} & & \overset{k1}{\rightarrow} & & \overset{k2}{\rightarrow} \\ CCC & & & OC & & L \\ k4\updownarrow k6 & & & k3\updownarrow k5 & & \\ CCC^* & & & OC^* & & \end{array}$$

It is of interest that these reversible steps are only of minor importance below the spermidine concentrations of 6mM when DNA is uncondensed. However, they take on a significant role upon DNA condensation at and above 6mM spermidine (table 5.1). This can be seen from the calculated equilibrium constants, where the side reactions involving the formation of DNA structures resistant to cleavage by EcoKI become significant only once DNA condensation has occurred. Similar models were used to fit the data using the other DNA substrates (as discussed in section 3.4) with the same condensation dependence on reversible rate constants observed (data not shown). It is also interesting that the same model can be used to fit the data from the inhibition of dyes and condensation, possibly implying a similar mechanism in their inhibitory effects.

The rate constant of restriction of supercoiled pBR322 was affected by the condensation of DNA by spermidine (figure 5.9) in a similar way to the ATP hydrolysis experiments. Almost all restriction activity is lost when the DNA is condensed with 6-10mM spermidine. It can be seen that the rate constants are consistently higher for the restriction of nicked DNA into linear forms, than supercoiled into nicked DNA, which are higher than linear DNA into fragments. The same overall trend of loss of restriction activity upon DNA condensation is seen when EcoKI cuts supercoiled pBR322 (figure 9A), linear pBR322 (figure 9B), supercoiled pBRsk1 (figure 9C) and linear pBRsk1 (figure 9D). Although rate constants increase with a slight addition of spermidine (2-4mM), these increases are not significant within experimental error.

[Sp] (mM)	Rate constants (s^{-1})						Equilibrium constants	
	k_1	k_2	k_3	k_4	k_5	k_6	k_3/k_5	k_4/k_6
0	**0.0150** ±0.0030	**0.0262** ±0.0100	**$1.93x10^{-8}$** ±0.0030	**$1.13x10^{-9}$** ±0.0110	**0.0020** ±0.0010	**0.1563** ±1.8	**$9.65x10^{-6}$**	**$7.22x10^{-9}$**
2	**0.0187** ±0.0003	**0.0276** ±0.0075	**$1.93x10^{-8}$** ±0.0019	**$1.13x10^{-9}$** ±0.0011	**0.0041** ±0.0016	**0.0051** ±0.0037	**$4.71x10^{-6}$**	**$2.21x10^{-7}$**
4	**0.0197** ±0.0029	**0.0331** ±0.0087	**$1.93x10^{-8}$** ±0.0016	**$1.13x10^{-9}$** ±0.0008	**0.0019** ±0.0006	**0.0044** ±0.0027	**$1.01x10^{-5}$**	**$2.57x10^{-7}$**
6	**0.0037** ±0.0002	**0.0083** ±0.0020	**0.0152** ±0.0006	**0.0033** ±0.0001	**0.0003** ±0.0001	**0.0004** ±0.0001	**50.67**	**8.25**
8	**0.0020** ±0.0001	**0.0020** ±0.0006	**0.0079** ±0.0004	**0.0025** ±0.0001	**0.0002** ±0.0001	**0.0004** ±0.0001	**39.5**	**6.25**
10	**0.0002** ±0.0001	**0.0002** ±0.0001	**0.0093** ±0.0004	**0.0022** ±0.0001	**0.0029** ±0.0005	**0.0017** ±0.0001	**3.20**	**1.29**

Table 5.1. Effect of spermidine concentration on EcoKI rate constants of restriction. Rate constants for the restriction of supercoiled pBRsk1 by EcoKI with varying concentrations of spermidine were calculated by Dynafit using the mechanism described in the text. The equilibrium constants for the reversible reaction steps are also shown. A graphical representation of rate constants k1 and k2 are shown in figure 5.9C.

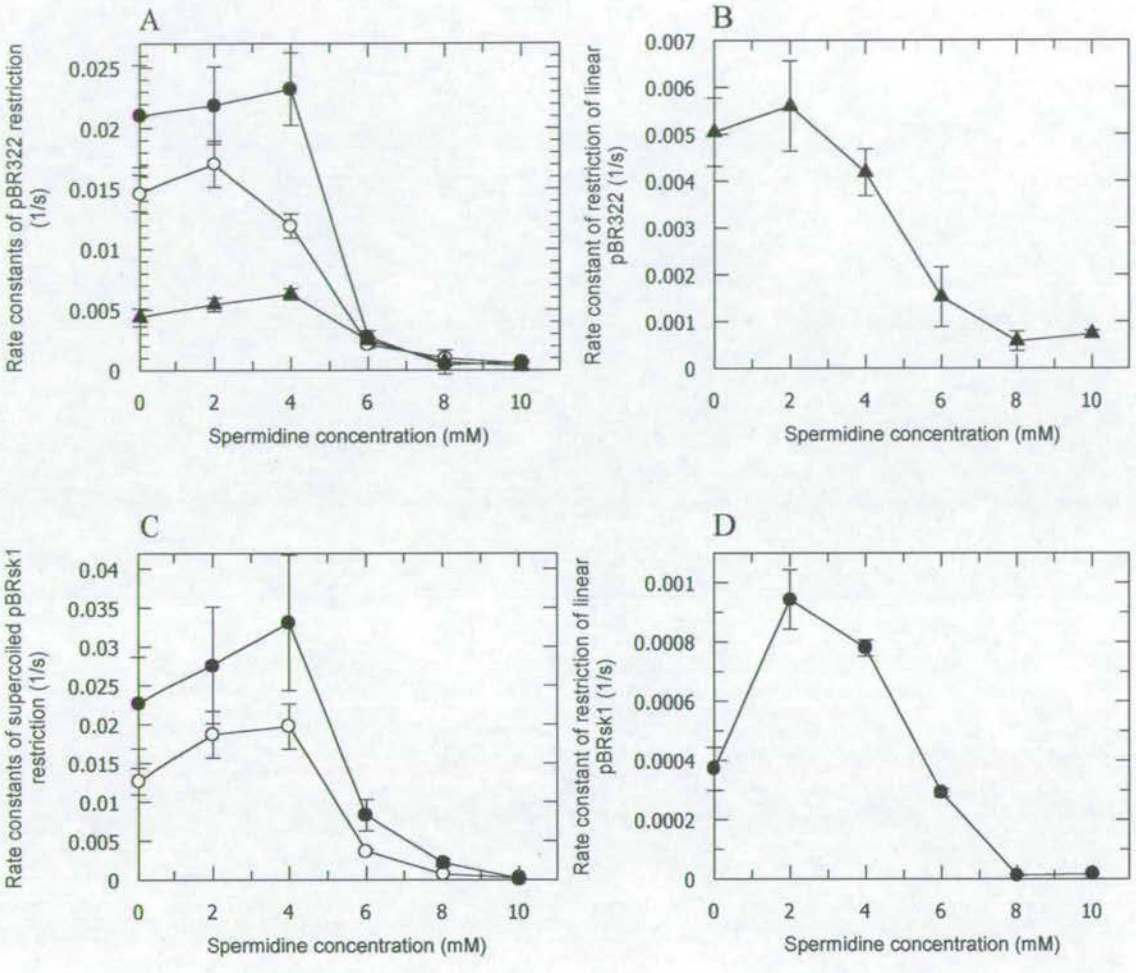

Figure 5.9. Effect of spermidine concentration on the restriction of supercoiled and linear pBR322 and pBRsk1 by EcoKI. The reactions were carried out in low salt EcoKI buffer, pH 7.9, with the ionic strength made up to 100mM with NaCl. Reactions contained 50nM DNA with 134nM EcoKI for pBR322 and 67nM EcoKI for pBRsk1. A) This graph represents the effect of spermidine concentration on the rate constant of restriction of supercoiled pBR322 into nicked form (open circles), nicked DNA into linear form (filled circles), and linear DNA into fragments (closed triangles). B) This graph represents the effect of spermidine concentration on the rate constant of restriction of linear pBR322 into fragments. C) This graph represents the effect of spermidine concentration on the rate constant of restriction of supercoiled pBRsk1 into nicked form (open circles), and nicked DNA into linear form (filled circles). D) This graph represents the effect of spermidine concentration on the rate constant of restriction of linear pBRsk1 into fragments. Each point shows the mean rate constants of 2 separate experiments. (See Appendix C).

5.4. Summary

Ligation of linearised plasmid was increased by low spermidine concentrations but inhibited at higher concentrations, with varying ionic strength. AFM showed condensed structures of DNA with the addition of spermidine, with toroidal condensates observed at high spermidine concentration. At a constant ionic strength of 100mM, the DNaseI assay found linearised and supercoiled plasmid DNA was condensed at 6mM spermidine. It was found that the addition of YOYO at 50bp per YOYO raised this condensation point to 10mM spermidine. Condensation is dependent upon ionic strength, where condensation is followed by decondensation of plasmid DNA as the spermidine concentration is increased with an accompanying increase in ionic strength. The condensed structure of DNA inhibits the ATP hydrolysis and restriction activities of EcoKI.

Chapter 6:

StpA

6.1. Introduction

The nucleoid of growing bacteria occupies only a small volume in the centre of the cell. This compact conformation of the host chromosome is partly due to the binding of condensation-inducing nucleoid-associated proteins. These include StpA, which is 58% homologous to the well-studied condensing protein H-NS. This protein forms dimers that oligomerise, and bind DNA. Each monomer of the dimer is thought to bind to DNA and therefore the dimer can bridge two separate DNA helices together, thus condensing the DNA (Esposito *et al.*, 2002). The concentration of such nucleoid-associated proteins changes throughout the cell cycle. Upon exposure to an environment that can damage the DNA, such as UV light or nalidixic acid, the bacterial nucleoid has been seen to reorganise itself into a highly condensed conformation with the DNA helices in parallel arrays (Minsky, 2003). It has been found that another nucleoid-associated protein, Dps, that is induced by starvation is involved in the organisation of such a nucleoidal conformation (Frenkiel-Krispin *et al.*, 2004).

The effects of StpA on the structure of DNA and the resultant effects on EcoKI activity may further elucidate the situation encountered by EcoKI and other DNA-binding proteins within the bacterial cell.

6.2. Effect of StpA on DNA conformation

6.2.1. StpA-induced condensation of linear DNA

The DNaseI assay was used to look at the condensed structure of DNA with varying concentrations of StpA. It was found that linear pBR322 was protected from DNaseI digestion by a concentration of 64bp per StpA, and partially protected at a concentration of 96bp per StpA (figure 6.1). A very faint band can also be seen when 128bp per StpA is used, although the majority of DNA at this concentration has been digested. All other concentrations of StpA are insufficient to protect linear pBR322 from DNaseI and it is therefore digested. Some slight smearing can be seen at concentrations of 256-171bp per StpA indicating that the accessibility of DNaseI to the DNA is partially inhibited, showing that the DNA structure has been altered at these concentrations of StpA.

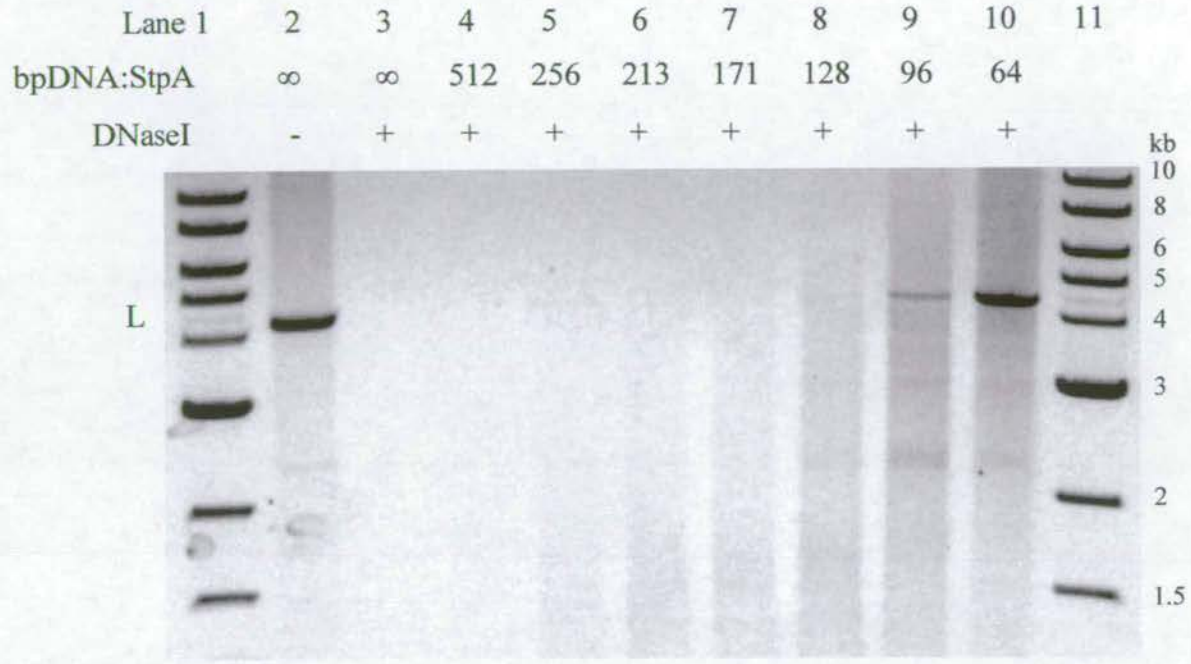

Figure 6.1. Effect of StpA concentration on DNase I digestion of linear pBR322. Linear pBR322 (L) was digested with 0.1μg/ml DNase I for 1h at 25°C in high salt EcoKI buffer, pH7.9. The gel shows undigested DNA as a band of 4.4kb (L), with digested DNA being absent from the gel, or present as a faint smear. Lanes 1 and 11 contain linear DNA 1kb markers of sizes indicated.

6.2.2. StpA-induced condensation of supercoiled DNA

The effect of StpA concentration on DNaseI digestion of supercoiled pBRsk1 was also studied (figure 6.2). Supercoiled pBRsk1 was protected from DNaseI digestion by a concentration of 256bp per StpA, and partially protected at a concentration of 384bp per StpA. A very faint linear band can also be seen when 512bp per StpA is used, although the majority of DNA at this concentration has been digested. All other concentrations of StpA are insufficient to protect supercoiled pBR322 from DNaseI and it is therefore digested. The proportions of the protected DNA change as the StpA concentration is increased. This can be seen with the decrease in the intensity of linear DNA, and increasing intensity of supercoiled DNA. This indicates that the DNA is becoming less accessible to DNaseI attack with increasing StpA concentration, therefore implying a change in DNA structure. Although it is possible that StpA is physically blocking the potential cutting sites of DNaseI and thereby preventing digestion, this is unlikely due to the low concentrations of StpA (256bp:StpA) required to inhibit DNaseI. At this low concentration, the relatively small size of StpA would be unable to sufficiently protect the DNA from the indiscriminate cutting of DNaseI.

No concentration of StpA studied was capable of completely protecting the supercoiled form of pBRsk1, as the DNaseI was always able to at least nick the plasmid. This nicking activity was not seen with linear pBR322. This may be as nicked linear substrate is indistinguishable from intact linear substrate by agarose gel electrophoresis. Therefore StpA-induced condensation may not be able to protect the linear pBR322 from the nicking activity of DNaseI.

These results suggest that StpA can condense both linear pBR322 and supercoiled pBRsk1. However, it is also possible that StpA inhibits the DNaseI enzyme directly. This was shown not to be the case by a control experiment shown in figure 6.3. In this control, a concentration of StpA was used which caused DNaseI inhibition of supercoiled pBRsk1 (171bp:StpA), but with 3 times the concentration of DNA, reducing the DNAbp:StpA ratio below the inhibition level (512bp:StpA). As the total concentration of StpA had not changed, if StpA inhibited DNaseI directly, this reaction would have resulted in no digestion of the DNA. However, the DNA was digested and therefore the effect of StpA upon DNA structure appears to be the DNaseI inhibiting factor.

Figure 6.2. Effect of StpA concentration on DNase I digestion of supercoiled pBRsk1. Supercoiled pBRsk1 (CCC) was digested with 0.1µg/ml DNase I for 1h at 25°C in high salt EcoKI buffer, pH7.9. The gel shows undigested DNA (CCC), with digested DNA being absent from the gel, and DNA protected from digestion is present as linear (L) and nicked (OC) species. Lanes 1 contains linear DNA 1kb markers of sizes indicated.

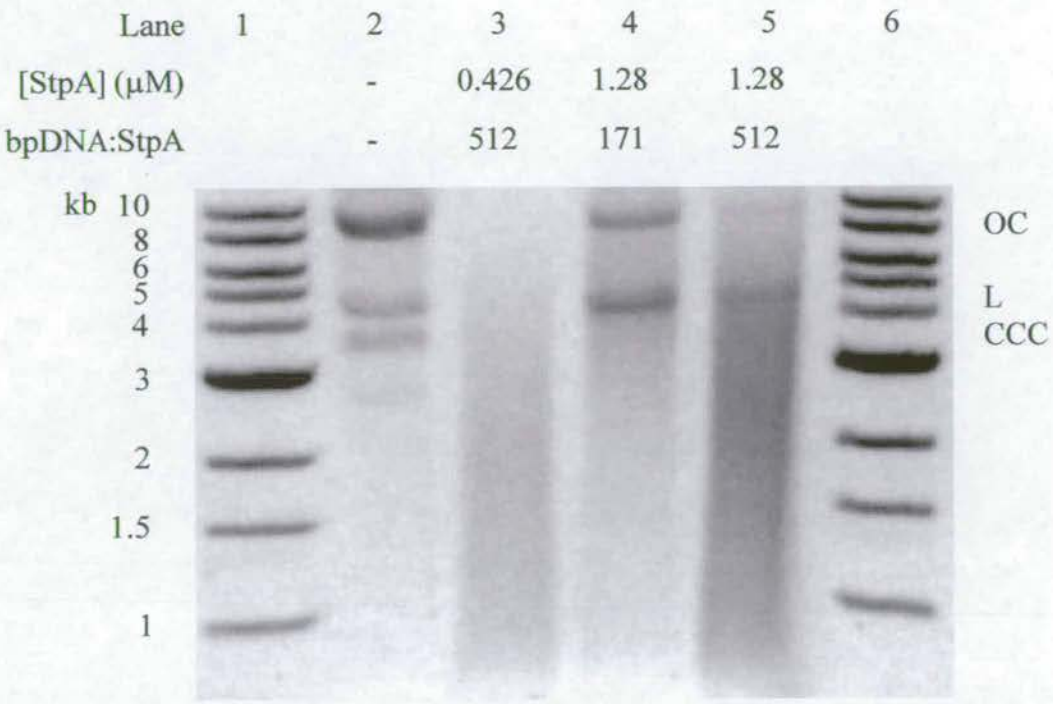

Figure 6.3. Agarose gel showing effect of StpA concentration on inhibition of DNase I digestion of supercoiled pBRsk1. Supercoiled pBRsk1 was digested by 0.1μg/ml DNase I in low salt EcoKI buffer, pH 7.9, at 25°C. Lane 3 shows how 50nM DNA is digested by DNase I with 512bp DNA per StpA, with a StpA concentration of 0.426μM. Lane 4 shows DNase I digestion of 50nM DNA at 171bp per StpA (1.28μM StpA). Lane 5 shows how 150nM DNA is digested by DNase I with 512bp per StpA, at an StpA concentration of 1.28μM. Lane 2 is a marker containing supercoiled (CCC), nicked (OC) and linear (L) pBRsk1. Lanes1 and 6 contain 1kb linear DNA markers of sizes indicated.

The experiment described in figure 6.3 also shows how the effect of StpA on DNA is dependent upon the bp:StpA ratio and not the actual StpA concentration. This is different to the way that spermidine effects DNA structure and may be explained by their different mechanisms of condensation. Therefore these experiments show that linearised plasmid is condensed by a higher concentration of StpA than supercoiled plasmid DNA.

6.3. Effect of StpA-induced condensation on EcoKI activity

6.3.1. EcoKI ATP hydrolysis

As the conditions of DNA condensation with StpA have been determined, the effect of this conformation on EcoKI activity can be studied. Figure 6.4 shows the effect of StpA concentration on the ATP hydrolysis activity of EcoKI. The rate of ATP hydrolysis of linear pBRsk1 decreases only slightly with addition of StpA up to 171bp per StpA (0.00585StpA:bp). A large decrease in ATP hydrolysis rate to around a fifth of the uninhibited rate is seen with addition of StpA up to a concentration of 96bp per StpA (0.0104StpA:bp). Upon further addition of StpA up to 64bp per StpA (0.0156StpA:bp) there is little change in the ATP hydrolysis rate, which levels off at around a sixth of its uninhibited rate.

The rate of ATP hydrolysis of supercoiled pBRsk1 decreases only slightly with addition of StpA up to 384bp per StpA (0.0026StpA:bp). A large decrease in ATP hydrolysis rate to around a fifth of the uninhibited rate is seen with addition of StpA up to a concentration of 171bp per StpA (0.00585StpA:bp). Upon further addition of StpA there is little change in the ATP hydrolysis rate up to 64bp per StpA (0.0156StpA:bp) where it levels off at around a tenth of the uninhibited rate.

Linear and supercoiled DNA follow the same trend in their response to increasing StpA concentrations. However, a higher concentration of StpA is required to inhibit the ATP hydrolysis activity of EcoKI with linear rather than supercoiled pBRsk1 substrate. The rate of EcoKI ATP hydrolysis of both supercoiled and linear pBRsk1 is inhibited by concentrations of StpA that condense DNA. It therefore appears that the condensed structure of DNA induced by StpA inhibits EcoKI ATP hydrolysis activity.

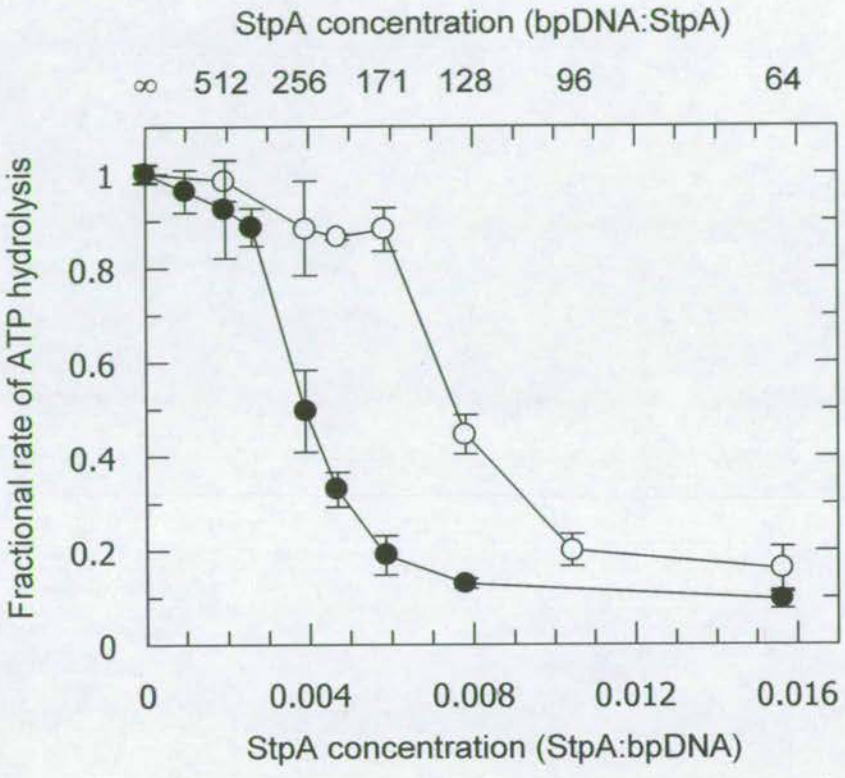

Figure 6.4. Effect of StpA concentration on the relative rate of ATP hydrolysis of EcoKI with linear and supercoiled substrates. The StpA concentrations are indicated as bp per StpA on the top x axis and as the number of StpA molecules per bp on the bottom x axis. The relative rate of ATP hydrolysis by EcoKI is shown when supercoiled pBRsk1 (closed circles) and linear pBRsk1 (open circles) were used as substrates. Reactions took place in high salt EcoKI buffer, pH 7.9, with 5nM DNA.

6.3.2. EcoKI restriction activity

6.3.2.1. Linear DNA

Figure 6.5 shows the effect of StpA concentration on the restriction of linear pBR322 after 20min incubation with EcoKI. It can be seen that EcoKI restriction of linear pBR322 is inhibited by high concentrations of StpA. In the absence of StpA, restriction of linear pBR322 does not go to completion, although most DNA has been restricted after 20min. However, no EcoKI cutting of linear pBR322 is visible after 20min at concentrations up to 96bp per StpA. EcoKI restriction is also inhibited by 128bp per StpA, but a small amount of smearing (indicating cutting) can be seen. Concentrations of 256-171bp per StpA appear to be slightly inhibitory to EcoKI restriction. The usual cutting pattern of EcoKI restriction of EcoRI-linearised pBR322 (band at 3.9kb and smear from this), as seen in absence of StpA, is not seen at these concentrations of StpA. This implies that concentrations of 256-171bp linear pBR322 per StpA reduce the rate and alter the mechanism of restriction by EcoKI.

6.3.2.2. Supercoiled DNA

It can be seen from figure 6.6 that EcoKI restriction of supercoiled pBRsk1 is also inhibited by high concentrations of StpA. In the absence of StpA, supercoiled pBRsk1 is completely cut into linear DNA. However, no EcoKI cutting of supercoiled pBRsk1 is visible after 20min at concentrations up to 256bp per StpA. EcoKI restriction is also inhibited by 512bp per StpA, but a small amount of restricted linear DNA can be seen. A faint supercoiled band can also be seen when DNA is cut at a concentration of 1024bp per StpA, indicating that the reaction has not gone to completion and is therefore slightly inhibited.

Figure 6.7 shows a control experiment to check that StpA was not inhibiting EcoKI directly. This involved cutting supercoiled pBRsk1 with an StpA concentration that inhibited EcoKI (171bp per StpA), but using three times the concentration of DNA, thereby bringing the bp:StpA ratio to level which caused less inhibition of EcoKI (512bp:StpA). As the StpA total concentration has not changed, if EcoKI was directly inhibited by StpA, then this DNA should still be uncut by EcoKI. In fact the DNA was cut and therefore it appears that StpA inhibits EcoKI by its affect on DNA structure.

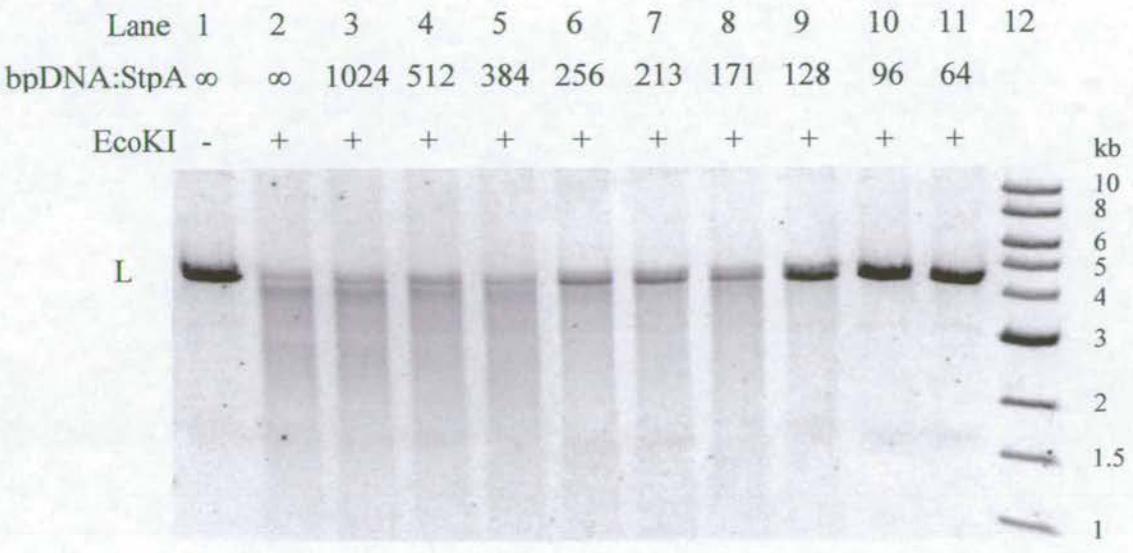

Figure 6.5. Effect of StpA concentration on the restriction of EcoKI on EcoRI-linearised pBR322. 50nM linear pBR322 was cut in high salt EcoKI buffer, pH 7.9, with varying concentrations of StpA for 20min. pBR322 is cut from DNA that forms a distinct band of 4.4kb (L), into a smear of lower molecular weight. Lane 12 contains a linear 1kb DNA ladder of sizes indicated.

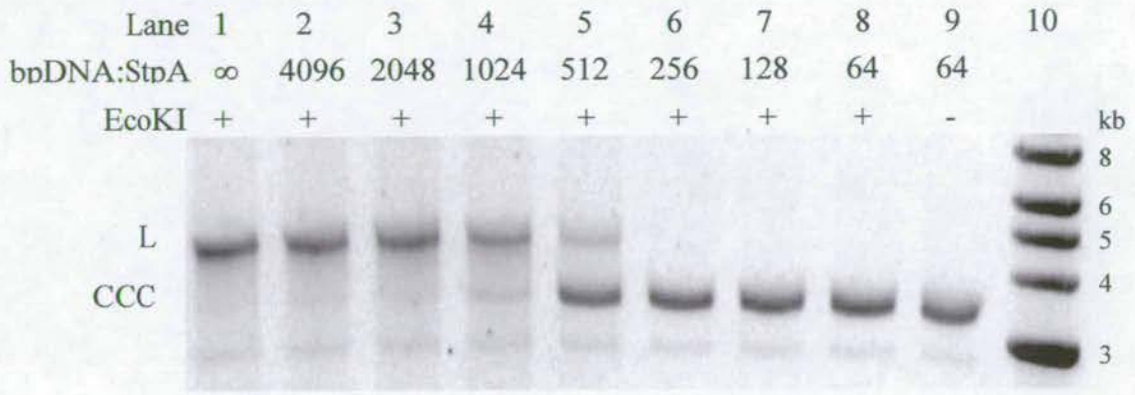

Figure 6.6. Effect of StpA concentration on the restriction of EcoKI on supercoiled pBRsk1. 50nM supercoiled pBRsk1 was cut in high salt EcoKI buffer, pH 7.9, with varying concentrations of StpA for 20min. pBRsk1 is cut from supercoiled DNA (CCC), into a linear band of 4.4kb (L). Lane 10 contains a linear 1kb DNA ladder of sizes indicated.

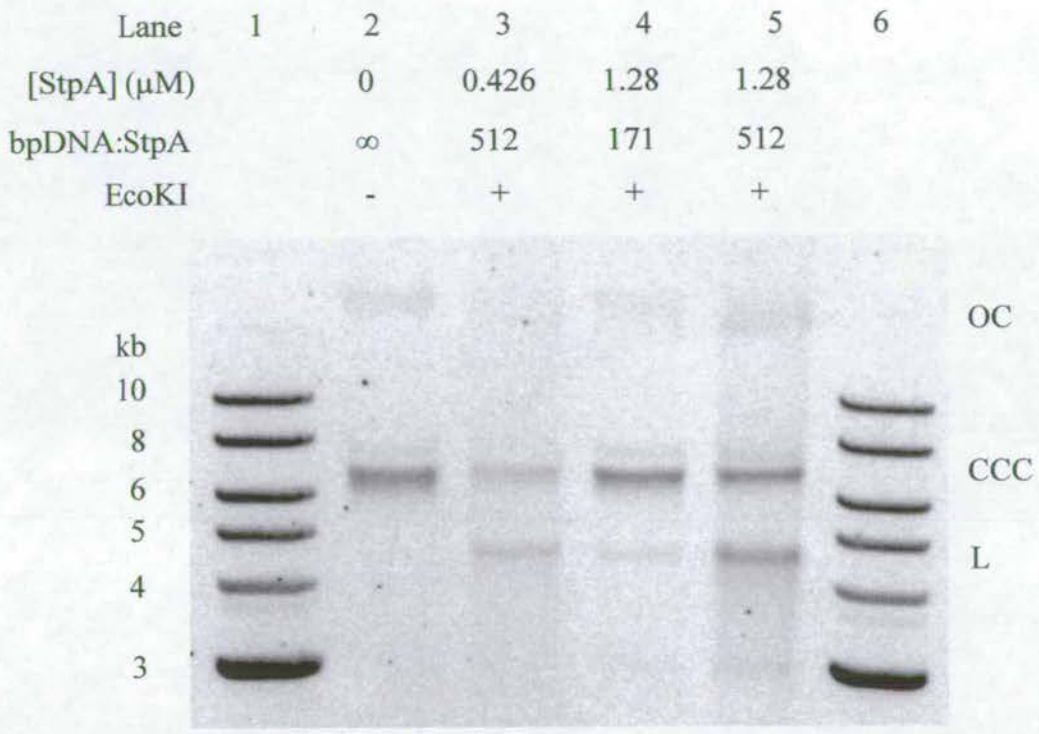

Figure 6.7. Agarose gel showing effect of StpA concentration on inhibition of EcoKI restriction of supercoiled pBRsk1. Supercoiled pBRsk1 was restricted by EcoKI in low salt EcoKI buffer, pH 7.9, at 25°C. Lane 3 shows how 50nM DNA is restricted by EcoKI with 512bp DNA per StpA, with a StpA concentration of 0.426μM. Lane 4 shows EcoKI restriction of 50nM DNA at 171bp per StpA (1.28μM StpA). Lane 5 shows how 150nM DNA is restricted by EcoKI with 512bp per StpA, at an StpA concentration of 1.28μM. Lane 2 is a marker containing supercoiled (CCC) pBRsk1 with a small amount of nicked (OC) DNA, without any StpA. Lanes1 and 6 contain 1kb linear DNA markers of sizes indicated.

EcoKI restriction is inhibited by StpA-induced condensation of supercoiled pBRsk1. Although there is a major inhibition at the condensation point, there also seems to be a more general inhibition of EcoKI that varies with StpA concentration and may agree with the altered structure of DNA seen with the DNaseI assay. It should be noted that this other, more general inhibition is not so evident from the ATP hydrolysis data, although there is a slight decrease in the ATP hydrolysis rates prior to the condensation point with increasing concentrations of StpA.

The fact that supercoiled DNA is condensed at lower concentrations of StpA than linear DNA may give some insight into the condensation mechanism. Inter-helix linking is thought to be a major function of StpA in its condensing role. DNA supercoiling would facilitate this by the close proximity of the helices to each other due to its covalently closed and twisted structure. This would allow StpA dimers to bind to two DNA helices in supercoiled DNA more easily than in linear DNA where the helices are further apart.

6.4. Summary

The DNaseI assay shows that StpA condenses linearised plasmid DNA at a higher concentration than is required to condense supercoiled plasmid. This StpA-induced condensation of DNA inhibits the ATP hydrolysis and restriction activities of EcoKI.

Chapter 7:

Crowding

7.1. Introduction

Any DNA entering the cytoplasm of the bacterial cell will have its conformation immediately affected by crowding. This is due to the extremely high concentrations of macromolecules present in the cytoplasm, which take up a large volume of the cell interior. Crowding also affects the nucleoid structure, helping to compact it into a small volume in the centre of the cell. Crowding not only affects DNA structure, but also the rate at which it interacts with proteins. This is mainly due to 'volume exclusion', which acts to increase the relative concentrations of the reactants and hence speed up reactions. However, as a solution becomes more crowded, it also becomes more viscous. Viscosity tends to slow down reactions as restricted diffusion effects make it more difficult for reactants to meet.

It is therefore of interest to see how viscosity and crowding affect the activity of EcoKI, as this is more representative of the situation in which EcoKI encounters invading bacteriophage DNA in the cytoplasm. In order to separate the effects of viscosity and crowding, a method of measuring the viscosity of the reaction solutions was required.

7.2. Viscosity measurement

The viscosities of various concentrations of PEG 8000 and glycerol were measured in low salt EcoKI buffer made up to 100mM ionic strength with NaCl. As the concentrations of PEG 8000 and glycerol increased, so did the viscosity, as shown in figure 7.1. It was found that PEG 8000 forms more viscous solutions than glycerol. These results can be used to form solutions of PEG 8000 and glycerol with equal viscosity. For example, if an experiment was carried out in 15% PEG 8000, a control experiment with glycerol of an equivalent viscosity would be carried out in 54% glycerol.

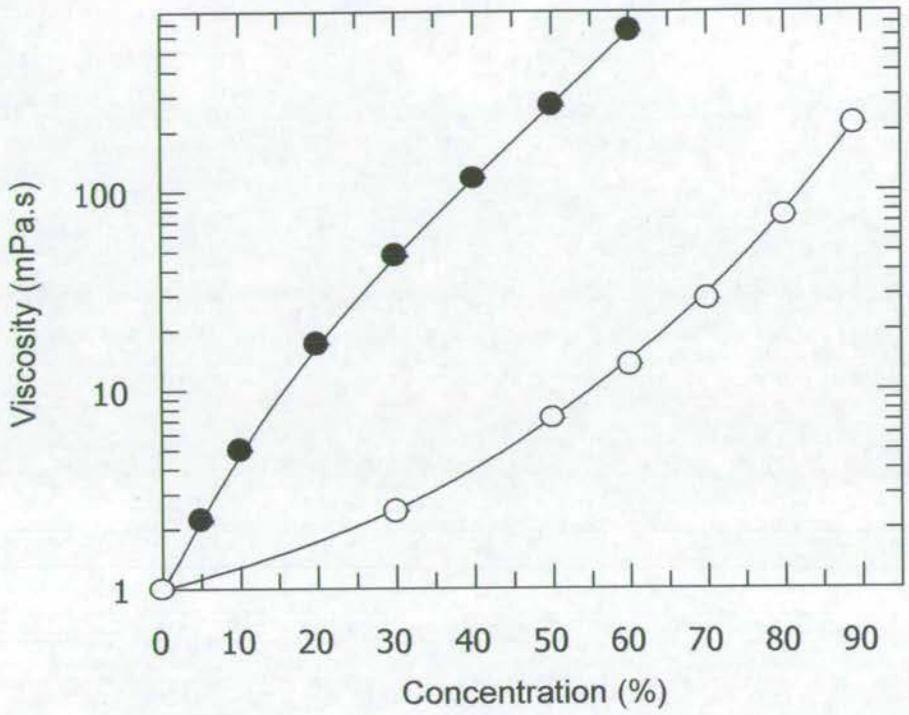

Figure 7.1. Calibration of PEG 8000 and glycerol viscosities. Viscosities were measured in low salt EcoKI buffer, pH 7.9, at 25°C with the ionic strength made up to 100mM with NaCl. PEG 8000 viscosities were measured from 0-60% solutions (closed circles). Glycerol viscosities were measured from 0-89% solutions (open circles). Points show the mean of 2 separate experiments. (see Appendix D).

7.3. Effect of crowding on EcoKI activity

7.3.1. EcoKI ATP hydrolysis activity

In order to change the absorbances at 630nm obtained from the P_i ATP hydrolysis assay into the concentration of P_i produced, a calibration graph is required. This was obtained by measuring the absorbances of solutions of known KH_2PO_4 concentrations at 630nm and is shown in figure 7.2. The calibration graphs form straight lines up to a concentration of 0.75mM potassium dihydrogen phosphate at an absorbance at 630nm. However, it was found that lower absorbances were obtained for KH_2PO_4 when the experiments were done in the presence of PEG 8000. Therefore a separate graph was required for the calibration of absorbances at 630nm to KH_2PO_4 concentration in the presence of PEG 8000.

Reactions were carried out with 50nM linear pBR322 with 134nM EcoKI in low salt EcoKI buffer, pH7.9, made up to 100mM ionic strength with NaCl. These results in figure 7.3 show how the amount of P_i produced by EcoKI varies with time in buffers containing 5% PEG 8000 and 27.5% glycerol. Both these solutions have the same viscosity. It can be seen that the production of P_i follows the same trend in both solutions (and as in absence of PEG 8000 and glycerol, figure 3.12), with an initial rapid rate, followed by a slowing and levelling off of P_i produced. It can be seen from the graph that EcoKI produced more P_i more quickly in the presence of 5% PEG 8000 than in the presence of 27.5% glycerol.

The initial rate of P_i production can be calculated at each concentration of PEG 8000 and glycerol. These rates are compared in figure 7.4. This graph shows how EcoKI ATP hydrolysis activity (production of P_i) is inhibited by increasing concentrations of glycerol and therefore increasing viscosity. However, increasing the concentration of PEG 8000 has a different effect. As the PEG 8000 concentration is increased from 0 to 5%, the initial rate of P_i production increases. Further increases in PEG 8000 concentration inhibit the initial rate of P_i production, but to a lesser extent than the inhibition achieved by the same viscosities of glycerol. This indicates that factors other than viscosity, such as crowding, are affecting initial reaction rates of P_i production in the presence of PEG 8000.

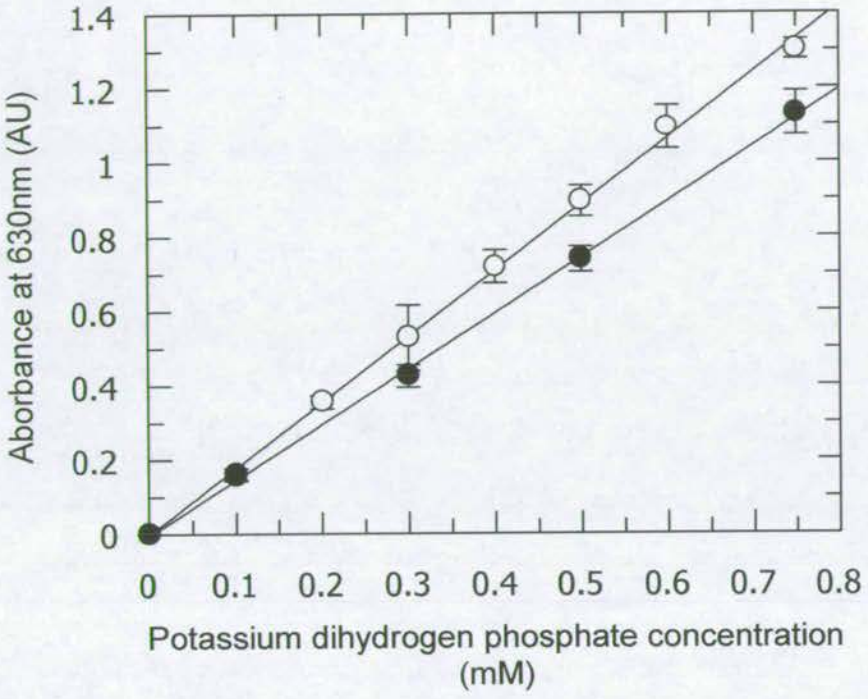

Figure 7.2. Calibration of KH_2PO_4 concentration with absorbance at 630nm. The absorbance at 630nm was measured 100s after the addition of mixed reagent to sample. Separate calibration graphs were required for samples containing PEG 8000 (closed circles) and containing glycerol or water (open circles). Points shown are the mean of 3 separate experiments (open circles), and the mean of 5 separate experiments (closed circles).

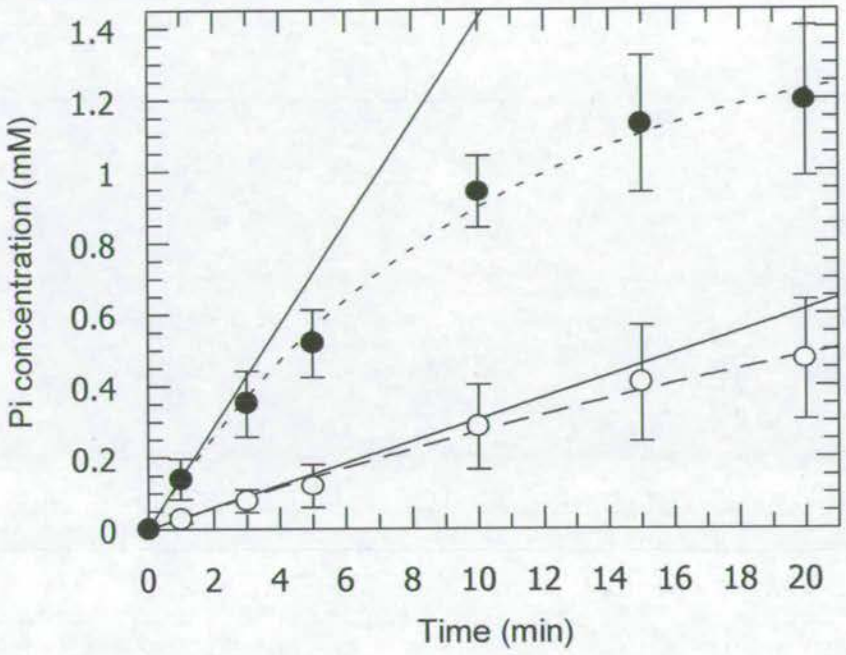

Figure 7.3. Effect of PEG 8000 and glycerol on the production of P_i by EcoKI. Reactions were carried out in low salt EcoKI buffer, pH 7.9, with 50nM linear pBR322 and 134nM EcoKI. Reactions were stopped with EDTA and absorbances at 630nm measured after 100s incubation with mixed reagent. The absorbances at 630nm were converted into P_i concentrations by use of the calibration graphs (figure 7.2). The graph shows the amount of P_i produced in isoviscous reactions containing 5% PEG 8000 (closed circles and dotted line) and 27.5% glycerol (open circles and dashed line). The complete lines represent the initial rates of reactions. All points represent the mean of 4 separate experiments.

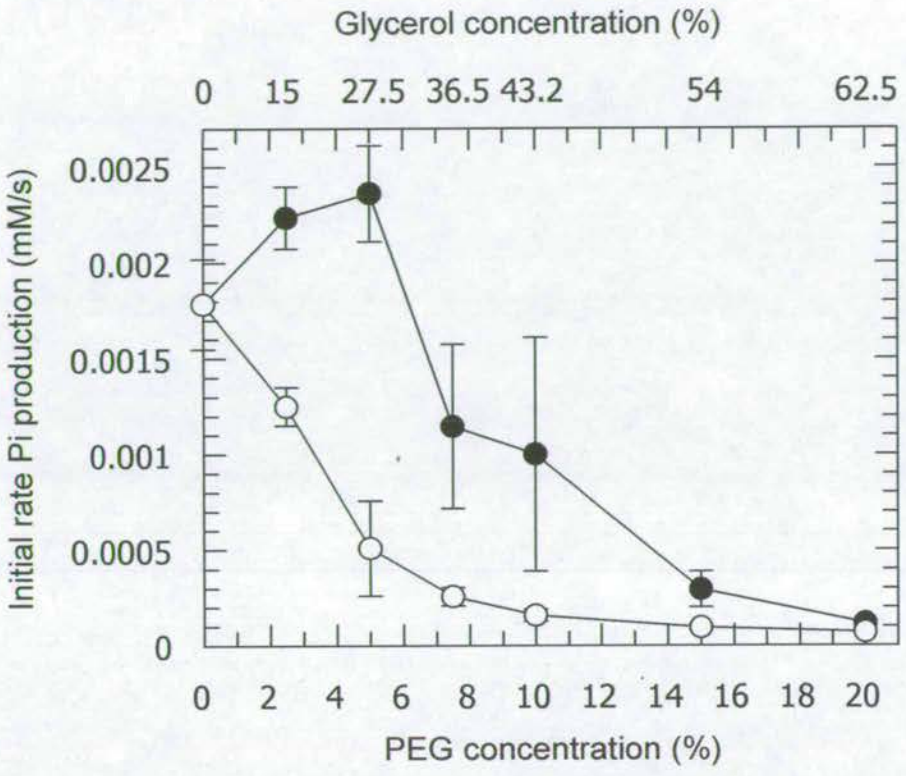

Figure 7.4. Effect of PEG 8000 and glycerol concentrations on initial rate of P_i production by EcoKI. Reactions were carried out as described in figure 7.3. The initial rates of P_i production by EcoKI with varying concentrations of PEG 8000 (closed circles) and glycerol (open circles) are shown. The bottom axis shows the concentration of PEG 8000, with the top axis giving the concentrations of glycerol used. The points are aligned to show solutions of equal viscosities. Each point represents the mean of 4 separate experiments. (see Appendix D).

Such a peak in activity is predicted by theory for reaction rates in crowded solutions (Zimmerman, 1993). Crowding increases the reaction rates by increasing the relative concentrations of reactants due to excluded volume effects. However, at higher concentrations crowding inhibits reactions due to the increased viscosity and slower diffusion, thereby preventing enzymes from locating their binding sites. In this respect, EcoKI represents an interesting enzyme to study crowding effects, as each EcoKI can only carry out a single restriction reaction. Therefore the usual resultant increased turnover rate with excluded volume effects does not account for any increase in reaction rates for EcoKI.

In an attempt to distinguish between crowding and viscosity effects, the differences between the rates of P_i production at isoviscous concentrations of PEG 8000 and glycerol were calculated. This can be seen in figure 7.5, which shows the effect of crowding on the initial rate of ATP hydrolysis (P_i production) where glycerol solutions act as viscosity blanks. This graph shows a peak at 5% PEG 8000 (27.5% glycerol). At all concentrations studied, the initial rates in PEG 8000 were higher than the corresponding initial rates obtained in glycerol as shown by the positive difference values.

This can be explained by the excluded volume principle of crowding. Glycerol forms homogenous viscous solutions. This viscosity acts to inhibit EcoKI binding as EcoKI is in a binding equilibrium with DNA, and will therefore release from its target site occasionally prior to the start of translocation. Once EcoKI has released its target site, it will be more difficult for it to rebind in highly viscous solutions. High viscosities of glycerol will also slow translocation due to the physical force required to pull a long length of DNA through a viscous solution. This is not the case with PEG 8000. PEG 8000 produces solutions that are viscous when measured on the macroscopic scale, but are inhomogeneous in composition at the molecular level. PEG 8000 forms a microarchitechture, where DNA and EcoKI are confined in a reduced volume, where they reside in a 'buffer bubble'. This therefore increases the relative concentrations of the reactants by reducing the volume that they occupy, without producing the problems of translocating DNA though a highly viscous environment. However, high PEG 8000 concentrations do become inhibitory, which can be explained if the PEG 8000 'cages' become so small they confine DNA-EcoKI complexes in a condensed state that act to inhibit EcoKI binding and/or translocation. Increases in ATP hydrolysis rate due to increased EcoKI concentrations and increased binding, have already been shown in figure 3.10. Crowding would mimic this as it acts to increase the relative concentration of EcoKI, and should therefore also increase the ATP hydrolysis rate.

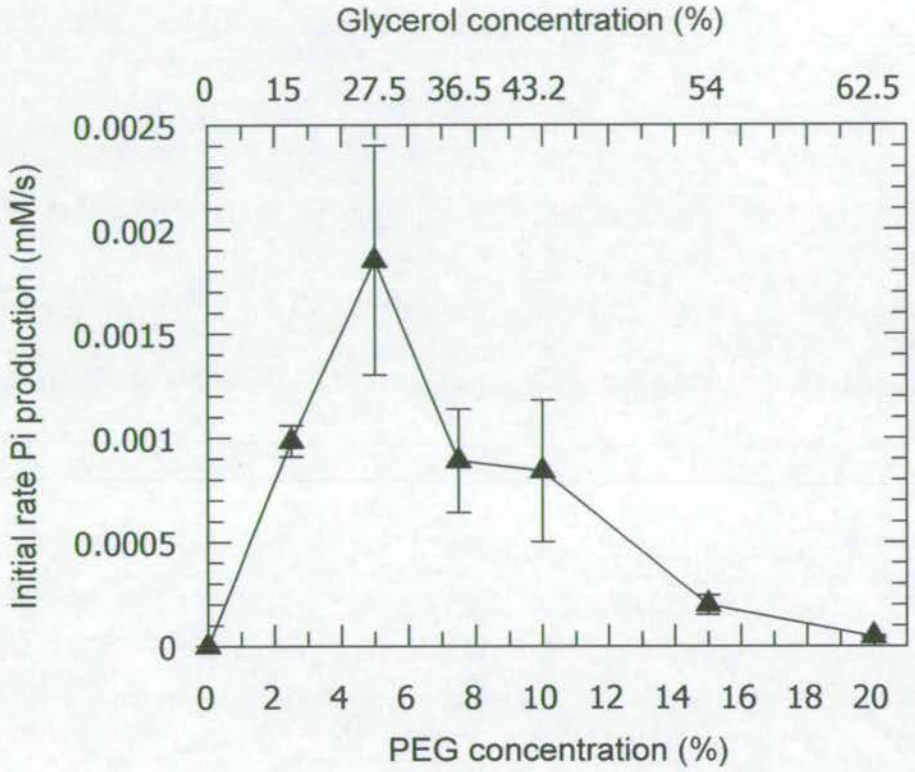

Figure 7.5. Difference between the initial rates of P_i production in the presence of PEG 8000 and glycerol. The initial rates of production of P_i in the presence of glycerol were taken away from the initial rates of production of P_i in the presence of PEG 8000 at equal viscosities (as shown in figure 7.4). The bottom axis shows the concentrations of PEG 8000 with the concentrations of glycerol used to give equal viscosities given on the top axis.

7.3.2. EcoKI restriction activity

Experiments were carried out to determine the effect of various concentrations of PEG 8000 and glycerol on the restriction activity of EcoKI on linear pBR322. These reactions were done under the same conditions as the P_i ATP hydrolysis experiments. The example results show that linear pBR322 is cut more quickly in 10% PEG 8000 compared to the 43.2% glycerol solution of equal viscosity (figure 7.6). The linear band that remains throughout the 20min time course with 43.2% glycerol, disappears after only 15min incubation with 10% PEG 8000 and EcoKI. This finding is shown more clearly in figure 7.6C, which represents these results graphically. With 10% PEG 8000 a rapid decrease in the fraction of DNA uncut can be seen, followed by a slower levelling off, with almost all the DNA being cut after 15min. In contrast, cutting in the presence of 43.2% glycerol shows a very slow decrease of uncut DNA, with only around a quarter total DNA being cut after 20min. Figure 7.6A shows that when the linear DNA is cut in the presence of 10% PEG 8000, the usual banding pattern of pBR322 cut by EcoKI is not seen (for comparison, see figure 3.6). In fact, no smearing is visible at all, indicating the DNA is cut into fragments too small to be seen on the gel. This implies a different mechanism of cutting in this crowded environment.

In order to determine whether non-specific restriction was occurring or if the observed DNA digestion was due to a contaminant present in the PEG 8000 or other buffer solutions, appropriate controls reactions in the absence of EcoKI or using methylated DNA were carried out. Under these conditions, no restriction of the DNA occurred after 20min incubation with any concentrations of PEG 8000 or glycerol investigated (figure 7.7). This indicates that the restriction reactions observed are due to the specific activity of EcoKI.

The rate constants of EcoKI restriction of linear pBR322 with different concentrations of PEG 8000 and glycerol are shown in figure 7.8. This graph shows how EcoKI restriction of linear pBR322 is inhibited by increasing concentrations of glycerol and therefore increasing viscosity. However, increasing the concentration of PEG 8000 has a different effect. As the PEG 8000 concentration is increased from 0 to 5%, the rate constant decreases. However, when the PEG 8000 concentration is increased to 7.5%, the rate constant increases. Upon further addition of PEG 8000, the rate constant decreases again, and levels off at around 15% PEG 8000. All concentrations of PEG 8000 used produce higher rate constants than the concentrations of glycerol at equal viscosities. This indicates that factors other than viscosity are affecting the rate constant of restriction of linear pBR322 in the presence of PEG 8000.

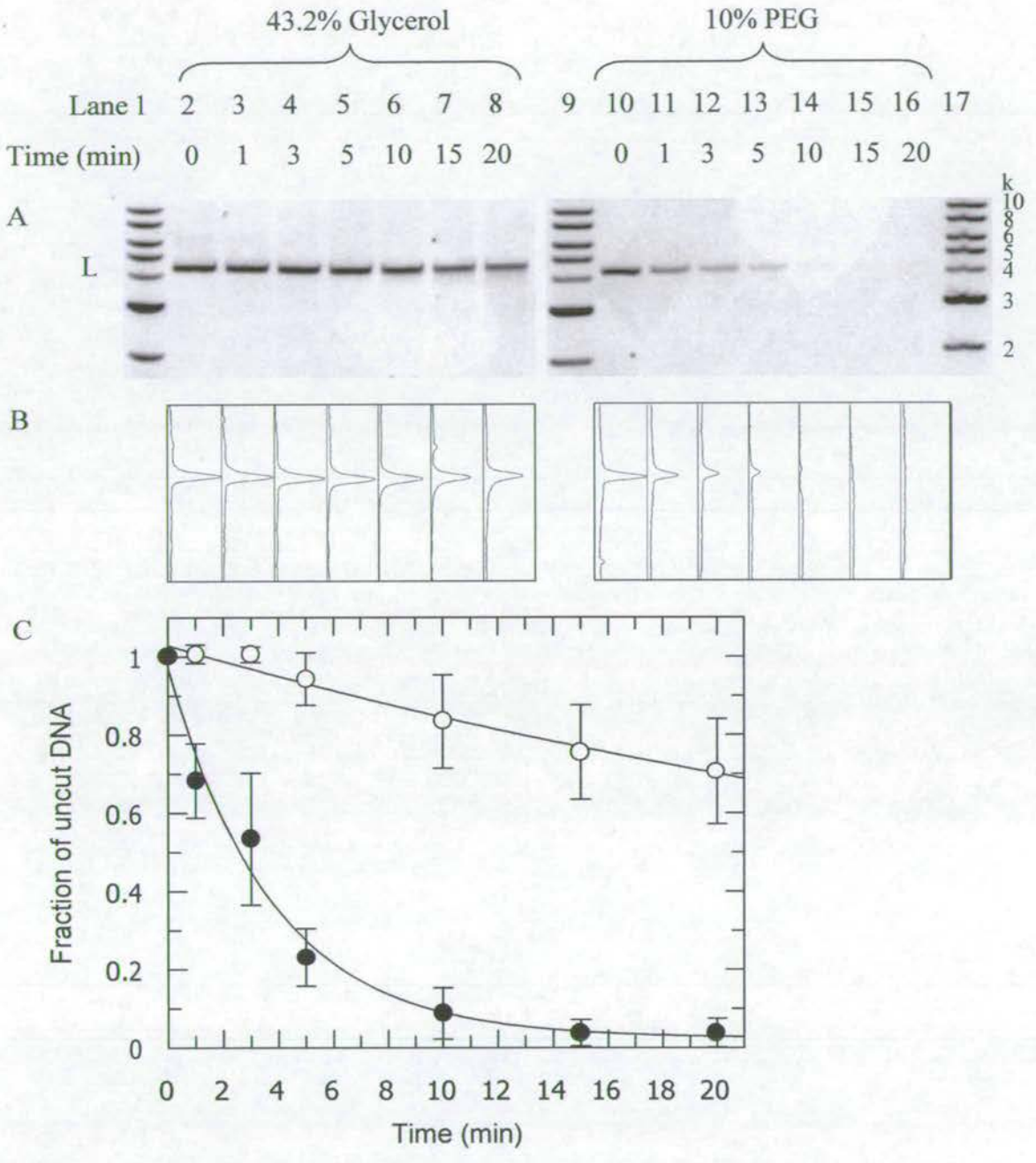

Figure 7.6. Effect of PEG 8000 and glycerol on the restriction of linear pBR322 by EcoKI. Reactions were carried out in low salt EcoKI buffer, pH7.9, with 50nM linear pBR322 and 134nM EcoKI. A) Agarose gels of linear pBR322 (L) being cut by EcoKI at specific time points. In lanes 2-8, buffer contained 43.2% glycerol, and in lanes 10-16 buffer contained 10% PEG 8000. Lanes 1, 9 and 17 contain 1kb linear DNA marker of sizes indicated. B) Densitometry of aligned gels using Scion Image software. C) Graph showing effect of 10% PEG 8000 (closed circles) and 43.2% glycerol (open circles) on the cutting of linear pBR322.

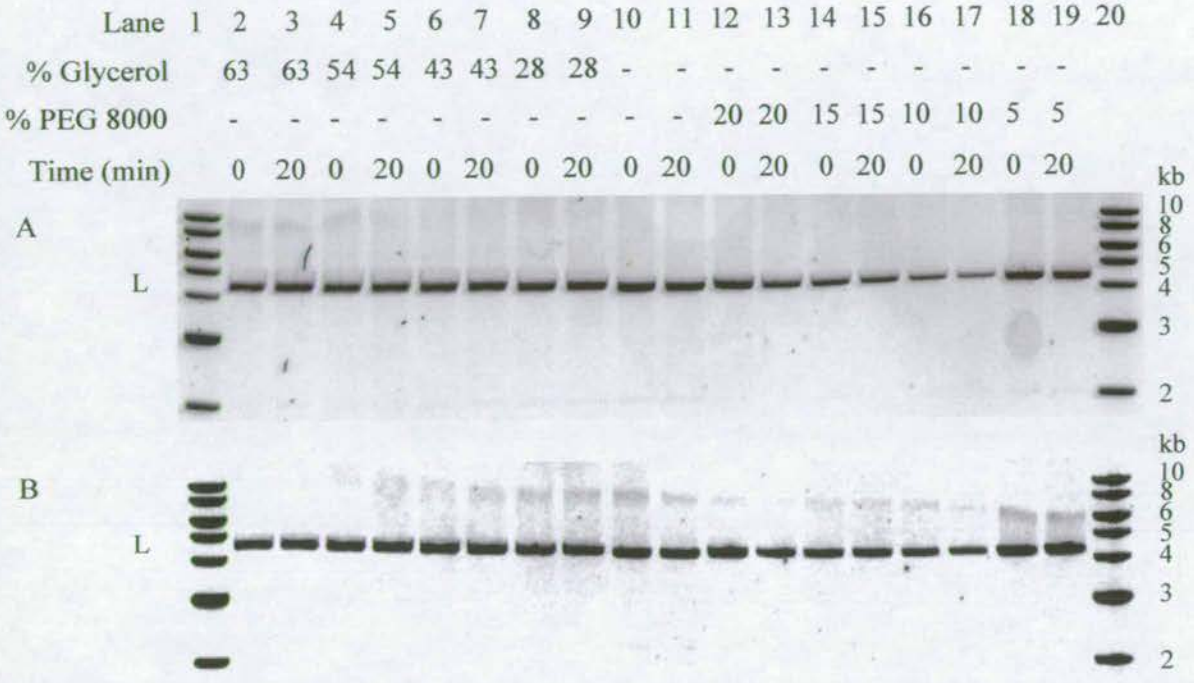

Figure 7.7. Crowding controls. 50nM linear pBR322 (L) was incubated with various concentrations of PEG 8000 or glycerol in low salt EcoKI buffer, pH 7.9 with 0.1mM SAM, 50µg/ml BSA, and 2mM ATP. (A) was carried out in the absence of EcoKI, whereas (B) was carried out in the presence of 134nM EcoKI with linear pBR322 methylated at the EcoKI target site. Reactions were stopped by addition of EDTA to a final concentration of 77mM, and heating to 68°C for 30min. Lanes 1 and 20 contain 1kb linear DNA markers of sizes indicated.

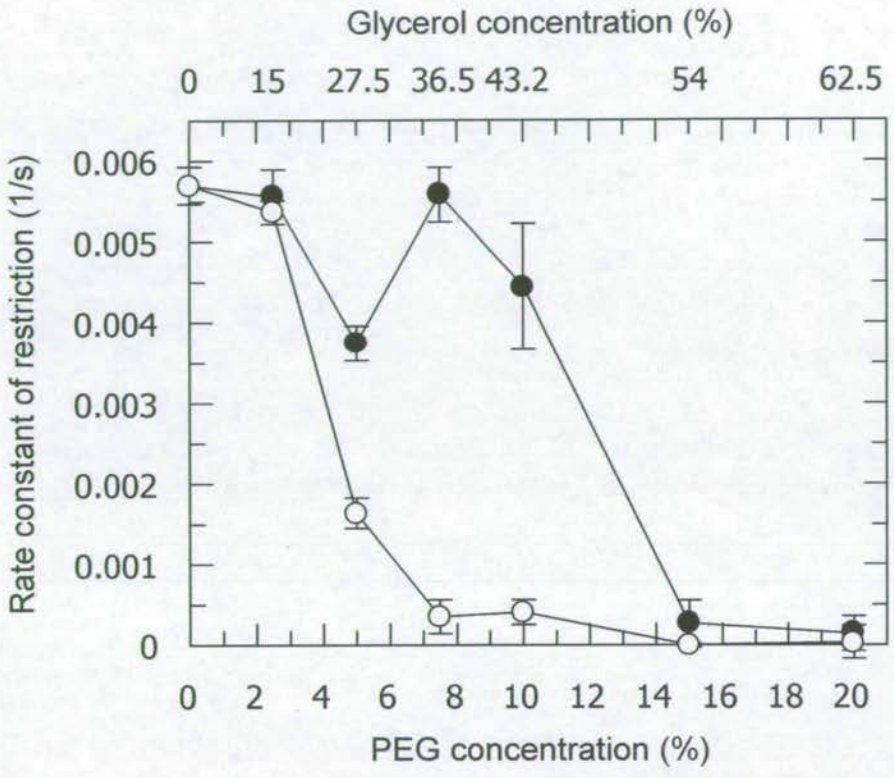

Figure 7.8. Effect of PEG 8000 and glycerol concentrations on the rate constant of restriction of linear pBR322 by EcoKI. Reactions were carried out in low salt EcoKI buffer, pH7.9, as described in figure 7.6. The rate constants of restriction by EcoKI with varying concentrations of PEG 8000 (closed circles) and glycerol (open circles) are shown. The bottom axis shows the concentration of PEG 8000, with the top axis giving the concentrations of glycerol used. The points are aligned to show solutions of equal viscosities. Each point represents the mean of 4 separate experiments. (see Appendix D).

The difference between the rate constants of restriction in the presence of PEG 8000 and glycerol shows the effect of crowding on the rate constants of restriction as glycerol solution are used as viscosity blanks (figure 7.9). This graph shows a peak at 7.5% PEG 8000 (36.5% glycerol). At all concentrations studied the rate constants in the presence of PEG 8000 were higher than the corresponding rate constants obtained in the presence of equal viscosities of glycerol as shown by the positive difference values.

The increased rate of restriction activity in the presence of PEG 8000 compared to glycerol can also be explained by the volume exclusion principle. Here, once again, an increase in binding in the caged environment of the 'buffer bubble' would explain the difference between restriction with PEG 8000 and the homogeneous viscous solutions of glycerol, where translocation and EcoKI binding are inhibited.

It is important to note that in these experiments, only one crowding agent (PEG 8000) and one viscosity control (glycerol) have been used. It is very possible that the effects on EcoKI activity by these agents are due to specific interactions of PEG 8000 and glycerol with EcoKI. For example, it has been found that glycerol decreases the volume of the interior of proteins, making them more rigid (Priev *et al.*, 1996). Therefore it is expected that proteins which require flexibility in order to function properly are likely to be affected by glycerol to a greater extent than proteins where flexibility is not so important. If such specific effects are taking place, the data analysis in reference to crowding and viscosity effects of PEG 8000 and glycerol on EcoKI activity is redundant. It would therefore be of great importance to repeat these experiments with other crowding agents and other viscosity controls in order to gain a clearer understanding of the reaction mechanisms taking place under such conditions.

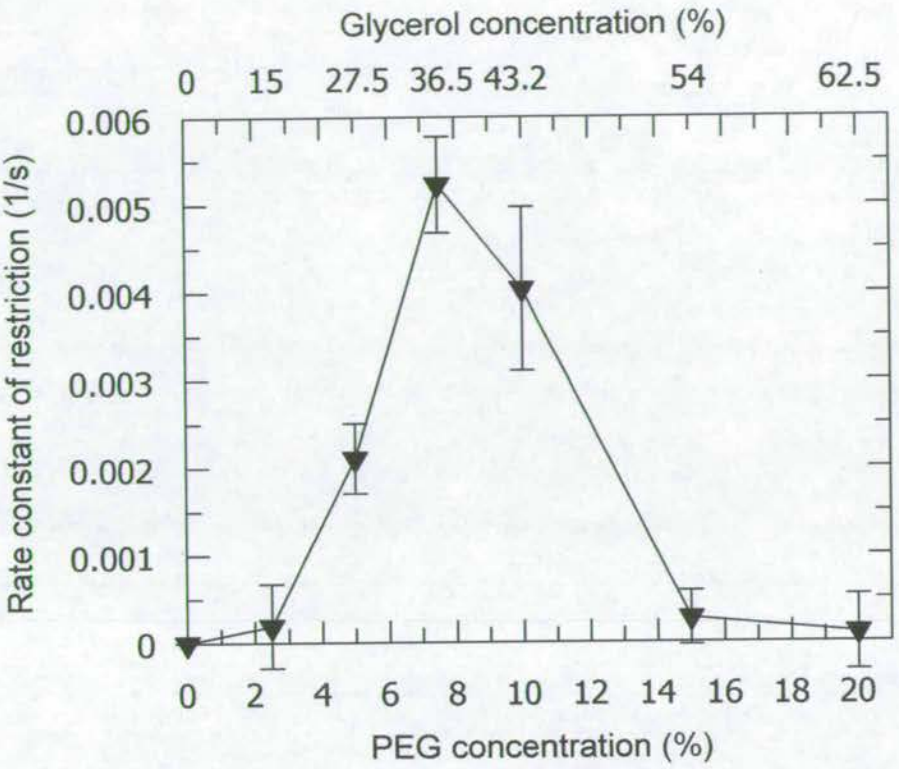

Figure 7.9. Difference between the rate constant of restriction of linear pBR322 by EcoKI in the presence of PEG 8000 and glycerol. The rate constants of restriction in the presence of glycerol were taken away from the rate constants of restriction in the presence of PEG 8000 at equal viscosities (as shown in figure 7.8). The bottom axis shows the concentrations of PEG 8000 with the concentrations of glycerol used to give equal viscosities given on the top axis.

7.4. Summary

ATP hydrolysis activity of EcoKI in solutions containing glycerol or PEG 8000 can be determined using separate calibration curves. Viscous solutions inhibit EcoKI ATP hydrolysis and restriction activities. PEG 8000 alters EcoKI activity by crowding effects, and therefore shows less inhibition of EcoKI than glycerol controls of the same viscosity. PEG 8000 crowding effects, compared to the glycerol viscosity controls, show peaks at 5% and 7.5% PEG 8000 for EcoKI ATP hydrolysis and restriction activity respectively. This effect can be explained as crowding will increase EcoKI binding to the DNA due to volume exclusion effects. The main effect of volume exclusion will be to increase the relative concentration of EcoKI, and therefore increase the binding to DNA. Increasing the EcoKI concentration has been already shown to increase the ATP hydrolysis rate of EcoKI (figure 3.10). However results need to be repeated with other crowding agents and viscous solutions in order to minimise specific effects.

Chapter 8:

Discussion

8.1. EcoKI restriction

The model of type I R/M restriction by Studier and Bandyopadhyay predicts restriction of DNA where two restriction enzymes bump into each other, causing a stall in translocation, triggering restriction (Studier and Bandyopadhyay, 1988). The results of EcoKI restriction of plasmid DNA containing one and two target sites, in linear and supercoiled form agree with this model. When a supercoiled substrate is restricted, production of a nicked intermediate can clearly be seen reinforcing the fact that restriction occurs as two single-stranded nicking events (Dreier and Bickle, 1996). However, linear DNA containing one EcoKI site is restricted very slowly. This is commonly seen with excess of enzyme and can also be explained by the proposed model if a translocating EcoKI bumps into a non-specifically bound enzyme and induces restriction (Janscak *et al.*, 1996; Szczelkun *et al.*, 1997).

At the ratio of 1.34 EcoKI per target site, all supercoiled DNA with one or two target sites is linearised. However, the linear DNA with two sites is not all restricted further into linear fragments. If linear DNA with two target sites is produced by restriction of plasmid by EcoRI, this substrate is also not all restricted to linear fragments by EcoKI. Why, at a saturating concentration of EcoKI that is sufficient to fully restrict supercoiled DNA is not all linear DNA being cut? It has been shown that the R subunits of EcoR124I can dissociate from the restriction complex (Seidel *et al.*, 2004). This could cause deficient cutting and could account for limited restriction of two-site DNA. However, R-subunit dissociation does not occur with EcoKI at the concentrations used (Dryden *et al.*, 1997) and one-site DNA would also undergo limited restriction in the same way, which does not occur in these results. Therefore, a possible explanation that could explain these results is that although there is enough EcoKI to saturate the sites, this excess is low. EcoKI binding will occur in equilibrium with association and dissociation from the target sites. It is possible that on DNA with two target sites, only one enzyme may be specifically bound. This would translocate past the other site and no restriction would be triggered, as the other enzyme is required to cause translocation to stall. However, if the substrate were supercoiled, the two-site plasmid would be restricted in the same way as a one-site plasmid. The finding that an increase in EcoKI concentration from 2 up to 10 EcoKI per target site produces a linear increase in ATP hydrolysis activity with all DNA substrates (linear and supercoiled DNA with one and two sites, figure 3.10) backs up this model. This situation of a low excess of EcoKI to target sites may be representative of the *in vivo* situation of a bacteria infected by many phage. Therefore, although saturating conditions were used, a higher concentration of enzyme may

have fully restricted two-site DNA, but also caused greater restriction of one-site linear DNA due to greater non-specific binding.

These strange kinetics of restriction of linear and supercoiled two-site pBR322 and linear one-site pBRsk1 need to be accounted for by a model in order to calculate the rate constants of restriction. The reversible steps to uncleavable forms included in the models have little effect on the overall rate constants of restriction but allow a much better fit of the data. The reversible steps can be justified by the proposals of insufficient binding of EcoKI in the case of linear and supercoiled two-site pBR322, where the binding of only one EcoKI would prevent the reaction going to completion until a second EcoKI was bound. Such intermediates produced could be termed uncleavable, and would be able to be cleaved upon binding of the second EcoKI, thereby making the reaction step reversible. The restriction of linear one-site pBRsk1 by collision between specifically and non-specifically bound EcoKI can also be explained by the same mechanism. Therefore, the good fit of this model to the data backs up the proposed mechanisms of restriction seen in these results.

8.2. EcoKI translocation

EcoKI ATP hydrolysis activity was successfully measured by the ATP hydrolysis coupled enzyme assay. The rates of ATP hydrolysis achieved using 5nM DNA with a single target site ranged from around 55nM/s to 88nM/s. This broadly agrees with previous results by Davies (2000), who obtained a range in ATP hydrolysis of around 50nM/s to 90nM/s also using 5nM DNA containing a single target site. A higher ATP hydrolysis rate is observed when using linear DNA compared to supercoiled DNA containing one target site. This agrees with the observations of Seidal *et al.*, (2004), who observed a reduction in translocation velocity of EcoR124I when using supercoiled substrate rather than linear DNA with one target site. However, Davies (2000), has observed a lower rate of ATP hydrolysis on linear DNA compared to supercoiled with a single target site. A direct comparison between the two sets of results is hindered by the different conditions used for this complex assay, as the experiments by Davies (2000) were carried out at a higher temperature and with a greater concentration of PK/LDH mix, which has been found to affect EcoKI activity due to the high ammonium sulphate content of the stock solution. With the pH and buffer conditions of the other reaction components not specified, it is likely that further differences may be present between our experiments and may be responsible for the inconsistencies

between our results. The quantity of type II enzyme used to produce the linearised plasmid also varies between these two sets of experiments and may also effect reaction rates, possibly due to the glycerol present in the EcoRI stock. However, if these results are taken together, it may be the case that EcoKI ATP hydrolysis activity with supercoiled and linear one-site DNA is similar. Interestingly, there was no difference seen between the ATP hydrolysis rates of EcoKI during reactions with supercoiled and linearised plasmids with two target sites. The rates of ATP hydrolysis of two-site DNA were in between the rates obtained for one-site linear and supercoiled DNA, but closer to the faster rate of one-site linear DNA. It is therefore possible that intramolecular dimerisation of EcoKI may help overcome any superhelical inhibition to translocation, caused by the constrained structure of circular DNA.

It should be noted that there was no change in the EcoKI ATP hydrolysis rate with any of the DNA substrates used over a reaction period of 30min (data not shown). Restriction assays have shown that EcoKI cutting of DNA substrates occurs within this time period in the ATP regenerating buffer used for the ATP hydrolysis coupled assay. Therefore, EcoKI appears to keep hydrolysing ATP at a constant rate before and after restriction has occurred. This is true even when using supercoiled one-site DNA where EcoKI continues to hydrolyse ATP at a constant rate even when it has restricted the DNA into its linear form. Using the same assay, Bianco (2004, personal communication) has seen a decrease in the rate of ATP hydrolysis by EcoR124I after restriction of supercoiled DNA with a single target site. His results showed that EcoR124I ATP hydrolysis activity was similar for linear and supercoiled DNA with one target site, until the supercoiled DNA was restricted, where ATP hydrolysis continued more slowly. As no (or little) restriction occurs on the linear DNA with one target site, there was no change in ATP hydrolysis rate. This change in rate following restriction was not seen with EcoKI, and can be explained by the ability of EcoR124I to dissociate from its R subunits. It has been proposed that the R subunits can dissociate upon restriction (Seidel *et al.*, 2004). As the R subunits are the motors of translocation, and hydrolyse the ATP, any dissociation will affect the ATP hydrolysis rate. Therefore this partial disassembly of EcoR124I upon restriction of supercoiled DNA can explain the change in ATP hydrolysis activity, rather than the change in DNA structure.

It should be noted that the continuing hydrolysis of ATP after restriction has occurred has been previously reported for type I restriction enzymes (reviewed in Bickle, 1993; Bickle and Kruger 1993). This 'futile cycling' of ATP has been used to propose a self-destruction mechanism of infected cells, where the recognition of foreign invading DNA would trigger a

massive consumption of ATP which could kill the cell, thereby reducing the chance of further phage infection (Dreier and Bickle, 1996). This 'futile cycling' of ATP has also been reported for the helicase PcrA, which continues to hydrolyse ATP, albeit at a reduced rate, once it reaches the 5' end of the DNA (Dillingham *et al.*, 2000). In this case the ATP hydrolysis must be decoupled from translocation, but it is unknown if this decoupling also occurs following restriction in type I R/M systems, or if translocation of the free ends of restricted DNA are continually translocated after resetting of the enzyme.

The ATP hydrolysis rate of linear DNA with two EcoKI target sites is 74nM/s with 5nM EcoKI target sites. This corresponds to around 15 ATP hydrolysed/EcoKI/s. It has been found that EcoR124I translocates DNA using 1 ATP/bp (Bianco and Szczelkun, 2004, personal communications). If this were true for EcoKI, this would produce a total translocation rate of around 15bp/s. As EcoKI translocates DNA bi-directionally, this translates to only 7.5bp/s in each direction. At this rate, EcoKI would take almost 5min to translocate the entire 4.4kb plasmid. However, Szczelkun has measured the translocation rate of EcoKI under slightly different buffer conditions (NEB buffer 4, 0.2mM SAM, 4mM ATP) at around 120bp/s (Szczelkun, 2004, personal communication). If EcoKI were translocating at this rate under the experimental conditions used in this thesis (EcoKI high salt buffer, 0.1mM SAM, 2mM ATP), this would correspond to EcoKI translocating around 16bp of DNA for every ATP hydrolysed.

EcoKI ATP hydrolysis activity using linear DNA with two target sites was also measured by the production of P_i. The rate of P_i production showed an initial rapid increase, followed by a levelling off. This levelling off may be due to the decrease in ATP or production of ADP or P_i that could inhibit the reaction. In this respect it was interesting that restriction of two-site linear DNA was more rapid in the presence of an ATP regenerating system, where the ADP and P_i are recycled and the ATP concentration is maintained, compared to normal buffer conditions, where ATP decreases and ADP and P_i increase. A similar levelling off was seen by Pullman *et al.*, (1960), when measuring the P_i production by mitochondrial ATPase. However, when the experiment was repeated under ATP-regenerating conditions, no levelling off was observed, and the rate produced was identical to the initial rate found under non-regenerating conditions. These results were explained by the inhibitory effects of ADP on the mitochondrial ATPase. For this reason the initial rate of P_i production was measured. This shape of curve was also seen by Janscak *et al.*, (1996), when using the same assay with EcoR124I. Under their assay conditions, EcoR124I produced P_i at an initial rate around 10

times faster than the initial rate of P_i production with EcoKI in this thesis, when DNA and enzyme concentrations are correlated. Although it should be noted that different buffer conditions and DNA substrates make such direct comparisons useful only as an approximate guide to relative activity levels.

The initial rate of EcoKI *Pi* production (1.8μM/s, with 50nM linear pBR322) translates to around 21 ATP hydrolysed/EcoKI/s. If one ATP were used to translocate a single DNA bp, then this would produce a total translocation rate of 21bp/s for EcoKI, or 10.5bp/s in each direction. However, if the measured translocation rate of 120bp/s (Szczelkun, 2004, personal communication) were occurring under these reaction conditions, this would correspond to around 11bp translocated per ATP hydrolysed. These results agree with the reactions using the ATP hydrolysis coupled assay. The slight difference in ATP hydrolysis rates measured may be due to the different buffer conditions used in each assay.

Work on EcoR124I translocation also found there was a short pause before the onset of translocation (Szczelkun, 2004, personal communication). Short time points were therefore taken for the ATP hydrolysis P_i assay, down to 10s, but no pause in translocation was observed for EcoKI.

8.3. EcoKI restriction site

It was found that restriction of a single site plasmid by EcoKI occurred at random positions. No specific bands were produced when further cut with either EcoRI or BsgI, indicating that cutting could occur at any position. This agrees with the results of Janscak *et al.*, who found EcoAI cut single site supercoiled plasmid at random positions (Janscak *et al.*, 1999). However, Szczelkun *et al.*, (1997), discovered that although the majority of EcoR124I restriction of a single site plasmid occurred at random positions, discrete cutting sites were also present in close proximity to the target site. These discrete cutting sites were also seen for the EcoR124I restriction of linear DNA with two target sites (Szczelkun *et al.*, 1997). The cutting of a two-site linear plasmid by EcoKI also revealed production of fragment sizes that can be accounted for by cutting at positions very close to the target sites. However, a large fraction of the DNA was also cut at random positions. Szczelkun *et al.*, (1997), found the target site restriction to occur within around 250bp of the site for EcoR124I, whereas the mean discrete cutting site for EcoKI was determined in this thesis to be within 189±73bp of

the target site. Although this agrees with the results for EcoR124I, it should be noted that accurate determination of the sizes of fragments is limited by comparison to size standards on agarose gels, and are all therefore only accurate to within 100bp. The discrete bands produced are also quite broad, indicating that a specific cutting site is not recognised, more that a region of the DNA is targeted for restriction. This could be explained if one EcoKI translocated up to the other EcoKI bound to its target site before it started to translocate. Translocation of the first EcoKI would stall when it bumped into the stationary EcoKI and restriction would be triggered at the other target site. This property would also be a function of EcoKI concentration, as if a higher concentration were used, binding to target sites would be increased and a greater proportion of EcoKI would be translocating at the same time. Translocation would therefore be more likely to occur at around half way between the target sites. However, this increase in concentration of EcoKI would also increase non-specific binding, which could potentially also trigger restriction at random positions (Janscak *et al.*, 1996).

This behaviour of cutting in close proximity to one of the target sites is reminiscent of restriction by type III restriction systems, which cut DNA at a fixed distance (25-27bp) from a single target site when two target sites are present in the correct orientation. The restriction mechanism is unknown and may share similarities with the reactions carried out by EcoKI under these experimental conditions.

As the distances between the two target sites in these experiments was large, DNA substrates containing two EcoKI sites with varying short distances between these sites were constructed. It was found that although substrates AB, AC and AD, with up to 117bp between the target sites were not restricted by EcoKI, the largest fragment AG with 317bp between the target sites was restricted by EcoKI, producing a smear on an agarose gel of between100-200bp, as well as a less intense smear at around 250bp. However, gel mobility shift assays appear to show that fragments AB and AG can both bind two EcoKI molecules simultaneously. EcoKI also exhibits ATP hydrolysis activity with all DNA fragments (AB, AC, AD, and AG). This implies that the footprint required for EcoKI to be able to restrict DNA is much larger than is required for binding and translocation. Dreier *et al.*, (1996), have shown that EcoR124II requires at least 40bp between its target site for restriction to occur. In these experiments, it appears that the level of restriction increases as this inter-site distance is gradually lengthened to 135bp. They concluded that the inability of the enzyme to cut DNA

with a shorter distance between the target sites was due to steric hindrance only allowing binding of a single EcoR124II enzyme.

Experiments carried out to determine the footprint of EcoKI using exonuclease III found that EcoKI only protected a region of 45bp when bound to DNA in the absence of ATP (Powell *et al.*, 1998b). This footprint was seen to shrink to 30bp when ATP was added and EcoKI bound specifically to its target site. However, it is possible that the R subunits, attached at either end of the complex, associate with the DNA to a distance greater than this, without offering any protection from exonuclease digestion. These R subunits would need to be able to associate with the DNA to drive translocation and restriction. Therefore, the footprint of EcoKI may be significantly larger than that measured by the exonuclease III assay. In agreement with these results, Bickle has also found EcoAI unable to restrict DNA when sites are closer than around 200bp apart (Bickle, 2004, personal communication).

It is therefore possible that EcoKI can bind to both sites on the small fragments (AB, AC, and AD) but steric hindrance prevents proper association of R subunits required for restriction. It is also possible that both EcoKI molecules can bind to the small substrates properly but a certain translocation distance must be reached before restriction can be successfully initiated. In this case, a certain momentum would have to be reached before a stall could trigger restriction. This mechanism would also imply that translocation involved acceleration. More detailed information about the structural arrangement of type I restriction enzymes may allow elucidation of the mechanism of restriction.

8.4. Effect of pH on EcoKI restriction activity

EcoKI restriction was found to have an optimal activity at pH 9.5 when bis-tris propane buffer was used. This was true for restriction of both supercoiled and linear DNA with one target site. The fact that the increase in restriction at high pH only occurred with unmethylated target sites and when all EcoKI cofactors were present, indicates this activity is due to the specific restriction activity of EcoKI, and not star activity or an impurity. The observation that the slow digestion of one-site linear DNA follows the same pH dependence trend as the specific restriction of the one-site supercoiled DNA is of particular interest. Restriction of this one-site linear substrate is thought to be triggered by the specifically

bound translocating enzyme bumping into a non-specifically bound enzyme on the DNA. This implies that increasing the pH to 9.5 may increase the binding of EcoKI to DNA.

It may also be of interest to note that over 80% of linear one-site DNA was restricted by EcoKI at pH 9.5 after 30min. However, there is only an excess of 1.34 EcoKI per target site, which would correspond to only one third of the specifically bound EcoKI having a chance of bumping into a non-specifically bound molecule. However, the non-specifically bound EcoKI are free to dissociate and associate with other DNA molecules and can therefore trigger these multiple restrictions. It seems unlikely that this small excess of enzyme could block 80% of the translocating EcoKI molecules before they reached the end of the DNA, which should occur within around 5min (at pH 7.9). Therefore, these results could provide evidence for the model where EcoKI resets itself after reaching the end of the DNA, and starts the translocation process again from the beginning. This would allow sufficient time the non-specifically bound EcoKI to cause a stall in the translocation of many more translocating EcoKI.

8.5. Dyes

YOYO, EtBr and H33258 all caused dramatic inhibition of EcoKI restriction of supercoiled DNA with one target site. EcoKI ATP hydrolysis activity was also analysed with respect to YOYO concentration, and a similarly dramatic inhibitory effect seen. This is not unexpected as EtBr has been previously shown to inhibit EcoKI methylase and restriction activity (Burkhardt *et al.*, 1981) as well as EcoR124II ATP hydrolysis activity (Dreier and Bickle, 1996).

The results show that substantial inhibition of both translocation and cleavage is achieved by even one dye molecule being present on average every 256 base pairs along the DNA. As a consequence of the slowed kinetics of ATP hydrolysis, DNA translocation and double-strand cleavage, a substantial amount of the DNA substrate is only subject to single-strand nicking. The presence of substantial quantities of nicked DNA rules out the simple idea that dyes achieve their inhibitory effect purely by blocking access of EcoKI to its binding site. If that were the case, then no accumulation of nicked open circular DNA would be observed. The presence of dye molecules on the DNA will undoubtedly hinder EcoKI in locating and binding to its target site due to competition. However, this cannot be the entire cause of the

observed reduction in activity since at least a proportion of the enzyme must be able to bind to its site, as all the binding processes are equilibrium processes. Once it has done so, it is committed to hydrolyse ATP and to introduce single-strand breaks in the DNA. The appearance of single-strand breaks and hydrolysis of ATP indicates that the translocation and cleavage processes are being hindered. It has previously been shown that a single protein bound to DNA is insufficient to halt a translocating type I R/M enzyme (Dreier *et al.,* 1996) but in experiments in this thesis it appears that multiple ligands bound in a non-specific manner to the DNA are a very effective block to the type I R/M enzyme. Given that EcoKI can translocate DNA bi-directionally, it appears that the motors are both moving DNA but are stalling before they can translocate all of the DNA. Instead of stalling by colliding with each other, they are stalling prematurely against the barriers formed by bound dye molecules. Each restriction subunit may then introduce a single-strand break in the DNA but since these two nicks are now unlikely to be adjacent to each other, the DNA is not linearised. In this case, the DNA would maintain its circular conformation due to the large number of non-covalent base pair attractions present between the nicks.

The cutting position of EcoKI in the presence of YOYO was investigated further by restriction of linear DNA containing two EcoKI target sites, with 1 YOYO bound per 256bp. The positions of the target sites within the linear DNA varied and therefore produced different banding patterns when restricted by EcoKI. The banding patterns produced were the same as in the absence of YOYO, implying that EcoKI can translocate DNA the same distance whether YOYO is present or not. However, the YOYO concentration used was only 256bp per YOYO, as sufficient DNA could not be restricted for visualisation by agarose gels at higher YOYO concentration. It is therefore possible that YOYO could stop EcoKI translocation at higher concentration.

The dyes could inhibit EcoKI activity in a number of ways: the dyes affect the structure of DNA upon binding by altering the helical repeat and increasing the persistence length (Meng *et al.,* 1996 and references therein), which could change the affinity of EcoKI for the DNA, and could therefore inhibit binding, translocation and restriction reactions; the dyes could physically block the target site, and therefore compete with EcoKI for binding; the dyes could also inhibit translocation by forming a physical block or; the dyes may bind to EcoKI and inhibit its activity directly.

As it is likely that non-specific binding of dyes within the binding site of EcoKI will occur and inhibit the binding of EcoKI, this property may be used to further analyse the data obtained. The car parking model is a useful extension of the work by McGhee and von Hippel (1974), and may be useful in determining the relevant footprints of enzymes. In this case YOYO was used as a block to EcoKI binding, with successful binding measured by ATP hydrolysis activity, and initial restriction rates. Draw backs of this method are that EcoKI may only be able to hydrolyse ATP at a reduced rate in the presence of YOYO due to slowed translocation, EcoKI may be able to bind to DNA even with YOYO bound, and EcoKI and YOYO will compete with each other for binding in an equilibrium process. However, the data predicts an EcoKI footprint of around 69bp for ATP hydrolysis activity and around 290bp for restriction activity, which are much larger than the footprint calculated by exonuclease III digestion (Powell *et al.*, 1998b). This finding that a larger footprint is required for restriction than ATP hydrolysis agrees with the experiments using the short DNA fragments with two EcoKI sites (AB, AC, AD, and AG), where EcoKI was able to bind and exhibit ATP hydrolysis activity on even the smallest fragment, without being able to cut it. The restriction footprint size of around 290bp corresponds to a requirement of around 277bp between targets sites for successful restriction. This also agrees with results using short DNA fragments as a fragment with 117bp between the target sites (AD) was not restricted whereas a fragment with 317bp between the target sites (AG) was successfully restricted. In relation to the results with YOYO, it is possible that EcoKI needs a certain distance to gather up enough momentum to dislodge a bound dye molecule or it requires to be travelling at a certain speed for a stall in translocation to trigger restriction. This would imply that the enzyme accelerates and does not just start translocation at full speed.

8.6. Spermidine

Cyclisation of bacteriophage λ DNA was used as a clear measure of DNA condensation state by Jary and Sikorav, (1999). In this study the cyclisation rate was increased by over six orders of magnitude due to spermidine-induced DNA condensation bringing the free ends into close proximity. However, such a significant and straight forward affect of condensation on joining of free ends was not seen in ligation experiments in this thesis, probably due to the requirement of the enzyme ligase, which adds a further complication to the interpretation of the results. Increasing spermidine concentrations produced an initial increase in ligation

rate followed by a dramatic inhibition at higher concentrations. This mirrors the results of Raae *et al.,* (1975) who studied the effect of spermidine on ligase activity using a DNA substrate too small to undergo toroidal condensation. Their results also showed a similar trend for tetravalent spermine, with both stimulation and inhibition of ligase activity occurring at lower concentrations. It should be noted that both sets of experiments allowed the total ionic strength to vary with polyamine concentration. Their results also showed a strong inhibition of ligase activity at high ionic strength using monovalent salts, and explained the inhibitory effect of polyamines on ligase activity as being due to decreased affinity of the enzyme for the DNA, due to charge neutralisation. They suggested that this effect would also be seen with high concentrations of monovalent salt. In agreement with this, they predicted and found that K_m values for ligase activity increased in the presence of polyamines and KCl. As the results for ligase activity dependence on spermidine concentration are the same in this thesis, the same explanation of decreased affinity due to spermidine association with the DNA can be extended to this work. However, interpretation of the results presented here is further complicated by the ability of the DNA to form toroidal condensates with free ends held in close proximity but potentially kept rigidly separated. Therefore, although it would be of interest to repeat these experiments with a constant ionic strength, the complexities of the ligation reaction and its dependence on so many variables make it unsuitable as a straightforward assay of DNA conformation.

AFM images illustrate condensed structures that can be produced by the addition of spermidine to plasmid DNA. However, although semi-condensed and toroidal conformations are seen at high spermidine concentrations, these images were only obtainable under conditions of low ionic strength due to the inability of this imaging technique to cope with conditions of high salt. Even under these low salt conditions, the high concentrations of spermidine used produce a noisy background, probably due to the presence of salt crystals. One previous AFM study using spermidine was unable to obtain high quality images at high concentrations due to this effect and was only able to observe semi-condensed intermediate DNA conformations (Fang and Hoh, 1998). Therefore, although these images show conformations that DNA may adopt upon addition of spermidine, they cannot be used to represent definite structures obtained under conditions of higher ionic strength, which are required for EcoKI activity. However, these images agree with many reports of toroidal condensates imaged by both AFM and electron microscopy (for examples see Hud and Downing, 2001; Baeza *et al.,* 1987). At polyamine concentrations below the critical

condensation-inducing concentrations, compact conformations of semi-condensed intermediates have also been visualised.

The DNA digestion by DNase I was carried out under the same buffer conditions as required for EcoKI activity and revealed the general state of DNA condensation. This assay has previously been successfully used for the determination of a spermidine-induced condensed state of pBR322 (Baeza *et al.,* 1987). It was found that the concentration of spermidine required to condense DNA increased with increasing ionic strength. This agrees with the counterion condensation theory (Manning, 1978) as well as many previous experimental observations (for example, see Matulis *et al.,* 2000). Furthermore, it was seen that no condensation occurred at any concentrations of spermidine up to 140mM when the total ionic strength was maintained at 681mM. However, when ionic strength is not maintained, the DNA condenses and then decondenses as the spermidine concentration increases. This also agrees with the previous experiments of Murayama *et al.,* (2003). They explained this decondensation by the idea that with increased spermidine concentration following condensation, charge neutralisation continues beyond the critical 89-90% required for condensation. Eventually the DNA has bound so much spermidine that the DNA will carry an overall positive charge. This will cause the DNA to lose its condensed structure by disruption of the attractive forces caused by charge correlation.

Under normal low salt EcoKI buffer conditions of 100mM ionic strength, supercoiled and linear plasmid DNA was condensed by 6mM spermidine. However, under identical conditions, linear and supercoiled plasmid DNA with one bisintercalating dye YOYO bound per every 50bp, was found to require 10mM spermidine before it adopted a condensed conformation. A similar result has been seen by Murayama and Sano, (2005), who found that YOYO inhibited DNA condensation by spermidine. They also found that binding of spermidine and condensation of the DNA caused a decrease in the binding of YOYO. They related these results to competition for binding between spermidine (3+) and YOYO (4+), with YOYO preferring to bind specific conformations of DNA. In a similar study using EtBr and spermine Lee *et al.,* (2001), postulated that effects on intercalative binding that alters the DNA structure by unwinding, lengthening and creating a kink, would be unfavourable to condensation. In relation to this, it is interesting to note that EtBr binding was found to cause dissociation of histones from DNA (McMurray and van Holde, 1991). In this way, intercalative binding of EtBr caused a decondensation of nucleosomal DNA. These results all indicate the dramatic effects small DNA-binding molecules can have upon the overall

conformation of DNA. The presence of high concentrations and tight regulation of molecules such as spermidine, are likely to have significant physiological consequences.

Our experiments show that the restriction activity of EcoKI is strongly compromised by the condensation of DNA by spermidine. Condensation inhibits the rates of hydrolysis of ATP required for DNA translocation and double-strand cleavage of supercoiled and linear DNA, containing either one or two target sites. Restriction of spermidine-condensed supercoiled DNA results in the production of a significant amount of nicked DNA that is not further restricted. Also, EcoKI ATP hydrolysis occurs at very low levels on condensed DNA. This implies that DNA condensation does not simply block EcoKI from the target site by blocking access of EcoKI to its binding site, as some EcoKI are able to translocate and nick the DNA.

It appears from the results that compromising EcoKI translocation by DNA condensation leads most often to single-strand breaks. They do not indicate if multiple single-strand breaks are introduced but if they are then they are too far apart for strand separation to easily occur or the breaks introduced by a particular restriction subunit are all on the same strand of DNA. Occasionally a double-strand break is made on the condensed DNA but the frequency is much reduced compared to uncondensed DNA. Previously it was shown for the EcoR124II type I R/M enzyme that nicks by themselves are not able to induce a second cleavage to produce a double-strand break (Dreier *et al.,* 1996) so it appears that the endonuclease domain in the restriction subunit is only able to make single-strand breaks on one strand of the DNA. During translocation on uncondensed pBRsk1, the two restriction subunits can cooperate with each other to make a double-strand break when the translocation stalls after the entire plasmid has been reeled in. However, stalling translocation of these subunits before they collide means the two nicks are uncoordinated and fail to lead to linearisation of the DNA.

The same models of EcoKI restriction can be used to fit the data when cleavage is inhibited by both dyes and spermidine-induced condensation. The reversible steps required for such models are due to the persistence of large amounts of uncleaved or nicked DNA after long incubations with EcoKI. The fact that DNA condensation as well as increasing dye concentrations both increase the importance of the reversible rate constants in the overall reaction mechanism, indicate that similar mechanisms of inhibition may be used in both situations.

8.7. StpA

The nucleoid-associated protein StpA was also able to condense DNA into a conformation that was resistant to digestion by DNase I. It was found that around one StpA per 64-96bp condensed linear DNA whereas supercoiled DNA required only one StpA per 256-384bp for condensation. At these DNA-condensing concentrations of StpA, EcoKI ATP hydrolysis and restriction activity with single-site linear and supercoiled plasmid DNA was inhibited. It was also shown that the actual concentration of StpA was not responsible for the inhibition of DNaseI or EcoKI, but rather the number of StpA per DNA bp was vital to inhibition of these enzymes. StpA therefore inhibits EcoKI activity by formation of a condensed structure of DNA which may prevent access of EcoKI to the target site or prevent translocation due to StpA bridging DNA helices together.

At concentrations of 256-171bp per StpA, a reduced level of restriction of linear pBR322 by EcoKI occurred, even though DNaseI activity was not inhibited at these concentrations. Also, the usual banding pattern for restriction of EcoRI-linearised pBR322, that occurs at lower StpA concentrations, was not seen. This implies that the position of EcoKI restriction is affected by the presence of bound StpA. In this way, StpA could cause a block to translocation, possibly by formation of interstrand links which could occur at concentrations of StpA too low to fully condense DNA.

It is interesting that StpA is able to condense supercoiled DNA more easily than linear DNA, as this effect was not seen with spermidine condensation. StpA is proposed to act in a similar way to H-NS, which forms oligomeric arrays that bind helices together (Azam *et al.*, 1999). This will be aided by supercoiling, which brings different regions of DNA into close proximity, with approximate parallel orientation (Minsky, 2004). This finding highlights the different mechanisms in which condensing agents act and how the physical structure of DNA can affect its overall conformation and activity.

It has been calculated by Azam *et al.*, (2000) that there is one StpA molecule per 190bp of DNA in *E.coli* cells during the exponential phase, as well as one H-NS per 220bp. This quantity of StpA would be enough to condense supercoiled DNA under these experimental conditions, and along with its homologue H-NS as well as the numerous other nucleoid-associated proteins that act to condense DNA, would be expected to condense linear DNA as well. Therefore, although under conditions of cell stress, the nucleoidal DNA has been seen

to arrange itself into highly organised parallel arrays of DNA helices (Levin-Zaidman, 2000; Minsky, 2004) that would be expected to be resistant to enzymes such as EcoKI, healthy cells in exponential growth phase may possess a nucleoidal conformation that is also resistant to EcoKI. However, such binding of nucleoid-associated proteins will depend sensitively upon the ionic conditions and may be present in levels too low to induce condensation *in vivo*. It has already been suggested that intracellular levels of nucleoid-associated proteins are too low to condense DNA *in vivo*, but that additional factors such as polyamines and crowding may aid in DNA compaction (Murphy and Zimmerman, 1995).

8.8. Crowding

Wenner and Bloomfield, (1999), used Ficoll 70 to crowd reactions involving the type II restriction enzyme EcoRV. They found that Ficoll had little effect on the overall rate of reaction due to its opposing effects on V_{max}, K_m and non-specific binding. They found that although the excluded volume effects of crowding increased V_{max} and non-specific binding, the resultant increase in viscosity decreases protein diffusion thereby increasing K_m. These forces appear to offset each other, allowing the overall reaction rate to be maintained between 0-20% Ficoll. Similar reaction complexities will be present in the reaction of EcoKI with PEG 8000 or glycerol. However, as EcoKI carries out only a single reaction, the inhibitory effects of non-specific binding should be reduced.

In fact glycerol and PEG 8000 were found to have very different effects on EcoKI activity. Glycerol had a greater inhibitory effect on EcoKI ATP hydrolysis and restriction activity than PEG 8000, even though reactions were carried out at equal viscosities. The largest difference in EcoKI ATP hydrolysis activity for reactions carried out in isoviscous solutions of glycerol and PEG 8000, occurred using 5% PEG 8000 and 27.5% glycerol. For EcoKI restriction, the largest difference in activity for reactions carried out in isoviscous solutions of glycerol and PEG 8000 occurred at 7.5% PEG 8000 and 36.5% glycerol. This increased activity of EcoKI in PEG 8000 compared to glycerol can be explained by the fact that glycerol inhibits EcoKI activity due to its viscosity, which restricts diffusion and could reduce binding and translocation. Although PEG 8000 has equal macroscopic viscosity under the experimental conditions, it is also a crowding agent. In this way it can increase the concentrations of individual reactants by volume exclusion. PEG 8000 can also act to cage the DNA and EcoKI reactions within a 'buffer bubble', which would not be so heavily

affected by the inhibitory effects of viscosity. This would act to increase the binding of EcoKI to DNA, resulting in the observed increases in ATP hydrolysis and restriction. The fact that an increase in EcoKI concentration has been shown to increase the rate of ATP hydrolysis (see section 3.5.1.2.), backs up the proposal that the increases in rate observed under crowded conditions using PEG 8000 are due to volume exclusion effects increasing the relative reactant concentrations.

However, although glycerol is used as a viscosity control in these experiments, it may have other effects upon EcoKI activity. Glycerol has been proposed to force proteins to release lubricating water from their interior, decreasing their conformational flexibility (Priev *et al.*, 1996) causing a collapse of these internal voids. Such an increase in rigidity would be expected to have a profound effect on an enzyme such as EcoKI, where flexibility is likely to be important in DNA translocation. As other specific effects upon EcoKI activity are also possible, assignment of the inhibitory effect of glycerol on EcoKI activity to viscosity alone would be misleading. Such unknown specific effects may also occur in the reaction between PEG 8000 and EcoKI. In this way, the effects of PEG 8000 on reaction rates may not be solely attributable to crowding. Therefore the discussion of these crowding results only gives an indication of the possible mechanisms of EcoKI reactions taking place in viscous and crowded solutions. Ideally these experiments should be repeated with other crowding agents as well as different viscosity controls to minimise the possibility of specific interactions.

8.9. Physiological consequences

The results indicate that DNA condensation, whether induced by the polyamine spermidine or the nucleoid-associated protein StpA is inhibitory to EcoKI activity. The tightly bound non-specific molecules such as YOYO, EtBr and H33258 also greatly inhibit EcoKI activity. However, the effects of the crowding agent PEG 8000 act to enhance EcoKI activity with respect to the inhibitory effects of isoviscous solutions of glycerol.

These observations can be related to those previously made on restriction alleviation and on the structure of the nucleoid. It is apparent that the type I R/M enzyme can find itself in three different situations, i. diffusing in the cytoplasm looking for protein-free 'naked' foreign DNA, ii. bound to the nucleoid during its replication when it is partially coated with

nucleoid-associated proteins or iii. bound to a fully condensed nucleoid which is undergoing repair.

It has been found that there are two sorts of restriction alleviation (RA) initiated under conditions of cell stress caused by 2-aminopurine, nalidixic acid or UV irradiation, or by the creation of potentially lethal r^+m^- mutant type I R/M enzymes or introduction of a new R/M system. These different mechanisms of RA are termed family-specific and general (Makovets *et al.*, 2004). The family-specific RA is due to a genotypic effect but no genotype has yet been found for general RA so it was suggested that this mechanism could be due to some feature of the structure of the nucleoid (Murray, 2002). These results on the inhibitory effects of spermidine and StpA-induced condensation and non-specific ligands, all of which mimic aspects of nucleoid structure, are strong evidence in support of this assertion. I believe that the experimental conditions used here, namely coating the DNA with non-specific dye molecules and condensing it with spermidine and StpA, mimic the nucleoid structure encountered by EcoKI and other type I R/M enzymes *in vivo*. Therefore, the *in vivo* implication of these results is that the EcoKI DNA translocation process on the nucleoid is drastically slowed by both condensation and non-specific protein binding and the enzyme stalls. Furthermore, the production of single and double-strand breaks in the host DNA by the R/M enzyme is strongly inhibited by nucleoid structure, particularly the structures induced by conditions of stress where the nucleoid becomes highly ordered and condensed (Frenkiel-Krispin *et al.*, 2001, 2004). Double-strand breaks, which have been observed by pulsed field gel electrophoresis of *E. coli* chromosomal DNA (Cromie and Leach, 2001), will still occur but very slowly, infrequently and in an uncoordinated manner. These cleavage events can be repaired by DNA ligase and recombination processes.

A similar argument can be made to explain the observation that bacterial cells can acquire new type I R/M systems easily by transformation, transduction and conjugation but the restriction activity, in contrast to modification, takes a long time to be manifest and RA is activated (Kulik and Bickle, 1996; Makovets *et al.*, 1998; O'Neill *et al.*, 1997; Prakash-Cheng and Ryu, 1993; Prakash-Cheng *et al.*, 1993). Upon introduction of the new system, protein is slowly made and assembled into the R/M enzyme. Some of this newly synthesized enzyme will clearly be able to attack the foreign DNA should it be unmodified; however, the bulk of the enzyme will be sequestered by binding to the nucleoid where it can either slowly carry out its methylation reaction or trigger the restriction reaction in response to the unmodified targets on the nucleoid. The results in this thesis show that if the restriction

reaction is triggered, the translocation and cleavage functions will be inhibited by the nucleoid structure, allowing the normal DNA repair processes to handle the occasional damage produced by the type I R/M enzyme.

In summary, the restriction activity of the type I R/M enzymes, which is completely dependent upon extensive translocation, is so inefficient on nucleoid DNA that it is not a major problem for the cell and the general RA phenomenon is observed. In addition to general RA, family-specific RA is an extra feature in which some of the type I R/M enzymes are subjected to clpXP-dependent proteolysis whilst they are attempting to move along the nucleoid DNA.

However, when phage attack a type I R/M proficient cell which is already under stress and showing RA, it is observed that restriction of the phage is not entirely abolished (Bertani and Weigle, 1953; Doronina and Murray, 2001; Efimova *et al.,* 1988; Glover and Colson, 1965; Makovets *et al.,* 1999) indicating that the unmodified, chemically identical, foreign and host DNA molecules can be distinguished by the restriction enzyme. This can be explained by the existence of two pools of type I R/M enzyme (Doronina and Murray, 2001; Holubova *et al.,* 2000, 2004). The pool of enzyme bound to the nucleoid will be dealt with by general and family-specific RA as described above but the cytoplasmic pool of the enzyme will bind to the incoming phage DNA. This foreign DNA will be in a highly crowded environment but uncondensed. This form of DNA is the perfect substrate for the translocation process prior to double-strand cleavage and this substrate will not induce RA. It would appear reasonable to suggest that in this situation, the type I R/M enzyme can complete its restriction reaction so rapidly that if it were susceptible to family-specific RA, then the clpXP enzyme would be physically unable to locate, bind, and destroy the restriction enzyme before the restriction enzyme had destroyed the incoming DNA. Translocation rates for type I R/M enzymes have been measured to be between 100 and 400 base pairs per second in each direction (Firman and Szcelkun, 2000; Garcia and Molineux, 1999; Studier and Bandyopadhyay, 1988) so even if two target sequences were 10000 base pairs apart, the clpXP would only have between 12 and 50 seconds to act. It is also perhaps noteworthy that EcoKI can form a large dimer species on unmethylated, random coil DNA if the DNA contains two target sequences (Berge *et al.,* 2000; Ellis *et al.,* 1999) even though this extra complexity is not essential for enzyme activity. Such a dimer is unlikely to be able to form on chromosomal DNA packaged in the nucleoid as it is unlikely that two target sequences will be in close physical proximity.

Perhaps this dimer species is not susceptible to clpXP family-specific RA whereas the monomer species bound on the nucleoid would still be susceptible?

In conclusion, I believe these results show that the answer to the question "how are unmodified sequences in the resident bacterial chromosome distinguished from those in DNA that has recently entered the bacterial cell?" (Makovets *et al.*, 2004; Murray, 2002) is that DNA in the nucleoid is condensed and coated with non-sequence specific ligands whereas foreign DNA is relatively naked and in a less compact conformation. These differences in the higher order structure have an enormous effect on the activity of the type I R/M enzymes.

These results also have wider implications, indicating that the varying conformations of DNA produced during the cell cycle, in response to damage, or free in the cytoplasm all possess different activities. DNA condensation appears to be a general mechanism used to exclude proteins when the cellular DNA is damaged, but even in a growing cell DNA is organised in the compacted nucleoid or crowded cytoplasm. This highlights the variability in effects that the structure of DNA and buffer environment can have upon enzyme activity. Physiological conditions should therefore be emulated *in vitro* in order to truly represent the reactions that take place within the cell interior.

References

Adzuma, K., and Mizuuchi, K. (1989). Interaction of proteins located at a distance along DNA: mechanism of target immunity in the Mu DNA strand-transfer reaction. Cell. 57:41-47.

Ames, B.N., and Dubin, D.T. (1960). The role of polyamines in the neutralization of bacteriophage deoxyribonucleic acid. J. Biol. Chem. 235:769-775

Arber, W. (1965). Host-controlled modification of bacteriophage. Annu. Rev. Microbiol. 19:365-378.

Arscott, A.G., Li, A-Z., and Bloomfield, V.A. (1990). Condensation of DNA by trivalent cations. 1. Effects of DNA length and topology on the size and shape of condensed particles. Biopolymers. 30:619-630.

Atkins, P.W. (1979). Physical chemistry. Second edition, Oxford University Press.

Ausubel, F.M., Brent, R., Kingston, R.E., Moore, D.D., Seidmen, J.G., Smith, J.A., and Struhl, K. (Editors). (1992). Short protocols in molecular biology. Second edition, Greene Publishing Associates and John Wiley and Sons.

Azam, T.A., Hiraga, S., and Ishihama, A. (2000). Two types of localization of the DNA-binding proteins within the *Escherichia coli* nucleoid. Genes Cells. 5:613-626.

Azam, T.A., and Ishihama, A. (1999). Twelve species of the nucleoid-associated protein from *Escherichia coli*. J. Biol. Chem. 274(46):33105-33113.

Azam, T.A., Iwata, A., Nishimura, A., Ueda, S., and Ishihama, A. (1999). Growth phase-dependent variation in protein composition of the *Escherichia coli* nucleoid. 181(20):6361-6370.

Baeza, I., Gariglio, P., Rangel, L.M., Chavez, P., Cervantes, L., Arguello, C., Wong, C., and Montanez, C. (1987). Electron microscopy and biochemical properties of polyamine-compacted DNA. Biochem. 26:6387-6392.

Battista, J.R. (1997). Against all odds: the survival strategies of *Deinococcus radiodurans*. Annu. Rev. Microbiol. 51:203-24.

Baumann, C.G., and Bloomfield, V.A. (1995). Large-scale purification of plasmid DNA for biophysical and molecular biology studies. BioTechniques. 19(6):884-890.

Baumann, C.G., Bloomfield, V.A., Smith, S.B., Bustamante, C., Wang, M.D., and Block, S.M. (2000). Stretching of single collapsed DNA molecules. Biophys. J. 78:1965-1978.

Berge, T., Ellis, D.J., Dryden, D.T., Edwardson, J.M., and Henderson, R.M. (2000). Translocation-independent dimerization of the EcoKI endonuclease visualized by atomic force microscopy. Biophys. J. 79:479-484.

Bertani, G., and Weigle, J.J. (1953). Host controlled variation in bacterial viruses. J. Bacteriol.. 65:113-121.

Bickle, T.A., Brack, C., and Yuan, R. (1978). ATP-induced conformational changes in the restriction endonuclease from *Escherichia coli* K-12. Poc. Natl. Acad. Sci. USA. 75:3099-3103.

Bickle, T.A., and Kruger, D.H. (1993). Biology of DNA restriction. Microbiol. Rev. 57:434-450.

Black, L.W. (1989). DNA packaging in dsDNA bacteriophages. Annu. Rev. Microbiol. 43:267-292.

Blagbrough, I.S., Geall, A.J., and Neal, A.P. (2003). Polyamines and novel polyamine conjugates interact with DNA in ways that can be exploited in non-viral gene therapy. Biochem. Soc. Trans. 31(2):397-406.

Bloomfield, V.A. (1991). Condensation of DNA by multivalent cations: Considerations on mechanism. Biopolymers. 31:1471-1481.

Bloomfield, V.A. (1996). DNA condensation. Curr. Opin. Struct. Biol. 6:334-341.

Bohrmann, B., Haider, M., and Kellenberger, E. (1993). Concentration evaluation of chromatin in unstained resin-embedded sections by means of low-dose ratio-contrast imaging in STEM. Ultramicroscopy. 49:235-251.

Bolivar, F. (1977). Construction and characterisation of new cloning vehicles. II. A multipurpose cloning system. Gene. 2:95-113.

Bourniquel, A.A., and Bickle, T.A. (2002). Complex restriction enzymes: NTP-driven molecular motors. Biochimie. 84:1047-1059.

Brewer, L.R., Corzett, M., and Balhorn, R. (1999). Protamine-induced condensation and decondensation of the same DNA molecule. Science. 286:120-123.

Brosh Jr, R.M., Karow, J.K., White, E.J., Shaw, N.D., Hickson, I.D., and Bohr, V.A. (2000). Potent inhibition of Werner and Bloom helicases by DNA minor groove binding drugs. Nucleic Acids Res. 28(12):2420-2430.

Burckhardt, J., Weisemann, J., Hamilton, D.L., and Yuan, R. (1981). Complexes formed between the restriction endonuclease EcoK and heteroduplex DNA. J. Mol. Biol. 153:425-440.

Burg, M.B. (2000). Macromolecular crowding as a cell volume sensor. Cell Physiol. Biochem. 10:251-256.

Carlsson, C., Jonsson, M., and Akerman, B. (1995). Double bands in DNA gel electrophoresis caused by bis-intercalating dyes. Nucleic Acids Res. 23(13):2413-2420.

Carlsson, C., Larsson, A., and Jonsson, M. (1996). Influence of optical probing with YOYO on the electrophoretic behaviour of the DNA molecule. Electrophoresis. 17:642-651.

Cerritelli, M.E., Cheng, N., Rosenberg, A.H., McPherson, C.E., Booy, F.P., and Steven, A.C. (1997). Encapsidated conformation of bacteriophage T7 DNA. Cell. 91:271-280.

Chan, K-M., Delfert, D., and Junger, K.D. (1986). A direct colorimetric assay for Ca^{2+}-stimulated ATPase activity. Anal. Biochem. 157:375-380.

Chen, A., Powell, L.M., Dryden, D.T.F., Murray, N.E., Brown, T. (1995). Tyrosine 27 of the specificity polypeptide of EcoKI can be UV crosslinked to a bromodeoxyuridine-substituted DNA target sequence. Nucleic Acids Res. 23:1177-1183.

Cheng, X., and Roberts, R.J. (2001). AdoMet-dependent methylation, DNA methyltransferases and base flipping. Nucleic Acids Res. 29(18):3784-3795.

Clark, D.J., and Thomas, J.O. (1988). Differences in the binding of H1 variants to DNA. Cooperativity and linker-length related distribution. Eur. J. Biochem. 178:225-233.

Colclasure, G.C., and Parker, J.C. (1991). Cytosolic protein concentration is the primary volume signal in dog red cells. J. Gen. Physiol. 98(5):881-892.

Crothers, D.M., Drak, J., Kahn, J.D., and Levene, S.D. (1992).DNA bending, flexibility, and helical repeat by cyclization kinetics. Methods Enzymol. 212:3-29.

Daly, M.J., and Minton, K.W. (1995). Resistance to radiation. Science. 270:1318.

Damadian,R. (1971). Biological ion exchanger resins. I. Quantitative electrostatic correspondence of fixed charge and mobile counter ion. Biophys. J. 11:739-760.

Dame, R.T., Wyman, C., and Goosen, N. (2000). H-NS mediated compaction of DNA visualised by atomic force microscopy. Nucleic Acids Res. 28(28):3504-3510.

Daujotyte, D., Serva, S., Vilkaitis, G., Merkiene, E., Venclovas, C., and Klimasauskas, S. (2004). HhaI DNA methyltransferase uses the protruding Gln237 for active flipping of its target cytosine. Structure. 12:1047-1055.

Davies, G.P. (2000). Motifs in the HsdR subunit of EcoKI necessary for ATP-dependent DNA translocation and DNA cleavage. Ph.D. Thesis. University of Edinburgh.

Davies, G.P., Kemp, P., Molineux, I.J., and Murray, N.E. (1999). The DNA translocation and ATPase activities of restriction-deficient mutants of Eco KI. J. Mol. Biol.292(4):787-96.

Davies, G.P., Martin, I., Sturrock, S.S., Cronshaw, A., Murray, N.E. and Dryden, D.T.F. (1999). On the structure and function of type I DNA restriction enzymes. J. Mol. Biol. 290:565-579.

Davies, G.P., Powell, L.M., Webb, J.L., Cooper, L.P., and Murray, N.E. (1998). EcoKI with an amino acid substitution in any one of seven DEAD-box motifs has impaired ATPase and endonuclease activities. Nucleic Acids Res. 26:4828-4836.

Dillingham, M.S., Spies, M., and Kowalczykowski, S.C. (2003). RecBCD enzyme is a bipolar DNA helicase. Nature. 423:893-897.

Dillingham, M.S., Wigley, D.B., and Webb, M.R. (2000). Demonstration of unidirectional single-stranded DNA translocation by PcrA helicase: Measurement of step size and translocation speed. Biochem. 39:205-212.

Dixon, D.A., and Kowalczykowski S.C. (1993). The recombination hotspot χ is a regulatory sequence that acts by attenuating the nuclease activity of the *E. coli* Rec BCD enzyme. Cell 73:87-96.

Doronina, V.A., and Murray, N.E. (2001). The proteolytic control of restriction activity in *Escherichia coli* K-12. Mol. Microbiol. 39:416-428.

Dreier, J., and Bickle, T.A. (1996). ATPase activity of the type C restriction-modification system EcoR124II. J. Mol. Biol. 257:960-969.

Dreier, J., MacWilliams, M.P., and Bickle, T.A. (1996). DNA cleavage by the type IC restriction-modification enzyme EcoR124II. (1996). J. Mol. Biol. 264, 722-733.

Dryden, D.T.F., Cooper, L.P., and Murray, N.E. (1993). Purification and characterization of the methyltransferase from the type I restriction and modification system of *Escherichia coli* K12. J Biol. Chem. 268:13228-13236.

Dryden, D.T.F., Cooper, L.P., Thorpe, P.H., and Byron, O. (1997). The *in vitro* assembly of the EcoKI type I DNA restriction/modification enzyme and its in vivo implications. Biochem. 36:1065-1076.

Dryden, D.T.F., Davies, G.D., Martin, I., Powell, L.M., Murray, N.E., Ellis, D.J., Berge, T., Edwardson, J.M., and Henderson, R.M. (1999). Molecular interactions in complex proteins and nucleic acids. Biochem. Soc. Trans. 27(4):691-696.

Dryden, D.T.F., Murray, N.E., and Rao, D.N. (2001). Nucleoside triphosphate-dependent restriction enzymes. Nucleic Acids Res. 29(18):3728-3741.

Dryden, D.T.F., Sturrock, S.S., and Winter, M. (1995). Structural modelling of a type I DNA methyltransferase. Nat. Struct. Biol. 2:632-635.

Efimova, E.P., Delver, E.P., and Belogurov, A.A. (1988). 2-aminopurine and 5-bromouracil induce alleviation of type I restriction in *Escherichia coli*: Mismatches function as inducing signals? Mol. Gen. Genet. 214:317-320.

Eggleston, A.K., Rahim, N.A., and Kowalczykowski, S.C. (1996). A helicase assay based on the displacement of fluorescent, nucleic acid binding ligands. Nucleic Acids Res. 24(7):1179-1186.

Ellis, D.J., Dryden, D.T.F., Berge, T., Edwardson, J.M., and Henderson, R.M. (1999). Direct observation of DNA translocation and cleavage by the EcoKI endonuclease using atomic force microscopy. Nat. Struct. Biol. 6:15-17.

Ellis, R.J., and Minton, A.P. (2003). Join the crowd. Nature. 425:27-28

Embleton, M.L., Siksnys, V., and Halford, S.E. (2001). DNA cleavage reactions by type II restriction enzymes that require two copies of their recognition sites. J. Mol. Biol. 311:503-514.

Endlich, B., and Linn, S. (1985). The DNA restriction endonuclease of *Escherichia coli* B. II. Further studies of the structure of DNA intermediates and products. J. Biol. Chem. 260, 5729-5738.

Eskin, B., and Linn, S. (1972). The deoxyribonucleic acid modification and restriction enzymes of *Escherichia coli* B. J. Biol. Chem. 247(19):6192-6196.

Esposito, D., Petrovic, A., Harris, R., Ono, S., Eccleston,. J.F., Mbabaali, A., Haq, I., Higgins, C.F., Hinton, J.C.D., Driscoll, P.P., and Ladbury, J.E. (2002). H-NS oligomerization domain structure reveals the mechanism for high order self-association of the intact protein. J. Mol. Biol. 324:841-850.

Fang, Y., and Hoh, J.H. (1998). Early intermediates in spermidine-induced DNA condensation on the surface of mica. J. Am. Chem. Soc. 120(35):8903-8909.

Firman, K., and Szczelkun, M.D. (2000). Measuring motion on DNA by the type I restriction endonuclease EcoR124I usingtriplex displacement. EMBO J. 19:2094-2102.

Flink, I., and Pettijohn, D.E. (1975). Polyamines stabilise DNA folds. Nature. 253:62-63.
Golan, R., Pietrasanta, L.I., Hsieh, W., and Hansma, H.G. (1999). DNA toroids: Stages in condensation. Biochem. 38:14069-14076.

Frenkiel-Krispin, D., Ben-Avraham, I., Englander, J., Shimoni, E., Wolf, S.G., and Minsky, A. (2004). Nucleoid restructuring in stationary-state bacteria. Mol. Microbiol. 51(2):395-405.

Frenkiel-Krispin, D., Levin-Zaidman, S., Shimoni, E., Wolf., S.G., Wachtel, E.J., Arad, T., Finkel, S.E., Kolter, R., and Minsky, A. (2001). Regulated phase transitions of bacterial chromatin: A non-enzymatic pathway for generic DNA protection. EMBO J. 20(5):1184-1191.

Friedhoff, P., Lurz, R., Luders, G., and Pingoud, A. (2001). Sau3AI, a monomeric type II restriction endonuclease that dimerizes on the DNA and thereby induces DNA loops. J. Biol. Chem. 276(26):23581-23588.

Fuller-Pace, F.V., Bullas, L.R., Delius, H., and Murray, N.E. (1984). Genetic recombination can generate altered restriction specificity. Proc. Natl. Acad. Sci. USA. 81:6095-6099.

Gann, A.F., Campbell, A.J.B., Collins, J.F., Coulson, A.F.W., and Murray, N.E. (1987). Reassortment of DNA recognition domains and the evolution of new specificities. Mol. Microbiol. 1:13-22.

Garcia, L.R. and Molineux, I.J. (1999). Translocation and specific cleavage of bacteriophage T7 DNA *in vivo* by EcoKI. Proc. Natl. Acad. Sci. USA. 96:12430-12435.

George, J.W., Ghate, S., Matson, S.W., and Besterman, J.M. (1992). Inhibition of DNA helicase II unwinding and ATPase activities by DNA-interacting ligands. Kinetics and specificity. J. Biol. Chem. 267:10683-10689.

Gerard, F., Dri, A.M., and Moreau, P.L. (1999). Role of *Escherichia coli* RpoS, LexA, and H-NS global regulators in metabolism and survival under aerobic, phosphate-starvation conditions. Microbiol. 145:1547-1562.

Goppelt, M., Langowski, J., Pingoud, A., Haupt, W., Urbanke, C., Mayer, H., and Maass, G. (1981). The effect of several nucleic acid binding drugs on the cleavage of d(GGAATTCC) and pBR 322 by the Eco RI restriction endonuclease. Nucleic Acids Res. 9(22):6115-6127.

Gorbalenya, A.E., and Koonin, E.V. (1991). Endonuclease (R) subunits of type-I and type-III restriction-modification enzymes contain a helicase-like domain. FEBS Lett. 291:277-281.

Gormley, N.A., Bath, A.J., and Halford S.E. (2000). Reactions of BglI and other type II restriction endonucleases with discontinuous recognition sites. J. Biol. Chem. 275(10):6928-6936.

Gosule, L.C., and Schellman, J.A. (1976). Compact form of DNA induced by spermidine. Nature. 259:333-335.

Ha, B-Y., and Liu, A.J. (2001). Physical questions posed by DNA condensation. Physical chemistry of polyelectrolytes. Edited by Radeva, T. Marcel Dekker, NY. Pages 163-180.

Hagerman, P.J. (1988). Flexibility of DNA. Annu. Rev. Biophys. Biophys. Chem. 17:265-286.

Halford, S.E. (2001). Hopping, jumping and looping by restriction enzymes. Biochem. Soc. Trans. 29:363-374.

Halford, S.E., Welsh, A.J., and Szczelkun, M.D. (2003). Enzyme-mediated DNA looping. Annu. Rev. Biophys. Biomol. Struct. 33:1-24.

Harris DA, (1987) in: Spectrophotometry and spectropfluorimetry. A practical approach (Harris, D.A. and Bashford, C.L. eds.) IRL Press, Oxford.

Havas, K., Flaus, A., Phelan, M., Kingston, R., Wade, P.A., Lilley, D.M.J., AND Owen-Hughs, T. (2000). Generation of superhelical torsion by ATP-dependent chromatin remodelling activities. Cell. 103:1133-1142.

Hayashi, K., Nakazawa, M., Ishizaki, Y, Hiraoka, N., and Obayashi, A. (1985). Stimulation of intermolecular ligation with E. coli DNA ligase by high concentrations of monovalent cations in polyethylene glycol solutions. Nucleic Acids Res. 13(22):7979-7992.

Horiuchi, K., and Zinder, N.D. (1972). Cleavage of bacteriophage f1 DNA by the restriction enzyme of *Escherichia coli* B. Proc. Natl. Acad. Sci. USA. 69:3220-3224.

Huang, N., Banavali, N.K., and MacKerell, A.D. (2003). Protein-facilitated base flipping in DNA by cytosine-5-methyltransferase. Proc. Natl. Acad. Sci. USA. 100(1):68-73.

Hud, N.V. Allen, M.J., Downing, K.H., Lee, J., and Balhorn, R. (1993). Identification of the elemental packing unit of DNA in mammalian sperm cells by atomic force microscopy. Biochem. Biophys. Res. Commun. 193:1347-1354.

Hud, N.V., and Downing, K.H. (2001). Cryoelectron microscopy of λ phage DNA condensates in vitreous ice: The fine structure of DNA toroids. PNAS. 98(26):14925-14930.

Hud, N.V., Downing, K.H., and Balhorn, R. (1995). A constant radius of curvature model for the organization of DNA in toroidal condensates. Proc. Natl. Acad. Sci. USA. 92:3581-3585.

Janscak, P., Abadjieva, A., and Firman, K. (1996). The type I restriction endonuclease R.EcoR124I: over-production and biochemical properties. J. Mol. Biol. 257:977-991.

Janscak, P., and Bickle, T.A. (2000). DNA supercoiling during ATP-dependent DNA translocation by the type I restriction enzyme EcoAI. J. Mol. Biol. 295:1089-1099.

Janscak, P., MacWilliams, M.P., Sandmeier, U., Nagaraja, V., and Bickle, T.A. (1999). DNA translocation blockage, a general mechanism of cleavage site selection by type I restriction enzymes. EMBO J. 18:2638-2647.

Janscak, P., Sandmeier, U., and Bickle, T.A. (1999). Single amino acid substitutions in the HsdR subunit of the type IB restriction enzyme EcoAI uncouple the DNA translocation and DNA cleavage activities of the enzyme. Nucleic Acids Res. 27:2638-2643.

Jary, D., and Sikorav, J-L. (1999). Cyclization of globular DNA. Implications for DNA-DNA interactions *in vivo*. Bichem. 38(11):3223-3227.

Jeltsch, A., Alves, J., Maas, G., and Pingoud, A. (1992). On the catalytic mechanism of EcoRI and EcoRV. A detailed proposal based on biochemical results, structural data and molecular modelling. FEBS Lett. 304:4-8.

Jen-Jacobson, L., Engler, L.E., Lesser, D.R., Kurpiewski, M.R., Yee, C., and McVerry, B. (1996). Structural adaptations in the interaction of EcoRI endonuclease with methylated GAATTC sites. EMBO J. 15:2870-2882.

Kaiser, A.D., and Inman, R.B. (1965). Cohesion and the biological activity of bacteriophage lambda DNA. J. Mol. Biol. 13:78-91.

Kan, N.C., Lautenberger, J.A., Edgell, M.H., and Hutchison, C.A. (1979). The nucleotide sequence recognized by the *Escherichia coli* K12 restriction and modification enzymes. J. Mol. Biol. 130:191-209.

Kao-Huang, Y., Revzin, A., Butler, A.P., O'Conner, P., Noble, D.W., and von Hippel, P.H. (1977). Nonspecific DNA binding of genome-regulating proteins as a biological control mechanism: measurement of DNA-bound *Escherichia coli* lac repressor *in vivo*. Proc. Natl. Acad. Sci. USA. 74(10):4228-4232.

Keatch, S.A., Su, T.J., Dryden, D.T.F. (2004). Alleviation of restriction by DNA condensation and non-specific DNA binding ligands. Nucleic Acids Res. 32(19):5841-5850.

Kelleher, J.E., Daniel, A.S., and Murray, N.E. (1991). Mutations that confer *de novo* activity upon a maintenance methyltransferase. J. Mol. Biol. 221:431-440.

Kleinschmidt, A.K., Lang, D., Jacherts, D., and Zahn, R.K. (1962). Preparation and length measurements of the total deoxyribonucleic acid content of T2 bacteriophages. Biochem. Biophys. Acta. 61:857-864

Klimasauskas, S., Kumar, S., Roberts, R.J., and Cheng, X. (1994). HhaI methyltransferase flips its target base out of the DNA helix. Cell. 76:357-369.

Klimasauskas, S., and Roberts, R.J. (1995). M.HhaI binds tightly to substrates containing mismatches at the target base. Nucleic Acids Res. 23(8):1388-1395.

Kobayashi, I. (2001). Behavior of restriction-modification systems as selfish mobile elements and their impact on genome evolution. Nucleic Acids Res. 29:3742-3756

Korona, R., Korona, B., and Levin, B.R. (1993). Sensitivity of naturally occurring coliphages to type I and type II restriction and modification. Gen. Microbiol. 139(Pt 6):1283-1290.

Krasnow, M.A., and Cozzarelli, N.R. (1982). Catenation of DNA rings by topoisomerases. J. Biol. Chem. 257(5):2687-2693.

Kruger, D.H., Schroeder, C., Reuter, M., Bogdarina, I.G., Buryanov, Y.I., and Bickle, T.A. (1985). DNA methylation of bacterial viruses T3 and T7 by different DNA methylases in *Escherichia coli* K12 cells. Eur. J. Biochem. 150(2):323-330.

Kuosmanen, M., and Poso, H. (1985). Inhibition of the activity of restriction endonucleases by spermidine and spermine. FEBS Lett. 179(1):17-20.

Kuzmic, P. (1996). Program DYNAFIT for the Analysis of Enzyme Kinetic Data: Application to HIV Proteinase. Anal. Biochem. 237:260-273.

Laemmli, U.K. (1975). Characterization of DNA condensates induced by poly(ethylene oxide) and polylysine. Proc. Natl. Acad. Sci. U S A. 72(11):4288-4292.

Lambert O, Letellier L, Gelbart WM, Rigaud JL. (2000). DNA delivery by phage as a strategy for encapsulating toroidal condensates of arbitrary size into liposomes. Proc. Natl. Acad. Sci. USA. 97(13):7248-53.

Langst, G., Bonte, E.J., Corona, D.F., and Becker, P.B. (1999). Nucleosome movement by CHRAC and ISWI without disruption or *trans*-displacement of the histone octamer. Cell. 97:843-852.

Lee, C.Y., Ryu, H-W., and Ko, T-S. (2001). Binding features of ethidium bromide and their effects on nuclease susceptibility of calf thymus DNA in the presence of spermine. Bull. Korean. Chem. Soc. 22(1):87-89.

Lerman, S. (1971). A transition to a compact form of DNA in polymer solutions. Proc. Natl. Acad. Sci. USA. 68:1886-1890.

Levin-Zaidman, S., Englander, J., Shimoni, E., Sharma, A.K., Minton, K.W., and Minsky, A. (2003). Ringlike structure of the Deinococcus radiodurans genome: A key to radioresistance? Science. 299:254-256.

Levin-Zaidman, S., Frenkiel-Krispin, D., Shimoni, E., Sabanay, I., Wolf, S.G., and Minsky, A. (2000). Ordered intracellular RecA-DNA assemblies: A potential site of *in vivo* RecA-mediated activities. Proc. Natl. Acad. Sci. USA. 97:6791-6796.

Lewin B. Genes VII. 2000. Oxford UniversityPress.

Lia, G., Bensimon, D., Croquette, V., Allemand, J-F., Dunlap, D., Lewis, D.E.A., Adhya, S., and Finzi, L. (2003). Supercoiling and denaturation in Gal repressor/heat unstable nucleoid protein (HU)-mediated DNA looping. Proc. Natl. Acad. Sci. USA. 100(20):11373-11377.

Lin, Z., Wang, C., Feng, X., Liu, M., Li, J., and Bai, C. (1998). The observation of th elocal ordering characteristics of spermidine-condensed DNA: Atomic force microscopy and polarizing microscopy studies. Nucleic Acids Res. 26(13):3228-3234.

Liquori, A.M., Costantino, L., Crescenzi, V., Elia, V., Giglio, E., Puliti, R., DeSantis Savino, M., and Vitagliano, V. (1967). Complexes between DNA and polyamines: A molecular model. J. Mol. Biol. 24:113-122.

Liu, G., Molas, M., Grossman, G.A., Pasumarthy, M., Perales, J.C., cooper, M.J., and Hanson, R.W. (2001). Biological properties of poly-L-lysine-DNA complexes generated by cooperative binding the polycation. J. Biol. Chem. 276:34379-34387

Ma, C., and Bloomfield, V.A. (1994). Condensation of supercoiled DNA induced by $MnCl_2$. Biophys. J. 67:1678-1681.

Ma, C., Sun, L., and Bloomfield, V.A. (1995). Condensation of plasmids enhanced by Z-DNA conformation of d(CG)n inserts. Biochem. 34:3521-3528.

Mahdi, A.A., Briggs, G.S., Sharples, G.J., Wen, Q., and Lloyd, R.G. (2003). A model for dsDNA translocation revealed by a structural motif common to RecG and Mfd proteins. EMBO. J. 22(3):724-734.

Makita, N., and Yoshikawa, K. (2002). Proton concentration (pH) switches the high-order structure of DNA in the presence of spermine. Biophys. Chem. 99:43-53.

Makovets, S., Doronina, V.A., and Murray, N.E. (1999). Regulation of endonuclease activity by proteolysis prevents breakage of unmodified bacterial chromosomes by type I restriction enzymes. Proc. Natl. Acad. Sci. USA. 96:9757-9762.

Makovets, S., Powell, L.M., Titheradge, A.J.B., Blakely, G.W., and Murray, N.E. (2004). Is modification sufficient to protect a bacterial chromosome from a resident restriction endonuclease? Mol. Microbiol. 51:135-147.

Makovets, S., Titheradge, A.J.B., and Murray, N.E. (1998). ClpX and ClpP are essential for the efficient acquisition of genes specifying type IA and IB restriction systems. Mol. Microbiol. 28:25-35.

Manning, G.S. (1978). The molecular theory of polyelectrolyte solutions with applications to the electrostatic properties of polynucleotides. Q. Rev. Biophys. 11:179-246.

Mannisto, M., Vanderkerken, S., Toncheva, V., Elomaa, M., Ruponen, M., Schacht, E., and Urtti, A. (2002). Structure-activity relationships of poly(L-lysines): Effects of pegylation and molecular shape on physicochemical and biological properties in gene delivery. J. Cont. Rel. 83:169-182.

Marquet, R., and Houssier, C. (1991). Thermodynamics of cation-induced DNA condensation. J. Biomol. Stuct. Dyn. 9:159-167.

Marquet, R., Wyart, A., and Houssier, C. (1987). Influence of DNA length on spermine-induced condensation. Importance of the bending and stiffening of DNA. Biochim. Biophys. Acta. 909:165-172.

Matsuura, S-I., Komatsu, J., Hirano, K., Yasuda, H., Takashima, K., Katsura, S., and Mizuno, A. (2001). Real-time observation of a single DNA digestion by λ exonuclease under fluorescence microscope field. Nucleic Acids Res. 29(16):E79

Matulis, D., Rouzina, I., and Bloomfield, V.A. (2000). Thermodynamics of DNA binding and condensation: Isothermal titration calorimetry and electrostatic mechanism. J. Mol. Biol. 296(4):1053-1063.

McGhee, J.D., and von Hippel, P.H. (1974). Theoretical aspects of DNA-protein interactions: Co-operative and non-co-operative binding of large ligands to a one-dimensional homogeneous lattice. J. Mol. Biol. 86:469-489.

McMurray, C.T., and van Holde, K.E. (1991). Binding of ethidium to the nucleosome core particle. 1. Binding and dissociation reactions. Biochem. 30(23):5631-5643.

Meisel, A., Bickle, T.A., Kruger, D.H., and Schroeder, C. (1992). Type III restriction enzymes need two inversely oriented recognition sites for DNA cleavage. Nature. 355:467-469.

Meisel, A., Mackeldanz, P., Bickle, TA., Kruger, D.H., Schroeder, C. (1995). Type III restriction endonucleases translocate DNA in a reaction driven by recognition site-specific ATP hydrolysis. EMBO J. 14:2958-2966.

Meng, X., Cai, W., and Schwartz, D.C. (1996). Inhibition of restriction endonuclease activity by DNA binding fluorochromes. J. Biomol. Struct. Dyn. 13(6):945-951.

Mernagh, D.R., and Kneale, G.G. (1996). High resolution footprinting of a type I methyltransferase reveals a large structural distortion within the DNA recognition site. Nucleic Acids Res. 24:4853-4858.

Milkman, R., Raleigh, E.A., McKane, M., Cryderman, D., Bilodeau, P., and McWeeny, K. (1999). Molecular evolution of the *Escherichia coli* chromosome. V. Recombination patterns among strains of diverse origin. Genetics. 153:539-554.

Minsky, A. (2004). Information content and complexity in the high-order organization of DNA. Annu. Rev. Biophys. Biomol. Struct. 33:317-342.

Minsky, A. (2003). Structural aspects of DNA repair: The role of restricted diffusion. Mol. Microbiol. 50(2):367-376.

Minton, A.P. (2000a). Effect of a concentrated "inert" macromolecular cosolute in the stability of a globular protein with respect to denaturation by heat and by chaotropes: A statistical-thermodynamic model. 78(1):101-109.

Minton, A.P. (2000b). Protein folding: Thickening the broth. Curr. Biol. 10:R97-99

Minton, A.P. (1998). Molecular crowding: Analysis of effects of high concentrations of inert cosolutes on biochemical equilibria and rates in terms of volume exclusion. Methods Enzym. 295:127-149.

Minton, A.P. (2001). The influence of macromolecular crowding and macromolecular confinement on biochemical reactions in physiological media. J. Biol. Chem. 276(14):10577-10580.

Milsom, S.E., Halford, S.E., Embleton, M.L., and Szczelkun, M.D. (2001). Analysis of DNA looping interactions by type II restriction enzymes that require two copies of their recognition sites. J. Mol. Biol. 311:515-527.

Moat and Foster. (1995). Microbial Physiology. Third edition, (page 11), Wiley-Liss.

Moe, J.G., and Russu, I.M. (1992). Kinetics and energetics of base-pair opening in 5'-d(CGCGAATTCGCG)-3' and a substituted dodecamer containing G.T mismatches. Biochemistry. 31:8421-8428.

Morris, P.D. and Raney, K.D. (1999). DNA helicases displace streptavidin from biotin-labelled oligonucleotides. Biochem. 38:5164-5171.

Murayama, H., and Yoshikawa, K. (1999). Thermodynamics of the collapsing phase transition in a single duplex DNA molecule. J. Phys. Chem. 103:10517-10523.

Murayama, Y., and Sano, M. (2005). Exchange of counterions in DNA condensation. Preprint, to appear in Biopolymers.

Murayama, Y., Sakamaki, Y., and Sano, M. (2003). Elastic response of single DNA molecules exhibits a reentrant collapsing transition. Phys. Rev. Lett. 90(1):018102-1-4.

Murphy, L.D., and Zimmerman, S.B. (2001). A limited loss of DNA compaction accompanying the release of cytoplasm from cells of *Escherichia coli*. J. Struct. Biol. 133:75-86.

Murphy, L.Z., and Zimmerman, S.B. (1995). Condensation and cohesion of λ DNA in cell extracts and other media: Implications for the structure and function of DNA in prokaryotes. Biophys. Chem. 57:71-92.

Murphy, L.D., and Zimmerman, S.B. (1994). Macromolecular crowding effects on the interaction of DNA with *Escherichia coli* DNA-binding proteins: A model for bacterial nucleoid stabilization. Biochim. Biophys. Acta. 1219(2):277-284.

Murphy, L.D., and Zimmerman, S.B. (2000). Multiple restraints to the unfolding of spermidine nucleoids from *Escherichia coli*. J. Struct. Biol. 132:46-62.

Murray, N.E. (2002). Immigration control of DNA in bacteria: self versus non-self. Microbiol. 148:3-20.

Murray, N.E. (2000). Type I restriction systems: Sophisticated molecular machines (a legacy of Bertani and Weigle). Microbiol. and Mol. Biol. Rev. 64(2):412-434.

Murray, N.E., Batten, P.L., and Murray, K. (1973). Restriction of bacteriophage lambda by *Escherichia coli* K. J. Mol. Biol. 81:395-407.

Oana, H., Tsumoto, K., Yoshikawa, Y., and Yoshikawa, K. (2002). Folding transition of large DNA completely inhibits the action of a restriction endonuclease as revealed by single-chain observation. FEBS Lett. 530:143-146.

O'Gara, M., Horton, J.R., Roberts, R.J., and Cheng, X. (1998). Structures of HhaI methyltransferase complexed with substrates containing mismatches at target base. Nature Structural Biology. 5(10):872-877.

O'Gara, M., Zhang, X., Roberts, R.J., and Cheng, X. (1999). Structure of a binary complex of HhaI methyltransferse with S-adenosyl-L-methionine formed in the presence of a short non-specific DNA oligonucleotide. J. Mol. Biol. 287:201-209.

Oh, T.J., and Kim, I.G. (1999). The expression of *Escherichia coli* SOS genes *recA* and *uvrA* is inducible by polyamines. Biochem. Biophys. Res. Commun. 264(2):584-589.

O'Neill, M., Chen, A., and Murray, N.E. (1997). The restriction-modification genes of *Escherichia coli* K-12 may not be selfish: They do not resist loss and are readily replaced by alleles conferring different specificities. Proc. Natl. Acad. Sci. USA. 94:14596-14601.

O'Neill, M., Dryden, D.T.F., and Murray, N.E. (1998). Localization of a protein-DNA interface by random mutagenesis. EMBO J. 17:7118-7127.

O'Neill, M., Powell, L.M., and Murray, N.E. (2001). Target recognition by EcoKI: The recognition domain is robust and restriction-deficiency commonly results from the proteolytic control of enzyme activity. J. Mol. Biol. 307:951-963.

Ostrovsky, B., Bar-Yarn, Y. (1995). Motion of polymer ends in homopolymer and heteropolymer collapse. Biophys. J. 68:1694-1698.

Parolin, C., Montecucco, A., Ciarrocchi, G., Pedrali-Noy, G., Valisena, S., Palumbo, M., and Palu, G. (1990). The effect of the minor groove binding agent DAPI (2-amidino-diphenyl-indole) on DNA-directed enzymes: An attempt to explain inhibition of plasmid expression in *Escherichia coli*. FEMS Microbiol. Lett. 68:341-346.

Paul and Clark. (1996). Soil Microbiology and Biochemistry. Second edition, (pages 50-54). Academic Press.

Pingoud, A. (1985). Spermidine increases the accuracy of type II restriction endonucleases. Suppression of cleavage at degenerate, non-symmetrical sites. Eur. J. Biochem. 147:105-109.

Pingoud, A., and Jeltsch, A. (1997). Recognition and cleavage of DNA by type-II restriction endonucleases. Eur. J. Biochem. 246:1-22.

Pingoud, A., and Jeltsch, A. (2001). Structure and function of type II restriction endonucleases. Nucleic Acids Res. 29(18):3705-3727.

Pingoud, A., Urbanke, C., Alves, J., Ehbrecht, H-J., Zabeau, M., and Gualerzi, C. (1984). Effect of polyamines and basic proteins on cleavage of DNA by restriction endonucleases. Biochem. 23:5697-5703.

Porschke, D. (1984). Dynamics of DNA condensation. Biochem. 23:4821-4828.

Porter, D.J.T., Sort, S.A., Hanlon, M.H., Preufschat, F., Wilson, J.E., Willard, D.H., and Consler, T.G. (1998). Product release is the major contributer to k_{cat} for the hepatitis C virus helicase-catalysed strand separation of short duplex DNA. J. Biol. Chem. 273:18906-18914.

Post, C.B., and Zimm, B.H. (1982). Theory of DNA condensation: collapse versus aggregation. Biopolymers. 21:2123-2137.

Powell, L.M., Connolly, B.A., and Dryden, D.T.F. (1998)a. The DNA binding characteristics of the trimeric EcoKI methyltransferase and its partially assembled dimeric form determined by fluorescence polarisation and DNA footprinting. J. Mol. Biol. 283:947-961.

Powell, L.M., Dryden, D.T.F., and Murray, N.E. (1998)b. Sequence-specific DNA binding by EcoKI, a type IA DNA restriction enzyme. J. Mol. Biol. 283:963-976.

Powell, L.M., Dryden, D.T.F., Willcock, D.F., Pain, R.H., and Murray, N.E. (1993). DNA recognition by the EcoK methylatransferase: the influence of DNA methylationand the cofactor S-adenosyl-L-methionine. J. Mol. Biol. 234:60-71.

Powell, L.M., and Murray, N.E. (1995). S-adenosyl methionine alters the DNA contacts of the EcoKI methyltransferase. Nucleic Acids Res. 23:967-974.

Prakash-Cheng, A., and Ryu, J. (1993). Delayed expression of *in vivo* restriction activity following conjugal transfer of *Escherichia coli* hsd_K (restriction-modification) genes. J. Bacteriol. 175:4905-4906.

Priev, A., Almagor, A., Yedgar, S., and Gavish, B. (1996). Glycerol decreases the volume and compressibility of protein interior. Biochem. 35:2061-2066.

Pullman, M.E., Penefsky, H.S., Datta, A., and Racker, E. (1960). Partial resolution of the enzymes catalysing oxidative phosphorylation. J. Biol. Chem. 235(11):3322-3329.

Raae, A.J., Kleppe, R.K., and Kleppe, K. (1975). Kinetics and effect of salts an dpolyamines on T4 polynucleotide ligase. Eur. J. Biochem. 60:437-443.

Ragkousi, K., Cowan, A.E., Ross, M.A., and Setlow, P. (2000). Analysis of nucleoid morphology during germination and outgrowth of spores of *Bacillus* species. J. Bacteriol. 182:5556-55562.

Rao, D.N., Saha, S., and Krishnamurthy, V. (2000). ATP-dependent restriction enzymes. Prog. Nucl. Acids. Res. Mol. Biol. 64:1-63.

Raspaud, E., de la Cruz, O., Sikorav, J-L., and Livolant, F. (1998). Precipitation of DNA by polyamines: A polyelectrolyte behaviour. Biophys. J. 74:381-393.

Rau, D.C., and Parsegian, V.A. (1992). Direct measurement of temperature-dependent solvation forces between DNA double helices. Biophys. J. 61:260-271.

Reich, Z., Ghirlando, R., and Minsky, A. (1992). Nucleic acids packaging process: Effects of adenine tracts and sequence-dependent curvature. J. Biomol. Struct. Dyn. 9:1097-1109.

Reich, Z., Levin-Zaidman, S., Gutman, S.B., Arad, T, and Minsky, A. (1994). Supercoiling-regulated liquid-crystalline packaging of topologically-constrained, nucleosome-free DNA molecules. Biochem. 33:14177-14184.

Richey, B., Cayley, D.S., Mossing, M.C., Kolka, C., Anderson, C.F., Farrar, T.C., and Record, M.T. Jr. Variability of the intracellular ionic environment of *Escherichia coli*. Differences between *in vitro* and *in vivo* effects of ion concentrations on protein-DNA interactions and gene expression. J. Biol. Chem. 262(15):7157-7164.

Rill, R.L. (1986). Liquid crystalline phases in concentrated aqueous solutions of Na+ DNA. Proc. Natl. Acad. Sci. USA. 83:342-346.

Ringrose, L., Chabanis, S., Angrand, P-O., Woodroofe, C., and Stewart, A.F. (1999). Quantitative comparison of DNA looping in vitro and in vivo: Chromatin increases effective DNA flexibility at short distances. EMBO J. 18:6630-6641.

Roberts, R.J., and Cheng, X. (1998). Base flipping. Annu. Rev. Biochem. 67:181-198.

Roberts, R.J., Vincze, T., Posfai, J., and Macelis, D. (2003). REBASE - restriction enzymes and methylases. Nucleic Acids Res. 31:418-420.

Roca, A.I., and Cox, M.M. (1997). RecA protein: Structure, function, and role in recombinational DNA repair. Prog. Nucl. Acid Res. Mol. Biol. 56:129-223.

Roman, L.J., Eggleston, A.K. and Kowalczykowski, S.C. (1992). Processivity of the DNA helicase activity of *Escherichia coli* RecBCD enzyme. J. Biol. Chem. 267:4207-4214.

Rubin, R. (1977). Spermidine-deoxyribonucleic acid interaction *in vitro* and in *Escherichia coli*. J. Bacteriol. 129(2):916-925.

Ruiz-Herrera, J., Ruiz-Medrano, R., and Dominguez, A. (1995). Selective inhibition of cytosine-DNA methylases by polyamines. FEBS Lett. 357:192-196.

Rye, H.S., Yue, S., Wemmer, D.E., Quesada, M.A., Haugland, R.P., Mathies, R.A., and Glazer, A.N. (1992). Stable fluorescent complexes of double-stranded DNA with bis-intercalating asymmetric cyanine dyes: Properties and applications. Nucleic Acids Res. 20(11):2803-2812.

Saminathan, M., Thomas, T., Shirahata, A., Pillai, C.K.S., and Thomas, T.J. (2002). Polyaminestructural effects on the induction and stabilization of liquid crystalline DNA: Potential applications to DNA packaging, gene therapy and polyamine therapeutics. Nucleic Acids Res. 30(17):3722-3731.

Schellman, J.A., and Parthasarathy, N. (1984). X-ray diffraction studies on cation-collapsed DNA. J. Mol. Biol. 175(3):313-329.

Schleif, R. (1992). DNA looping. Annu. Rev. Biochem. 61:199-223.

Seidel, R., van Noort, J., van der Scheer, C., Bloom, J.G.P., Dekker, N.H., Dutta, C.F., Blundell, A., Robinson, T., Firman, K., and Dekker, C. (2004). Real-time observation of DNA translocation by the type I restriction modification enzyme EcoR124I. Nat. Struct. Mol. Biol. 11(9):838-843.

Shore, D., Langowski, J., and Baldwin, R.L. (1981). DNA flexibility studied by covalent closure of short fragments into circles. Proc. Natl. Acad. Sci. USA. 78(8):4833-4837.

Sikorav, J-L., and Church, G.M. (1991). Complementary recognition in condensed DNA: Accelerated DNA renaturation. J. Mol. Biol. 222(4):1085-1108.

Sikorav, J.L., Pelta, J., and Livolant, F. (1994). A liquid crystalline phase in spermidine-condensed DNA. Biophys. J. 67:1387-1392.

Singleton, M.R., Dillingham, M.S., Gaudier, M., Kowalczykowski, S.C., and Wigley, D.B. (2004). Crystal structure of RecBCD enzyme reveals a machine for processing DNA breaks. Nature. 432:187-193.

Singleton, M.R., and Wigley, D.B. (2002).Modularity and specialization in superfamily 1 and 2 helicases. J. Bacteriol. 184(7):1819-1826.

Smith, B.T., Grossman, A.D., and Walker, G.C. (2002). Localization of UvrA and effect of DNA damage on the chromosome of *Bacillus subtilis*. J. Bacteriol. 184:488-493.

Smith, G.R. (2001). Homologous recombination near and far from DNA breaks: Alternative roles and contrasting views. Annu. Rev. Genet. 35:243-274.

Smith, J.D., Arber, W., and Kuhnlein, U. (1972). Host specificity of DNA produced by *Escherichia coli* XIV. The role of nucleotide methylation in *in vivo* B-specific modification. J. Mol. Biol. 63:1-8.

Sonnenfield, J.M., Burns, C.M., Higgins, C.F., and Hinton, J.C.D. (2001). The nucleoid-associated protein StpA binds curved DNA, has a greater DNA-binding affinity than H-NS and is present in significant levels in *hns* mutants. Biochimie. 83:243-249.

Soslau, G., and Pirollo, K. (1983). Selective inhibition of restriction endonuclease cleavage by DNA intercalators. Biochem. Biophys. Res. Commun. 115(2):484-491.

Soultanas, P., Dillingham, M.S., Wiley, P., Webb, M.R., and Wigley, D.B. (2000). Uncoupling DNA translocation and helicase activity in PcrA: direct evidence for an active mechanism. EMBO J. 19(14):3799-3810.

Soultanas, P., Dillingham, M.S., Papadopoulos, F., Philips, S.E.V., Thomas, C.D., and Wigley, D.B. (1999). Plasmid replication initiator protein RepD increases the processivity of PcrA DNA helicase. Nucleic Acids Res., 27:1421-1428.

Soultanas, P., and Wigley, D.B. (2000). DNA helicases: 'inching forward'. Curr. Opin. Struct. Biol. 10:124-128.

Soultanas, P., and Wigley, D.B. (2001). Unwinding the 'Gordonian knot' of helicase action. Trends Biochem. Sci. 26(1):47-54.

Spies, M., Bianco, P.R., Dillingham, M.S., Handa, N., Baskin, R.J., and Kowalczykowski, S.C. (2003). A molecular throttle: The recombination hotspot χ controls DNA recombination by the Rec BCD helicase. Cell. 114:647-654.

Spurio, R., Durrenberger, M., Falconi, M., La Teana, A., Pon, C.L., and Gualerzi, C.O. (1992). Lethal overproduction of the *Escherichia coli* nucleoid protein H-NS: ultramicroscopic and molecular autopsy. Mol. Gen. Genet. 231:201-211.

Srivenugopal, K.S., Wemmer, D.E., and Morris, D.R. (1987). Aggregation of DNA analogs of spermidine; enzymatic and structural studies. Nucleic Acids Res. 15(6):2563-2580.

Stahl, F.W., Crasemann, J.M., and Stahl, M.M. (1975). Rec-mediated recombinational hotspot activity in bacteriophage λ. III. χ mutations are site-mutations stimulating rec-mediated recombination. J. Mol. Biol. 94:203-212.

Stanford, N.P., Szczelkun, M.D., Marko, J.F., and Halford, S.E. (2000). One- and three-dimensional pathways for proteins to reach specific DNA sites. EMBO J. 19(23):6546-6557.

Studier F.W., and Bandyopadhyay, P.K. (1988). Model for how type I restriction enzymes select cleavage sites in DNA. Proc. Natl. Acad. Sci. USA. 85:4677-4681.

Studier, F.W. and Movva, N.R. (1976). SAMase gene of bacteriophage T3 is responsible for overcoming host restriction. J. Virol. 19:136-145.

Sturrock, S.S., and Dryden, D.T.F. (1997). A prediction of the amino acids and structures involved in DNA recognition by type I DNA restriction and modification enzymes. Nucleic Acids Res. 25(17):3408-3414.

Suri, B., and Bickle, T.A. (1985). EcoA: the first member of a new family of type I restriction modification systems. Gene organization and enzymatic activities. J. Mol. Biol. 186:77-85.

Szczelkun M.D. (2002). Kinetic models of translocation, head-on collision, and DNA cleavage by type I restriction endonucleases. Biochem. 41:2067-2074.

Szczelkun, M.D., Janscak, P., Firman, K., and Halford, S.E. (1997). Selection of non-specific DNA cleavage sites by the type IC restriction endonuclease EcoR124I. J. Mol. Biol. 271:112-123

Tabor, C.W., and Tabor, H. (1976). 1,4-Diaminobutane (putrescine), spermidine, and spermine. Annu. Rev. Biochem. 45:285-306.

Tabor, H., Tabor, C.W., and Irreverre, F. (1973). Quantitative determination of aliphatic diamines and polyamines by an automated liquid chromatography procedure. Anal. Biochem. 55(2):457-467.

Taylor, A.F., and Smith, G.R. (2003). RecBCD enzyme is a DNA helicase with fast and slow motors of opposite polarity. Nature. 423:889-893.

Taylor, I., Patel, J., Firman, K., and Kneale, G. (1992). Purification and biochemical characterisation of the EcoR124 type I modification methylase. Nucleic Acids Res. 20:179-186.

Taylor, I., Watts, D., and Kneale, G.G. (1994). DNA binding induces a major structural transition in a type I methyltransferase. EMBO J. 13:5772-5778.

Thielking, V., Selent, U., Kohler, E., Landgraf, Z., Wolfes, H., Alves, J., and Pingoud, A. (1992). Mg^{2+} confers DNA binding specificity to the EcoRV restriction endonuclease. Biochem. 31:3727-3732.

Thielking, V., Selent, U., Kohler, E., Wolfes, H, Pieper, U., Geiger, R., Urbanke, C., Winkler, F.K., and Pingoud, A. (1991). Site-directed mutagenesis studies with EcoRV restriction endonuclease to identify regions involved in recognition and catalysis. Biochem. 30:6416-6422.

Thomas, T.J. and Thomas, T. (1994). Polyamine-induced Z-DNA conformation in plasmids containing (dA-dC)n(dG-dT)n inserts and increased binding of lupus autoantibodies to the Z-DNA form of the plasmids. Biochem. J. 298:485-491.

Voet, D., and Voet, J.G. (1995). Biochemistry. Second edition, Wiley.

Vovis, G.F., Horiuchi, K., and Zinder, N.D. (1974). Kinetics of methylation of DNA by a restriction endonuclease from *Escherichia coli* B. Proc. Natl. Acad. Sci. USA. 71:3810-3813.

Walkinshaw, M.D., Taylor, P., Sturrock, S.S., Atanasiu, C., Berge, T., Henderson, R.M., Edwardson, J.M., and Dryden, DT. (2002). Structure of Ocr from bacteriophage T7, a protein that mimics B-form DNA. Mol. Cell. 9(1):187-194.

Wang, J.C., and Davidson, N. (1968). Cyclization of phage DNAs. Cold Spring Harb. Symp. Quant. Biol. 33:409-415.

Watson, M.A., Gowers, D.M., and Halford, S.E. (2000). Alternative geometries of DNA looping: An analysis using the SfiI endonuclease. J. Mol. Biol. 298:461-475.

Wenner, J.R., and Bloomfield, V.A. (1999). Crowding effects on EcoRV kinetics and binding. Biophys. J. 77:3234-3241.

Whitehouse, I., Stockdale, C., Flaus, A., Szczelkun, M.D., and Owen-Hughs, T. (2003). Evidence for DNA translocation by the ISWI chromatin-remodelling enzyme. Mol. Cell. Bio. 23(6):1935-1945.

Willcock, D.F., Dryden, D.T.F., and Murray, N.E. (1994). A mutational analysis of the two motifs common to adenine methyltransferases. EMBO J. 13:3902-3908.

Williams, R.M., and Rimsky, S. (1997). Molecular aspects of the *Escherichia coli* nucleoid-associated protein H-NS: A central controller of gene regulatory networks. FEMS Microbiol. Lett. 156:175-185.

Wilson, R.W., and Bloomfield, V.A. (1979). Couterion-induced condensation of deoxyribonucleic acid, A light scattering study. Biochem. 18:2192-2196.

Wilson, W.D. (1990). In Nucleic Acids in Chemistry and Biology. Eds. Blackburn, G. M., and Gait, M. J. Oxford University Press, New York. Pages 295-336.

Wolffe, A. Chromatin. Structure and Function. (1998). Third edition, Academic Press.

Yin, H., Wang, M.D., Svoboda, K., Landick, R, Block, S.M., Gelles, J. (1995). Transcription against an applied force. Science. 270:1653-1657.

Yoshikawa, K. (2001). Controlling the higher-order structure of giant DNA molecules. Adv. Drug Del. Rev. 52:235-244.

Yuan, R., Hamilton, D.L., and Burckhardt, J. (1980). DNA translocation by the restriction enzyme from *E. coli* K. Cell 20:237-244.

Zhang, A., and Belfort, M. (1992). Nucleotide sequence of a newly-identified *Escherichia* gene, *stpA*, encoding and H-NS-like protein. Nucleic Acids Res. 20:6735.

Zimmerman, S.B. (1993). Macromolecular crowding: Biochemical, biophysical, and physiological consequences. Annu. Rev. Biophys. Biomol. Struct. 22:27-65.

Zimmerman, S.B., and Pheiffer, B.H. (1983). Macromolecular crowding allows blunt-end ligation by DNA ligases from rat liver or *Escherichia coli*. Proc. Natl. Acad. Sci. USA. 80(19):5852-5856.

Zimmerman, S.B., and Murphy, L.D. (1996). Macromolecular crowding and the mandatory condensation of DNA in bacteria. FEBS Lett. 390:245-248.

Zimmerman, S.B., and Trach, S.O. (1991). Estimation of macromolecule concentrations and excluded volume effects for the cytoplasm of *Escherichia coli*. J. Mol. Biol. 222(3):599-620.

Appendix A

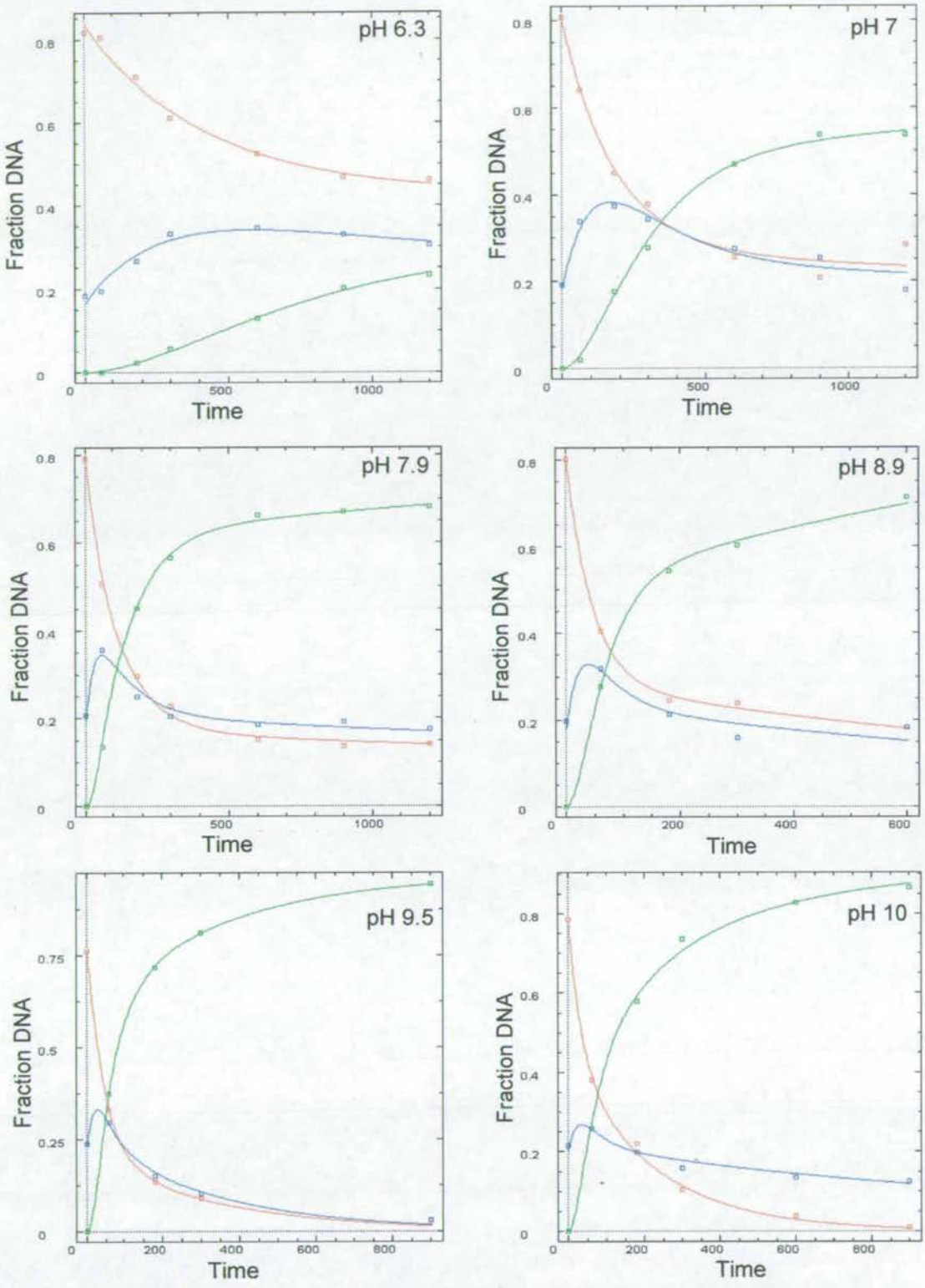

Appendix A.i. Time courses of restriction of supercoiled pBRsk1 by EcoKI at varying pH. Supercoiled DNA (red) is cut into nicked intermediate (blue) and linear product (green) at the different pHs indicated. Each point represents the mean of 2 separate experiments. Curves were fitted using Dynafit, and rate constants calculated and shown in figures 3.24 and 3.25.

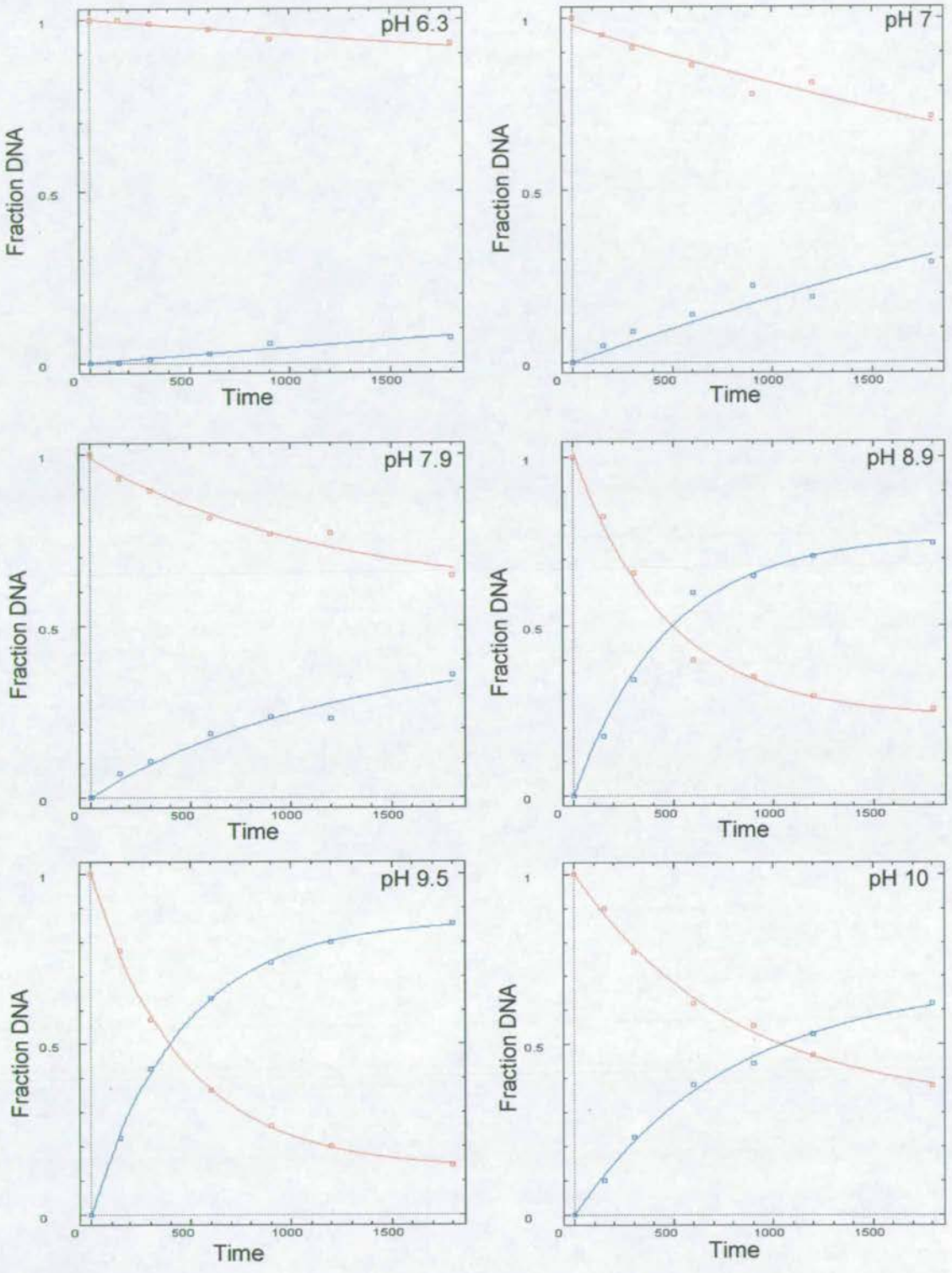

Appendix A.ii. Time courses of restriction of linear pBRsk1 by EcoKI at varying pH. Linear DNA (red) is digested into a smear (blue) at the different pHs indicated. Each point represents the mean of 2 separate experiments. Curves were fitted using Dynafit, and rate constants calculated and shown in figure 3.26.

Appendix B

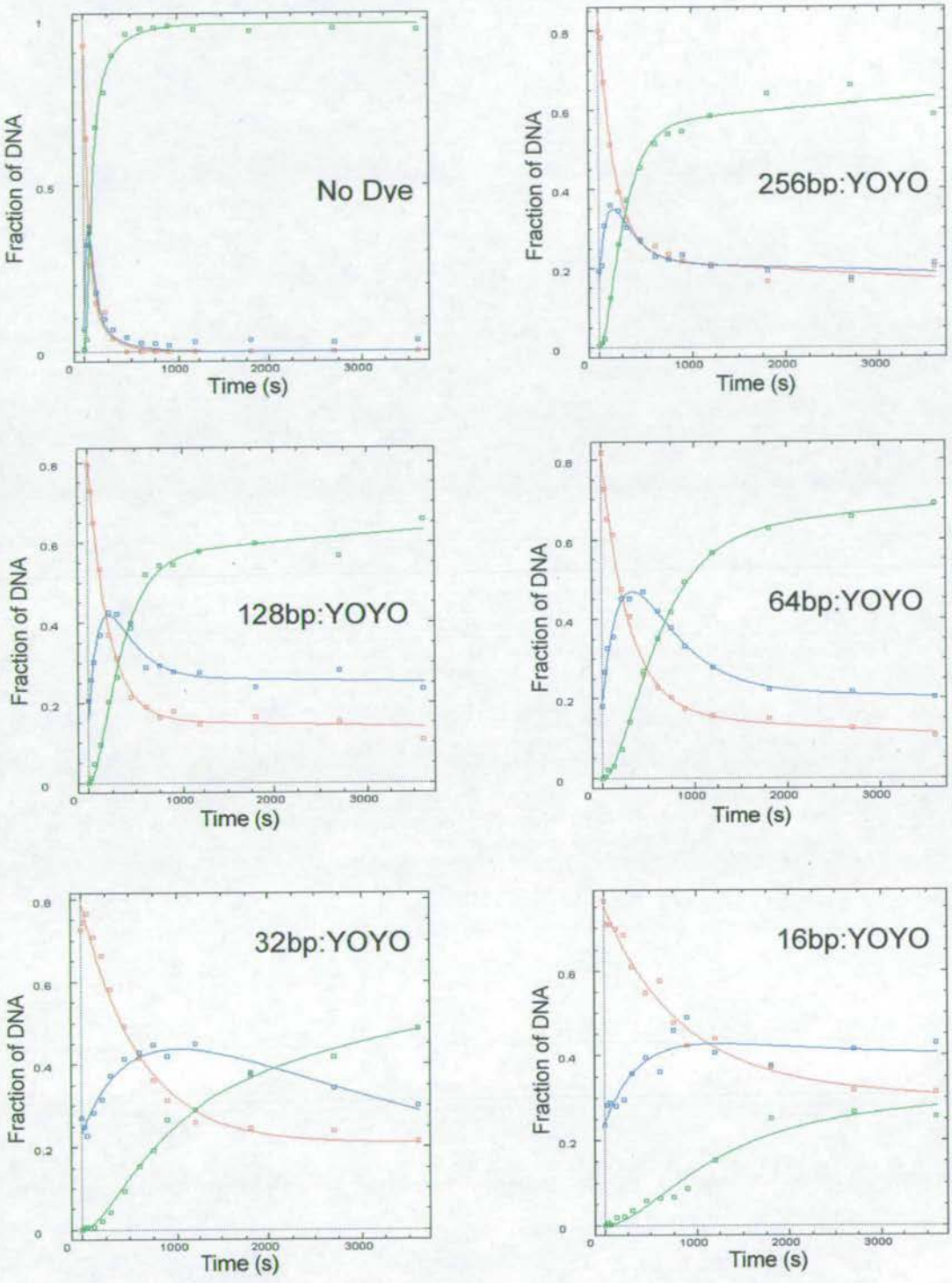

Appendix B.i. Effect of YOYO concentration on restriction of supercoiled pBRsk1 by EcoKI. Supercoiled DNA (red) is cut into nicked intermediate (blue) and linearised product (green) with different concentrations of YOYO as indicated. Points show the mean of 4 separate experiments. Curves were fitted with Dynafit, and rate constants calculated and shown in figure 4.2.

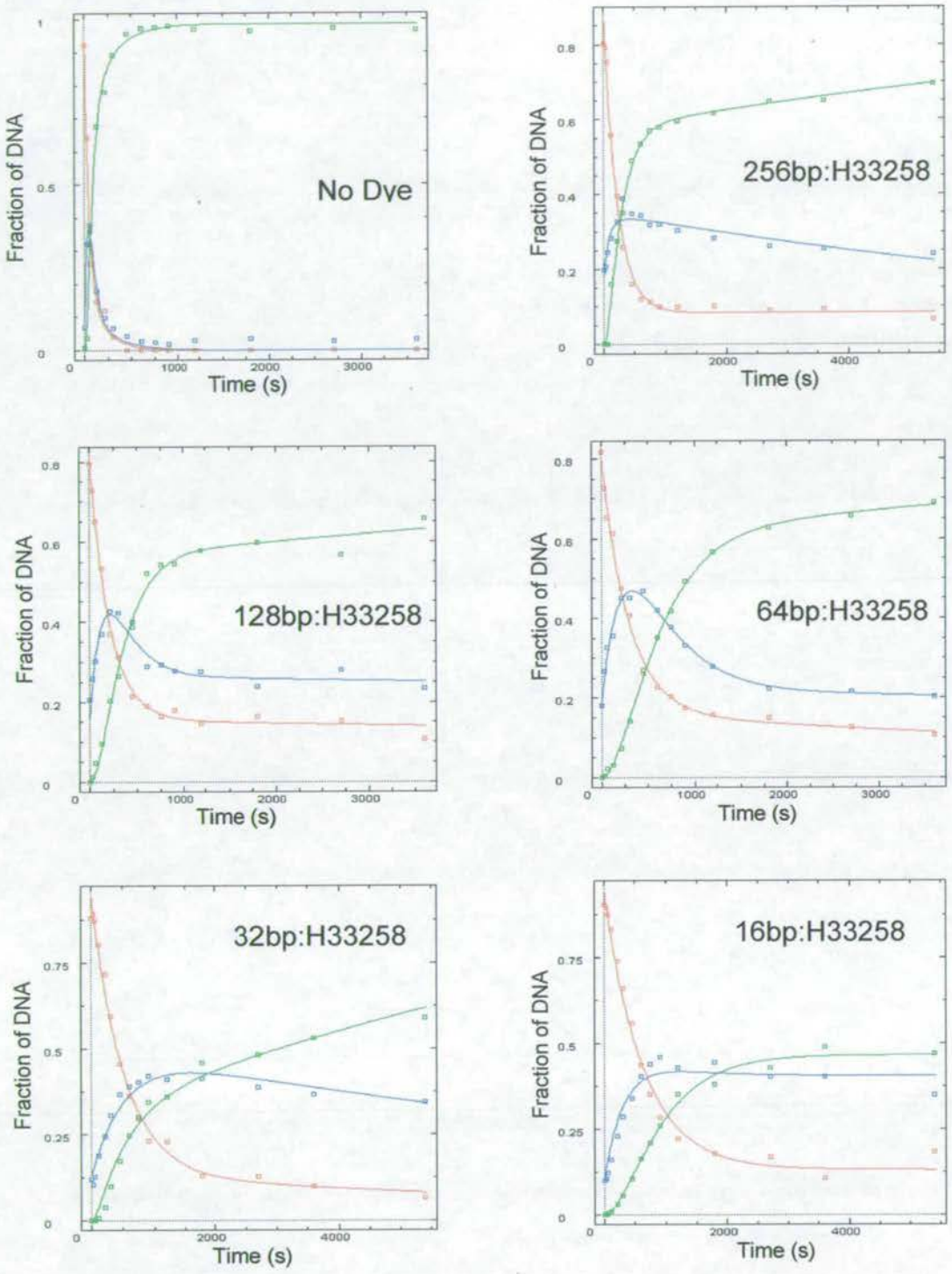

Appendix B.ii. Effect of H33258 concentration on restriction of supercoiled pBRsk1 by EcoKI. Supercoiled DNA (red) is cut into nicked intermediate (blue) and linearised product (green) with different concentrations of H33258 as indicated. Points represent the fraction of DNA restricted in a single experiment. Curves were fitted with Dynafit, and rate constants calculated and shown in figure 4.3.

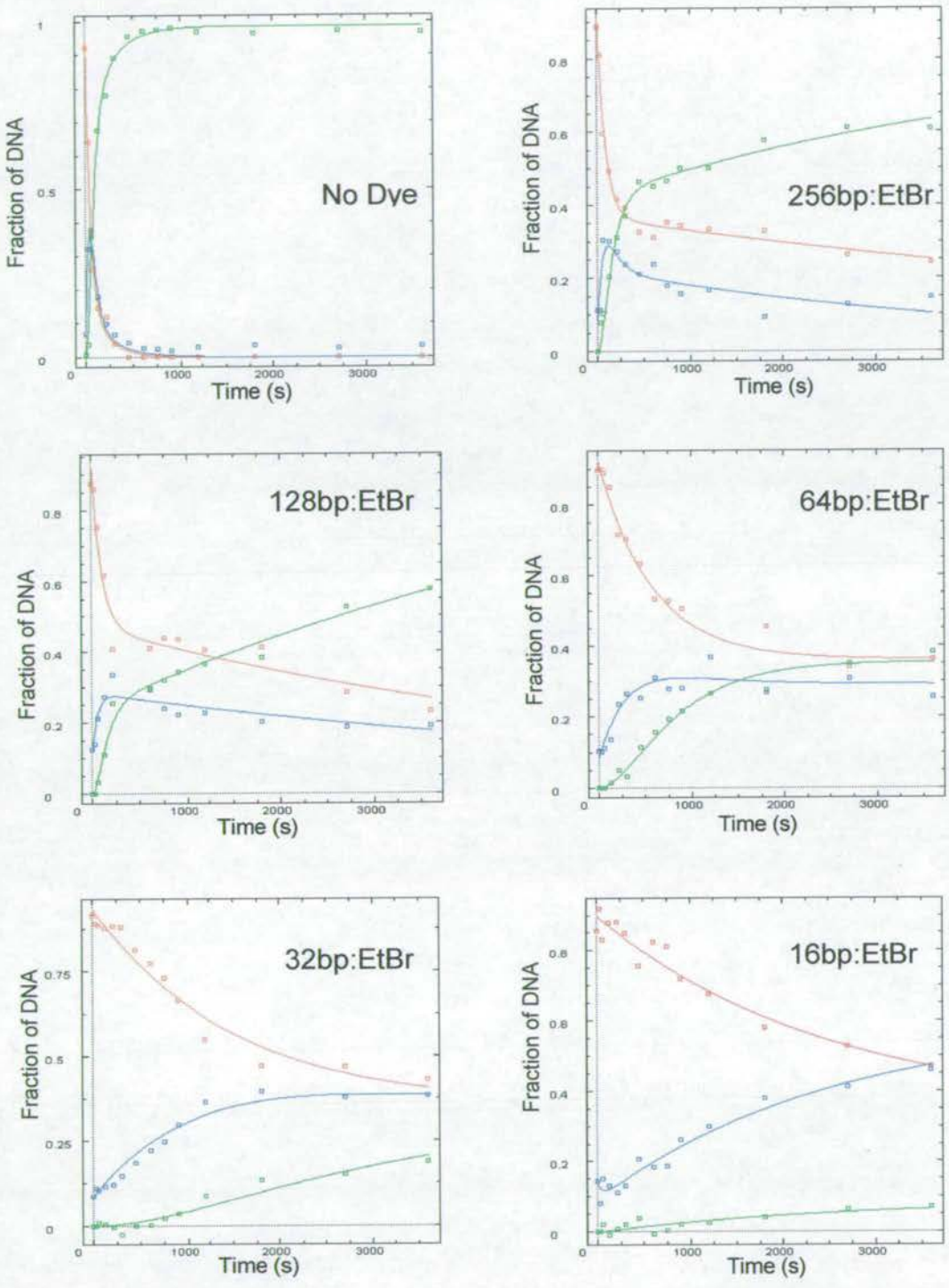

Appendix B.iii. Effect of EtBr concentration on restriction of supercoiled pBRsk1 by EcoKI. Supercoiled DNA (red) is cut into nicked intermediate (blue) and linearised product (green) with different concentrations of EtBr as indicated. Points represent the fraction of DNA restricted in a single experiment. Curves were fitted with Dynafit, and rate constants calculated and shown in figure 4.4.

	128bp:YOYO			64bp:YOYO		
Time (s)	CCC	OC	L	CCC	OC	L
0	0.017118	0.017118	0	0.04297	0.043022	0
30	0.029667	0.030092	0.017363	0.127249	0.121645	0.008028
60	0.012745	0.064172	0.072323	0.117019	0.096155	0.02505
120	0.020275	0.044759	0.027878	0.088327	0.084902	0.007562
210	0.066574	0.031661	0.045295	0.102978	0.118839	0.021516
300	0.022328	0.059264	0.053459	0.109019	0.106228	0.035264
450	0.046026	0.10099	0.115929	0.089201	0.07337	0.076301
600	0.035985	0.087811	0.060615	0.07098	0.048349	0.066603
750	0.05525	0.059194	0.055986	0.066023	0.040372	0.096552
900	0.035278	0.074023	0.047499	0.05091	0.073817	0.113471
1200	0.010101	0.077173	0.076089	0.045545	0.107576	0.143633
1800	0.035502	0.091818	0.056973	0.058396	0.140089	0.178174
2700	0.041886	0.039857	0.002738	0.04581	0.145638	0.189653
3600	0.00645	0.088894	0.091553	0.050878	0.150258	0.199192

	32bp:YOYO			16bp:YOYO		
Time (s)	CCC	OC	L	CCC	OC	L
0	0.158921	0.158921	0	0.099543	0.099543	0
30	0.120404	0.122861	0.011613	0.09609	0.086644	0.009446
60	0.086919	0.088523	0.013498	0.104593	0.102501	0.002092
120	0.089306	0.091072	0.013964	0.115056	0.087636	0.02742
210	0.106622	0.101284	0.041406	0.091742	0.062576	0.029166
300	0.122189	0.109163	0.064171	0.028719	0.019852	0.048572
450	0.066017	0.085097	0.073873	0.063264	0.018402	0.081666
600	0.074373	0.184552	0.121465	0.148675	0.059234	0.089441
750	0.035071	0.129634	0.113857	0.046318	0.045816	0.092134
900	0.040711	0.088786	0.114623	0.039179	0.084244	0.123423
1200	0.041544	0.085963	0.071658	0.080658	0.044378	0.03628
1800	0.028839	0.061656	0.077562	0.005642	0.069322	0.06368
2700	0.037405	0.086546	0.117128	0.071432	0.004296	0.067136
3600	0.070898	0.066256	0.11677	0.076642	0.008269	0.08491

Appendix B iv. Tables indicating standard deviation errors for the fraction of DNA restricted by EcoKI with varying concentrations of YOYO over time, for graphs shown in Appendix B i.

Appendix C

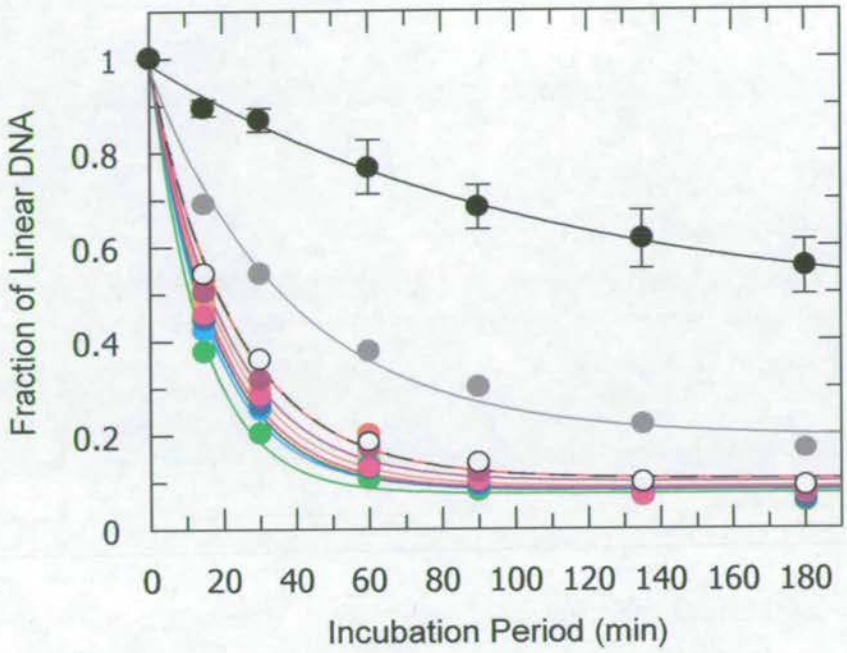

Appendix C.i. Effect of spermidine concentrations on ligation of linear DNA. Graph shows the loss of full length EcoRI-linearised pBR322 as ligase forms ligated products by joining the ends of the same molecule and other molecules together. The ligation rate was measured with spermidine concentrations of 0 (red), 0.25mM (orange), 0.5mM (yellow), 0.75mM (green), 1mM (cyan), 1.25mM (blue), 1.5mM (pink), 1.75mM (purple), 2mM (white), 3mM (grey), and 5mM (black). Points represent the mean of 3 separate experiments. Representative error bars are on data collected with 5mM spermidine. Error bars are not shown on other data for clarity. Rate constants were calculated and are shown in figure 5.2.

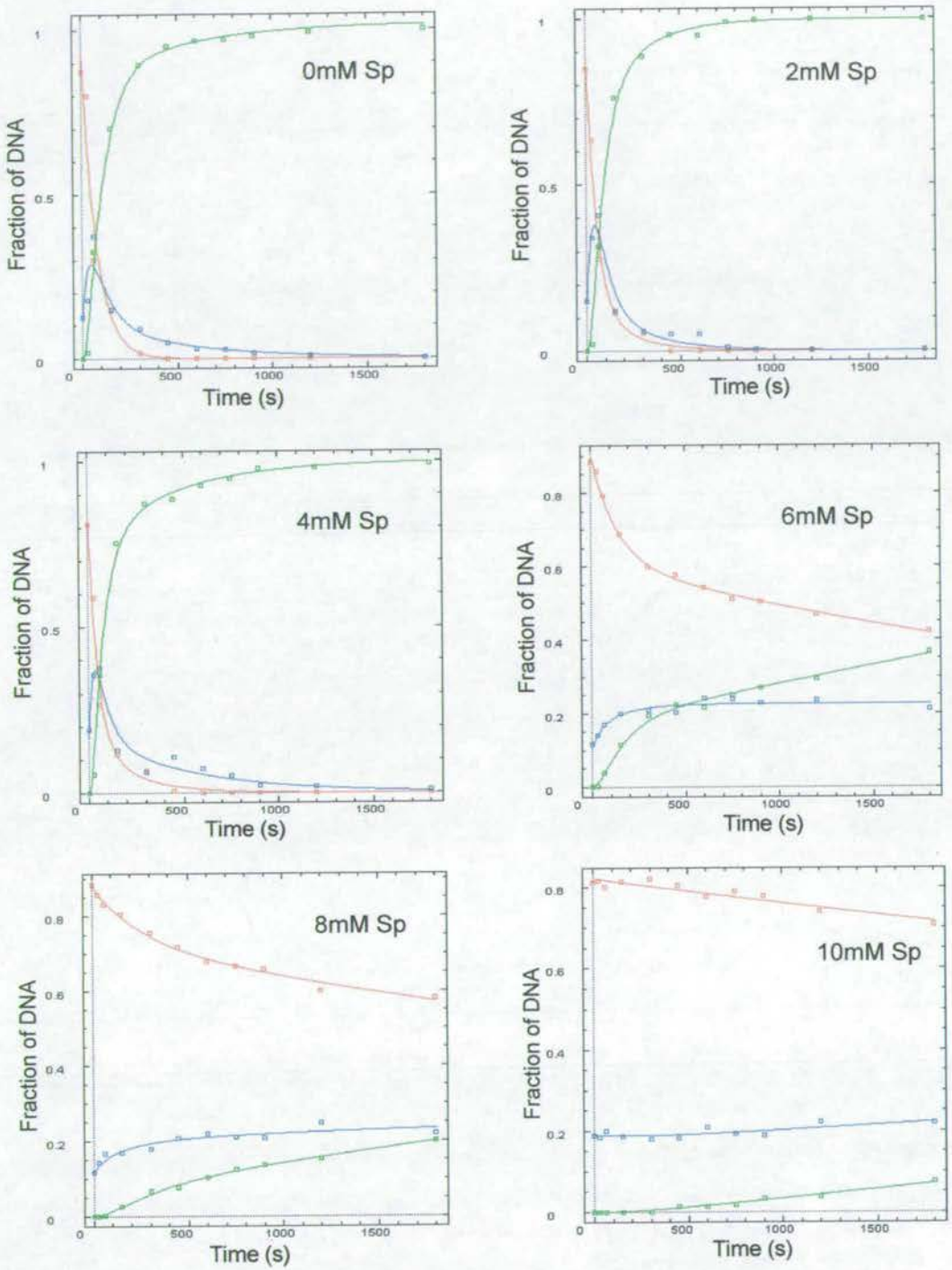

Appendix C.ii. Effect of spermidine concentration on restriction of supercoiled pBRsk1 by EcoKI. Supercoiled DNA (red) is cut into nicked intermediate (blue) and linearised product (green) with different concentrations of spermidine as indicated. Points show the mean of 2 separate experiments.Curves were fitted with Dynafit, and rate constants calculated and shown in figure 5.9C.

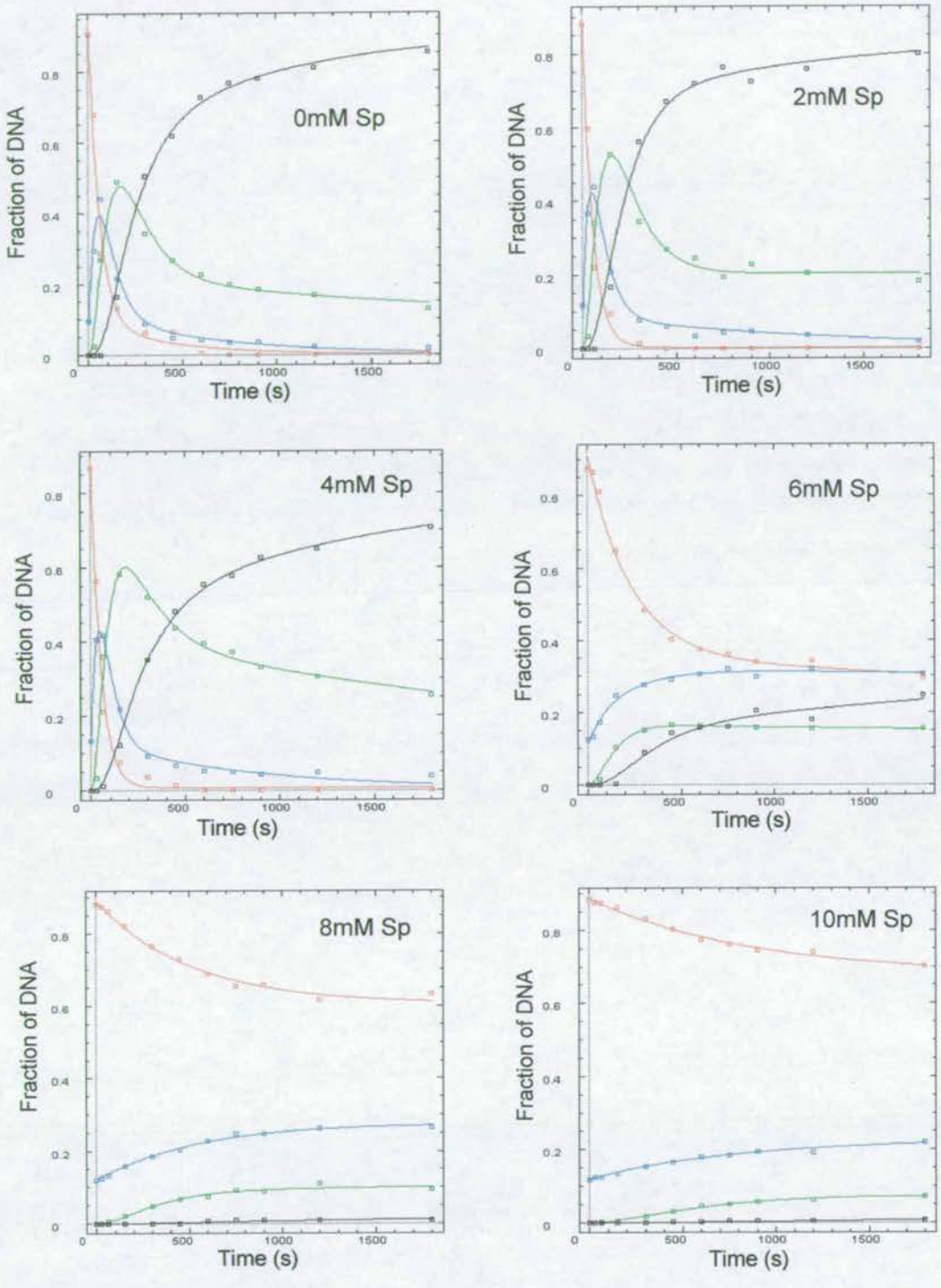

Appendix C.iii. Effect of spermidine concentration on restriction of supercoiled pBR322 by EcoKI. Supercoiled DNA (red) is cut into nicked intermediate (blue) and linear intermediate (green) and finally linear fragments (black) with different concentrations of spermidine as indicated. Points show the mean of 2 separate experiments. Curves were fitted with Dynafit, and rate constants calculated and shown in figure 5.9A.

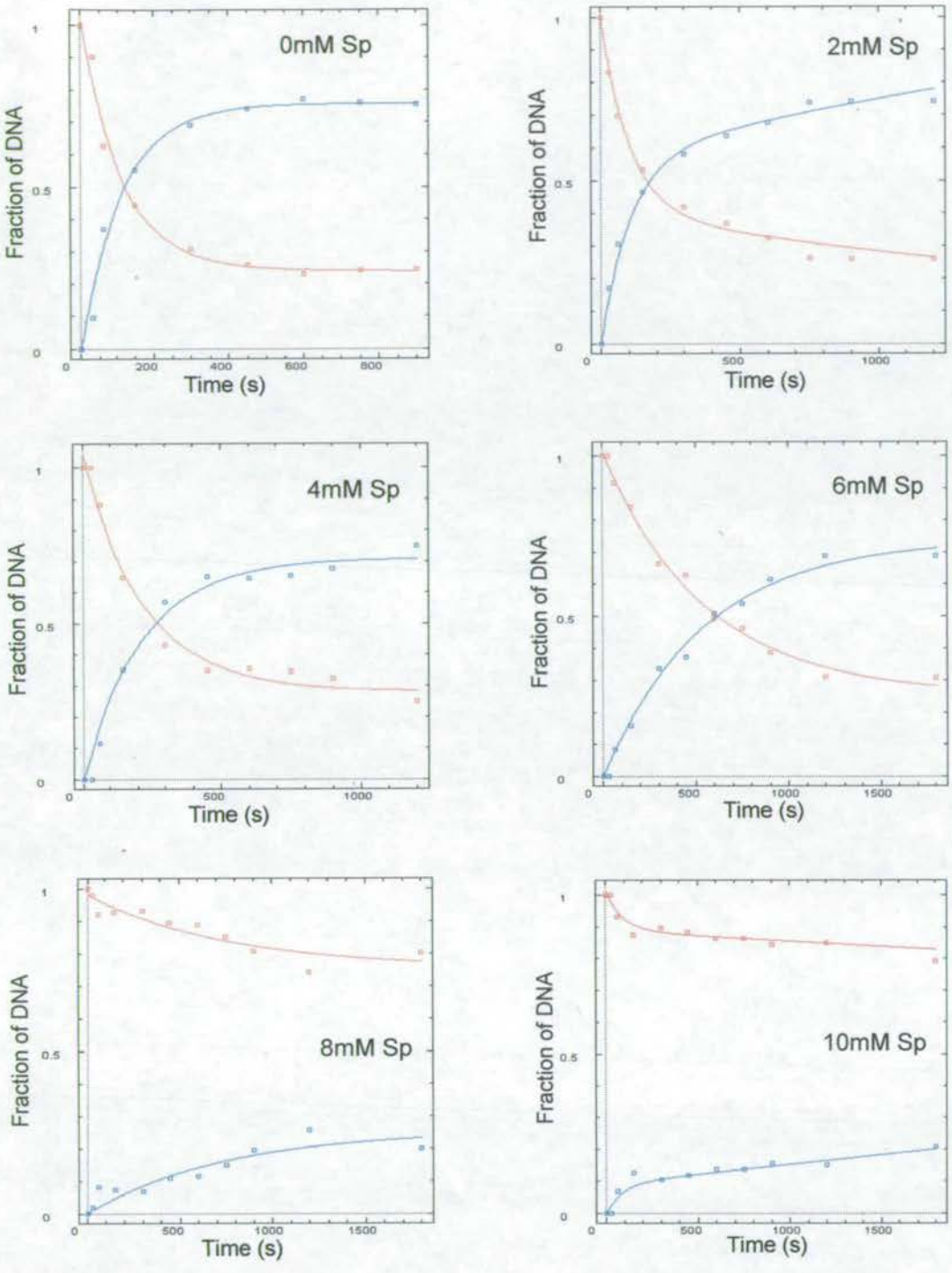

Appendix C.iv. Effect of spermidine concentration on restriction of linear pBR322 by EcoKI. Linear DNA (red) is cut into linear fragments (blue) with different concentrations of spermidine as indicated. Points show the mean of 2 separate experiments. Curves were fitted with Dynafit, and rate constants calculated and shown in figure 5.9B.

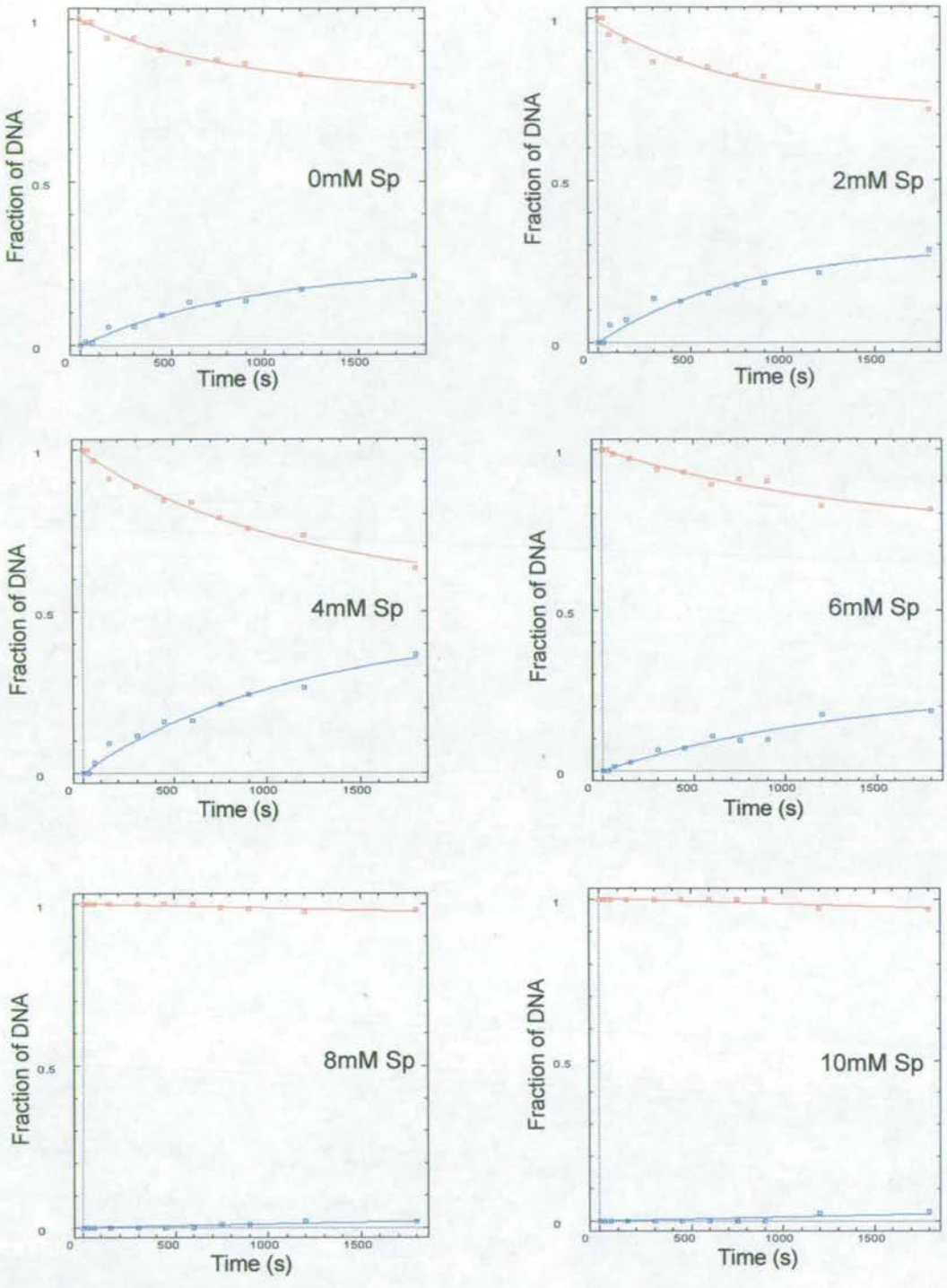

Appendix C.v. Effect of spermidine concentration on restriction of linear pBRsk1 by EcoKI. Linear DNA (red) is digested into a smear (blue) with different concentrations of spermidine as indicated. Points show the mean of 2 separate experiments. Curves were fitted with Dynafit, and rate constants calculated and shown in figure 5.9D.

Supercoiled pBRsk1						
	0mM Spermidine					
Time (s)	CCC (i)	CCC (ii)	OC (i)	OC (ii)	L (i)	L (ii)
0	0.905387	0.843172	0.094613	0.156828	0	0
30	0.785024	0.818459	0.175508	0.181541	0.0394683	0
60	0.232637	0.371671	0.369693	0.376063	0.3976699	0.252266
150	0.087244	0.214538	0.165705	0.12863	0.7470518	0.656832
300	0	0.032347	0.055788	0.123156	0.9442120	0.844497
450	0	0	0.037685	0.06044	0.9623149	0.93956
600	0	0	0.038259	0.023952	0.9617414	0.976048
750	0	0	0.027439	0.029412	0.9725610	0.970588
900	0	0	0.034286	0	0.9657143	1
1200	0	0	0.015238	0	0.9847619	1
1800	0	0	0	0	1	1

Supercoiled pBRsk1						
	2mM Spermidine					
Time (s)	CCC (i)	CCC (ii)	OC (i)	OC (ii)	L (i)	L (ii)
0	0.888442	0.810328	0.111558	0.189672	0	0
30	0.642671	0.629447	0.344608	0.34036	0.0127204	0.030193
60	0.256675	0.299567	0.424757	0.391418	0.3185680	0.309014
150	0.064671	0.166497	0.125722	0.116168	0.8096069	0.717335
300	0	0.107058	0.056558	0.063105	0.9434416	0.829836
450	0	0	0.035049	0.064257	0.9649507	0.935743
600	0	0	0.044944	0.058201	0.9550562	0.941799
750	0	0	0.023653	0	0.9763469	1
900	0	0	0.010624	0	0.9893758	1
1200	0	0	0.005525	0	0.9944751	1
1800	0	0	0.006803	0	0.9931973	1

Supercoiled pBRsk1						
	4mM Spermidine					
Time (s)	CCC (i)	CCC (ii)	OC (i)	OC (ii)	L (i)	L (ii)
0	0.844955	0.774805	0.155045	0.225195	0	0
30	0.612414	0.56589	0.353387	0.354821	0.0341988	0.07929
60	0.262074	0.272066	0.347506	0.408452	0.3904206	0.319482
150	0.089255	0.144818	0.120885	0.135029	0.7898597	0.720153
300	0.024544	0.10745	0.071091	0.051659	0.9043657	0.840891
450	0	0.012904	0.052798	0.159921	0.9472017	0.827175
600	0	0	0.049251	0.096096	0.9507495	0.903904
750	0	0	0.03944	0.065041	0.9605598	0.934959
900	0	0	0.044226	0	0.9557740	1
1200	0	0	0.038108	0	0.9618922	1
1800	0	0	0.015152	0	0.9848485	1

Supercoiled pBRsk1						
	6mM Spermidine					
Time (s)	CCC (i)	CCC (ii)	OC (i)	OC (ii)	L (i)	L (ii)
0	0.884967	0.882743	0.115033	0.117257	0	0
30	0.861287	0.854175	0.138713	0.142061	0	0.003763
60	0.774768	0.812409	0.173364	0.164259	0.0518672	0.023332
150	0.673866	0.700291	0.193724	0.203908	0.1324106	0.095801
300	0.590024	0.606472	0.190156	0.226779	0.2198203	0.166749
450	0.589321	0.561257	0.19391	0.206975	0.2167693	0.231768
600	0.54799	0.537856	0.227296	0.253631	0.2247133	0.208514
750	0.54096	0.48037	0.209057	0.266872	0.2499834	0.252759
900	0.482755	0.525092	0.21519	0.239902	0.3020552	0.235006
1200	0.504337	0.434292	0.208644	0.264116	0.2870185	0.301592
1800	0.456107	0.388168	0.229078	0.191736	0.3148151	0.420096

Supercoiled pBRsk1						
	8mM Spermidine					
Time (s)	CCC (i)	CCC (ii)	OC (i)	OC (ii)	L (i)	L (ii)
0	0.906376	0.861114	0.093624	0.138886	0	0
30	0.877215	0.838727	0.122785	0.161273	0	0
60	0.845078	0.815989	0.154922	0.177953	0	0.006058
150	0.806792	0.802192	0.162633	0.174011	0.0305751	0.023796
300	0.741407	0.764642	0.173462	0.185625	0.0851309	0.049733
450	0.702211	0.728752	0.215618	0.200207	0.0821714	0.071041
600	0.6798	0.675883	0.221242	0.216078	0.0989581	0.108039
750	0.684897	0.647104	0.208731	0.212845	0.1063723	0.14005
900	0.672665	0.642114	0.187141	0.226889	0.1401947	0.130997
1200	0.607963	0.590164	0.238073	0.259563	0.1539635	0.150273
1800	0.603202	0.556779	0.215165	0.223943	0.1816327	0.219278

Supercoiled pBRsk1						
	10mM Spermidine					
Time (s)	CCC (i)	CCC (ii)	OC (i)	OC (ii)	L (i)	L (ii)
0	0.790356	0.831404	0.209644	0.168596	0	0
30	0.810442	0.819752	0.189558	0.180248	0	0
60	0.806202	0.794121	0.193798	0.205879	0	0
150	0.825918	0.801478	0.174082	0.198522	0	0
300	0.824595	0.815848	0.175405	0.184152	0	0
450	0.813226	0.797581	0.178769	0.18283	0.0080046	0.019589
600	0.777269	0.777344	0.208569	0.209559	0.0141621	0.013097
750	0.767383	0.810573	0.211034	0.174855	0.0215830	0.014571
900	0.77553	0.783555	0.19146	0.184615	0.0330103	0.03183
1200	0.730292	0.751847	0.220904	0.220374	0.0488043	0.027778
1800	0.700599	0.712276	0.231045	0.207021	0.0683564	0.080703

Appendix C.vi. Tables showing individual measurements of fractional DNA level produced by EcoKI restriction of supercoiled pBRsk1 with varying concentrations of spermidine. Supercoiled (CCC), nicked (OC) and linear (L) DNA levels are shown for each experiment ((i) and (ii)) with the mean values depicted graphically in Appendix C.ii.

Supercoiled pBR322								
	6mM Spermidine							
Time (s)	CCC (i)	CCC (ii)	OC (i)	OC (ii)	L (i)	L (ii)	lf (i)	lf (ii)
0	0.86463	0.88314	0.13537	0.11686	0	0	0	0
30	0.86160	0.87129	0.13840	0.12871	0	0	0	0
60	0.81025	0.81178	0.17729	0.16953	0.01246	0.01869	0	0
150	0.63557	0.66072	0.25207	0.23944	0.11236	0.09487	0	0.00497
300	0.44597	0.51878	0.25881	0.29511	0.15927	0.14289	0.13596	0.04321
450	0.39165	0.41060	0.28472	0.29795	0.17725	0.15147	0.14637	0.13998
600	0.35548	0.39121	0.28391	0.32745	0.17404	0.15047	0.18657	0.13087
750	0.32848	0.39252	0.29143	0.34775	0.16008	0.16089	0.22001	0.09884
900	0.29253	0.38817	0.26947	0.32774	0.16390	0.14909	0.27410	0.13499
1200	0.28676	0.40068	0.29289	0.34887	0.15686	0.15203	0.26348	0.09842
1800	0.25517	0.33346	0.29217	0.31902	0.15912	0.14986	0.29354	0.19766

Supercoiled pBR322								
	8mM Spermidine							
Time (s)	CCC (i)	CCC (ii)	OC (i)	OC (ii)	L (i)	L (ii)	lf (i)	lf (ii)
0	0.87457	0.88619	0.12543	0.11381	0	0	0	0
30	0.86860	0.88029	0.13140	0.11971	0	0	0	0
60	0.85668	0.86712	0.13631	0.12773	0.00701	0.00515	0	0
150	0.81811	0.82244	0.15878	0.15615	0.02311	0.02141	0	0
300	0.76011	0.77188	0.19249	0.17888	0.04739	0.04923	0	0
450	0.72957	0.73107	0.20426	0.20315	0.06617	0.06577	0	0
600	0.68621	0.69014	0.23163	0.22627	0.08217	0.06806	0	0.01552
750	0.66688	0.64370	0.25266	0.23972	0.08046	0.09955	0	0.01703
900	0.66192	0.65332	0.25867	0.23363	0.07942	0.09660	0	0.01644
1200	0.63077	0.60541	0.26427	0.26096	0.10495	0.11568	0	0.01794
1800	0.63838	0.62726	0.26195	0.26694	0.09967	0.08794	0	0.01786

Supercoiled pBR322								
	10mM Spermidine							
Time (s)	CCC (i)	CCC (ii)	OC (i)	OC (ii)	L (i)	L (ii)	lf (i)	lf (ii)
0	0.88135	0.88417	0.11865	0.11583	0	0	0	0
30	0.87431	0.87776	0.12569	0.12224	0	0	0	0
60	0.87373	0.87268	0.12325	0.12732	0.00302	0	0	0
150	0.86353	0.85941	0.12729	0.14059	0.00918	0	0	0
300	0.83061	0.82899	0.14719	0.15954	0.02220	0.01147	0	0
450	0.80091	0.80348	0.16837	0.16268	0.03072	0.02948	0	0.00437
600	0.76754	0.77840	0.17732	0.17996	0.05514	0.03619	0	0.00545
750	0.75249	0.77036	0.18660	0.17972	0.06092	0.04105	0	0.00887
900	0.73653	0.75316	0.18970	0.19784	0.07377	0.03872	0	0.01028
1200	0.72299	0.75859	0.19997	0.18241	0.07704	0.04816	0	0.01084
1800	0.68324	0.71849	0.22834	0.21360	0.08842	0.05630	0	0.01161

Appendix C.vii. Tables showing individual measurements of fractional DNA level produced by EcoKI restriction of supercoiled pBR322 with varying concentrations of spermidine. Levels of supercoiled (CCC), nicked (OC), linear (L) and linear fragments (lf) of DNA are shown for each experiment ((i) and (ii)) with the mean values depicted graphically in Appendix C.iii.

Linear pBR322								
	0mM Spermidine				2mM Spermidine			
Time (s)	L (i)	L (ii)	lf (i)	lf (ii)	L (i)	L (ii)	lf (i)	lf (ii)
0	1	1	0	0	1	1	0	0
30	0.80783	1	0.19216	0	0.71109	0.94849	0.28891 233	0.05151
60	0.49739	0.76258	0.50261	0.23741	0.53963	0.85205	0.46037	0.14795
150	0.30176	0.58853	0.69823	0.41146	0.41431	0.65699	0.58569	0.34300
300	0.16394	0.45055	0.83605	0.54945	0.26125	0.57799	0.73875	0.42201
450	0.1219	0.39632	0.87809	0.60368	0.18093	0.55151	0.81907	0.44849
600	0.11319	0.34657	0.88680	0.65342	0.16657	0.48110	0.83343	0.51889
750	0.10234	0.37855	0.89766	0.62145	0.17363	0.35054	0.82636	0.64945
900	0.10163	0.38685	0.89837	0.61315	0.16177	0.35629	0.83822	0.64371
1200					0.15355	0.36572	0.84645	0.63428

Linear pBR322								
	4mM Spermidine				6mM Spermidine			
Time (s)	L (i)	L (ii)	lf (i)	lf (ii)	L (i)	L (ii)	lf (i)	lf (ii)
0	1	1	0	0	1	1	0	0
30	1	1	0	0	1	1	0	0
60	0.76665	1	0.23336	0	0.84250	0.98650	0.15749	0.01349
150	0.63612	0.65883	0.36388	0.34117	0.71284	0.96978	0.28715	0.03021
300	0.42793	0.43593	0.57206	0.56407	0.46073	0.8656	0.53926	0.13440
450	0.34067	0.35918	0.65932	0.64081	0.45754	0.80033	0.54245	0.19967
600	0.33029	0.37812	0.66971	0.62188	0.32101	0.66389	0.67898	0.33610
750	0.30507	0.38855	0.69493	0.61144	0.26689	0.65547	0.73310	0.34452
900	0.23370	0.41293	0.76629	0.58706	0.25831	0.50968	0.74168	0.49031
1200	0.16523	0.33429	0.83476	0.66571	0.18978	0.43137	0.81021	0.56862
1800					0.14607	0.47398	0.85393	0.52601

Linear pBR322								
	8mM Spermidine				10mM Spermidine			
Time (s)	L (i)	L (ii)	lf (i)	lf (ii)	L (i)	L (ii)	lf (i)	lf (ii)
0	1	1	0	0	1	1	0	0
30	1	0.96169	0	0.03830	1	1	0	0
60	0.89647	0.94400	0.10352	0.05599	0.86607	1	0.13392	0
150	0.94206	0.91286	0.05793	0.08713	0.84934	0.89922	0.15065	0.10077
300	0.90418	0.96189	0.09581	0.03810	0.81075	0.98007	0.18924	0.01992
450	0.93153	0.85428	0.06846	0.14571	0.86294	0.90228	0.13705	0.09771
600	0.93609	0.84012	0.06390	0.15987	0.84205	0.88335	0.15794	0.11664
750	0.87240	0.82942	0.12759	0.17057	0.80984	0.91574	0.19015	0.08425
900	0.91454	0.69846	0.08545	0.30153	0.82671	0.86127	0.17328	0.13872
1200	0.86461	0.62106	0.13538	0.37893	0.82289	0.87548	0.17710	0.12451
1800	0.96088	0.64082	0.03911	0.35917	0.87288	0.71300	0.12711	0.28699

Appendix C.viii. Tables showing individual measurements of fractional DNA level produced by EcoKI restriction of linear pBR322 with varying concentrations of spermidine. Levels of linear (L) and linear fragments (lf) of DNA are shown for each experiment ((i) and (ii)) with the mean values depicted graphically in Appendix C.iv.

Linear pBRsk1								
	0mM Spermidine				2mM Spermidine			
Time (s)	L (i)	L (ii)	Smear (i)	Smear (ii)	L (i)	L (ii)	Smear (i)	Smear (ii)
0	1	1	0	0	1	1	0	0
30	1	0.97727	0	0.02272	1	1	0	0
60	1	0.98305	0	0.01694	0.96314	0.93036	0.03685	0.06963
150	0.93655	0.94926	0.06344	0.05074	0.92066	0.93839	0.07933	0.06160
300	0.95414	0.93181	0.04585	0.06818	0.87326	0.85765	0.12673	0.14234
450	0.95825	0.85918	0.04174	0.14081	0.89234	0.85248	0.10766	0.14751
600	0.89464	0.84172	0.10536	0.15827	0.87861	0.81884	0.12138	0.18115
750	0.90942	0.84234	0.09057	0.15765	0.83935	0.80617	0.16065	0.19382
900	0.89199	0.83710	0.10800	0.16289	0.86758	0.76761	0.13241	0.23238
1200	0.88732	0.77305	0.11267	0.22695	0.8223	0.75094	0.1777	0.24905
1800	0.85122	0.73053	0.14878	0.26946	0.77288	0.65869	0.22711	0.34130

Linear pBRsk1								
	4mM Spermidine				6mM Spermidine			
Time (s)	L (i)	L (ii)	Smear (i)	Smear (ii)	L (i)	L (ii)	Smear (i)	Smear (ii)
0	1	1	0	0	1	1	0	0
30	1	1	0	0	1	1	0	0
60	0.96459	0.96894	0.03540	0.03105	1	0.97393	0	0.02606
150	0.90723	0.91107	0.09276	0.08892	0.96531	0.98169	0.03468	0.01830
300	0.88293	0.88619	0.11706	0.11380	0.90211	0.96945	0.09788	0.03055
450	0.82142	0.86153	0.17857	0.13846	0.90816	0.95249	0.09183	0.04750
600	0.81898	0.85533	0.18101	0.14467	0.84708	0.93468	0.15291	0.06531
750	0.78616	0.78921	0.21383	0.21078	0.92817	0.88503	0.07182	0.11496
900	0.75288	0.76178	0.24712	0.23822	0.90304	0.90315	0.09695	0.09684
1200	0.72479	0.74430	0.27520	0.25569	0.74463	0.90488	0.25537	0.09511
1800	0.66199	0.60241	0.33801	0.39759	0.75401	0.87193	0.24598	0.12806

Linear pBRsk1								
	8mM Spermidine				10mM Spermidine			
Time (s)	L (i)	L (ii)	Smear (i)	Smear (ii)	L (i)	L (ii)	Smear (i)	Smear (ii)
0	1	1	0	0	1	1	0	0
30	1	1	0	0	1	1	0	0
60	1	1	0	0	1	1	0	0
150	1	1	0	0	1	1	0	0
300	1	1	0	0	1	1	0	0
450	1	1	0	0	1	1	0	0
600	1	1	0	0	1	1	0	0
750	0.97838	1	0.02161	0	1	1	0	0
900	0.97684	1	0.02315	0	1	1	0	0
1200	0.95537	1	0.04462	0	0.94919	1	0.05080	0
1800	0.96511	1	0.03488	0	0.93945	1	0.06054	0

Appendix C.ix. Tables showing individual measurements of fractional DNA level produced by EcoKI restriction of linear pBRsk1 with varying concentrations of spermidine. Levels of linear (L) and restricted (Smear) of DNA are shown for each experiment ((i) and (ii)) with the mean values depicted graphically in Appendix C.v.

Appendix D

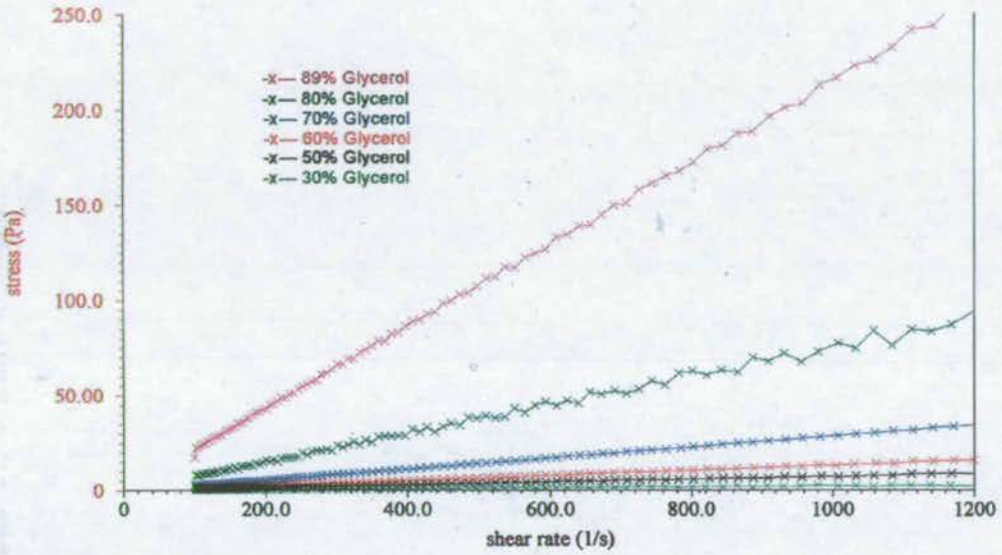

Appendix D.i. Viscosity of various concentrations of glycerol. Graph showing rheology data of measured stress as shear rate is varied. From this data it is possible to calculate the viscosities of the solutions, as shown if figure 7.1.

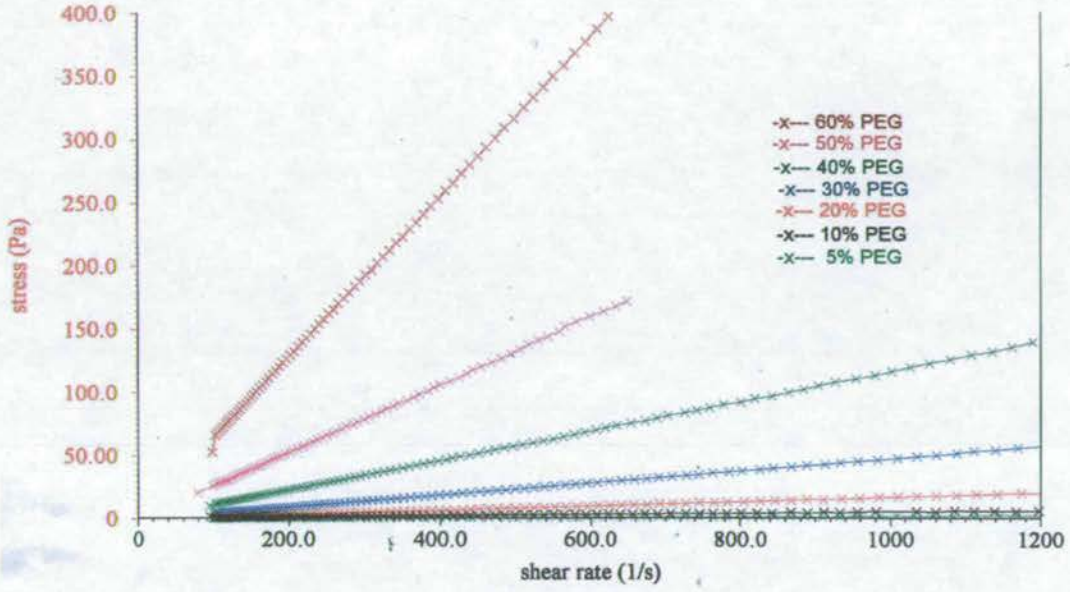

Appendix D.ii. Viscosity of various concentrations of PEG 8000. Graph showing rheology data of measured stress as shear rate is varied. From this data it is possible to calculate the viscosities of the solutions, as shown in figure 7.1.

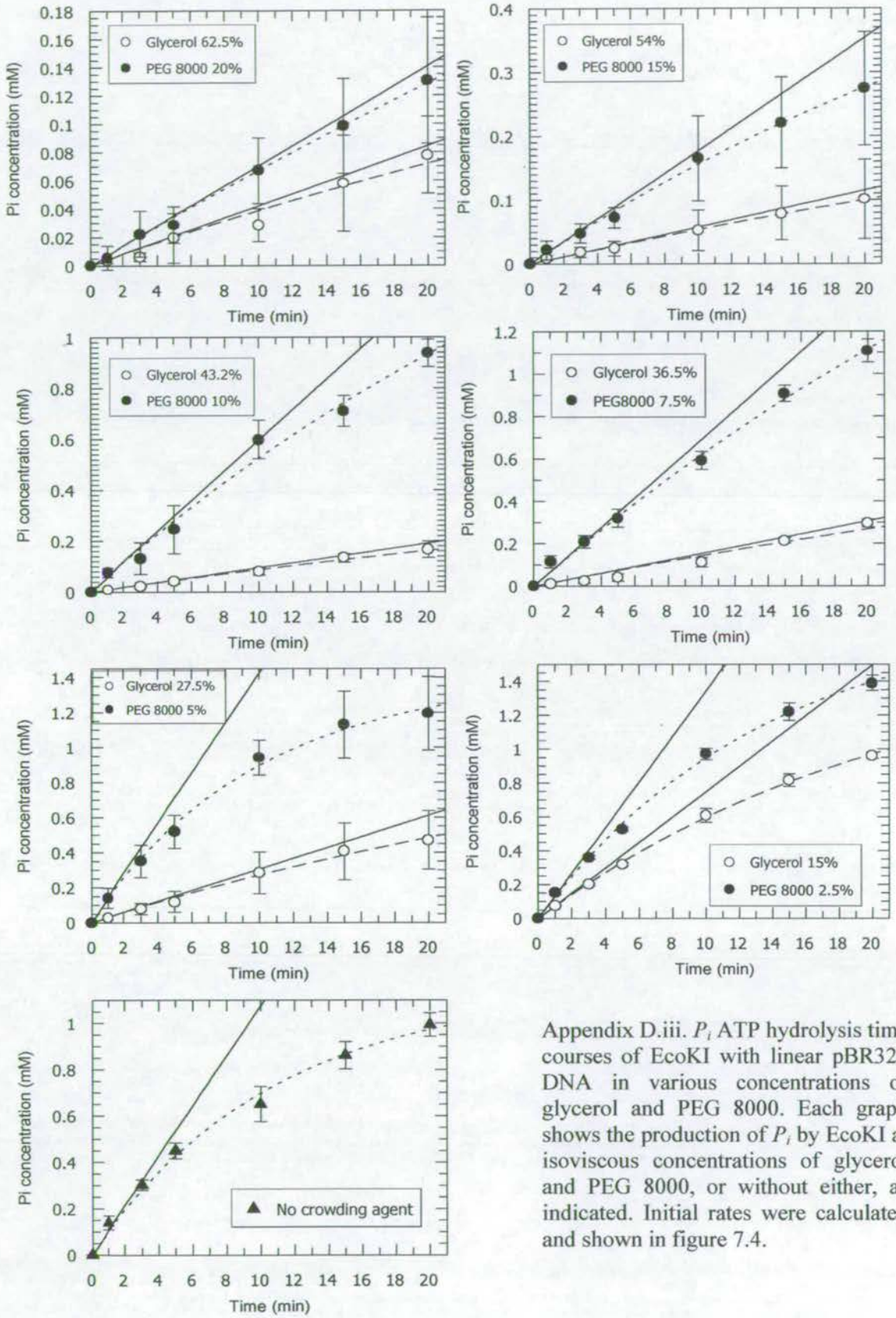

Appendix D.iii. P_i ATP hydrolysis time courses of EcoKI with linear pBR322 DNA in various concentrations of glycerol and PEG 8000. Each graph shows the production of P_i by EcoKI at isoviscous concentrations of glycerol and PEG 8000, or without either, as indicated. Initial rates were calculated and shown in figure 7.4.

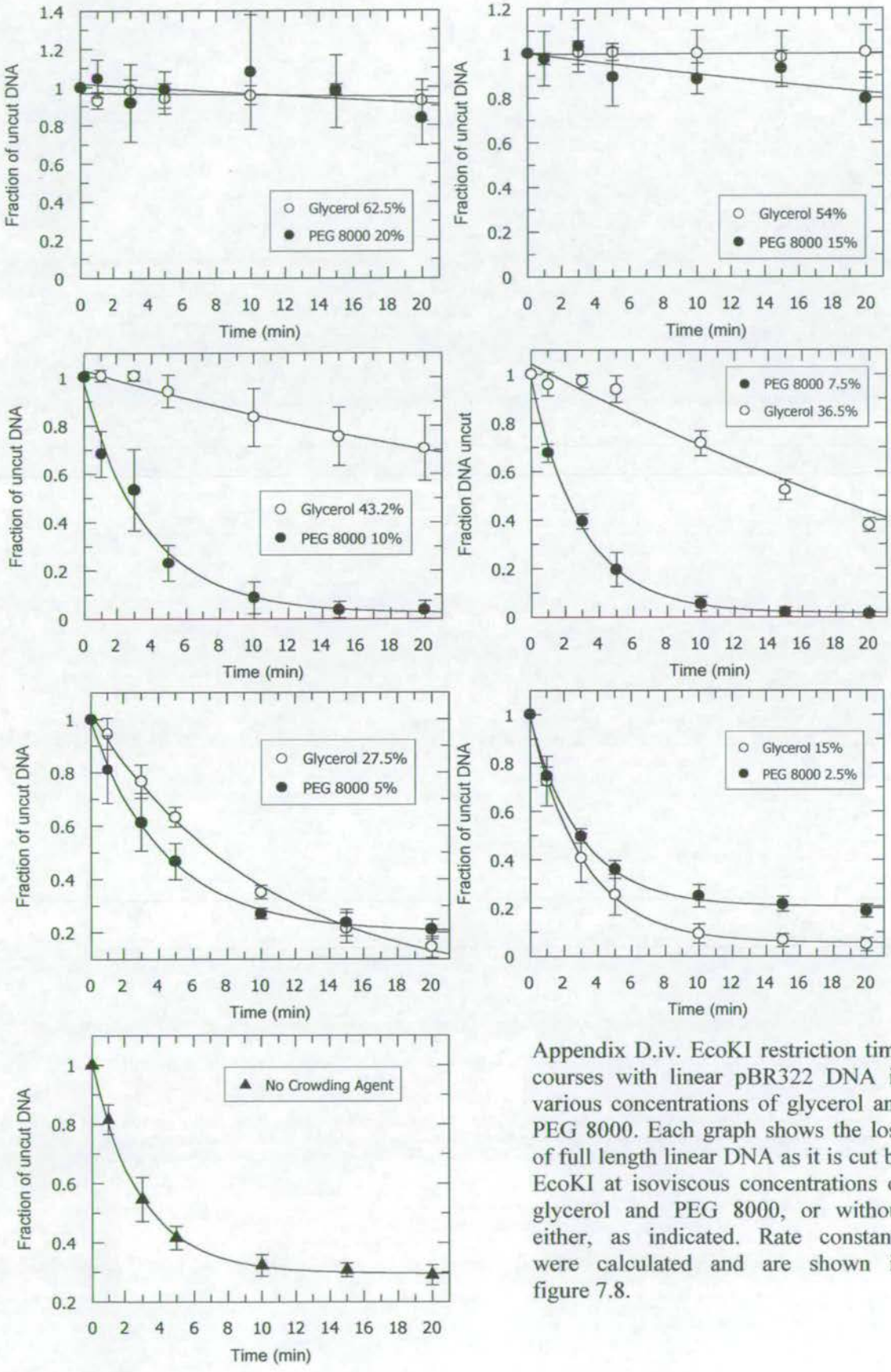

Appendix D.iv. EcoKI restriction time courses with linear pBR322 DNA in various concentrations of glycerol and PEG 8000. Each graph shows the loss of full length linear DNA as it is cut by EcoKI at isoviscous concentrations of glycerol and PEG 8000, or without either, as indicated. Rate constants were calculated and are shown in figure 7.8.

Appendix E

A secspBR322ccc4mMSp

Time , (s)	CCC
0	0.867091562
30	0.562012584
60	0.211672872
150	0.076425736
300	0.03542993
450	0.014892654
600	0
750	0
900	0
1200	0
1800	0

B secspBR322oc4mMSp

Time , (s)	OC
0	0.132908438
30	0.404640044
60	0.417089304
150	0.219540646
300	0.093465188
450	0.06747415
600	0.051588836
750	0.049175906
900	0.043822808
1200	0.046423189
1800	0.03811518

C secspBR322l4mMSp

Time , (s)	L
0	0
30	0.033347372
60	0.359260378
150	0.583194152
300	0.519425579
450	0.436130379
600	0.395600879
750	0.372606217
900	0.331901281
1200	0.305027792
1800	0.256356756

D secspBR322lf4mMSp

Time , (s)	LF
0	0
30	0
60	0.011977446
150	0.120839465
300	0.351679303
450	0.481502818
600	0.552810285
750	0.578217877
900	0.624275912
1200	0.64854902
1800	0.705528064

Appendix E.i. Data for EcoKI restriction of supercoiled pBR322 in EcoKI low salt buffer, pH7.9, with 4mM spermidine at a total ionic strength of 100mM. The fraction of DNA occuring as supercoiled (CCC), nicked (OC), linear (L) and linear fragments (LF) are shown for restriction timecourses A-D respectively. Data represents the mean of 2 separate experiments. This data was fitted to curves using Dynafit and tasks scripted in Appendix E.ii. The appropriate file names for these functions are given above the data. The original files were in notepad.

Task File for fitting data from Appendix E.i to reaction mechanisms using Dynafit:

```
[task]

  data = progress
  task = fit
  model = steven4 ?

[mechanism]

  CCC --> OC      : K1
  OC --> L        : K2
  OC --> OC*      : K5
  CCC --> CCC*    : K4
  L --> LF        : K3
  L --> L*        : K6

[constants]

 K1 = 0.0154666667 ? , K2 = 0.02 ? , K5=0.00000002 ? , K4=0.0026? , K3 = 0.046
? , K6 = 0.0001 ?

[concentrations]

  CCC =46 ?; nM
  OC*=10.55  ?; nM
  CCC*=4.7  ?; nM
  L*= 0  ; nM

[progress]

  variable  time

  file
c:/Ausers/SAKeatch/DYNAFIT/dynafitdata/spermidine/secspBR322ccc4mMSp.txt
  response CCC  = 0.0196 ?
  response CCC* = 0.00405?

  file
c:/Ausers/SAKeatch/DYNAFIT/dynafitdata/spermidine/secspBR322oc4mMSp.txt
  response OC  = 0.0234 ?
  response OC* = 0.004 ?

  file
c:/Ausers/SAKeatch/DYNAFIT/dynafitdata/spermidine/secspBR322l4mMSp.txt
  response L  = 0.0167 ?
  response L* = 0.0233 ?
```

```
file
c:/Ausers/SAKeatch/DYNAFIT/dynafitdata/spermidine/secspBR322lf4mMSp.txt
  response LF = 0.0195 ?

[output]
  directory ./examples/nuclease/output

; ********************************************

[task]

  data = progress
  task = fit
  model = steven6 ?

[mechanism]

  CCC --> OC     : K1
  OC --> L       : K2
  L --> LF    : K3

[constants]

  K1 = 0.0154666667 ? ,  K2 = 0.02 ? ,  K3 = 0.0046 ?

[concentrations]

  CCC =46 ?; nM

[progress]

  variable  time

  file
c:/Ausers/SAKeatch/DYNAFIT/dynafitdata/spermidine/secspBR322ccc4mMSp.txt
  response CCC  = 0.0196 ?

  file
c:/Ausers/SAKeatch/DYNAFIT/dynafitdata/spermidine/secspBR322oc4mMSp.txt
  response OC  = 0.0234 ?

  file
c:/Ausers/SAKeatch/DYNAFIT/dynafitdata/spermidine/secspBR322l4mMSp.txt
  response L  = 0.0167 ?

file
c:/Ausers/SAKeatch/DYNAFIT/dynafitdata/spermidine/secspBR322lf4mMSp.txt
```

```
  response LF = 0.0195 ?

[output]
  directory ./examples/nuclease/output

; ********************************************

[task]

  data = progress
  task = fit
  model = steven5 ?

[mechanism]

  CCC --> OC        : K1
  OC --> L          : K2
  OC <--> OC*       : K5 K8
  CCC <--> CCC*     : K4 K7
  L --> LF          : K3
  L <--> L*         : K6 K9

[constants]

  K1 = 0.0154666667 ? ,  K2 = 0.02 ? ,  K5=0.00000002 ? , K4=0.0026? , K3 =
0.046 ? , K6 = 0.0001 ? , K7 = 0.0001 ? , K8 = 0.0001 ? , K9 = 0.0001 ?

[concentrations]

  CCC =46 ?; nM
  OC*=10.55  ?; nM
  CCC*=4.7  ?; nM
  L*= 0  ; nM


[progress]

  variable  time

  file
c:/Ausers/SAKeatch/DYNAFIT/dynafitdata/spermidine/secspBR322ccc4mMSp.txt
  response CCC  = 0.0196 ?
  response CCC* = 0.00405?

  file
c:/Ausers/SAKeatch/DYNAFIT/dynafitdata/spermidine/secspBR322oc4mMSp.txt
  response OC  = 0.0234 ?
  response OC* = 0.004 ?
```

```
  file
c:/Ausers/SAKeatch/DYNAFIT/dynafitdata/spermidine/secspBR322l4mMSp.txt
  response L  = 0.0167 ?
  response L* = 0.0233 ?

file
c:/Ausers/SAKeatch/DYNAFIT/dynafitdata/spermidine/secspBR322lf4mMSp.txt
  response LF = 0.0195 ?

[output]
  directory ./examples/nuclease/output

; ***********************************************

[end]
```

Appendix E.ii. Script file for Dynafit to fit curves to the data in Appendix E.i, using several models (steven4,5, and 6). The mechanisms for these models are indicated in the [mechanism] sections of each task. The best model to fit the data is chosen by the program, and hence the reaction mechanism is deduced. CCC and CCC* represents supercoiled DNA in its cuttable and uncuttable forms respectively. OC and OC* represents nicked DNA in its cuttable and uncuttable forms respectively. L and L* represents linear DNA in its cuttable and uncuttable forms respectively. LF represents DNA linear fragments. The original file was in notepad.

A

model	data (n)	parameters	squares(S)	status	comment
steven4 [a]	44	16	0.000792444	reject	poor fit
steven6 [b]	44	8	0.00440031	reject	poor fit
steven5 [c]	44	19	0.000563601	accept	best fit

B

Parameter	Initial	Fitted	Error	%Error
K1	0.0154667	0.01193	0.001	8.4
K2	0.02	0.02324	0.003	13
K5	2e-008	1.037e-005	0.0012	11000
K8	0.0001	0.001846	0.00039	21
K4	0.0026	0.00745	0.00074	9.9
K7	0.0001	0.0002763	0.0001	38
K3	0.046	0.006279	0.00046	7.4
K6	0.0001	0.000418	2.5e-005	6
K9	0.0001	0.0005086	0.00014	28

C

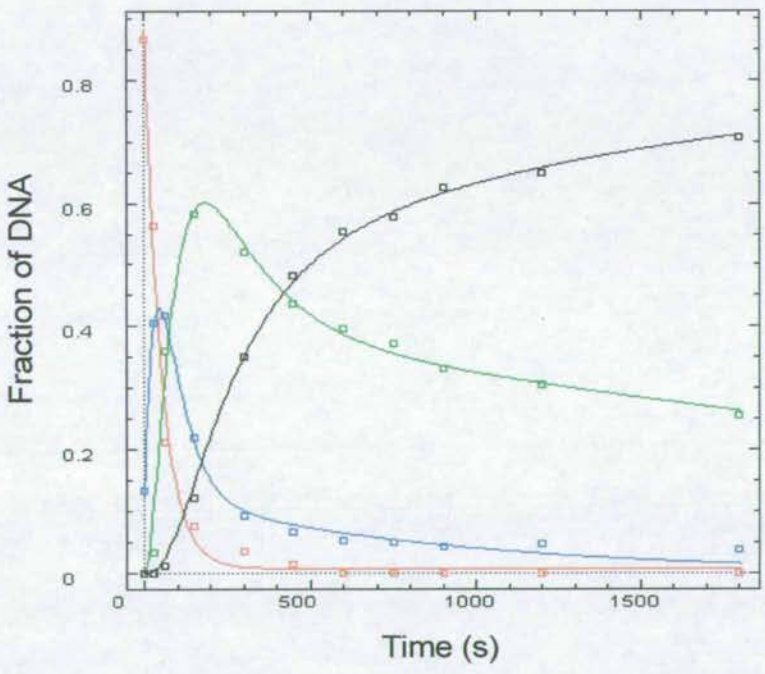

Appendix E.iii. Curve-fitting by Dynafit. Using the script file shown in Appendix E.ii, with data provided in Appendix E.i, Dynafit produced the output table shown (A), indicating that of the models suggested, model 5 (steven5) produced the best fit. The rate constants calculated using model 5 are also indicated (B). The data fitted using model 5 is also shown (C), with the fraction of supercoiled (red), nicked (blue), linear (green) and linear fragmented (black) DNA indicated.

Appendix F

Published online November 1, 2004

Nucleic Acids Research, 2004, Vol. 32, No. 19 ***5841–5850***
doi:10.1093/nar/gkh918

Alleviation of restriction by DNA condensation and non-specific DNA binding ligands

Steven A. Keatch, Tsueu-Ju Su and David T. F. Dryden*

School of Chemistry, The University of Edinburgh, The King's Buildings, Edinburgh, EH9 3JJ, UK

Received September 17, 2004; Revised and Accepted October 13, 2004

ABSTRACT

During conditions of cell stress, the type I restriction and modification enzymes of bacteria show reduced, but not zero, levels of restriction of unmethylated foreign DNA. In such conditions, chemically identical unmethylated recognition sequences also occur on the chromosome of the host but restriction alleviation prevents the enzymes from destroying the host DNA. How is this distinction between chemically identical DNA molecules achieved? For some, but not all, type I restriction enzymes, alleviation is partially due to proteolytic degradation of a subunit of the enzyme. We identify that the additional alleviation factor is attributable to the structural difference between foreign DNA entering the cell as a random coil and host DNA, which exists in a condensed nucleoid structure coated with many non-specific ligands. The type I restriction enzyme is able to destroy the 'naked' DNA using a complex reaction linked to DNA translocation, but this essential translocation process is inhibited by DNA condensation and the presence of non-specific ligands bound along the DNA.

INTRODUCTION

In every cell, it is important to be able to distinguish between different DNA molecules, for example between replicated DNA versus non-replicated DNA or host DNA versus foreign DNA. In both these situations, the cell contrives to ensure that the DNA molecules are chemically different. In both eukaryotes and prokaryotes, DNA methylation, where cytosine is modified to C5-methyl-C or N4-methyl-C and adenine is modified to N6-methyl-A, is of particular importance for this chemical distinction. These different chemical modifications allow various enzyme systems to distinguish between the methylation states of the DNA and carry out appropriate reactions. However, there are situations such as cell stress and DNA damage in which chemically identical DNA molecules have to be differentiated by an enzyme. The normally impressive chemical ability of an enzyme to discriminate between different substrates is of no use in this situation, so how is this discrimination achieved?

This question is raised most clearly by the phenomenon of restriction alleviation (RA) in bacteria, the existence of which has been known for many years (1,2) but which is only partially understood at a molecular level. In the RA process, the DNA restriction/modification (R/M) system of the host bacterium is switched off or reduced in effectiveness for a period of time to allow, for example, repair of DNA damage induced by UV irradiation (1,3,4) or by chemical agents (5–8) or, when introducing an R/M system into a naïve host, the establishment of modification upon the chromosome (9–13). It can also be induced by the loss of the modification function by mutation (3,14). R/M systems either modify (methylate) newly replicated, hemimethylated host DNA, which contains the methylated parental strand and the unmethylated daughter strand, or destroy unmethylated foreign DNA. In situations of incomplete modification of the host DNA, R/M systems can be lethal. It is known that type I R/M systems have RA control to prevent lethality (9,11) whilst type II R/M systems function as selfish genetic elements (15) and kill their hosts.

RA raises two important questions about the nature of the DNA in the cell. First, when the chromosomal DNA sequences recognized by the R/M system exist in a partly methylated state during DNA repair or a fully unmethylated state when a new R/M system is acquired by a naïve host, how does the host cell control the potentially lethal activity of the host type I R/M system on its chromosome (7,16)? Second, during RA a reduced level of restriction activity is still present and forms a barrier to phage infection (1–3,5,6) indicating that the unmodified target sequences on the phage DNA can be distinguished from the unmodified target sequences on the host DNA by the resident type I R/M system. How is this accomplished when both DNA molecules are chemically identical (7,16)? We wish to address these two questions in this paper.

The RA phenomenon appears to apply only to type I R/M systems, which combine both restriction endonuclease and modification methyltransferase activities within a single multifunctional enzyme complex [reviewed in (16–19)]. These systems, despite their complexity, are very widespread in prokaryotes occurring in at least 50% of bacteria (20). Type I R/M systems are grouped into four families, IA to ID (21). Type I R/M enzymes contain two restriction subunits, two modification subunits and a single sequence specificity subunit; they usually prefer to modify host DNA when it exists in a hemimethylated state following DNA replication and to destroy foreign DNA, which usually contains unmodified target sequences. The complex restriction reaction commences with an irreversible attachment to the unmodified target sequence followed by reeling in of the DNA on either side of the target sequence towards the enzyme (often referred to as

*To whom correspondence should be addressed. Tel: +44 131 650 4735; Fax: +44 131 650 6453; Email: david.dryden@ed.ac.uk

DNA translocation driven by ATP hydrolysis) with concomitant formation of DNA loops and eventual double-strand cleavage of the DNA when translocation is halted by some obstruction to further translocation. These obstructions are usually another type I R/M enzyme (22), a Holliday junction (23,24) or complete translocation of circular DNA containing only a single target sequence [e.g. (25)]. The restriction subunits are responsible for both the ATP-hydrolysis dependent DNA translocation and for DNA cleavage as they contain essential amino acid motifs for DNA helicase motor activity and for Mg^{2+}-dependent endonuclease activity (26–30). At the collision site, each endonuclease domain, one in each restriction subunit, introduces a single-strand break. Since the breaks are in close proximity to each other, the overlapping DNA ends melt and the DNA is cleaved. The nature of the cleaved ends is still not clear (31–33). Furthermore, once cleavage has occurred, the enzyme apparently remains bound to the DNA (34) and continues to hydrolyse ATP without turnover in the complete restriction process (32,35,36).

There appear to be (at least) two forms of RA. For type IA and IB R/M systems, RA has been linked to a genotypic effect (11–13) involving the products of the clpXP genes (10). We will refer to this as 'family-specific RA', which so far is known for only the type IA and IB families. ClpXP is a proteolytic enzyme complex, which degrades the restriction subunits of the type I R/M enzyme but only if the R/M enzyme has commenced the complex restriction process (3). It is the translocation process during restriction, which signals the clpXP protease to attack the type I R/M enzyme and degrade the restriction subunits. In this manner, the potentially lethal effects of the type I R/M enzyme on the chromosome are prevented at least for the IA and IB families. However, not all type I R/M systems are subject to RA via the clpXP protease but RA is still observed and no specific genotype has so far been associated with this second form of RA (7). We will refer to this as 'general RA' and, on the basis of our results, we propose that it applies to all type I R/M systems including those which also have family-specific RA. The two forms of RA, general and family-specific are effective in limiting damage to the host chromosome. The physical basis of general RA is not known, but it has been suggested that it may be related to the difference between the higher order structure of the chromosomal DNA present in the nucleoid and foreign DNA, which will adopt a random coil conformation as it enters the cytoplasm of the cell (7,16). Thus, the type I R/M enzyme will see two different DNA structures, and it effectively exists in two different 'compartments' in the cell, either associated with the nucleoid where its main function is to maintain methylation or in the cytoplasm where its role is to intercept foreign unmethylated DNA. There is some evidence that when in the cytoplasmic fraction the enzyme can associate with the inner membrane (3,37,38).

The structure of the nucleoid has been the focus of much attention for many years (39,40). In the absence of cell stress, the nucleoid is always partially coated with a range of 'histone-like' proteins (40,41) and their concentration varies depending on growth conditions (42). Such an extensive array of non-sequence-specific ligands bound along the DNA is likely to hinder a translocating type I R/M enzyme. Although it has been demonstrated that a single repressor protein bound to DNA does not hinder translocation (43), it is noteworthy that the presence of saturating concentrations of intercalating dye molecules does substantially hinder restriction (44,45) implying that a barrier of non-specifically bound ligands would pose a problem for translocation by type I R/M enzymes. Whilst the nucleoid DNA is typically only partially compacted by bound protein thereby allowing DNA replication to proceed, under conditions of stress which induce RA, it has recently been observed that the nucleoid can slowly convert to a semicrystalline form and undergoes a well-known process termed 'condensation' in which the DNA double strands become aligned with each other in compact arrays (46–48). This condensed DNA is not available for replication or transcription as these processes are shut down during conditions of DNA damage to allow time for DNA repair. Hence, it is therefore possible that the condensed nucleoid is also generally resistant to restriction. It has been shown that a variety of simple type II restriction enzymes are inhibited *in vitro* by DNA condensation (49,50) but for these enzymes there is no indication of any association with the RA phenomenon (4,5,7). Condensation is likely to be an even more acute problem for a type I R/M system dependent upon DNA translocation.

In this paper, we compare the activity of EcoKI on 'naked' DNA with that on DNA coated with non-sequence specific ligands and with DNA condensed by the addition of a polyamine to address the questions about general RA posed by Murray (16) concerning the difference between self and foreign DNA when both are unmethylated. DNA condensation is achieved by the addition of the polyamine spermidine (Sp^{3+}), a well-known physiological condensing agent and as non-specific DNA binding ligands, we use several dyes including a dye which binds in the minor groove of DNA, Hoechst 33258, and two dyes which intercalate between base pairs, ethidium bromide (EtBr) and the cyanine dye YOYO.

MATERIALS AND METHODS

EcoKI purification

EcoKI was prepared from 8 l of NK311 cells (6) containing the plasmid pBE3 (11) as previously described (51). Concentration of enzyme was determined by UV absorption at 280 nm. Buffers used for all experiments were either a 'high-salt' EcoKI buffer comprising 33 mM Tris-acetate, 10 mM Magnesium acetate, 66 mM potassium acetate, 0.5 mM DTT, pH 7.9 or a 'low-salt' EcoKI buffer comprising 10 mM Tris-acetate, 10 mM Magnesium acetate, 7 mM 2-mercaptoethanol, pH 7.9.

DNA plasmid preparation

Plasmid DNA was purified from *E.coli* strain ER2426 as described in (52). This strain lacks the EcoKI R/M system hence the DNA contains unmodified EcoKI sites. Plasmid pBR322 and its derivative, pBRsk1 (27) were used in our experiments. pBR322 contains two target sites for EcoKI, whereas pBRsk1 contains only one EcoKI target site. Both plasmids contain one EcoRI site. When linear DNA was required, plasmid DNA was cut with EcoRI in high-salt EcoKI buffer. DNA concentration was determined by UV spectroscopy and purity by agarose gel electrophoresis

using 1× TBE (10× TBE: 0.89 M Tris base, 0.89 M boric acid, 20 mM EDTA) and DNA loading buffer (10× DNA loading buffer: 20% Ficoll 400, 0.1 M Na_2EDTA, 1% SDS, 0.25% (w/v) bromophenol blue, pH 8).

DNA condensation by spermidine and binding of dyes to DNA

Spermidine (Sigma Aldrich) was dissolved in low-salt EcoKI buffer and the pH adjusted to pH 7.9 if required. This stock solution was added to DNA solutions and left for 30 min before adding EcoKI and its reaction ingredients. The dyes ethidium bromide (EtBr), Hoechst 33258 and YOYO (Molecular Probes) were added to DNA at various dye molecule to DNA base-pair ratios and incubated for 30 min at 45°C before adding EcoKI and its reaction ingredients.

DNase digestion

Assays were carried out in low-salt EcoKI buffer with 1 mM $CaCl_2$ and the ionic strength adjusted using NaCl. Plasmid pBRsk1 DNA (50 nM) was incubated with 0.1 µg/ml DNase I at 37°C. The reaction was stopped by the addition of EDTA to a final concentration of 77 mM. Samples were then run on 0.8% agarose gels, in 1× TBE with EtBr staining.

Restriction assays

Assays were typically carried out in low-salt EcoKI buffer with the ionic strength adjusted with NaCl. Reactions were carried out with 50 nM plasmid DNA, 0.1 mM S-adenosylmethionine (SAM, New England Biolabs), 50 µg/ml BSA (New England Biolabs) and 2 mM ATP (Roche). EcoKI (67 nM) was used for digestion of DNA containing one EcoKI target site and 134 nM EcoKI for DNA with two sites. Reactions were typically carried out in 180 µl total volume, with 22 µl being removed at specific time points and added to EDTA (77 mM final concentration) in order to stop the reaction. EcoKI was denatured by heating the sample to 68°C for 30 min. This treatment also served to displace Hoechst and YOYO from the DNA and allow their replacement with EtBr. It is known that YOYO makes the DNA migrate differently from DNA stained with EtBr (53) and this treatment allowed all densitometry to be performed in the same manner with EtBr. Loading buffer was then added to samples before being run on 0.8% agarose gels in 1× TBE buffer. EtBr was used to stain the DNA, which was visualized using a UV transilluminator (UVP, TFM-30) and images acquired using a digital camera (Fujifilm FinePix S602Zoom) with a 3 mm thick, 570 nm cut-on filter (Schott, Germany) and Adobe Photoshop software. Densitometry was carried out on gel images using Scion Image software (Scion Corporation). In order to analyse the data thoroughly, a conversion factor was determined to allow direct comparison between supercoiled, nicked or linear DNA as these different topological forms bind varying amounts of dye.

Translocation assays

EcoKI translocation was measured by a coupled enzyme ATPase assay (54). In this reaction, the rate of decrease in NADH is proportional to the rate of ATP hydrolysis by EcoKI and is measured via absorbance at 340 nm. For this assay, 5 nM DNA with one EcoKI target site or 2.5 nM DNA with two EcoKI target sites was incubated with 10 nM EcoKI, 50 µg/ml BSA, 0.1 mM SAM, 1 mM phosphoenol pyruvate (Sigma), 250 µM NADH (Sigma), in low-salt EcoKI buffer, pH 7.9, with a final reaction volume of 300 µl. Pyruvate kinase/lactate dehydrogenase (Roche) was dialysed against low-salt EcoKI buffer and used fresh on the day of experiment at a concentration of 13 µg/ml. A baseline was recorded at 340 nm before starting the reaction by adding ATP to 2 mM. The rate of decrease of NADH was recorded and the corresponding rate of ATP hydrolysis calculated using an extinction coefficient for NADH of 6.22 for a 1 mM solution, 1 cm pathlength at 340 nm.

Data analysis was performed using Grafit (Erithacus Software, UK) and Dynafit (55).

RESULTS

Determination of conditions for condensation of plasmid DNA

DNA condensation has been shown to be highly dependent not only on the nature of the condensing agent but also on the ionic strength and pH of the solution (56). Given that spermidine carries a charge of 3+ and is strongly basic, these two parameters must be carefully controlled when attempting to assay the EcoKI activity. An assay for condensation using the non-specific nuclease DNaseI was successfully used under the solution conditions appropriate for assaying EcoKI. DNaseI was only able to digest both linear and circular DNA at Sp^{3+} concentrations of <6 mM as shown by the presence of undigested DNA on agarose gel electrophoresis, Figure 1. Slight protection was observed at 5 mM Sp^{3+} but full protection of linear DNA and maintenance of circular DNA, albeit with

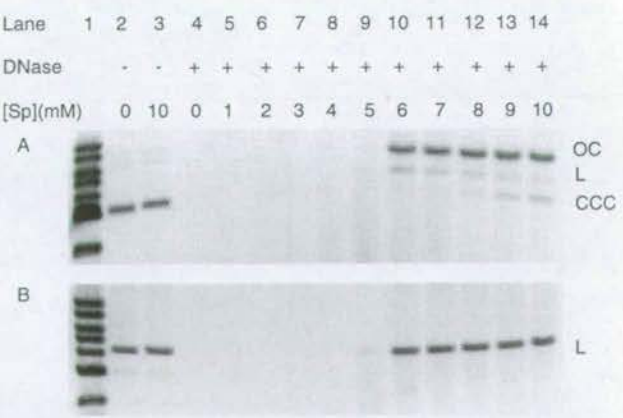

Figure 1. Effect of spermidine-induced condensation on digestion of DNA by DNase I. DNase (1 µg/ml) was used to digest 50 nM supercoiled (**A**) and linear (**B**) pBRsk1 at 37°C in low-salt EcoKI buffer with the ionic strength made up to 100 mM with NaCl. Lane 1 contains a DNA size marker (10, 8, 6, 5, 4, 3 and 2 kb from top to bottom). Lanes 2–14 contain DNA in the presence (plus sign) or absence (minus sign) of DNaseI and varying concentrations of spermidine ranging from 0 to 10 mM as indicated. The different conformations of DNA are as follows: CCC, covalently closed circular (supercoiled); OC, open circular (nicked) and L, linear DNA. Both CCC and L pBRsk1 were condensed by 6 mM spermidine. It can be seen that although the L DNA appears completely condensed at 6 mM spermidine, the CCC DNA is mainly in an OC conformation with some L DNA.

some single-strand nicking, was only observed when the spermidine concentration equalled or exceeded 6 mM. These results are consistent with spermidine-induced compaction of the DNA under these experimental conditions (56).

EcoKI restriction activity on plasmid pBRsk1 as a function of condensation and intercalation

Having defined the conditions which lead to the onset of DNA condensation in the EcoKI assay buffer, we analysed the DNA cleavage rates of EcoKI as either spermidine or intercalating dyes were added whilst maintaining pH and ionic strength constant. Figure 2 shows the progressive digestion of pBRsk1 supercoiled plasmid by EcoKI. It is clear that the closed circular form of the plasmid is converted to a nicked open circular form and then to a linear form but the rates at which these steps occur decreases significantly as both [Sp^{3+}] and [dye] increase (EtBr results not shown). After lengthy incubations, the linear product is gradually digested further. This secondary cleavage of DNA is often observed with type I enzymes. In the uninhibited assay, Figure 2A, the level of nicked DNA rapidly accumulates and then is further degraded by the acquisition of a second nick which must be in close proximity to the first. Of greatest interest is the accumulation of nicked plasmid once the DNA has condensed or the dye to base pair ratio reaches 1:32, Figure 2B, C and D. In the presence of condensation or dyes, the level of nicked DNA builds up ~5–10 times slower compared with the uninhibited

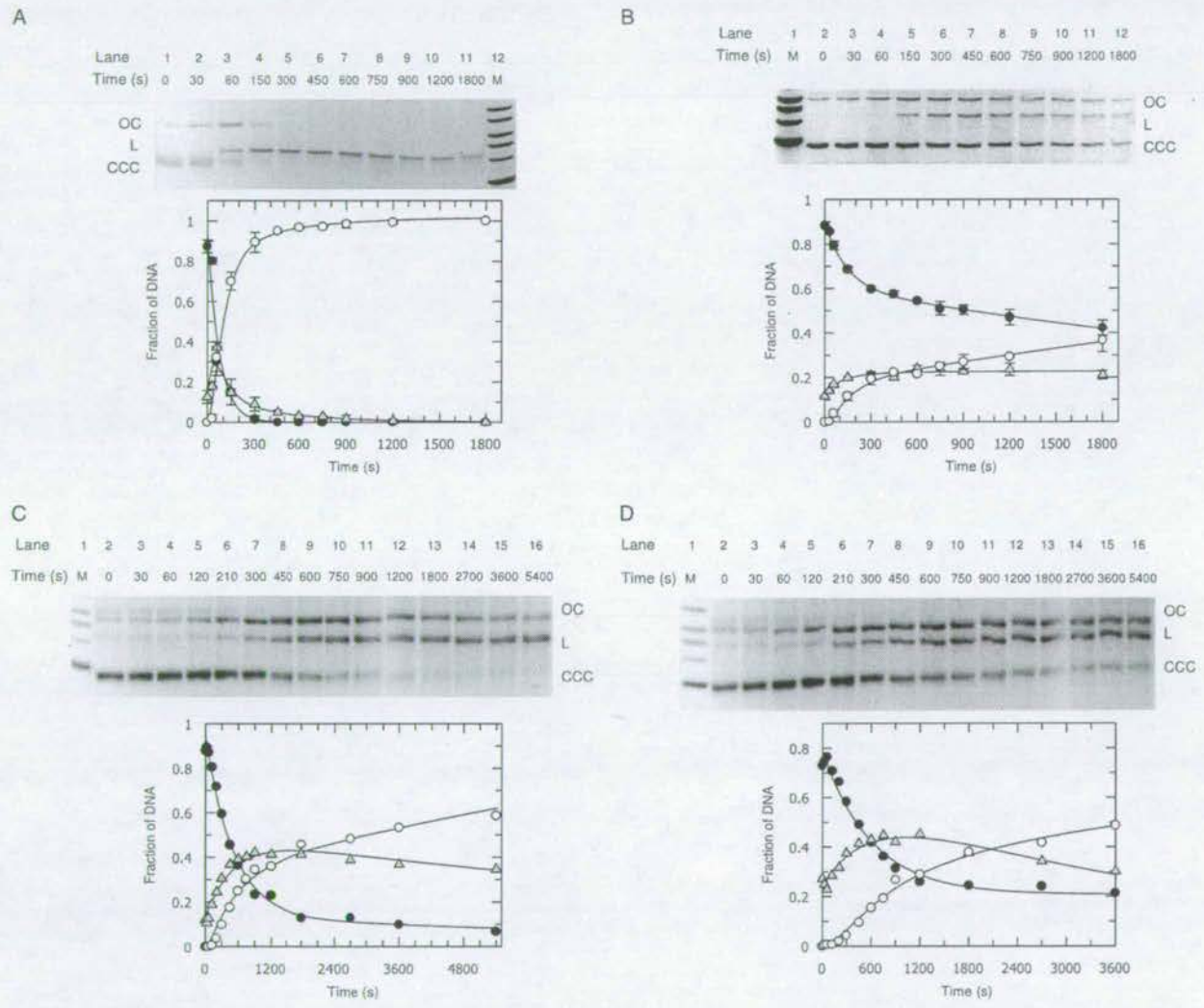

Figure 2. Degradation of 50 nM CCC pBRsk1 by 67 nM EcoKI in low-salt EcoKI buffer with the ionic strength made up to 100 mM with NaCl. The gels show the time course of DNA digestion with CCC DNA being converted to OC then to L DNA. DNA markers of the sizes indicated are shown in lanes marked with an M. The results of densitometry of these gels are shown below each gel with the proportion of CCC DNA shown as filled circles, OC DNA as shaded triangles and L DNA as open circles. The fitted lines are derived from the kinetic model described in the text. All experiments were repeated at least in duplicate (Hoechst 33258) or in triplicate (other data sets) and representative error bars for SD are shown in sections A and B. (**A**) pBRsk1 being digested by EcoKI. Markers 10, 8, 6, 5, 4 and 3 kb from top to bottom. (**B**) Digestion of the DNA preincubated and condensed with 6 mM spermidine. Markers 6, 5, 4 and 3 kb from top to bottom. (**C**) Digestion of the DNA preincubated with Hoechst 33258 at a dye to base pair ratio of 1:32. Markers 6, 5, 4 and 3 kb from top to bottom. (**D**) Digestion of DNA preincubated with YOYO at a dye to base pair ratio of 1:32. Markers 8, 6, 5, 4 and 3 kb from top to bottom.

assay, but then breaks down even more slowly to linear DNA. The level of nicked plasmid reaches 20% or more of the total DNA when the spermidine concentration reaches 6 mM and 40% when the dye to base-pair ratio reaches 1:32. It appears that at least a proportion of the nicked DNA is either completely or very nearly completely resistant to cleavage to a linear form. Perhaps in these situations, further nicking does occur but the nicks are too far away from the initial nick to allow denaturation of the DNA to a linear form.

Kinetic modelling of the rate of DNA cleavage

In the absence of spermidine or dye, the restriction reaction pathway proceeds from closed circular (CCC) to open circular (OC) to linear (L) DNA and the restriction data obtained can be described by the model below.

$$\mathrm{CCC} \xrightarrow{k_1} \mathrm{OC} \xrightarrow{k_2} \mathrm{L}$$

However, the presence of even small amounts of spermidine or dye slows the progression through this reaction pathway, and the persistence of large amounts of uncleaved or nicked DNA after long periods of incubation suggests that these additives can sequester the DNA in uncleavable forms, CCC* for closed circular DNA and OC* for open circular DNA. As the binding of both spermidine and the dyes to DNA are not irreversible processes, we assumed that the formation of CCC* and OC* was reversible. Therefore, we added two additional steps to describe the reaction in the presence of spermidine or dye. The densitometric data, some of which is shown in Figure 2, has been fitted to the following model.

$$\mathrm{CCC} \xrightarrow{k_1} \mathrm{OC} \xrightarrow{k_2} \mathrm{L}$$

$$\mathrm{CCC} \underset{k_6}{\overset{k_4}{\leftrightarrow}} \mathrm{CCC}^*$$

$$\mathrm{OC} \underset{k_5}{\overset{k_3}{\leftrightarrow}} \mathrm{OC}^*$$

This more complex model applied equally well to both the spermidine data and the dye data, and the derived rate constants for spermidine are given in Table 1. It is apparent from the rate constants and the derived equilibrium constants that the two kinetic steps involving CCC* and OC* are of minor importance, and therefore difficult to measure accurately, at spermidine concentrations <6 mM where the DNA is uncondensed but becomes very significant upon condensation. Similarly, as the dye concentration increases they become more important (data not shown). Figure 3 shows the rate constants k_1 and k_2 as a function of [Sp^{3+}] or [dye]. It is apparent that both these rate constants are significantly slowed by condensation and by dye binding as expected from a qualitative inspection of Figure 2. Prior to DNA condensation, however, the rate constants increase significantly indicating that at low concentrations, spermidine actually enhances the restriction reaction. This effect was noted many years ago for the EcoAI type I R/M enzyme (57) and for some type II restriction enzymes (49,50).

Either condensation or the presence of intercalating dyes strongly inhibits the restriction process of EcoKI. The collapse of DNA due to Sp^{3+} into a tightly packed structure would be expected to restrict access of EcoKI to its target site, but we can see that perhaps surprisingly this is not too severe as the rate of nicking is still appreciable indicating that the enzyme can compete effectively with the Sp^{3+} to find its target site. Perhaps more surprising is the dramatic effect of the dyes. Even very small amounts of dye, where on an average one dye molecule is bound for every few hundred base pairs, reduces the rate of conversion of closed circular DNA to open circular DNA and then to linear DNA. These small dyes are clearly a severe block to either protein–DNA binding or EcoKI activity or both.

ATP hydrolysis

The ATP hydrolysis assay measures ATP consumption throughout the restriction process and does not distinguish between any particular binding, translocation or cutting event. However, it is observed that the rate of hydrolysis remains constant for any particular set of experimental conditions. Figure 3A shows the variation in rate as a function of spermidine. The rate is slightly decreased by low concentrations of spermidine but drops by 2/3 to 3/4 of its uninhibited value at 6 mM spermidine and still further at higher concentrations as condensation is completed. Even at the highest concentrations of spermidine where all of the DNA will be

Table 1. Rate constants for the degradation of closed circular plasmid pBRsk1 by EcoKI determined using the model described in the text

[Sp^{3+}] mM	Rate constants (s^{-1}) k_1	k_2	k_3	k_4	k_5	k_6	Equilibrium constants k_3/k_5	k_4/k_6
0	0.0150 ± 0.0030	0.0262 ± 0.0100	$1.93 \times 10^{-8} \pm 0.0030$	$1.13 \times 10^{-9} \pm 0.0110$	0.0020 ± 0.0010	0.1563 ± 1.8	9.65×10^{-6}	7.22×10^{-9}
2	0.0187 ± 0.0003	0.0276 ± 0.0075	$1.93 \times 10^{-8} \pm 0.0019$	$1.13 \times 10^{-9} \pm 0.0011$	0.0041 ± 0.0016	0.0051 ± 0.0037	4.71×10^{-6}	2.21×10^{-7}
4	0.0197 ± 0.0029	0.0331 ± 0.0087	$1.93 \times 10^{-8} \pm 0.0016$	$1.13 \times 10^{-9} \pm 0.0008$	0.0019 ± 0.0006	0.0044 ± 0.0027	1.01×10^{-5}	2.57×10^{-7}
6	0.0037 ± 0.0002	0.0083 ± 0.0020	0.0152 ± 0.0006	0.0033 ± 0.0001	0.0003 ± 0.0001	0.0004 ± 0.0001	50.67	8.25
8	0.0020 ± 0.0001	0.0020 ± 0.0006	0.0079 ± 0.0004	0.0025 ± 0.0001	0.0002 ± 0.0001	0.0004 ± 0.0001	39.50	6.25
10	0.0002 ± 0.0001	0.0002 ± 0.0001	0.0093 ± 0.0004	0.0022 ± 0.0001	0.0029 ± 0.0005	0.0017 ± 0.0001	3.20	1.29

It is clear from the equilibrium constants that the side reactions involving the formation of DNA structures resistant to cleavage by EcoKI become significant only once DNA condensation has occurred.

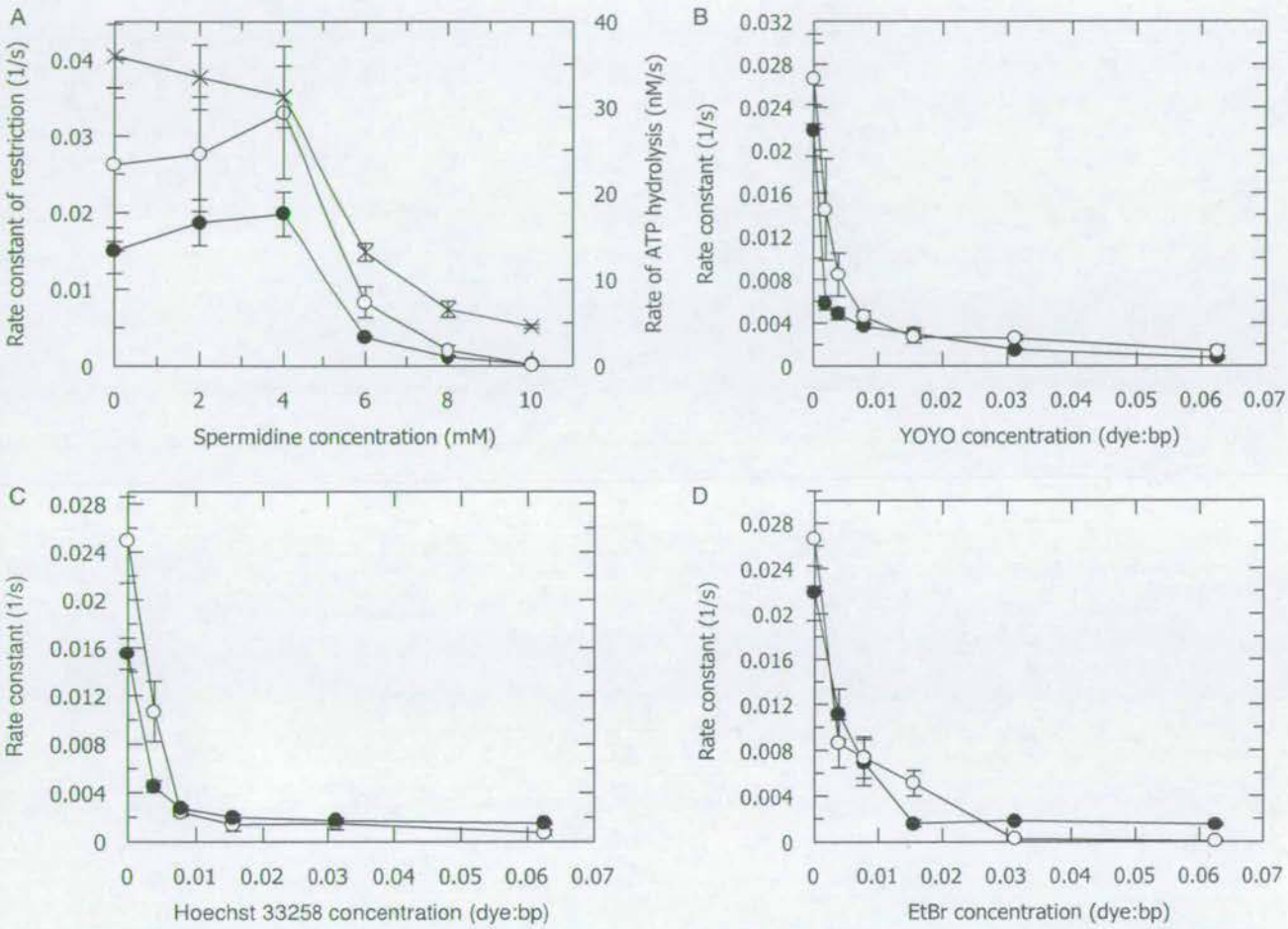

Figure 3. The effect of spermidine and dye molecules on the rates of the endonuclease and ATP hydrolysis reactions of EcoKI on CCC pBRsk1. The rate constants for the cleavage of CCC DNA to OC form (filled circles), OC DNA into L form (open circles) derived by fitting data, such as those shown in Figure 2 collected at different concentrations of spermidine or dye, to the full kinetic model given in the text are shown. The rate of ATP hydrolysis (×) derived from the ATPase assay in the presence of varying amounts of spermidine is also shown. (**A**) Effect of spermidine concentration on EcoKI activity. It can be seen that at low concentrations of spermidine the rate of cleavage is enhanced but once condensation occurs at 6 mM spermidine or greater, the activity is greatly reduced. The rate of ATP hydrolysis decreases as spermidine is added, particularly at high concentrations once the DNA has condensed. (**B**) Effect of YOYO concentration on DNA cleavage by EcoKI. (**C**) Effect of Hoechst 33258 concentration on DNA cleavage by EcoKI. (**D**) Effect of EtBr concentration on DNA cleavage by EcoKI.

condensed, ATP hydrolysis is observed indicating that the enzyme can still locate its target site on the condensed DNA and at least attempt to translocate DNA. The presence of YOYO also has a strong inhibitory effect on ATP hydrolysis (data not shown) with 50% inhibition achieved with 1 dye molecule per 128 bp of DNA.

Other DNA substrates

The above experiments were also repeated for closed circular pBR322 and pBR322 linearized with EcoRI, both of which contain two target sites for EcoKI (data not shown), and for linear pBRsk1 which has one target site. The presence of two target sites allows the enzyme to continue degrading the DNA after conversion to the linear form. This results in a smear of small fragments on agarose gels and requires the addition of a further kinetic step for linear DNA degrading to these fragments. This further complicates the kinetic analysis without revealing any significant new features. ATP hydrolysis occurs at similar rates for all DNA substrates tested including the linear DNA molecule, which contains only a single EcoKI site (data not shown) even though this molecule is virtually resistant to cleavage.

DISCUSSION

Our experiments show that the restriction activity of EcoKI is strongly compromised by the condensation of DNA by spermidine and by the presence of multiple ligands bound non-specifically along the DNA lattice. Condensation or the

presence of dye molecules inhibits the rates of hydrolysis of ATP required for DNA translocation and double-strand cleavage of the DNA. As a consequence of the slowed kinetics of ATP hydrolysis, DNA translocation and double-strand cleavage, a substantial amount of the DNA substrate is only subject to single-strand nicking. Although obstruction of EcoKI binding must occur to some extent, the presence of substantial quantities of nicked DNA rules out the simple idea that condensation or intercalating dyes achieve their inhibitory effect purely by blocking access of EcoKI to its binding site.

It has been shown that type I R/M enzymes make a double-strand break once translocation has stalled either by collision with another translocating type I R/M enzyme (22) or by a strong blockage to translocation such as a junction in the DNA (23,24) or complete translocation of a circular plasmid containing a single target sequence [e.g. (25)]. It appears from our results that compromising the translocation by DNA condensation leads most often to single-strand breaks. Our results do not indicate if multiple single-strand breaks are introduced. If multiple nicks are introduced, then they are either too far apart for strand separation to easily occur or the breaks introduced by a particular restriction subunit are all on the same strand of DNA. Occasionally a double-strand break is made on the condensed DNA, but the frequency is much reduced compared to uncondensed DNA. Previously, it was shown for the EcoR124II type I R/M enzyme that nicks by themselves are not able to induce a second cleavage to produce a double-strand break (43), so it appears that the endonuclease domain in the restriction subunit is only able to make single-strand breaks on one strand of the DNA. During translocation on uncondensed pBRsk1, the two restriction subunits can cooperate with each other to make a double-strand break when the translocation stalls after the entire plasmid has been reeled in. However, stalling translocation of these subunits before they collide means that the two nicks are uncoordinated and fail to lead to linearization of the DNA.

The restriction process is also strongly inhibited by the coating of the DNA with non-specific binding ligands such as dyes. Previously, it has been found that saturating amounts of the intercalator EtBr block restriction activity (44,45). Such inhibition has also been demonstrated for the type II restriction enzyme EcoRI (58). Our results show that substantial inhibition of both translocation and cleavage is achieved by even one dye molecule being present on an average for every 256 bp along the DNA. The presence of dye molecules on the DNA will undoubtedly hinder EcoKI in locating and binding to its target site as the three dye molecules, Hoechst 33258 (59,60), EtBr (61) and YOYO (53) have high nanomolar to micromolar binding affinity for DNA comparable to the binding affinity of EcoKI. However, competition for DNA binding between dye and EcoKI cannot be the entire cause of the observed reduction in activity since at least a proportion of the enzyme must be able to bind to its site as all the binding processes are equilibrium processes. Once EcoKI has bound to the DNA, it is committed to hydrolyse ATP and to introduce single-strand breaks in the DNA. The appearance of single-strand breaks and hydrolysis of ATP indicates that the translocation and cleavage processes are being hindered not only indirectly by competition between the enzyme and the dye for the EcoKI target sequence but also directly in the same manner as found when spermidine is present. It has previously been

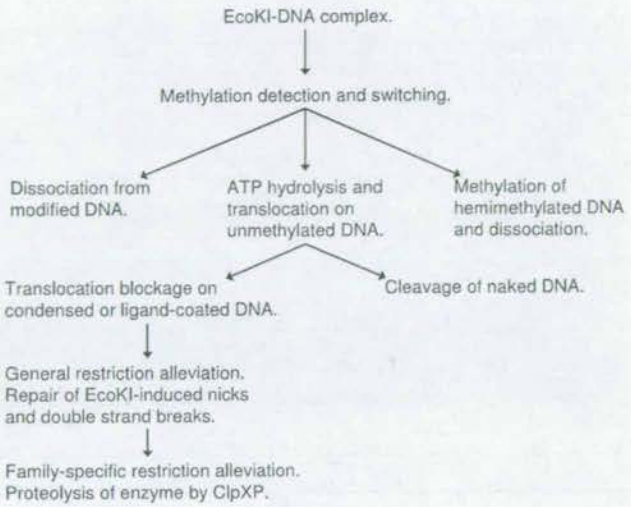

Figure 4. Diagrammatic representation of the pathways followed by the EcoKI type I R/M enzyme during restriction and restriction alleviation.

shown that a single protein bound to DNA is insufficient to halt a translocating type I R/M enzyme (43), but in our experiments it appears that multiple ligands bound in a non-specific manner to the DNA are a very effective block to the type I R/M enzyme. Given that EcoKI can translocate DNA bi-directionally, it appears that the motors are both moving DNA but are stalling before they can translocate the entire DNA. Instead of stalling by colliding with each other, they are stalling prematurely against the barriers formed by bound dye molecules. Each restriction subunit may then introduce a single-strand break in the DNA but since these two nicks are now unlikely to be adjacent to each other, the DNA is not linearized.

We wish to relate our observations, summarized in Figure 4, to those previously made on restriction alleviation and on the structure of the nucleoid. It is apparent that the type I R/M enzyme can find itself in three different situations: (i) diffusing in the cytoplasm looking for protein-free 'naked' foreign DNA; (ii) bound to the nucleoid during DNA replication when it is partially coated with histone-like proteins; or (iii) bound to a fully condensed nucleoid formed under conditions of cell stress.

The nucleoid and RA

Cell stress. It has been found that there are two sorts of RA, family-specific and general, initiated under conditions of cell stress caused by 2-aminopurine, nalidixic acid or UV irradiation, or by the creation of potentially lethal r^+m^- mutant type I R/M enzymes or introduction of a new R/M system (7). The family-specific RA, as explained earlier, is due to a genotypic effect but no genotype has yet been found for general RA so it was suggested that this mechanism could be due to some feature of the structure of the nucleoid (16).

We believe that the experimental conditions used here, namely coating the DNA with non-specific dye molecules and condensing it with spermidine, mimic the nucleoid structure encountered by EcoKI and other type I R/M enzymes *in vivo*. Therefore, the *in vivo* implication of our results is that the EcoKI DNA translocation process on the nucleoid

is drastically slowed by both condensation and non-specific protein binding and the enzyme stalls. Furthermore, the production of single and double-strand breaks in the host DNA by the R/M enzyme is strongly inhibited by nucleoid structure, particularly the structures induced by conditions of stress where the nucleoid becomes highly ordered and condensed (47,48). Double-strand breaks, which have been observed by pulsed field gel electrophoresis of *E.coli* chromosomal DNA (62), will still occur but very slowly, infrequently and in an uncoordinated manner. These cleavage events can be repaired by DNA ligase and recombination processes.

Acquisition of new type I R/M systems. A similar argument can be made to explain the observation that bacterial cells can acquire new type I R/M systems easily by transformation, transduction and conjugation, but the restriction activity, in contrast to modification, takes a long time to become manifest and RA is activated (9–13). Upon introduction of the new R/M system, protein is slowly synthesized and assembled into the R/M enzyme. Some of this newly synthesized enzyme will clearly be able to attack the foreign DNA should it be unmodified; however, the bulk of the enzyme will be sequestered by binding to the nucleoid where it can either slowly carry out its methylation reaction or trigger the restriction reaction in response to the unmodified targets on the nucleoid. Our *in vitro* data suggest that should the restriction reaction be triggered *in vivo*, the translocation and cleavage functions will be inhibited by the nucleoid structure allowing the normal DNA repair processes to handle the occasional damage produced by the type I R/M enzyme.

By extrapolating from our *in vitro* results to the situation prevailing *in vivo*, we conclude that the restriction activity of the type I R/M enzymes, which is completely dependent upon extensive translocation, would be so inefficient on nucleoid DNA that restriction will not be a major problem for the cell and one observes the general RA phenomenon, Figure 4. In addition to general RA, family-specific RA is an extra feature in which some of the type I R/M enzymes are subjected to clpXP-dependent proteolysis whilst they are attempting to move along the nucleoid DNA.

Nucleoid structure versus uncondensed foreign DNA

When phage attacks a type I R/M proficient cell, which is already under stress and showing RA, it is observed that restriction of the phage is not entirely abolished (1–3,5,6). This indicates that the unmodified, chemically identical, foreign and host DNA molecules can be distinguished by the restriction enzyme. This can be explained by the existence of two pools of type I R/M enzyme (3,37,38). The pool of enzyme bound to the nucleoid will be dealt with by general and family-specific RA as described above but the cytoplasmic pool of the enzyme will bind to the incoming phage DNA. This foreign DNA will be in an uncondensed, random coil form. This form of DNA is the perfect substrate for the translocation process prior to double-strand cleavage and this substrate will not induce general RA. It would appear reasonable to suggest that in this situation, the type I R/M enzyme can complete its restriction reaction so rapidly that if it were susceptible to family-specific RA, then the clpXP enzyme would be physically unable to locate, bind and destroy the restriction enzyme before the restriction enzyme had destroyed the incoming DNA. Translocation rates for type I R/M enzymes have been measured to be between 100 and 550 bp/s in each direction (22,63–65) so even if two target sequences were 10 000 bp apart, the clpXP would only have between 12 and 50 s to act. It is also perhaps noteworthy that EcoKI can form a large dimer species on unmethylated, random coil DNA if the DNA contains two target sequences (66,67) even though this extra complexity is not essential for enzyme activity and therefore seemingly superfluous. Such a dimer is unlikely to be able to form on chromosomal DNA packaged in the nucleoid as the two target sequences will rarely be in close physical proximity. Perhaps this dimer species is not susceptible to clpXP family-specific RA, whereas the monomer species bound on the nucleoid would still be susceptible? One final point of interest arises by comparing the maximum forces generated by the EcoR124I type I R/M enzyme and those generated by polymerases and by the forces required to disrupt nucleosomes. Single molecule experiments reveal that the EcoR124I R/M enzyme cannot move against forces >5 pN (65), whereas the polymerases can move against forces of 20 pN or more and nucleosomes require 20–40 pN to be disrupted [reviewed in (68)]. It would appear that the type I R/M enzymes do not generate enough force to drive their way past obstructions or through condensed DNA.

CONCLUSION

We believe our results show the answer to the question 'how are unmodified sequences present in the resident bacterial chromosome either because of DNA damage or because the host has no R/M system, distinguished from those in foreign DNA that has recently entered the bacterial cell?' (7,16) to be that DNA in the nucleoid is condensed and coated with non-sequence-specific ligands whereas foreign DNA is relatively naked and in a random coil conformation. These differences in the higher order structure have an enormous effect on the activity of the type I R/M enzymes.

ACKNOWLEDGEMENTS

We thank Professor Noreen Murray and Dr Garry Blakeley, Institute of Cell and Molecular Biology, University of Edinburgh for many useful discussions about restriction alleviation. This work was supported by a studentship to S.A.K. awarded by the MRC and a grant from the EPSRC.

REFERENCES

1. Bertani,G. and Weigle,J.J. (1953) Host controlled variation in bacterial viruses. *J. Bacteriol.*, **65**, 113–121.
2. Glover,S.W. and Colson,C. (1965) The breakdown of the restriction mechanism in zygotes of *Escherichia coli*. *Genet. Res.*, **6**, 153–155.
3. Doronina,V.A. and Murray,N.E. (2001) The proteolytic control of restriction activity in *Escherichia coli* K-12. *Mol. Microbiol.*, **39**, 416–428.
4. Thoms,B. and Wackernagel,W. (1982) UV-induced alleviation of lambda restriction in *Escherichia coli* K-12: kinetics of induction and specificity of this SOS function. *Mol. Gen. Genet.*, **186**, 111–117.
5. Efimova,E.P., Delver,E.P. and Belogurov,A.A. (1988) 2-aminopurine and 5-bromouracil induce alleviation of type I restriction in *Escherichia coli*: mismatches function as inducing signals? *Mol. Gen. Genet.*, **214**, 317–320.

6. Makovets,S., Doronina,V.A. and Murray,N.E. (1999) Regulation of endonuclease activity by proteolysis prevents breakage of unmodified bacterial chromosomes by type I restriction enzymes. *Proc. Natl Acad. Sci. USA*, **96**, 9757–9762.
7. Makovets,S., Powell,L.M., Titheradge,A.J.B., Blakely,G.W. and Murray,N.E. (2004) Is modification sufficient to protect a bacterial chromosome from a resident restriction endonuclease? *Mol. Microbiol.*, **51**, 135–147.
8. Thoms,B. and Wackernagel,W. (1984) Genetic control of damage-inducible restriction alleviation in *Escherichia coli* K12: an SOS function not repressed by lexA. *Mol. Gen. Genet.*, **197**, 297–303.
9. Kulik,E.M. and Bickle,T.A. (1996) Regulation of the activity of the type IC EcoR124I restriction enzyme. *J. Mol. Biol.*, **264**, 891–906.
10. Makovets,S., Titheradge,A.J.B. and Murray,N.E. (1998) ClpX and ClpP are essential for the efficient acquisition of genes specifying type IA and IB restriction systems. *Mol. Microbiol.*, **28**, 25–35.
11. O'Neill,M., Chen,A. and Murray,N.E. (1997) The restriction-modification genes of *Escherichia coli* K-12 may not be selfish: they do not resist loss and are readily replaced by alleles conferring different specificities. *Proc. Natl Acad. Sci. USA*, **94**, 14596–14601.
12. Prakash-Cheng,A. and Ryu,J. (1993) Delayed expression of *in vivo* restriction activity following conjugal transfer of *Escherichia coli* hsdk (restriction-modification) genes. *J. Bacteriol.*, **175**, 4905–4906.
13. Prakash-Cheng,A., Chung,S.S. and Ryu,J.-I. (1993) The expression and regulation of hsdK genes after conjugative transfer. *Mol. Gen. Genet.*, **241**, 491–496.
14. O'Neill,M., Powell,L.M. and Murray,N.E. (2001) Target recognition by EcoKI: the recognition domain is robust and restriction-deficiency commonly results from the proteolytic control of enzyme activity. *J. Mol. Biol.*, **307**, 951–963.
15. Kobayashi,I. (2001) Behavior of restriction-modification systems as selfish mobile elements and their impact on genome evolution. *Nucleic Acids Res.*, **29**, 3742–3756.
16. Murray,N.E. (2002) Immigration control of DNA in bacteria: self versus non-self. *Microbiology*, **148**, 3–20.
17. Bourniquel,A.A. and Bickle,T.A. (2002) Complex restriction enzymes: NTP-driven molecular motors. *Biochimie*, **84**, 1047–1059.
18. Dryden,D.T.F., Murray,N.E. and Rao,D.N. (2001) Nucleoside triphosphate-dependent restriction enzymes. *Nucleic Acids Res.*, **29**, 3728–3741.
19. Murray,N.E. (2000) Type I restriction systems: sophisticated molecular machines. *Microbiol. Mol. Biol. Rev.*, **64**, 412–434.
20. Roberts,R.J., Vincze,T., Posfai,J. and Macelis,D. (2003) REBASE—restriction enzymes and methylases. *Nucleic Acids Res.*, **31**, 418–420.
21. Titheradge,A.J., King,J., Ryu,J. and Murray,N.E. (2001) Families of restriction enzymes: an analysis prompted by molecular and genetic data for type ID restriction and modification systems. *Nucleic Acids Res.*, **29**, 4195–4205.
22. Studier,F.W. and Bandyopadhyay,P.K. (1988) Model for how type I restriction enzymes select cleavage sites in DNA. *Proc. Natl Acad. Sci. USA*, **85**, 4677–4681.
23. Janscak,P., MacWilliams,M.P., Sandmeier,U., Nagaraja,V. and Bickle,T.A. (1999) DNA translocation blockage, a general mechanism of cleavage site selection by type I restriction enzymes. *EMBO J.*, **18**, 2638–2647.
24. Taylor,A.F. and Smith,G.R. (1990) Action of RecBCD enzyme on cruciform DNA. *J. Mol. Biol.*, **211**, 117–134.
25. Szczelkun,M.D., Janscak,P., Firman,K. and and Halford,S.E. (1997) Selection of non-specific DNA cleavage sites by the type IC restriction endonuclease EcoR124I. *J. Mol. Biol.*, **271**, 112–123.
26. Davies,G.P., Powell,L.M., Webb,J.L., Cooper,L.P. and Murray,N.E. (1998) EcoKI with an amino acid substitution in any one of seven DEAD-box motifs has impaired ATPase and endonuclease activities. *Nucleic Acids Res.*, **26**, 4828–4836.
27. Davies,G.P., Kemp,P., Molineux,I.J. and Murray,N.E. (1999) The DNA translocation and ATPase activities of restriction-deficient mutants of Eco KI. *J. Mol. Biol.*, **292**, 787–796.
28. Davies,G.P., Martin,I., Sturrock,S.S., Cronshaw,A., Murray,N.E. and Dryden,D.T.F. (1999) On the structure and operation of type I DNA restriction enzymes. *J. Mol. Biol.*, **290**, 565–579.
29. Janscak,P., Sandmeier,U. and Bickle,T.A. (1999) Single amino acid substitutions in the HsdR subunit of the type IB restriction enzyme EcoAI uncouple the DNA translocation and DNA cleavage activities of the enzyme. *Nucleic Acids Res.*, **27**, 2638–2643.
30. Webb,J.L., King,G., Ternent,D., Titheradge,A.J.B. and Murray,N.E. (1996) Restriction by EcoKI is enhanced by cooperative interactions between target sequences and is dependent on DEAD box motifs. *EMBO J.*, **15**, 2003–2009.
31. Endlich,B. and Linn,S. (1985) The DNA restriction endonuclease of *Escherichia coli* B. II. Further studies of the structure of DNA intermediates and products. *J. Biol. Chem.*, **260**, 5729–5738.
32. Eskin,B. and Linn,S. (1972) The deoxyribonucleic acid modification and restriction enzymes of *Escherichia coli* B. II. Purification, subunit structure, and catalytic properties of the restriction endonuclease. *J. Biol. Chem.*, **247**, 6183–6191.
33. Murray,N.E., Batten,P.L. and Murray,K. (1973) Restriction of bacteriophage lambda by *Escherichia coli* K. *J. Mol. Biol.*, **81**, 395–407.
34. Bickle,T.A., Brack,C. and Yuan,R. (1978) ATP-induced conformational changes in the restriction endonuclease from *Escherichia coli* K-12. *Proc. Natl Acad. Sci. USA*, **75**, 3099–3103.
35. Eskin,B. and Linn,S. (1972) The deoxyribonucleic acid modification and restriction enzymes of *Escherichia coli* B. *J. Biol. Chem.*, **247**, 6192–6196.
36. Meselson,M. and Yuan,R. (1968) DNA restriction enzyme from *E. coli*. *Nature*, **217**, 1110–1114.
37. Holubova,I., Vejsadova,S., Weiserova,M. and Firman,K. (2000) Localization of the type I restriction-modification enzyme EcoKI in the bacterial cell. *Biochem. Biophys. Res. Commun.*, **270**, 46–51.
38. Holubova,I., Vejsadova,S., Firman,K. and Weiserova,M. (2004) Cellular localization of Type I restriction-modification enzymes is family dependent. *Biochem. Biophys. Res. Commun.*, **319**, 375–380.
39. Pettijohn,D.E. (1996) The nucleoid. In Neidhardt, F.C. (ed.), Escherichia coli *and* Salmonella typhimurium: *Cellular and Molecular Biology*. ASM Press, USA, pp. 158–166.
40. Robinow,C. and Kellenberger,E. (1994) The bacterial nucleoid revisited. *Microbiol Rev.*, **58**, 211–232.
41. Azam,T.A. and Ishihama,A. (1999) Twelve species of the nucleoid-associated protein from *Escherichia coli*. Sequence recognition specificity and DNA binding affinity. *J. Biol. Chem.*, **274**, 33105–33313.
42. Azam,T.A., Hiraga,S. and Ishihama,A. (2000) Two types of localization of the DNA-binding proteins within the *Escherichia coli* nucleoid. *Genes Cells*, **5**, 613–626.
43. Dreier,J., MacWilliams,M.P. and Bickle,T.A. (1996) DNA cleavage by the type IC restriction-modification enzyme EcoR124II. *J. Mol. Biol.*, **264**, 722–733.
44. Burckhardt,J., Weisemann,J., Hamilton,D.L. and Yuan,R. (1981) Complexes formed between the restriction endonuclease EcoK and heteroduplex DNA. *J. Mol. Biol.*, **153**, 425–440.
45. Dreier,J. and Bickle,T.A. (1996) ATPase activity of the type IC restriction-modification system EcoR124II. *J. Mol. Biol.*, **257**, 960–969.
46. Bloomfield,V.A., Crothers,D.M. and Tinoco Jr,I.T. (2000) *Nucleic Acids: Structures, Properties and Functions*. University Science Books, USA.
47. Frenkiel-Krispin,D., Levin-Zaidman,S., Shimoni,E., Wolf,S.G., Wachtel,E.J., Arad,T., Finkel,S.E., Kolter,R. and Minsky,A. (2001) Regulated phase transitions of bacterial chromatin: a non-enzymatic pathway for generic DNA protection. *EMBO J.*, **20**, 1184–1191.
48. Minsky,A. (2003) Structural aspects of DNA repair: the role of restricted diffusion. *Mol. Microbiol.*, **50**, 367–376.
49. Pingoud,A., Urbanke,C., Alves,J., Ehbrecht,H.J., Zabeau,M. and Gualerzi,C. (1984) Effect of polyamines and basic proteins on cleavage of DNA by restriction endonucleases. *Biochemistry*, **23**, 5697–5703.
50. Pingoud,A. (1985) Spermidine increases the accuracy of type II restriction endonucleases. suppression of cleavage at degenerate, non-symmetrical sites. *Eur. J. Biochem.*, **147**, 105–109.
51. Dryden,D.T.F., Cooper,L.P., Thorpe,P.H. and Byron,O. (1997) The *in vitro* assembly of the EcoKI type I DNA restriction/modification enzyme and its *in vivo* implications. *Biochemistry*, **36**, 1065–1076.
52. Baumann,C.G. and Bloomfield,V.A. (1995) Large-scale purification of plasmid DNA for biophysical and molecular biology studies. *Biotechniques*, **19**, 884–890.
53. Rye,H.S., Yue,S., Wemmer,D.E., Quesada,M.A., Haugland,R.P., Mathies,R.A. and Glazer,A.N. (1992) Stable fluorescent complexes of double-stranded DNA with bis-intercalating asymmetric cyanine dyes: properties and applications. *Nucleic Acids Res.*, **20**, 2803–2812.

54. Ali,J.A., Jackson,A.P., Howells,A.J. and Maxwell,A. (1993) The 43-kilodalton N-terminal fragment of the DNA gyrase B protein hydrolyzes ATP and binds coumarin drugs. *Biochemistry*, **32**, 2717–2724.
55. Kuzmic,P. (1996) Program DYNAFIT for the analysis of enzyme kinetic data: application to HIV proteinase. *Anal. Biochem.*, **237**, 260–273.
56. Raspaud,E., Olvera de la Cruz,M., Sikorav,J.L. and Livolant,F. (1998) Precipitation of DNA by polyamines: a polyelectrolyte behavior. *Biophys. J.*, **74**, 381–393.
57. Suri,B. and Bickle,T.A. (1985) EcoA: the first member of a new family of type I restriction modification systems. Gene organization and enzymatic activities. *J. Mol. Biol.*, **186**, 77–85.
58. Goppelt,M., Langowski,J., Pingoud,A., Haupt,W., Urbanke,C., Mayer,H. and Maass,G. (1981) The effect of several nucleic acid binding drugs on the cleavage of d(GGAATTCC) and pBR 322 by the Eco RI restriction endonuclease. *Nucleic Acids Res.*, **9**, 6115–6127.
59. Breusegem,S.Y., Clegg,R.M. and Loontiens,F.G. (2002) Base-sequence specificity of Hoechst 33258 and DAPI binding to five (A/T)4 DNA sites with kinetic evidence for more than one high-affinity Hoechst 33258-AATT complex. *J. Mol. Biol.*, **315**, 1049–1061.
60. Neidle,S. (2001) DNA minor-groove recognition by small molecules. *Nat. Prod. Rep.*, **18**, 291–309.
61. Morgan,A.R., Lee,J.S., Pulleyblank,D.E., Murray,N.L. and Evans,D.H. (1979) Ethidium fluorescence assays. Part 1. Physicochemical studies. *Nucleic Acids Res.*, **7**, 547–569.
62. Cromie,G.A. and Leach,D.R. (2001) Recombinational repair of chromosomal DNA double-strand breaks generated by a restriction endonuclease. *Mol. Microbiol.*, **41**, 873–883.
63. Firman,K. and Szczelkun,M.D. (2000) Measuring motion on DNA by the type I restriction endonuclease EcoR124I using triplex displacement. *EMBO J.*, **19**, 2094–2102.
64. Garcia,L.R. and Molineux,I.J. (1999) Translocation and specific cleavage of bacteriophage T7 DNA *in vivo* by EcoKI. *Proc. Natl Acad. Sci. USA*, **96**, 12430–12435.
65. Seidel,R., Van Noort,J., Van Der Scheer,C., Bloom,J.G., Dekker,N.H., Dutta,C.F., Blundell,A., Robinson,T., Firman,K. and Dekker,C. (2004) Real-time observation of DNA translocation by the type I restriction modification enzyme EcoR124I. *Nature Struct. Mol. Biol.*, **11**, 838–843.
66. Berge,T., Ellis,D.J., Dryden,D.T.F., Edwardson,J.M. and Henderson,R.M. (2000) Translocation-independent dimerization of the EcoKI endonuclease visualized by atomic force microscopy. *Biophys. J.*, **79**, 479–484.
67. Ellis,D.J., Dryden,D.T.F., Berge,T., Edwardson,J.M. and Henderson,R.M. (1999) Direct observation of DNA translocation and cleavage by the EcoKI endonuclease using atomic force microscopy. *Nature Struct. Biol.*, **6**, 15–17.
68. Zlatanova,J. and Leuba,S.H. (2003) Chromatin fibers, one-at-a-time. *J. Mol. Biol.*, **331**, 1–19.